



Division of Molecular and cellular Science/School of Pharmacy

PROFILING POST TRANSLATIONAL MODIFICATIONS OF HISTONE AND p53 IN HUMAN BREAST CARCINOMAS

Magdy Korashy Abdelghany
MB BCH, MSc

Thesis submitted to the University of Nottingham for
the degree of Doctor of Philosophy

September 2011

DECLARATION OF ORIGINALITY

Unless otherwise stated in the text, this thesis is the result of my own work.

Abstract

Breast cancer is one of the most common cancers in females in the western world, and despite the advances in diagnosis and treatment it is still associated with significant morbidity. Thus, improvements to existing treatment modalities remain a priority. Understanding the molecular mechanisms controlling tumour growth and its modulation will be key to developing new therapies. In recent years it has been shown that posttranslational modifications (PTMs) of histones and p53 are functionally important in the regulation of cellular processes such as proliferation, differentiation and DNA damage repair. Thus, this study assessed the incidence of histone and p53 PTMs in breast tumours, and investigated how small molecule inhibitors of acetyltransferases can manipulate the levels of these PTMs in tumour cells.

Our initial study demonstrated that hypoacetylation of H4K16 is associated with higher grade breast tumours (Elsheikh et al., 2009). Therefore, the expression levels of enzymes that are known to modulate H4K16 acetylation *in vivo* was assessed using immunohistochemical staining of 880 human breast tumour tissue microarrays. This led to the identification of a cluster of biomarkers (hMOF, H4K16ac, H3K9me3 and SUV39H1) which are significantly associated with patient outcome. We also assessed in tumours the incidence of other potential biomarkers including selected p53 PTMs such as p53K373ac and p53 K386ac. These were also found to be associated with favourable patient outcome in Kaplan-Meier survival analysis. Other potential biomarkers were also assessed such as the histone variant H2A.Z and its hyperacetylated form. H2A.Z correlated with Estrogen Receptor status of the tumours, consistent with a report that the

Abstract

gene encoding this histone variant is estrogen-regulated. In summary, this study has revealed that histone and p53 PTMs in breast tumours are potentially useful biomarkers for the classification of tumour type and as prognostic indicators, for use in conjunction with other clinicopathological indicators, and other well established biomarkers such as estrogen receptor and HER2.

In a second aspect of the study, we investigated the effects of the acetyltransferase inhibitors curcumin and garcinol on a breast cancer cell model (MCF-7 cells). Garcinol blocked transcription-related PTMs such as H3K18ac, but surprisingly induced hyperacetylation of H4K16. This was found to be correlated with increased TIP60 expression, and correlated with increased incidence of DNA damage and cell cycle arrest. Other changes in cancer - associated PTMs were also observed, including increased H4K20 trimethylation. Garcinol compounds also reduced colony formation by MCF-7 cells and augmented sensitivity to etoposide. In summary, the data shows that histone and p53 PTMs constitute novel biological prognostic markers in breast cancer, and that targeting the enzymes that regulate these events may provide new avenues to drug therapies.

Acknowledgments

I dedicate this work to my parents who devoted their lives to raising their sons. I am also indebted to my wife and daughters, as without their support this work would not have been accomplished. Finally, to the souls of the Egyptian revolutionaries who gave their lives for the sake of Egypt, my beloved country.

I am very grateful to Professor David M Heery for his role as my project supervisor and a research group leader; his principles will be guidance in my future in academia. Under his supervision, laboratory experiments became a source of joy and writing up became a challenge to achieve excellence.

A large part of my work wouldn't be done without the collaboration with Prof Ian Ellis and Dr Andy Green, who provided access to tumour samples and laboratory resources to accomplish important parts of my work.

I am really grateful for the great help from Dr Hilary Collins, Dr Karin Kindle and Dr Akhmed Aslam who introduced me to Molecular Biology techniques. They were a constant source of assistance and advice throughout my study.

This study was performed under the financial support of the Ministry of Higher Education, Egypt to whom I am indebted.

LIST OF CONTENTS

1	INTRODUCTION.....	
1.1	What is Cancer?.....	1
1.1.1	Breast Cancer Incidence and Mortality	2
1.1.2	Physiology and Symptoms of Breast Tumours	3
1.1.3	Detection and Diagnosis.....	5
1.1.4	Classification of Breast Tumours	7
1.1.5	Staging of Breast Cancer.....	20
1.1.6	Histological Grading of Breast Cancer	23
1.1.7	Tumour Prognosis	25
1.1.8	Models to Study Breast Cancer-Cell Lines	28
1.2	Molecular Pathology of Breast Cancer.....	28
1.2.1	From DNA to Protein	28
1.2.2	Overview of Chromatin Structure	30
1.2.3	Epigenetic Modifications in Chromatin	32
1.2.4	Common Epigenetic Changes in Cancer.....	33
1.2.5	DNA Methylation in Cancer	34
1.2.6	DNA Methylation in Breast Cancer	35
1.2.7	Histone Methyltransferases	36
1.2.8	Histone Post Translational Modifications (PTMs) in Cancer	38
1.2.9	Histone Variants in Cancer.....	48
1.2.10	Tumour Suppressor p53: Post Translational Modifications (PTMs) and its Role in Cancer	55
1.2.11	Histone Acetyltransferases (HATs).....	62
1.2.12	HATs Inhibitors.....	67

1.2.13	Histone Deacetylases (HDACs)	71
1.2.14	HDAC inhibitors and Cancer	76
1.3	Aims of This Thesis.....	80
2	MATERIALS AND METHODS	82
2.1	General.....	83
2.2	Breast Tumour Tissue.....	83
2.2.1	The Tissue Microarrays (TMAs).....	83
2.2.2	Construction of the Tissue Microarray Blocks.....	84
2.2.3	Immunohistochemistry (IHC) Staining and Data Analysis.....	84
2.2.4	Statistical analysis	88
2.3	Cell Culture.....	90
2.3.1	Reagents	90
2.3.2	Cell Line Maintenance	90
2.3.3	Freezing Down Cells for Liquid Nitrogen Stocks.....	93
2.3.4	Thawing Cells from Liquid Nitrogen Stocks	93
2.3.5	Harvesting adherent cells	93
2.4	Biochemical Techniques.....	94
2.4.1	Solutions and Buffers	94
2.4.2	Antibodies	97
2.4.3	Total Protein Assay	97
2.4.4	Protein Separation and Transfer to Nitrocellulose	98
2.4.5	Western Blotting and Immunodetection.....	98
2.4.6	Immunocytochemistry and Fluorescence Microscopy.....	99
2.4.7	Bivariate Flow Cytometric Analysis of the Cell Cycle.....	100
2.4.8	Colony formation study.....	102

2.5	Bacterial Manipulations.....	102
2.5.1	Reagents, cells, media, supplements	102
2.5.2	Culture of <i>E. coli</i> DH5 α	103
2.5.3	Preparation of <i>Escherichia coli</i> (<i>E. coli</i>) competent cells.....	103
2.5.4	Plasmid DNA Transformation into <i>E. coli</i> cells.....	104
2.6	Molecular biology techniques.....	106
2.6.1	Plasmid Purification from <i>E.coli</i>	106
2.6.2	Determination of Nucleic Acid Concentration.....	106
2.6.3	Sequencing of Plasmid DNA	106
2.6.4	Calcium Phosphate-Mediated Transfection of Adherent Cells	107
2.6.5	Data bank analysis.....	107
2.6.6	RNA interference	108
3	EVALUATION OF HISTONE PTMs IN BREAST TUMOURS	110
3.1	Evaluation of the H4K16ac Regulatory Axis as a Novel Biomarker Set in Breast Tumours	111
3.1.1	Enzymes that Regulate H4K16 Acetylation: The H4K16ac Axis	112
3.1.2	TMA profiling of the H4K16ac Regulatory Axis in Breast Tumours	
		117
3.2	: Histone Variants in Breast Cancer.....	158
3.2.1	Detection of Histone Variants in Breast Tumour TMAs	161
4	EVALUATION OF p53 PTMs AND THEIR MODULATORS IN BREAST CANCER.....	185
4.1	p53 Post Translational Modifications (PTMs)	186
4.1.1	Acetylation of p53 in breast cancer	186
4.1.2	Detection of p53 Acetylation in Breast Tumour Tissue.....	187

4.2	p53 Acetylation Modulators	212
4.2.1	Detection of p53 Acetylation Modulators in Breast Tumour TMA	
	214	
4.2.2	Tumour Outcome in relation to p53 Acetylation Marks and their Modulators.....	233
4.2.3	Cluster analysis of p53 PTMs and their regulators	239
5	THE EFFECT OF THE HAT INHIBITORs ON HISTONE AND p53 PTMs AND MCF-7 CELL CYCLE PROLIFERATION	253
5.1.1	HAT inhibitors Alter Histone H3 and H4 Acetylation.....	254
5.1.2	HATi treatment Alters Histone H3 and H4 Methylation	260
5.1.3	Effects of HATi on HATs and HDACs Expression.....	265
5.1.4	Garcinol induces DNA Damage <i>in vivo</i>	269
5.1.5	HATi Alters p53 Function.....	271
5.1.6	HATi Treatment Alters p53 Function	280
5.1.7	HATi Treatment Sensitizes MCF-7 Cells to Etoposide and Reduces Colony Formation.....	288
5.1.8	Summary of Results: HATi Treatment can Reverse the Loss of Histone and p53 PTMs in Breast Cancer Cells.....	291
6	CONCLUDING REMARKS	295
7	REFERENCES.....	305
8	APPENDIX	344

LIST OF TABLES

TABLE 1:1: FREQUENCY AND 5-YEAR SURVIVAL FOR BREAST CANCER HISTOPATHOLOGICAL TYPES.....	8
TABLE 1:2: BREAST CANCER TUMOUR SUBTYPES BY CDNA HIERARCHICAL CLUSTERING.....	15
TABLE 1:3: BREAST CANCER TNM STAGING	22
TABLE 1:4: CLASSES OF HUMAN HDACS	73
TABLE 2:1: MAMMALIAN CELL LINES USED IN THE STUDY.....	92
TABLE 2:2: SOLUTION COMPOSITIONS FOR PREPARING RESOLVING GELS FOR TRIS-GLYCINE SDS-POLYACRYLAMIDE GEL ELECTROPHORESIS.	96
TABLE 2:3: PLASMIDS USED IN THE STUDY.....	105
TABLE 3:1: H4K16AC REGULATORY AXIS DETECTION LEVELS IN RELATIONSHIP TO TUMOUR HISTO-PATHOLOGICAL TYPES.	123
TABLE 3:2: H4K16AC REGULATORY AXIS DETECTION LEVELS IN RELATIONSHIP TO TUMOUR PHENOTYPE GROUPS OF BREAST CANCER AS DEFINED BY NIELSEN ET AL (NIELSEN ET AL., 2004).....	124
TABLE 3:3: H4K16AC REGULATORY AXIS DETECTION LEVELS AND PHENOTYPE GROUPS OF BREAST CANCER AS DEFINED BY ABE EL-REHIM ET AL (ABD EL-REHIM ET AL., 2005).	125
TABLE 3:4: H4K16AC, HMOF AND SIRT1 DETECTION LEVELS IN RELATIONSHIP TO TUMOUR CLINICOPATHOLOGICAL PARAMETERS; BIOLOGICAL FACTORS...129	129
3:5: H3K9ME3, DBC1 AND SUV39H1 DETECTION LEVELS IN RELATIONSHIP TO TUMOUR CLINICOPATHOLOGICAL PARAMETERS; BIOLOGICAL FACTORS...132	132
TABLE 3:6: H4K16AC, HMOF AND SIRT1 DETECTION LEVEL AND HISTONE PTMS AND THEIR MODULATORS.....	136
TABLE 3:7: H3K9ME3, DBC1 AND SUV39H1 DETECTION LEVEL AND HISTONE PTMS AND THEIR MODULATORS.....	140
TABLE 3:8: COX PROPORTIONAL HAZARD MODEL SHOWING HAZARD RATIOS FOR BCSS AND DFS CONFERRED BY H4K16AC, HMOF, SUV39H1 AND CLINICOPATHOLOGICAL VARIABLES	146

TABLE 3:9: HISTONE VARIANTS DETECTION LEVELS IN DIFFERENT TUMOUR HISTO-PATHOLOGICAL TYPES.....	167
TABLE 3:10: HISTONE VARIANTS DETECTION LEVELS AND PHENOTYPE GROUPS OF BREAST CANCER AS DEFINED BY NIELSEN AND COLLEAGUES (NIELSEN ET AL., 2004).....	168
TABLE 3:11: HISTONE VARIANTS DETECTION LEVELS AND PHENOTYPE GROUPS OF BREAST CANCER AS DEFINED BY ABE EL-REHIM AND COLLEAGUES (ABD EL- REHIM ET AL., 2005).....	169
TABLE 3:12: RELATION BETWEEN HISTONE VARIANTS DETECTION LEVELS AND CLINICO-PATHOLOGICAL PARAMETERS AND BIOLOGICAL FACTORS.	172
TABLE 3:13: CORRELATION BETWEEN HISTONE VARIANTS LEVELS AND HISTONE PTMS AND THEIR MODULATORS.	175
TABLE 3:14: COX PROPORTIONAL HAZARD MODEL SHOWING HAZARD RATIOS FOR BCSS AND DFS CONFERRED BY H2A.Z AND CLINICOPATHOLOGICAL VARIABLES	179
TABLE 4:1:P53 PTMS DETECTION LEVELS IN RELATIONSHIP TO TUMOUR HISTOPATHOLOGICAL TYPES.....	195
TABLE 4:2: P53 PTMS DETECTION LEVELS IN RELATIONSHIP TO TUMOUR PHENOTYPE GROUPS OF BREAST CANCER AS DEFINED BY NIELSEN AND COLLEAGUES (NIELSEN ET AL., 2004).	196
TABLE 4:3: P53 PTMS DETECTION LEVELS AND PHENOTYPE GROUPS OF BREAST CANCER AS DEFINED BY ABE EL-REHIM AND COLLEAGUES (ABD EL-REHIM ET AL., 2005).	197
TABLE 4:4: RELATION BETWEEN P53 PTMS DETECTION LEVELS AND CLINICO- PATHOLOGICAL PARAMETERS AND BIOLOGICAL FACTORS.....	201
TABLE 4:5: P53 PTMS IN RELATION TO HISTONE PTMS AND THEIR MODULATORS.	208
TABLE 4:6: THE DETECTION LEVEL OF P53 ACETYLATION MODULATORS IN DIFFERENT TUMOUR HISTOPATHOLOGICAL TYPES.	220

TABLE 4:7: THE DETECTION LEVEL OF P53 ACETYLATION MODULATORS AND PHENOTYPE GROUPS OF BREAST CANCER AS DEFINED BY NIELSEN AND COLLEAGUES (NIELSEN ET AL., 2004).....	221
TABLE 4:8: THE RELATIONSHIP OF P53 ACETYLATION MODULATORS TO PHENOTYPE GROUPS OF BREAST CANCER AS DEFINED BY ABD EL-REHIM AND COLLEAGUES (ABD EL-REHIM ET AL., 2005).....	222
TABLE 4:9: THE RELATIONSHIP BETWEEN DETECTION LEVELS OF THE P53 ACETYLATION MODULATORS AND CLINICO-PATHOLOGICAL PARAMETERS AND BIOLOGICAL FACTORS.....	225
TABLE 4:10: P53 PTM ACETYLATION MODULATORS DETECTION LEVELS IN RELATIONSHIP TO HISTONE PTMS AND THEIR MODULATORS.....	230
TABLE 4:11: COX PROPORTIONAL HAZARD MODEL SHOWING HAZARD RATIOS FOR BCSS AND DFS CONFERRED BY P53K373AC AND P53K386AC AND CLINICOPATHOLOGICAL VARIABLES	238

LIST OF FIGURES

FIGURE 1.1: TERMINAL DUCT LOBULAR UNIT (TDLU).....	4
FIGURE 1.2: BREAST CANCER TUMOURS CLUSTERING BASED ON IHC STAINING DATA.....	19
FIGURE 1.3: NOTTINGHAM GRADING SYSTEM.....	24
FIGURE 1.4: NOTTINGHAM PROGNOSTIC INDEX	27
FIGURE 1.5: THE NUCLEOSOME IS THE BASIC UNIT OF CHROMATIN	31
FIGURE 1.6: COVALENT MODIFICATIONS OF THE N-TERMINAL TAIL OF THE CORE HISTONES.....	40
FIGURE 1.7: P53 PTMS.....	58
FIGURE 1.8: MDM2, MDM4 AND P53 REGULATORY LOOP.....	61
FIGURE 1.9: HISTONE ACETYLATION STATUS OF CHROMATIN	63
FIGURE 3.1: THE H4K16AC AXIS.	116
FIGURE 3.2: DETECTION OF THE H4K16AC REGULATORY AXIS IN BREAST CANCER TMAS AS DETERMINED BY IHC	119
FIGURE 3.3: H4K16AC REGULATORY AXIS AND PATIENT OUTCOME.	145
FIGURE 3.4: K-MEANS CLUSTERING ALGORITHM FOR BREAST CANCER TUMOUR TMA IN REGARDS TO H4K16AC REGULATORY AXIS DETECTION LEVELS AND VALIDITY INDICES TESTS.	149
FIGURE 3.5: PAM CLUSTERING ALGORITHM FOR BREAST CANCER TUMOUR TMA IN REGARDS TO H4K16AC REGULATORY AXIS DETECTION LEVELS AND VALIDITY INDICES TESTS.	150
FIGURE 3.6: COMMON CLUSTERING OF H4K16AC REGULATORY AXIS, CLUSTER 2 CORRELATES WITH FAVOURABLE TUMOUR GRADE AND BETTER SURVIVAL.	151
FIGURE 3.7: HISTONE PTMS, HATS AND HDACS RELATIONSHIP	160
FIGURE 3.8: DETECTION OF MH2A IN BREAST CANCER TMAS AS DETERMINED BY IHC.....	162
FIGURE 3.9: DETECTION OF H2A.Z IN BREAST CANCER TMAS AS DETERMINED BY IHC.....	163

FIGURE 3.10: DETECTION OF H2A.ZAC IN BREAST CANCER TMAS AS DETERMINED BY IHC	164
FIGURE 3.11: HIGH H2A.ZAC LEVEL CORRELATES WITH BETTER PATIENT SURVIVAL	178
FIGURE 4.1: DETECTION OF P53K120 ACETYLATION MARK IN BREAST CANCER AS DETERMINED BY IHC	189
FIGURE 4.2: DETECTION OF P53K373 ACETYLATION MARK IN BREAST CANCER AS DETERMINED BY IHC	190
FIGURE 4.3: DETECTION OF P53K386 ACETYLATION MARK IN BREAST CANCER AS DETERMINED BY IHC	191
FIGURE 4.4: P53 PTMS, HATS AND HDACS AND THEIR EFFECTS ON CELL CYCLE PROGRESSION	213
FIGURE 4.5: DETECTION OF TIP60 IN BREAST CANCER TMAS AS DETERMINED BY IHC STAINING	215
FIGURE 4.6: DETECTION OF CBP IN BREAST CANCER TMAS AS DETERMINED BY IHC STAINING	216
FIGURE 4.7: DETECTION OF HDAC1 IN BREAST CANCER TMAS AS DETERMINED BY IHC STAINING	217
FIGURE 4.8: TUMOUR OUTCOME IN BREAST CANCER TMA STAINED FOR P53 ACETYLATION MARKS AND THEIR ACETYLATION MODULATORS	235
FIGURE 4.9: TUMOUR OUTCOME IN BREAST CANCER TMA STAINED FOR P53 ACETYLATION MODULATORS	236
FIGURE 4.10: K-MEANS CLUSTERING ALGORITHM AND VALIDITY INDICES TESTS FOR BREAST CANCER TUMOUR TMA WITH REGARD TO P53K373AC, CBP, SIRT1 AND SUV39H1 DETECTION LEVELS	241
FIGURE 4.11: PAM CLUSTERING ALGORITHM FOR BREAST CANCER TUMOUR TMA WITH REGARDS TO P53K373AC, CBP, SIRT1 AND SUV39H1 DETECTION LEVELS	242
FIGURE 4.12: CLUSTERING OF (P53K373, CBP, SIRT1 AND SUV39H1), CORRELATION WITH TUMOUR GRADE AND TUMOUR OUTCOME	243

FIGURE 4.13: K-MEANS CLUSTERING ALGORITHM AND VALIDITY INDICES TESTS FOR BREAST CANCER TUMOUR TMA IN REGARDS TO P53K386AC, HMOF AND SIRT1 DETECTION LEVELS.....	246
FIGURE 4.14: PAM CLUSTERING ALGORITHM AND VALIDITY INDICES TESTS FOR BREAST CANCER TUMOUR TMA IN REGARDS TO P53K386AC, HMOF AND SIRT1 DETECTION LEVELS.	247
FIGURE 4.15: CLUSTERING OF (P53K386AC, HMOF AND SIRT1) AND TUMOUR OUTCOME.....	248
FIGURE 5.1: DIFFERENTIAL EFFECTS OF HATI TREATMENT ON HISTONE H3 AND H4 ACETYLATION.	257
FIGURE 5.2: HISTONE PTMS IN MRC-5 CELLS AFTER HATI TREATMENT	259
FIGURE 5.3: HAT INHIBITORS TREATMENT ALTERS HISTONE METHYLATION.....	263
FIGURE 5.4: HAT INHIBITORS INDUCE ALTERATIONS IN THE LEVELS OF HISTONE ACETYLATION REGULATORS.	268
FIGURE 5.5: HATI INDUCES HIGH LEVELS OF DNA DAMAGE RESPONSE MARKERS.	270
FIGURE 5.6: CURCUMIN ALTERS P53 ACETYLATION.	272
FIGURE 5.7: GARCINOL ALTERS P53 ACETYLATION.....	276
FIGURE 5.8: CONT. GARCINOL ALTERS P53 ACETYLATION, VALIDATION OF P53 PTMS ANTIBODIES.	277
FIGURE 5.9: HATI TREATMENT ALTERS P53 ACETYLATION AT K386, K373 AND K120 IN MRC-5 CELLS.	279
FIGURE 5.10: HATI TREATMENT ALTERS P53 TRANSCRIPTIONAL ACTIVITY.....	282
FIGURE 5.11: GARCINOL, ISOGARCINOL AND LTK14 TREATMENT IMPEDES PROLIFERATION OF MCF-7 CELLS BY BLOCKING S PHASE.....	285
FIGURE 5.12: CURCUMIN TREATMENT IMPEDES PROLIFERATION OF MCF-7 CELLS BY BLOCKING S PHASE.....	286
FIGURE 5.13: CELL CYCLE CHANGES IN MRC-5 CELLS UPON HATI TREATMENT... .	287
FIGURE 5.14: EFFECTS OF HATI ON MCF-7 CELLS PROLIFERATION.....	289

6.1: THE POSSIBLE PATHWAYS THROUGH WHICH GARCINOL TREATMENT ALTERS CELL PROLIFERATION	303
--	-----

LIST OF ABBREVIATIONS

BCSS: Breast cancer specific survival

BSE: Breast self examination

CBP: CREB binding protein

CK: cytokeratin

DAB: Diaminobenzidine

DBC1: Deleted in Breast Cancer 1

DCIS: Ductal carcinoma *in situ*

DDP: cisplatin

DFS: disease free survival

DNMT: DNA methyltransferase

DOX: doxorubicin

EGFR: epidermal growth factor receptor

ER: oestrogen receptor

FNA: Fine Needle Aspiration

FFPE: formalin fixed paraffin embedded

FGFR1: fibroblast growth factor receptor 1

H&E: haematoxylin and Eosin

H3K9ac: acetylated H3K9

H3K12ac: acetylated H3K12

H3K18ac: acetylated H3K18

H3K4me2: dimethylated H3K4

H4K16ac: acetylated H3K16

H4K20me3: trimethylated H4K20

H4R3me2: dimethylated H4R3

HATs: histone acetyltransferases

HATi: histone acetyltransferase inhibitors

HDACs: histone deacetylases

HD: high detection

HMT: histone methyltransferase

LD: low detection

MI: mitotic index

NC: not classified

NHS: National Health Service
NICE: National Institute of Clinical Excellence
NOS: not otherwise specific
NPI: Nottingham Prognostic Index
PTMs: Post Translational Modifications
PR: progesterone receptor
TNM: Tumour, Node, Metastases
UK: United Kingdom
USA: United States of America
WHO: World Health Organisation

Abbreviations used in Materials and Methods

APS: Ammonium persulphate
BSA: Bovine Serum Albumin
dH₂O: distilled water
DNA: Deoxyribonucleic acid
DTT: Dithiothreitol
ECL: Enhanced Chemi-Luminescence
EDTA: ethylenediamine tetra-acetic acid
FACS: Fluorescence activated cell sorting (Flow cytometry)
FCS: Foetal calf serum
H-score: Histo-score
HRP: Horseradish peroxidise
IHC: immunohistochemistry
IF: immunofluorescence
kD: kiloDalton
LB: broth Luria-Bertrani broth
NSS: Normal Swine Serum
PAM: Partitioning Around Medoids
SPSS: Statistical Package for Social Scientists
PAGE: Polyacrylamide gel electrophoresis
PBS: Phosphate buffered saline
PCR: Polymerase chain reaction
PSA: Ammonium Persulfate

rpm: revolutions per minute

RT: room temperature

SDS: Sodium dodecyl sulphate

TBS: Tris buffered saline

TBS-T: Tris buffered saline-Tween

TEMED: N, N, N, 'N-tetramethylethylenediamine

TMA: tissue microarray

Tween: 20 polyoxyethylene-sorbitanmonolaurate

WB: western blotting

INTRODUCTION

1.1 What is Cancer?

Body tissues are made up of highly specialised cells that have become differentiated to perform specific functions. The growth, homeostasis and death of normal cells in these tissues are highly regulated. Cancer describes a wide range of diseases in which unregulated cell growth leads to a cell mass or tumour, which may be benign or malignant. Tumours can stimulate the growth of blood vessels to supply their nutrients, and malignant tumours can infiltrate mesenchymal tissues and enter the blood and lymphatic systems to metastasise to other sites in the body.

Some of the earliest evidence for tumours in man has come from paleopathological studies, in particular the mummified remains of ancient Egyptian and Incan cultures. For example, in 2001 researchers at the Czech Institute of Egyptology identified a benign nerve sheath tumour (schwannoma) inside the sacrum of the mummy of Imahetkherresnet, sister of priest Iufaa (Strouhal and Nemeckova, 2009). Another study identified four malignant tumours among 325 samples, providing clear evidence that malignant tumours were not rare in the ancient Egyptian population (Zink et al., 1999). Moreover, papyrus documents from Egypt dating from 1500 B.C. describe cases of breast tumours and their treatment by “fire drill”, a form of cauterization. Interestingly, natural remedies used by the ancient Egyptians to treat cancers included beverages made from fermented medicinal plants. In a recent review of drug discovery among ancient populations, two case studies from ancient Egypt and China were used to illustrate how ancient medicines can be reconstructed from

chemical and archaeological data and their active compounds delimited for testing their anticancer or other medicinal uses (McGovern et al., 2010). As will be demonstrated in this thesis, medicinal plants continue to be an important potential source of bioactive compounds in the search for new antitumour agents. My study is just one more step in the journey of understanding cancer and discovering a cure.

1.1.1 Breast Cancer Incidence and Mortality

Recent statistics reveal that breast cancer is currently the most commonly diagnosed cancer in females in the UK (<http://info.cancerresearchuk.org/cancerstats/>.), and similar trends are seen worldwide (Parkin et al., 2001, Ott et al., 2010, Barrett, 2010, Westlake S, 2008). In 2006, precisely 45,822 new cases of breast cancer were diagnosed in the UK: over 99% (45,508) in women and less than 1% (314) in men. The UK has the highest age standardised incidence in the world. Among women aged 50, the incidence approaches 2 per 1000 women per year and increases particularly among the older age group aged 50-64. Over the last 30 years, the epidemiology of breast cancer has been dynamic, although the incidence of breast cancer in the UK is on the increase, survival rates are improving due to earlier diagnosis and advances in treatments (Miller et al., 2005, Coleman, 2000).

1.1.2 Physiology and Symptoms of Breast Tumours

Cancer of the breast originates from the epithelial cells that line the terminal duct lobular unit (TDLU) (Sainsbury et al., 2000), which is also identified as a breast lobule (Fig 1.1). The TDLU consists of 10-100 acini that drain into terminal ducts. A single breast cancer cell has to undergo at least 30 doublings to reach 1cm, to be clinically palpable (Mittra et al., 2000). The terminal duct drains into larger ducts and finally into the main duct of the lobe that eventually drains into the nipple. The breast contains 15-20 lobes; each one contains 20-40 lobules. Most invasive cancers arise from the TDLU (Tot, 2010, Petersen et al., 2003).

Signs of early disease include a palpable mass, nipple discharge, nipple scaling or ulceration or with Paget's disease, axillary mass, skin dimpling, oedema and erythema. Symptoms of early disease may include breast pain and axillary discomfort. Advanced disease will typically present as a fixed mass to the chest, which sometimes can be associated with oedema of the arm. Patients in advanced stage of breast cancer usually complain from breast enlargement, breast ulceration, back pain, bone pain, jaundice and weight loss.

Figure 1.1: Terminal Duct Lobular Unit (TDLU).



Breast carcinoma originates from the epithelial cells that line the terminal duct lobular unit (TDLU) which is also identified as a breast lobule (Highlight in right panel). The TDLU consists of 10-100 acini that drain into terminal ducts (Arrow head). The terminal duct drains into larger ducts and finally into the main duct of the lobe that eventually drains into the nipple (Left panel). Reproduced from (Pijnappel, 2008).

1.1.3 Detection and Diagnosis

Mammography

The NHS National Breast Screening Programme began inviting women for screening in 1990 and national coverage was achieved by 1993. It invites women in their late 40s and up to the age of 73. Women are invited for the screening every 3 years; women over the age of 70 who are not automatically invited for breast screening are still encouraged to go for screening every three years. The programme is carried through a regular breast screening and self examination. The first step involves an x-ray of each breast; in which a mammogram is taken while carefully compressing the breast. Mammograms can detect small changes in breast tissue which may indicate cancers that are too small to be felt either by the woman herself or by a doctor. Noticeably, early diagnosis has contributed to the reduction in breast cancer related mortality in the past 20 years (Quinn and Allen, 1995, McPherson et al., 2000).

Breast Awareness

Women are also encouraged to perform regular Breast Self Examination (BSE). The aim of BSE is to help women to familiarize themselves with their own breasts in order to discover what is normal for them and to recognise any irregularities. The breast is subjected to regular changes as a reflection of menstrual cycle changes; hence, it has been suggested that BSE one week after the onset of menstruation is beneficial for breast mass detection (Austoker, 2003). Although BSE is widely encouraged, some researchers do not think early detection through

screening or BSE has much impact on the patient survival within groups with the same individual stages (Richards et al., 1999).

Diagnosis

Upon presentation of a breast lump, triple assessments are performed, including; clinical examination, imaging the breast by mammography (see before) and/or ultrasound and needle biopsy (Blamey et al., 2000). Fine needle aspiration cytology (FNAC) of breast lumps-which is performed by a histopathologist- is both cost effective and reduces the need for an open biopsy that has a risk of complications. FNAC is currently considered the first choice for obtaining tissue for diagnosis of a palpable lump (National Institute for Clinical Excellence, 2002).

Recent technology in breast cancer early diagnosis

Human plasma assays for selected biomarkers have been marketed for breast cancer detection; this assay is measured by Mass spectrometry based MRM (Multiple Reaction Monitoring) technology; which is used to measure the level of

25 proteins in patient plasma sample (<http://www.nextgensciences.com/assays/breast.php>). This technology is also available for other human cancers like lung, liver, prostate and others (http://www.nextgensciences.com/indices/Plasma%20Assay%20Product%20Overview%20brochure_03-2011final.pdf). The manufacturer claims that this assay overcomes issues related to antibody availability, specificity and reproducibility.

1.1.4 Classification of Breast Tumours

Breast tumours can be classified according to histopathological type, biomolecular markers, and immunohistological staining phenotype. In addition, more recently, molecular profiling by transcript microarray analysis has characterized several prognostic gene expression signatures. Gene expression profiling potentially outperforms histopathological factors in identifying low-risk patients in specific breast cancer subgroups, with high predictive values (90%). This promises a potential role for a clinical application. Caldas *et al.* proposed that further improvements and insights may come from integrative expression pathway analyses that dissect prognostic signatures into modules related to cancer hallmarks (Teschendorff *et al.*, 2010). In the following section, an overview of breast cancer classifications is presented.

Histopathological typing of breast tumours is a vital element in pathological diagnosis as it provides an insight for the tumour prognosis (Li *et al.*, 2005a) as shown in Table 1.1.

Table 1:1: Frequency and 5-year Survival for Breast Cancer Histopathological Types.

Histological type	Frequency (%)	5-year Survival (%)
Ductal Carcinoma <i>in situ</i> (DCIS)	3.6	>99
Lobular Carcinoma <i>in situ</i> (LCIS)	1.6	>99
Mixed Ductal and Lobular Carcinoma <i>in situ</i>	0.2	>99
Paget's disease	1	79
Infiltrating Duct Carcinoma	71.4	79
Infiltrating Lobular Carcinoma	9	84
Mixed Ductal and Lobular Carcinoma	7	85
Medullary Carcinoma	1.1	82
Mucinous Carcinoma	2.3	95
Papillary Carcinoma	0.5	96
Tubular Carcinoma	1.4	96

Data adapted from (Li et al., 2005a, Li et al., 2003), based on the International Classification of Diseases for Oncology (ICD-O) histological category approach.

In situ carcinoma is characterised by the proliferation of malignant epithelial cells within the lobules or ducts, where tumour cells have not penetrated the basement membrane (Goussia et al., 2006). These carcinomas are subdivided into ductal carcinoma *in situ* (DCIS) and lobular carcinoma *in situ* (LCIS), according to whether the lesion involves only the ducts in TDLU (DCIS), or both small ducts and lobules (LCIS) (Buerger et al., 2000).

Ductal carcinoma *in situ* (DCIS) is a heterogeneous group of lesions, with several microscopic variants. It has been subdivided according to a nuclear grade, which include differences in nuclear morphology (Nuclear atypia), cellular architectural patterns and a presence of necrosis. Three subtypes are known: firstly, low grade such as a cribriform and a clinging patterns, which are characterized by a mild nuclear atypia, a low number of mitotic cells and are devoid of necrosis; secondly, intermediate grade such as a solid pattern, which is characterized by moderate nuclear atypia, some necrosis and the presence of occasional mitosis; finally, high grade such as a “comedo” pattern which is characterized by marked nuclear pleomorphism, necrosis and a high number of mitotic figures (Rosai, 2004).

Lobular carcinoma *in situ* (LCIS) lesion is characterized by clusters of distended acini or solid expansion of ductules. The LCIS cells lack glandular/acinar formations; are characterized by loss of cell-cell cohesion and nuclear atypia. Notably, women with LCIS have an increased risk of getting breast cancer in the future (Afonso and Bouwman, 2008).

Infiltrating Ductal Carcinoma (IDC) is the most common type of breast cancer, accounting for two thirds of infiltrating breast tumours. It comprises multiple histological variants, among them the classical IDC not otherwise specified (NOS) which is considered the classical picture of IDC (Rosai, 2004). Other histological variants of IDC that are characterized by some biological differences include the following:

Tubular Carcinoma which is a well differentiated form of IDC. It is composed of regular rounded or angulated tubules scattered in a fibrous stroma without any lobular arrangement. The tubules are linked by a single layer of cells with bland-looking nuclei, and rare mitotic figures. In general, tubular tumours and tubular mixed tumours (>75% of the component is tubular) have an excellent prognosis (Sheppard et al., 2000).

Mucinous (Colloid) Carcinoma comprises approximately 2% of breast carcinomas. Cells of IDC NOS type usually contain discrete mucinous material, which is PAS^{+ve}, present in both tumour cells, as well as in the stroma (Komaki et al., 1988).

Medullary Carcinoma is another variant, in which the hallmark is the presence of solid sheets or nests of relatively poorly differentiated cells; surrounded by a mantle of plasma cells and lymphocytes, sometimes with germinal centres (Malyuchik and Kiyamova, 2008). Despite the nuclear features, medullary carcinomas have a more favourable prognosis than IDC NOS. Hence,

nuclear grading is not done for this special type of infiltrating cancer (Pedersen et al., 1995).

Papillary Carcinoma is formed of a spectrum of papillary patterns, micropapillae, solid areas, a cribriform growth and occasional cysts. Again, the prognosis is usually more favourable than IDC NOS (Chen et al., 2008a).

A number of breast tumour types are associated with poor prognosis. For example, metaplastic carcinoma which comprises 3.7% of breast cancers; the epithelial elements of the tumour undergo metaplastic changes to a non-glandular pattern, most frequently squamous (Breuer et al., 2007), or osseous (Lee et al., 2008) differentiation. Inflammatory carcinoma is another variant which is a clinical rather than histopathological designation; is characterized by a large, erythematous and painful mass showing purple discolouration of the skin. A patient with such a tumour is usually associated with unfavourable prognosis (Renz et al., 2008). Interestingly, invasive lobular carcinoma (ILC) which is usually composed of small uniform cells have a low mitotic rate; its cells have a characteristic pattern of stromal infiltration. The cells are arranged in a single-file, linear arrangement "Indian files". Cells can also seen or individually embedded in a fibroblastic stroma; or concentrically positioned around ducts and lobules described as a "targetoid pattern". The tumour can also show solid, alveolar or tubular patterns. Sometimes, frequent remnants of *in situ* lobular components are seen in the territory. Generally, the tumour cells are large characterized by hyperchromatic, pleomorphic nuclei (Rosai, 2004). Finally, Paget's disease of the nipple; the lesion is usually interpreted as an adenocarcinoma arising either

independently or from the underlying tumour. The lesion is characterized by the presence of large cells, abundant pale cytoplasm and large atypical nuclei on the surface epithelium (Caliskan et al., 2008).

Biomarker Sub-typing of Breast Tumours

Biomarker expression is also used to classify breast tumours. A major subtype comprises the Luminal/ER-positive breast tumours; which, are characterized by high expression of the estrogen receptors and tend to be more differentiated. In general they have a better clinical outcome to hormonal therapy; especially, if quantitative analysis of ER expression was assessed (Mazouni et al., 2010). HER2 is another subtype that is characterized by amplification of the ERBB2 oncogene; these tumours respond to Herceptin® (Trastuzumab) by targeting this receptor kinase (Kakar et al., 2000). Finally, basal-like tumours, which are distinguished by poor cellular differentiation, show high expression of cytokeratin 5/6 and a lack of hormone receptors and HER2. Generally, those tumours have a tendency towards the worst clinical outcome because of their propensity to develop distant metastases and a lack of targeted therapy (Nielsen et al., 2004).

Breast Cancer Molecular Profiling

Breast cancer is a heterogeneous disease with varying clinical outcome. Thus, as previously discussed, many efforts have been made to establish a hierarchical classification for breast cancer tumours based on histopathological features or biomarkers, which can inform clinical treatment. More recently, efforts have been

made to apply gene expression profiling to tumours using microarray analysis techniques. High throughput gene expression data has identified four distinct molecular groups: luminal epithelial/estrogen (ER) positive, HER2 positive, basal-like and normal breast-like (Perou et al., 2000). A follow up study by Sorlie *et al* (2001) extended the clustering by subdivision of the luminal tumours into three subtypes: luminal A, B and C (Sorlie et al., 2001). Each subtype is generally characterized by a distinct gene expression. Hierarchical clustering by cDNA microarray analysis revealed two main categories:

- The first category showed low or absent expression of the ER and contained three groups (Table1.2):
 1. **Normal breast-like** showed the highest expression of many genes (CD36 antigen collagen type, vascular adhesion protein and integrin alpha7) known to be expressed by adipose tissue and other nonepithelial cell types.
 2. **ERBB2** which are characterized by high expression of several genes in the ERBB2 amplicon at 17q22.24 including ERBB2, and GRB7.
 3. **Basal-like** which are characterized by high expression of keratins 5 and 17, laminin, and fatty acid binding protein 7.
- The second category is **luminal subtype**, which is characterized by positive expression of ER genes, it also contained three groups
 1. Luminal subtype **A** group that showed highest expression of the ER gene, GATA binding protein 3, X-box binding protein 1, trefoil factor 3, hepatocyte nuclear factor 3a, and estrogen-regulated LIV-1.

2. Luminal subtype **B** which is characterized by low to moderate expression of the luminal specific genes and the ER cluster.
3. Luminal subtype **C** is also characterized by low to moderate expression of the luminal specific genes and ER cluster and further distinguished from luminal subtypes A and B by the high expression of a novel set of genes whose coordinated function is unknown, which is a feature they share with the basal-like and ERBB2 subtypes.

Interestingly, gene expression profiling was found to predict clinical outcome of breast cancer (van 't Veer et al., 2002). Later, in 2003, Sorlie *et al.* eliminated subtype C; and classified breast tumours into 5 subgroups comprising normal breast tissue-like subgroup, in addition to the previous 4 subgroups: basal, ERBB2-overexpressing, luminal A, B (Sorlie et al., 2003). In the same year, Sotiriou *et al* (2003) demonstrated six similar groups: Luminal type 1, 2, 3, ERBB2, Basal 1 and 2. Later on, more studies proposed other classes and tried to assign a distinct prognostic pattern to each tumour class. Afterwards, a “combined test set” was shaped. It was created by combining the data sets of a number of the aforementioned studies; which, characterized tumour subtype classifications as objective methods for tumour classification and revealed some variations in between (Hu et al., 2006). In order to deal with the variation between different clusters, a ‘consensus clustering’ method was developed which focused on the comparison and concordance among different clustering methods and clustering validation (Monti et al., 2003).

Table 1:2: Breast Cancer Tumour Subtypes by cDNA Hierarchical Clustering.

	Subtype A Highest expression of the ER gene GATA binding protein 3 X-box binding protein 1 Trefoil factor 3 Hepatocyte nuclear factor 3a Estrogen-regulated LIV-1.
Luminal ER-positive	Subtype B Moderate expression of the luminal specific genes including the ER cluster.
	Subtype C Low expression of the Luminal specific genes including the ER cluster. High expression of a novel set of genes that share with the basal-like and ERBB21 subtypes
	ERBB2 (HER2) ERBB2 ^{+ve} GRB7 ^{+ve}
ER-negative	Basal Cytokeratins 5 ^{+ve} , Cytokeratins 17 ^{+ve} , Laminin ^{+ve} , Fatty acid binding protein 7 ^{+ve}
	Normal Breast- like CD36 antigen collagen type ^{+ve} vascular adhesion protein ^{+ve} integrin alpha7 ^{+ve}

Women presenting with breast cancer receive classic intervention (surgery followed by chemotherapy). However, only those who are likely to have breast cancer recurrence later in their life (15%) benefit from chemotherapy. Many efforts have been made to identify the high risk group that require chemotherapy and save the rest of patients from undergoing this treatment. Since 2004, a commercially available kit (Oncotype DX[®]) has been marketed in the United States. The kit has been used by half of the breast cancer patients in the USA and is used to detect the expression level of 21 genes to predict the likelihood of breast cancer recurrence. Oncotype DX was also shown to predict the benefit of chemotherapy in response to a variety of different chemotherapeutic regimes. These results suggested that the 21-gene test can generally predict the benefit from chemotherapy (<http://www.genomichealth.com/en-US/Pipeline/NextGeneration.aspx>). However, it is still too early to confirm if this test is better than conventionally established risk factors such as age, grade or standard biomolecular marks (Buchen, 2011).

Unfortunately, not all tumours can be assigned into the above categories, and moreover these categories are insufficient to predict outcome with high accuracy. Tumours within each molecular subtype described above are still fairly heterogeneous with respect to clinical outcome. In addition, many of them are placed in the grey zone between major molecular subtypes. Thus, molecular-based classifications may be oversimplified. Few molecular studies have attempted to analyze tumour progression from a population biology point of view. Allred *et al.* (2008) have taken on the challenging task of evaluating intertumoural and intratumoural diversity in DCIS of the breast. Their study found that DCIS

showed a broad distribution of conventional histological grades and standard biomarkers ranging from well differentiated to poorly differentiated, in which some tumours were nearly identical to Invasive Breast Cancer (IBCs). Moreover, microarray expression profiling studies showed the same intrinsic subtypes in DCIS as in IBCs. However, higher resolution analysis showed coexistence of multiple histological grades, biomarker phenotypes, and intrinsic subtypes within the same DCIS. In addition, diversity within cases of DCIS was highly correlated with p53 mutations (Allred et al., 2008). This supports the idea of Polyak (2008) that breast cancer tumours incorporate clonally diverse cells; which is considered a driving force of progression.

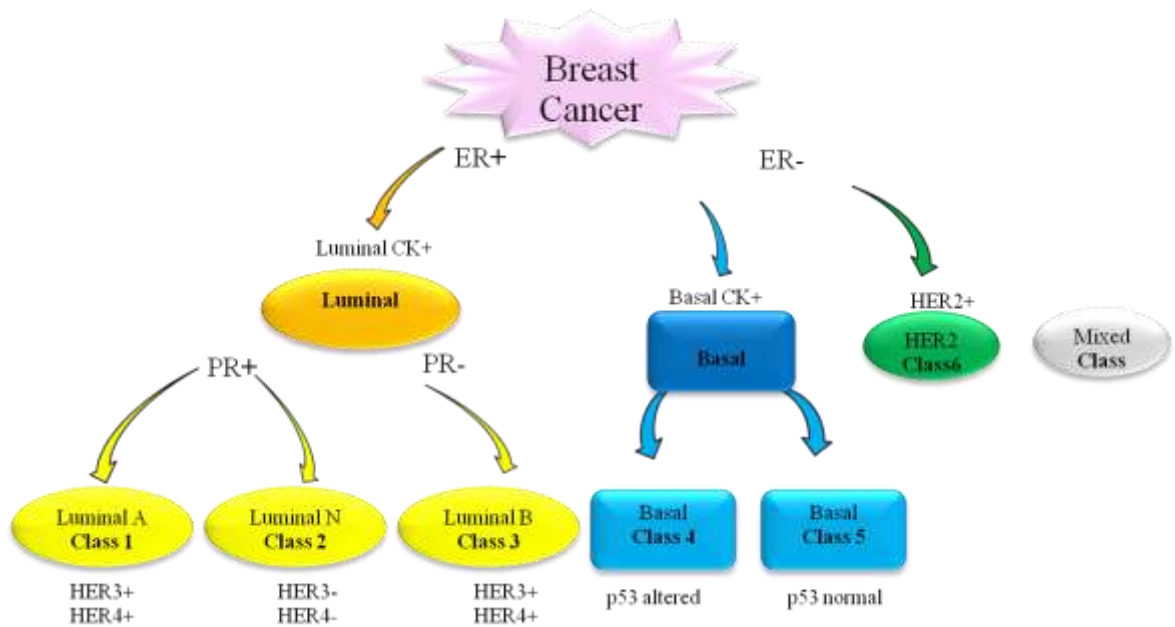
On this basis, we should keep in mind that on one level, breast tumours share some characteristics, which enable the pathologist to segregate them into distinctive histological types or biological categories. However, on a cellular basis, tumours are heterogeneous and a marked molecular difference is the hallmark of tumour cells. So, studying a tumour on multiple levels is important for proper tumour management.

Breast Cancer Tumour Clustering Based on IHC Staining

A clustering profile study was performed by the Breast Cancer Pathology Research Group in Nottingham, on a well characterized series of 1076 breast cancer patient. In that study, 25 commercially available antibodies were used against a known relevance for: tumour phonotypical type, hormonal receptors and a number of biological markers. Assessment of staining reactivity for each mark

was done by H-score (described later in Material and Methods); followed by hierarchical clustering analysis with Euclidean distance measure which revealed six cluster classes for breast cancer tumours (Abd El-Rehim et al., 2005). In 2010, Soria *et al.* used K-means and PAM clustering algorithms and further validated the clusters obtained with validity indexes (described later in Material and Methods). Six classes were described (Fig. 1.2) as follows: HER2 which were characterized by positive HER2 and negative ER expression; a broad basal class characterized by positive basal cytokeratin (CK5/6, CK14) and negative ER expression; and a broad luminal class (comprising A, B and N classes) which characterized by positive expression for luminal cytokeratin CK7/8, CK18 and CK19. Noteworthy, 38% of tumours did not fit into any of these six classes, referred to as mixed class. The basal class was subdivided into two subclasses according to mutant forms of p53 expression: p53 altered and p53 normal. The luminal tumours were subdivided according to progesterone receptor negative (Class B) or progesterone receptor positive status. The progesterone positive class can be further divided into class “A”, which is characterised by expression of HER3 and HER4, and class “N (HER3/HER4 negative) (Abd El-Rehim et al., 2005, Soria et al., 2010). Some data mentioned in this cluster class were used in the statistical analyses carried out in this thesis.

Figure 1.2: Breast Cancer Tumours Clustering based on IHC Staining data.



Adapted from (Soria et al., 2010).

1.1.5 Staging of Breast Cancer

Assessment of tumour stage and grade is complementary to tumour type in histopathological diagnosis. The most common world-wide used system is the TNM staging system of the American Joint Committee on Cancer (AJCC). It stands for 'tumour, node, and metastases'. It takes into account the size of the primary tumour, the draining lymph node, and whether the cancer has spread outside the primary site or not (Singletary et al., 2002). A summary of the TNM staging system for Breast cancer is emphasised in Table 1.3

Stage 0: DCIS, Cancer cells are present in the breast but no sign of spread.

Stage I: Breast tumours are very small and measure less than 2 centimetres in size. Which is considered "early breast cancer", no axillary lymph node (N) involved.

Stage IIA: The tumour (T) is between size 2-5 centimetres (cm), N negative; or T<2cm, N positive (<4 axillary nodes).

Stage IIB: T >5 cm, N negative; or T 2-5 cm and N positive (<4 axillary nodes)
No sign of spread of breast cancer to any other part of the body. This is still termed "early breast cancer".

Stage IIIA: T >5 cm, N positive; or T 2-5 cm and N positive in 4 or more axillary nodes.

Stage IIIB: The tumour extended to the chest wall or skin, N less than 10 positive lymph nodes

Stage IIIC: N is more than 10 Lymph nodes; one or more lymph nodes in subclavicular, infraclavicular or internal mammary lymph nodes. But there is

still no sign of disease spread any further throughout the body. This is known as "locally-advanced breast cancer"

Stage IV: Breast tumours are of any size. The lymph nodes are affected and the cancer has spread to other parts of the body, which known as "advanced or metastatic breast cancer". Tumour staging has a marked impact on tumour prognosis (Woodward et al., 2003).

Table 1:3: Breast Cancer TNM Staging.

Stage	Description
Stage 0	DCIS
Stage I	T <2cm, no nodal metastasis (N0)
Stage IIA	2≤ Size <5cm, N negative; or T<2cm, N positive (<4 axillary nodes)
Stage IIB	T >5 cm, N negative; or T 2-5 cm and N positive (<4 axillary nodes)
Stage IIIA	T >5 cm, N positive; or T 2-5 cm and N positive in ≥ 4 axillary nodes.
Stage IIIB	T extends to the chest wall or skin, N < 10 positive lymph nodes
Stage IIIC	N ≥ 10 Lymph nodes; involvement of subclavicular, infraclavicular or internal mammary N. No distant metastasis of the tumour (M0)
Stage IV	T has spread to other parts of the body (M1)

Where T, Tumour; N, Lymph node; and M, Metastasis. Data adapted from (Singletary et al., 2002).

1.1.6 Histological Grading of Breast Cancer

Histological grading is used widely to assess prognosis in breast cancer. The standard tumour grading system in use for breast cancer in the UK was developed by the Nottingham Breast Unit, with whom this collaborative project was performed. The current Nottingham grading system is a modification of the original Scarff-Bloom-Richardson (SBR). The system analyses three features, variation in the size and shape of nuclei, the degree of tubule formation and mitotic rate. In general, each element is given a score of 1 to 3 (1 being the best and 3 the worst) and the score of all three components are added together to give the "grade" as follow: Grade I, well differentiated, 3-5 points; Grade II, moderately differentiated, 6-7 points; Grade III, poorly differentiated, 8-9 points (Elston, 1984, Elston and Ellis, 1991) (Fig. 1.3). Histological grade in breast cancer was found to be strongly correlated with prognosis. For example, a study in Nottingham by Elston and Ellis (1991) on 1831 primary breast cancers revealed that survival for patients with grade I tumours is significantly better than those with grade II and III tumours, furthermore, a relatively large study (2219 cases) in Nottingham identified tumour grade in primary breast cancer tumours as an independent predictor for patient survival (Rakha et al., 2008).

Figure 1.3: Nottingham Grading System.



Mitotic count is carried out using the high power field (hpf) lens, data adapted from (Elston and Ellis, 1991).

1.1.7 Tumour Prognosis

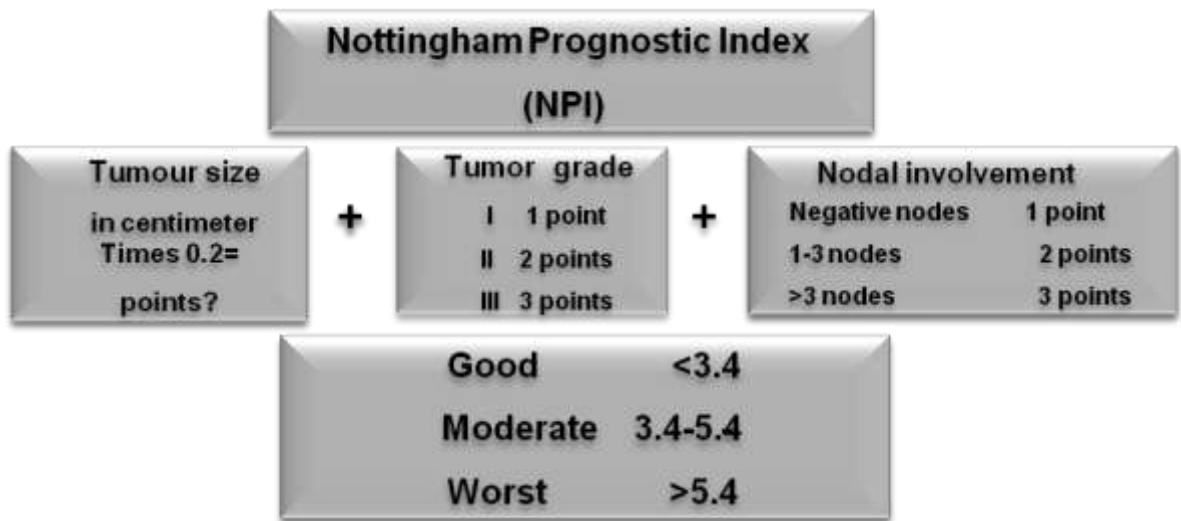
By definition tumour prognosis refers to the probable course and outcome of a tumour and the likelihood of patient recovery. A prognostic factor is a measurable factor in the primary tumour that can predict the tumour outcome and possibility of metastasis. Regarding breast cancer, the tumour prognosis strikingly varies from one patient to another. A predictive factor is a measurable factor that can predict the response to the treatment. Significant efforts over recent years have been made to identify tumour and host factors that would clearly predict tumour prognosis. Combinations of prognostic and predictive factors are used by clinicians, pathologists and oncologists during the process of tumour management to reach an accurate diagnosis measuring tumour differentiation, aggressiveness, rate of growth and metastatic potential and accordingly to decide the proper treatment modality based on sensitivity/ resistance to treatment (Pantel and Brakenhoff, 2004).

Prognostic factors in use: Considerable efforts have been done to further portray the prognosis of 70% of breast tumour patients, who 30% of them are going to develop metastasis in the future. A number of new prognostic markers have been established in specific patient groups. For example, lympho-vascular invasion in the nodal negative group is a poor prognostic marker; conversely, steroid receptor and HER2 protein positivity and their gene amplification is an established indicator for adjuvant therapy. In addition, uPA/PAI1 protein level is an independent prognostic factor associated with high metastatic risk. Overall,

gene expression profiling is still a focus for further investigation that proposes a bright future in breast cancer management (Weigelt et al., 2005).

Nottingham Prognostic Index (NPI) is used to work out the likely prognosis of the patient, according to information about the stage and grade of the breast cancer tumour. The calculation takes account of three factors: the size of the cancer; whether or not the cancer has spread to the axillary lymph nodes (and if so how many nodes are affected) and the grade of the cancer. The formula (as shown in Fig. 1.4) is as follow: $NPI = (0.2 * \text{tumour diameter in centimetres}) + \text{lymph node stage} + \text{tumour grade}$. Applying the formula gives scores which are grouped into 3 bands: a score of less than 3.4 suggests a good outcome with 80% overall survival (OS) and a high chance of cure. A score between 3.4 and 5.4 is considered intermediate which is characterized by 42% OS and suggests a moderate chance of a cure. Finally, any score of more than 5.4 suggests the worst outlook (13% OS) with a low chance of a cure. Generally, the NPI index is used as a guide to tumour outcome and considered as an important predictor of both disease free survival and overall survival. Furthermore, it can be influential in determining the treatment recommended (Galea et al., 1992).

Figure 1.4: Nottingham Prognostic Index.



Data adapted from (Galea et al., 1992)

1.1.8 Models to Study Breast Cancer-Cell Lines

In the last decade, exploring tumour biology in cell lines and xenografts has provided invaluable insights into tumour physiology. Gene expression profiles of 145 primary breast tumours and 51 breast cancer cell lines revealed similar genomic and transcriptional characteristics, although, some significant differences between cell line models and solid tumours were also documented (Neve et al., 2006). This study indicated that most of the genomic abnormalities in original tumours were retained in the cell lines derived from them. In addition, as shown for Trastuzumab (Herceptin®) monotherapy, cell lines can be useful models to measure tumour response to treatment, and can be used to identify molecular features that predict or indicate response to targeted therapies (Neve et al., 2006). Similarly, applying HDACi treatment (see section 1.2.14) in the H157 human lung cancer cell line sensitised the cells for etoposide, which suggests a possible use of histone acetylation modulators in combination with conventional chemotherapy (Hajji et al., 2009).

1.2 Molecular Pathology of Breast Cancer

1.2.1 From DNA to Protein

The genetic material of all cells is deoxyribonucleic acid (DNA) a long polymer made up of a sugar phosphate backbone and the 4 bases adenine (A), thymidine (T), guanine (G) and cytosine (C). DNA is double stranded, i.e. it consists of two complementary nucleic acid chains that form a double helix. Base pairing between A: T and G: C is facilitated by hydrogen bonds ensuring the anti-

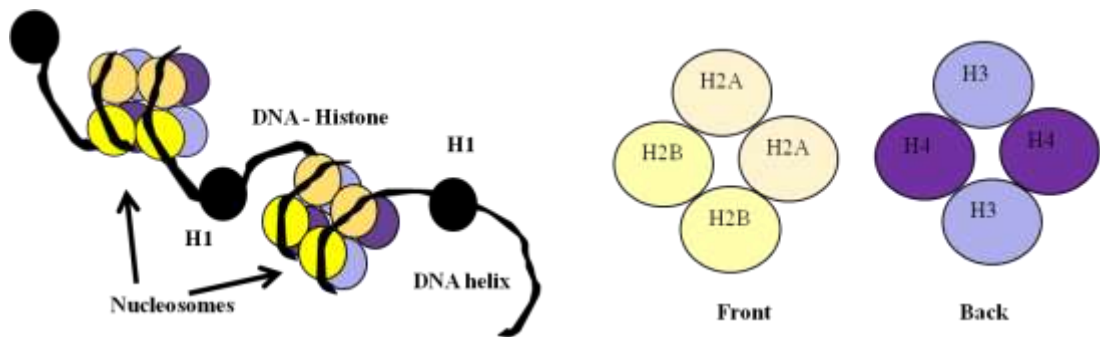
parallel DNA strands have complementary sequences. The DNA strands coil to form a right-handed double helix (B-DNA), with 10 nucleotide pairs per helical turn (Watson and Crick, 1953a, Watson and Crick, 1953b). The sequence of bases on the nucleic acid carries the genetic information, and an RNA copy is made by one of three RNA polymerases by the process known as transcription. *In vivo*, DNA strands are further assembled by structural proteins called histones to enable the compaction of ~ 1 meter DNA into ~ 10 µm cell nucleus in a well ordered structure that permit access to all the genomic material. The DNA sequence codes for the whole genomic information. The genome is formed of interrupted genes that consists of exons (representing the final RNA products) and introns (removed from the initial transcript) (Breathnach and Chambon, 1981). The process of splicing involves the deletion of introns from a primary transcript to give messenger RNA (mRNA) (Faustino and Cooper, 2003). Generation of mRNA is the 1st major step of gene expression; mRNA is generated from DNA double helix by RNA polymerases through a complementary base pairing process. The mRNA strand is complementary with the sequence of only one strand of DNA (the template strand) and is identical (apart from the replacement of T with U) with the other strand of DNA. Each mRNA consists of a non-translated 5' leader, a coding region, and a non-translated 3' region. Translation which is the 2nd stage of gene expression, involves the conversion of the nucleotide sequence of mRNA into the sequence of amino acid comprising a protein. mRNA is translated by ribosomes. A ribosome is an organelle composed of specialised ribonuclear proteins, arranged into small and large subunit, which provide the environment that control the recognition of a codon of mRNA and the anticodon of tRNA. The genetic code is a series of adjacent triplets. The ribosome translates

mRNA from the 5' end, where it translates each triplet codon into an amino acid as it proceeds toward the 3' end (Dintzis, 1961). The process of protein synthesis involves three main stages. The process is initiated by the binding of ribosome to the mRNA, forming initiation complex that contain the first aminoacyl-tRNA. Followed by the elongation step where amino acids are added to the first one; with synthesis of a series of peptide bonds between them to form amino acid chain. And finally, the termination step in which the completed peptide chain is released (Safer, 1989).

1.2.2 Overview of Chromatin Structure

Eukaryotic genomes are assembled as chromatin (DNA and histones), the basic unit of which is the nucleosome. The nucleosome consists of 147 base pairs of DNA wrapped 1.7 times around a histone octamer; built from two subunits of each of histones H2A, H2B, H3, and H4 (Fig. 1.5). The octamer is composed of a tetramer core of two H3 and two H4 histones, with H2A and H2B dimers on each side. Nucleosomes form a “beads on a string” structure, also known as the 10nm fibre, which can be further packaged into solenoids known as ‘30nm fibres’ or higher order structures. Linker histones such as H1 are located between core nucleosomes, to facilitate further compaction of chromatin (Khorasanizadeh, 2004, Luger, 2003). In addition to the core histones, a variety of histone variant proteins such as H2A.Z, macroH2A and γ H2A.X can replace H2A in the nucleosome, serving as landmarks for specific cellular functions (Gervais and Gaudreau, 2009). Specifically, epigenetic changes in canonical histone and histone variants have been found to play a critical role in regulating gene transcription (Sutcliffe et al., 2009).

Figure 1.5: The Nucleosome is the Basic Unit of Chromatin



A schematic representation of the chromatin where the nucleosomes (Arrows) are formed from DNA (black threads) wrapped 1.7 turns around two histone octamers. The front of the octamer is formed of two subunits of histones H2A, H2B; the back of the octamer is formed of two subunits of histones H3, and H4. Linker histone H1 (black sphere) is located between the core nucleosomes.

1.2.3 Epigenetic Modifications in Chromatin

Epigenetics is the study of meiotically and mitotically heritable changes in gene expression, which are not coded for in the DNA sequence (Egger et al., 2004); (Feinberg, 2004). Epigenetic signals include direct modification of the DNA (e.g. DNA methylation) and posttranslational modifications of histones. These inheritable and stable changes are responsible for maintaining tissue and cellular function (Lund and van Lohuizen, 2004b). Epigenetic changes differ from genetic changes in that they are (1) reversible, (2) they can affect more than one gene or locus, (3) can have positional effects, depending on their sequential or 3-dimensional proximity to other genes, (4) they are subjected to a high frequency of alteration, orders of magnitude greater than that of mutation and (5) can be altered by environmental factors i.e. regulation of histone modifications by natural products (Feinberg, 2004, Lund and van Lohuizen, 2004b).

Epigenetic changes modulate the accessibility of chromatin to transcription regulators and RNA polymerases, and also regulate other nuclear processes such as DNA replication, DNA repair and recombination. Epigenetic signals induce localised or global changes in the arrangement and composition of nucleosomes (Lund and van Lohuizen, 2004b). Structural studies have revealed that the N-terminal tails of core histones protrude from the nucleosomal core particles (Luger, 2003), and these are subjected to Post Translational Modifications (PTMs) (See section 1.2.8). These tails serve as regulatory subdomains onto which epigenetic signals can be written. The pattern of histone modifications determines the status of the chromatin at that site and is referred to

as the "histone code" (Jenuwein and Allis, 2001, Fingerman et al., 2008, Yue et al., 2007). Many of the enzymes that generate the histone code are recruited to chromatin as cofactors of transcription regulators. Other chromatin regulatory proteins contain histone PTM recognition modules such as the bromodomain, chromodomain or PHD domains. These domains use the epigenetic marks on the histone tails as recognition landmarks for chromatin binding to initiate downstream biological processes such as chromatin compaction, transcription regulation, or DNA repair (Lund and van Lohuizen, 2004b).

1.2.4 Common Epigenetic Changes in Cancer

In the past, the genetic model was used to explain the origin of cancer as a change in DNA sequence. One therefore may investigate the cancer mechanism by a search for mutations, deletions, rearrangements and gene amplification. The genetic model is able to explain most rare familial cancer syndromes, the cancer initiation of most common tumours and a number of mutations in a few genes have been shown to be responsible for cancer progression (Feinberg, 2004). In addition, an epigenetic model was proposed to further explain features of cancer. One therefore investigates the cancer mechanism by a search for changes in DNA methylation, chromatin modifications and gene imprinting errors (Feinberg, 2004). In addition, there is no doubt that histone modifications are contributing to carcinogenesis (Li et al., 2005b). Recently, it is well established that both models play together i.e. they are either combined or consecutive events (Feinberg, 2004).

1.2.5 DNA Methylation in Cancer

DNA methylation of the genome is a defence mechanism by which the repeated DNA (accounts for 50%) is transcriptionally silent. Demethylation of normally methylated DNA can result in activation of the corresponding genes (Li et al., 2005b). It has been found that a change in the methylation status of a gene promoter or first exon could cause the same effect of mutations of various tumour suppressor genes (TSGs) or protooncogenes (Jagodzinski, 2006).

Dysfunction of DNA methylation is tightly connected to cancer development. Global genomic hypomethylation abolishes oncogene activity; oncogenesis is promoted by local hypermethylation of tumour-suppressor genes (Lund and van Lohuizen, 2004a). DNA hypomethylation is linked to a number of cancers: MAGE in melanoma (De Smet et al., 1996), CA9 in renal cell cancer (Cho et al., 2001), cyclin D2 and maspin in gastric cancer (Oshimo et al., 2003), and hypomethylation of Cyclin D1 promoter as an underlying mechanism of its increased expression in gastric carcinoma development and progression (Oshimo et al., 2003).

A study of CpG methylation of human papilloma virus type 16 (HPV-16) DNA in cervical cancer cell lines revealed an efficiently targeted CpG methylation particularly in genomic segments overlying the late genes, while the LCR gene are unmethylated. Moreover, in 81 patient smears, the LCR gene of HPV-16 DNA were found to be hypermethylated in 52% of asymptomatic smears, 21.7% of precursor lesions, and 6.1% of invasive carcinomas; which suggested

that neoplastic transformation may be suppressed by CpG methylation, while demethylation occurs as the cause of or concomitant with neoplastic progression (Badal et al., 2003). In contrast, hypermethylation is associated with tumour suppressor gene silencing (Bestor, 2003), like E-cadherin in human breast and prostate carcinomas (Graff et al., 1995). Furthermore, CpG-island-promoter hypermethylation is associated with transcriptional silencing of tumour suppressor genes (Esteller, 2007b); hypermethylation of the pro-apoptotic gene caspase-8 is a common hallmark of relapsed glioblastoma multiforme (Martinez et al., 2007).

1.2.6 DNA Methylation in Breast Cancer

Regarding breast cancer tumours, an analysis of DNA sequence methylation in MCF-7 cells showing drug-resistance (to DOX and cisDDP) revealed dysfunction of the genes involved in estrogen metabolism, apoptosis and cell-cell contact. Cell line dysfunction was explained by the two opposing hypo- and hyper-methylation processes (Chekhun et al., 2007). In addition, Yang et al. (2001) pointed to the incidence of methylation of critical tumour suppressors and growth regulatory genes in breast cancer. Actually, they lie in several categories including: cell cycle regulating genes like p16/p16INK4A/CDKN2A/MTS; steroid receptor genes like ER α , PR, RAR β 2; tumour susceptibility like BRCA1; carcinogen detoxification like GSTP1; the cell adhesion gene E-cadherin and the matrix metalloproteinase (MMP) inhibitory gene TIMP-3 (Yang et al., 2001).

As these epigenetic changes are reversible events, they are a potential therapy targets in cancer (Das and Singal, 2004). There are two categories of drugs that epigenetically influence chromatin structure: DNA methyltransferase (DNMT) and histone deacetylase (HDAC) inhibitors (Jagodzinski, 2006). HDAC and DNMT inhibition are currently being evaluated in clinical trials with cancer patients (Issa et al., 2004, Garcia-Manero et al., 2008, Rudek et al., 2005). Moreover, Lan Yan (2001) suggested that inhibition of DNA methylation and histone deacetylation might be a therapeutic strategy in breast cancer especially for the ER and PR negative breast cancer phenotype. Recently, in a cell line model HDACi treatment sensitised the cancer cells to topoisomerase II (Hajji et al., 2009).

1.2.7 Histone Methyltransferases

Histone methyltransferases catalyze the addition of one or more methyl groups to a specific lysine or arginine residue within histones (Fingerman et al., 2008). Methylation of histones or combinations of post translational modifications can result in a variety of diverse biological processes. For example, trimethylation of lysine 9 in histone 3 (H3K9me3) is related to gene silencing/heterochromatin formation and trimethylation of lysine 4 in histone 3 (H3K4me3) is tightly linked to transcriptional regulation (Schotta et al., 2002, Tachibana et al., 2005, Lund and van Lohuizen, 2004b). Moreover, distinct effector molecules can read different methyl-lysine modification codes through specific interactions with the methylated histone. For example, heterochromatin protein 1 (HP1) mediates transcriptional repression via its high-affinity interactions with histone H3

methylated at K9 and K27 (Bannister et al., 2001). Several SET (SuVar39, Enhancer of Zeste and Trithorax) domain proteins have been established as histone methyltransferases capable of covalently altering the lysine residues of histone proteins. Many of those SET domain proteins have been tightly linked to cancer development (Lund and van Lohuizen, 2004b).

Several methyltransferases were found to be relevant to the histone modifications described in this study. The SUV39H1 protein is the first SET domain recognized as a histone methyltransferase (HMT) (Lund and van Lohuizen, 2004b). It methylates histone H3K9 and localizes to transcriptionally silent heterochromatin, where it recruits the transcriptional repressor HP1. SUV39H1 and HP1 have also been implicated in transcriptional repression at euchromatic loci (Bhaumik et al., 2007).

SUV420H1/2 were first identified in 2004 as two novel SET domain HMTases, that localize to pericentric heterochromatin in conjunction with HP1. SUV420H1/2 have been found to specifically trimethylate H4 at K20 (Schotta et al., 2004, Benetti et al., 2007). Reduced expression of SUV420H2 and loss of H4K20me3 were illustrated in human lung cancer (Van Den Broeck et al., 2008) and preneoplastic liver nodules in mice (Pogribny et al., 2006). In regards to breast cancer, loss of H4K20me3 was correlated with poor prognostic breast cancer subtypes (Elsheikh et al., 2009). In breast cancer cell lines, characterization of SUV420 enzymes in non- tumourigenic MCF-10-2A epithelial breast cells versus malignant cell lines (MCF-7, MDA-MB-231 and MDA-MB-231/S30) revealed a dysregulation of SUV420 and reduced H4K20me3 in

malignant cell lines especially MDA-MB-231 (Tryndyak et al., 2006). Moreover, diminished level of SUV420 expression was described in MCF-7 cells (Chekhun et al., 2007), suggesting an epigenetic role for SUV420 in breast cancer drug resistance.

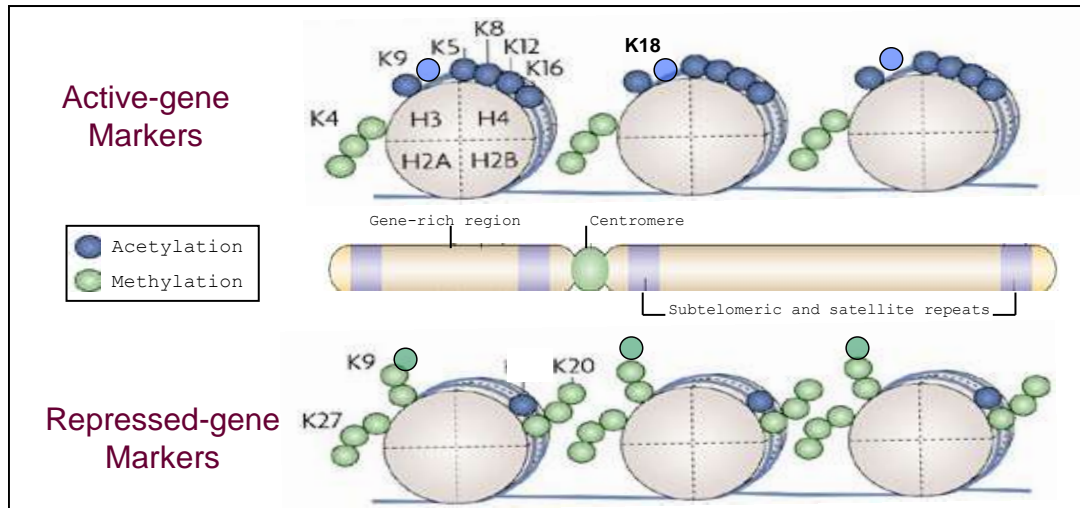
The methyltransferase Set7/9 is capable of the lysine methylation of histone tails which has important functions in many biological processes that include heterochromatin formation, X-chromosome inactivation and transcriptional regulation (Martin and Zhang, 2005). Also non-histone proteins can be methylated by Set7/9, in particular, it was shown to catalyze methylation of p53 at lysine 372 (p53K372me) and to modulate p53 activity in a human cancer cell line. Moreover, it is involved in the binding of the acetyltransferase TIP60 to p53 and for the subsequent acetylation of p53. So, lysine methylation of p53 by Set7/9 is important for p53 activation *in vivo* suggesting a mechanistic link between methylation and acetylation of p53 through TIP60 (Kurash et al., 2008).

1.2.8 Histone Post Translational Modifications (PTMs) in Cancer

As described above, histones have a key role in the regulation of gene transcription. The N-terminal tail of the histone is subjected to several post-translational modifications such as acetylation, deacetylation, methylation, phosphorylation, ubiquitination, sumoylation, and ADP-ribosylation (Khorasanizadeh, 2004). Together these modifications are referred to as the histone code (Jenuwein and Allis, 2001). Generally, histone hyperacetylation at gene promoters is correlated with transcription activity, whereas deacetylation is

correlated with inactive genes. Histone acetyltransferases (HATs) and histone deacetylases (HDACs) are the modulators for histone acetylation. Moreover, HMTs also play a similar role on histone modification and eventually gene regulation (Berger, 2002). For example, in prostate cancer, the expression of several tumour-associated genes were found to be associated with high levels of histone acetylation compared to normal cells (Li et al., 2005b). Another study in the same field by Tsubaki, Hwa *et al.* (2002), documented that treatment of prostate cancer cells with HDAC inhibitors increased the expression of genes such as insulin-like growth factor-binding protein 3 and carboxypeptidase A3 (CPA3); confirming the role for histone acetylation in gene regulation. Figure 1.6 is an overview of the modifications occurring in the histone tails which lead to changes in gene expression.

Figure 1.6: Covalent Modifications of the N-terminal tail of the Core Histones.



Acetylation and methylation marks are in green and blue circle, reproduced from (Esteller, 2007a) and modified.

Global Histone Modifications are Altered in Cancer

Seligson *et al.*, (2005) found that changes in bulk histone modifications are associated with cancer and that these changes are predictive of clinical outcome, independently of tumour stage, biomarkers, or capsular invasion. In addition, they proposed that the varied levels of specific histone modifications in prostate cancer may indicate an undiscovered molecular heterogeneity that might explain the broad range of clinical behaviour in cancer patients.

Our recent work on 880 breast cancer cases has showed that global histone PTMs are associated with tumour morphologic types, biomarker phenotype, tumour grade and clinical outcome (Elsheikh *et al.*, 2009). Altered global histone PTMs has also been found as a prognostic marker in other tumours such as renal cell carcinoma, glioma (Mosashvilli *et al.*, 2010, Liu *et al.*, 2010) and in inflammatory bowel disease (Tsaprouni *et al.*, 2011). In addition, targeting global histone modification levels was speculated as a future therapy in cancer especially pancreatic and prostatic cancer (Manuyakorn *et al.*, 2010, Reynoird *et al.*, 2010, Ellinger *et al.*, 2010). In the following section, I will discuss some of the most important histone PTMs that have a critical role in cellular function and tumourgenesis.

H3 lysine 9 methylation has been implicated in a variety of cell functions; such as, transcriptional silencing (Tachibana *et al.*, 2005). It was considered the primary signal sufficient for initiating a gene repression pathway *in vivo* (Snowden *et al.*, 2002). Generally, silenced or inactive promoters exhibit a loss of histone H3-acetylation and an increase in H3 lysine 9 trimethylation (H3K9me3)

(Groner et al., 2010). Regarding cancer, H3K9 methylation was illustrated in the silenced loci of three genes in colorectal cancer. Interestingly, treatment with the DNA methyltransferase inhibitor 5-aza-2'-deoxycytidine (5Aza-dC) rapidly reduced H3K9 methylation at silenced loci and resulted in reactivation of all three genes (Kondo et al., 2003). Furthermore, in DKO cells, the DNMT3B-deficient HCT116 colon cell line, elimination of H3K9 methylation from p16 (INK4a) gene resulted in profound changes in the surrounding histone PTMs; conversely, H3K9 methylation resulted in re-silencing of genes (Bachman et al., 2003).

H3K9me3 is a hallmark of heterochromatin formation; in conjunction with heterochromatic protein1 (HP1) family proteins they play a key role in constitutive heterochromatin formation (Bernstein et al., 2006, Wako and Fukui, 2007). H3K9me3 is recognized and recruited by HP1 to discrete regions of the genome, thereby regulating gene expression, chromatin packaging and heterochromatin formation (Dormann et al., 2006). In addition, H3K9me3 has a role in DNA double-strand break repair. The histone acetyltransferase TIP60 binds to H3K9me3 at heterochromatic sites, triggering acetylation and activation of DNA double-strand break repair factors (Fischle, 2009).

The role of H3k9me3 in cancer has been described; for example, dysregulation of H3K9me3 has been identified in acute myeloid leukaemia (AML). A decrease in H3K9me3 levels at promoter regions resulted in enhanced transcription factor activity at those sites. In addition, using the H3K9me3 signature in combination with established clinical prognostic markers outperformed prognosis prediction based on clinical parameters alone; and

enhanced AML outcome prediction (Muller-Tidow et al., 2010). In a mouse model, a study of hepatogenesis revealed that a methyl deficient diet resulted in altered global histone methylation/acetylation during tumourgenesis. They found altered levels of H4K20me3, H3K9me3, H4K16ac and H3K9ac and their modulators, the HATs and methyltransferases; this signifies the importance of histone PTMs in tumourgenesis (Pogribny et al., 2007). In prostate cancer, a recent study on 113 prostate cancer and 23 non-malignant samples revealed that levels of H3K9me3 were significantly reduced in cancer samples compared to non-malignant prostate tissue (Ellinger et al., 2010).

Multiple efforts have been made to modulate global H3K9me3 levels. Identification of GASC1, the putative oncogene which demethylates H3K9me3, delocalizes HP1 and reduces heterochromatin formation makes it a good target for anticancer therapy (Cloos et al., 2006). In addition, cobalt compounds have been implicated in reducing global H3K9me3 levels in A549 (a human lung carcinoma cell line) and Beas-2B, (a human bronchial epithelial cell line) by directly inhibiting JMJD2A demethylase activity (Li et al., 2009a). Finally, a mouse model study revealed that a methyl-deficient diet was found to induce malignant transformation in rat liver cells; mainly through an increase in global H3K9me3 in the formed tumours (Pogribny et al., 2007).

H3 Lysine 18 acetylation (H3K18ac), lower global/cellular levels of this acetyl mark were found to predict a higher risk of prostate cancer recurrence and poorer survival probabilities in both lung and kidney cancer groups (Seligson et al., 2009, Lall, 2008). In contrast, in oesophageal cancer, low expression of H3K18ac

correlated with a better prognosis, especially for those with early stage cancer, strengthened by a correlation between tumour differentiation and high H3K18ac levels (Tzao et al., 2008). CBP and p300, the histone acetyltransferases (HATs) are required for H3K18 acetylation (Horwitz et al., 2008, Lall, 2008).

H4 Lysine 16 acetylation (H4K16ac) specifically disrupts the formation of higher-order chromatin structures (Shogren-Knaak et al., 2006). An open chromatin configuration provides accessibility for specific transcription factors and the general transcription machinery (Glozak and Seto, 2007). H4K16ac was found to be lost at the promoters of certain tumour suppressor genes (Kapoor-Vazirani et al., 2008) and has been described as a common feature in human cancer (Pfister et al., 2008). This single histone PTM was found to have a key role in modulating both higher order chromatin structure and functional interactions between non-histone proteins and chromatin fibres (Shogren-Knaak et al., 2006).

H4K16ac is regulated by the histone acetyltransferase human MOF (hMOF) which is required for bulk H4K16 acetylation (Taipale et al., 2005). Knockdown of hMOF in HeLa and HepG2 cells caused a dramatic reduction of histone H4K16ac. In addition, hMOF has a role in DNA damage response during cell cycle progression. In HeLa cells, this reduction in hMOF levels by RNA interference resulted in an accumulation of cells in the G2 and M phases (Taipale et al., 2005). Moreover, down-regulation of hMOF results in decreased H4K16ac at the TMS1 gene loci (a tumour suppressor), a loss of nucleosomes positioning, and gene silencing. Interestingly, the induced gene silencing was independent of

histone methylation or DNA methylation and was reversed on hMOF re-expression (Kapoor-Vazirani et al., 2008).

Pfister *et al.*, (2008) examined the involvement of both H4K16ac and hMOF expression in breast cancer (n=100) and medulloblastomas (n=102) samples. mRNA expression profiling revealed down regulation of hMOF by 40% (breast cancer) and 11% (medulloblastoma). In addition, in a larger series of primary breast carcinomas (n=298) and primary medulloblastomas (n=180), immunohisto-chemistry (IHC) staining revealed low detection levels of both marks in both types of cancer compared to control non-malignant tissues (Pfister et al., 2008). In addition, hMOF protein expression was tightly correlated with acetylation of H4K16 in all tested samples (Pfister et al., 2008).

H4 Lysine 20 trimethylation (H4K20me3) dysregulation has been described in brain, breast and lung cancer (Liu et al., 2010, Elsheikh et al., 2009, Van Den Broeck et al., 2008). Loss of H4K20me3 has been found to play a crucial role in tumourgenesis of non-small cell lung carcinoma (Van Den Broeck et al., 2008). Cancer cells were found to display an aberrant pattern of histone H4 modifications, i.e. H4K16 hypo-acetylation and loss of H4K20me3 in comparison to normal lung tissue (Van Den Broeck et al., 2008). Methylation of H4 lysine 20 has been described in the DNA damage response in both yeast (Sanders et al., 2004) and Drosophila (Sakaguchi and Steward, 2007), especially in functional interaction with H4K16ac (Hsiao and Mizzen, 2010). The HMT SUV420H1 was found responsible for trimethylation of histone 4 at lysine 20 (Pannetier et al., 2008); Loss of H4K20 trimethylation in lung and breast cancer has been found

associated with a decrease in SUV420H2 expression (Van Den Broeck et al., 2008, Tryndyak et al., 2006). Using a mouse model of multistage skin carcinogenesis, Fraga *et al.*, (2005) reported loss of both H4K16ac and H4K20me3 during early stages of the tumourigenic process, in association with hypomethylation of DNA repetitive sequences, a well-known characteristic of cancer cells. This suggested that global loss of both monoacetylation and trimethylation of histone H4 is a common hallmark of human tumour cells.

H3K9me3, H4K20me3 and their Modulators, trimethylation of H3K9 is catalysed by the enzyme SUV39H1, (Bhaumik et al., 2007) the human homologue of the dominant Drosophila modifier of position-effect-variegation (PEV) Su (var) 3-9; (Aagaard et al., 1999). SUV39H1 co-localizes with methyl-lysine binding protein HP1, suggesting a regulatory role for SUV39H1 in higher order chromatin organisation (Aagaard et al., 2000). The SUV39H1-induced H3K9 trimethylation is associated with the repressed state of chromatin (O'Carroll et al., 2000, Rea et al., 2000, Bhaumik et al., 2007, Bannister et al., 2001). In addition to the involvement of SUV39H1-HP1 complex in heterochromatic gene silencing, it was also described in relation to Retinoblastoma protein (RB) repressive function at euchromatic genes *in vivo* (Nielsen et al., 2001). Modulation of heterochromatin formation has been proved to alter gene activity through stabilizing transcriptional "on" or "off" states. For example, in a mouse model study, over expression of SUV39H1 has been found to be associated with embryonic mice growth retardation (Czvitkovich et al., 2001).

The levels of H3K9me3 *in vivo* are indirectly regulated by the NAD-dependent acetyltransferase SIRT1. It has been reported that acetylation of SUV39H1 at K266 results in lower MTase activity of the enzyme. Reversal of this modification by SIRT1 stimulates SUV39H1 methyltransferase activity. Consistent with this, loss of SIRT1 greatly affects SUV39H1-dependent trimethylation of H3K9 and impairs localization with heterochromatin protein 1 (Vaquero et al., 2007). Moreover, Deleted in Breast Cancer 1 (DBC1), a negative regulator for SIRT1 (Kim et al., 2008) was found to inhibit SUV39H1 activity as well by disrupting the SUV39H1-SIRT1 protein complex (Li et al., 2009d).

Schotta *et al* (2004) reported that H3K9 trimethylation by SUV39H1 plays a critical role in the subsequent induction of H4-K20 trimethylation, although the H4 Lys 20 position is not an intrinsic substrate for SUV39H1. Like SUV39H1, both SUV420H1 and SUV420H2 can interact with HP1, suggesting the existence of a sequential mechanism to establish H3-K9 and H4-K20 trimethylation at pericentric heterochromatin (Schotta et al., 2004).

Crosstalk and Synergy between Histone PTMs, a profile for Active and Repressed Genes

While efforts are still underway to understand the functions of single histone PTMs, the histone code hypothesis predicts that histone PTMs act combinatorially to signal to chromatin regulators. Recent examples from the literature and unpublished data from our laboratory indicate that some chromatin binding proteins contain multiple modules such as chromo, bromo and PHD domains that

recognise multiple histone PTMs simultaneously (Ruthenburg et al., 2011, Deeves et al., unpublished). These combinatorial signals control nuclear processes such as transcription (Daujat et al., 2002), DNA damage response (van Attikum and Gasser, 2009) and transcriptional elongation (Zippo et al., 2009). Specifically, a study of TMS1/ASC, the pro-apoptotic gene that undergoes epigenetic silencing in human cancers revealed that, in active state of the TMS1 gene, the CpG island is marked by histone H4K16ac and H3K4 methylation. Conversely, silencing of this gene was accompanied by CpG loss of H4K16ac, H3K4 hypomethylation, and hypermethylation of H3K9. In addition, a single peak of histone H4K20me3 was observed near the transcription start site (Kapoor-Vazirani et al., 2008). Clearly, crosstalk and synergy between PTMs is therefore an important aspect of functional signalling in chromatin. Thus, it will be necessary to investigate the occurrence of multiple histone PTMs to discover new and informative cancer biomarkers.

1.2.9 Histone Variants in Cancer

Histone variants have evolved to perform different functions in the genome, such as chromosome segregation, DNA repair and gene regulation. Thus it is of interest to know whether global levels of histone variants were altered in breast tumours. In this study we investigated the expression of two variants of histone H2A, whose functions are outlined here.

Macro H2A (mH2A)

mH2A a member of the histone variant family (Abbott et al., 2004), which was first described in rat liver nucleosomes is nearly three times the size of conventional H2A histone. Although mH2A closely resembles the full length histone H2A, it contains a large C-terminal addition that is not conserved in other histone variants. The N-terminal region is 64 percent identical to full-length H2A (Pehrson and Fried, 1992). Two subtypes of macroH2A (macroH2A1.1 and macroH2A1.2) were described, which are likely to have distinct roles in chromatin structure and function (Pehrson et al., 1997).

mH2A has been described to be involved in a number of cellular functions. For example, nucleosome remodelling in repressed heterochromatin (Angelov et al., 2003) and in the inactive X chromosome study, where it was found preferentially (Costanzi and Pehrson, 1998). In addition, mH2A is also involved in transcriptional repression by interfering with the binding of the transcription factor NF-kappaB (Angelov et al., 2003), repression of p300- and Gal4-VP16-dependent polymerase II transcription (Doyen et al., 2006). Consistent with this, it was shown to be enriched at inactive genes as revealed in an immunopurification study; where mH2A.1 was found to be confined to the promoters of inactive genes in a complex containing PARP-1. mH2A.1 binding to PARP-1 inactivates its enzymatic activity and interferes with transcription (Ouararhni et al., 2006). mH2A.1 also has a role in heterochromatin formation; it consistently colocalizes with the heterochromatin markers (H3K27me2 and H3K27me3); while, mH2A2 colocalizes with the euchromatin marker, H3K4me3

(Araya et al., 2010). Thus the mH2A variant appears to function principally to suppress gene expression.

With regard to a potential role for mH2A in tumours, a study of mH2A function in a melanoma cell line revealed a favourable role for mH2A in controlling malignant melanoma tumour progression. Knockdown of mH2A in melanoma cells of low malignancy results in significantly increased proliferation and migration *in vitro* and enhanced growth and metastasis *in vivo* (Kapoor et al., 2010). Interestingly, mH2A binding to chromatin is not affected by the acetylation of the other core histones (Abbott et al., 2004).

Histone Variant H2A.Z

H2A.Z is another variant of the core histone H2A and represents 10% of the total H2A in the cells (Redon et al., 2002). In humans H2A.Z is incorporated into nucleosomes by Snf-2-related CREB-binding protein activator protein (SRCAP) and p400/TIP60 complexes (Gevry et al., 2007, Svetelis et al., 2009a); which catalyse nucleosome sliding and help ATP-dependent exchange of histone H2A/H2B dimers containing H2A.Z into nucleosomes (Cai et al., 2006). H2A.Z was found to contribute to biophysical property changes in the nucleosomes; for example, H2A.Z containing nucleosomes exhibited higher mobility and weaker correlations between internal motions compared to the respective canonical H2B and H2A containing nucleosome (Placek et al., 2005).

H2A.Z has a pleiotropic action and, most interestingly, has been proposed as an epigenetic marker for memory for repressed previously-active genes (Brickner et al., 2007). Other functions have also been suggested, such as a requirement for H2A.Z in heterochromatin integrity (Rangasamy et al., 2003), a guard against heterochromatin propagation (Shia et al., 2006), and roles in DNA damage repair (Ahmed et al., 2007, Gevry et al., 2007), chromosome segregation (Dhillon et al., 2006, Altaf et al., 2009), nucleosome stability (Jin and Felsenfeld, 2007) and for transcription factor recruitment (Fu et al., 2008, Draker and Cheung, 2009, Lemieux et al., 2008).

Importantly, H2A.Z is subjected to post translational modifications (PTMs) which appear to correlate with gene activity (Thambirajah et al., 2009). Acetylation of H2A.Z is linked to genome-wide gene activity in yeast (Millar et al., 2006), chicken (Bruce et al., 2005) and mammalian cells (Chen et al., 2006). In yeast, H2A.Zac is deacetylated by Sir2 prior to degradation via a ubiquitin/proteasome-dependent pathway (Chen et al., 2006, Seligson et al., 2009). In human cells, H2A.Z is incorporated into nucleosomes as an H2A.Z/H2B dimer by the SRCAP and p400/TIP60 complexes (Svtelis et al., 2009a). A study on SRCAP remodelling complexes revealed its role as a co-activator for a number of transcription factors (Svtelis et al., 2009a) as a result of its ability to promote incorporation of H2A.Z into chromatin (Ruhl et al., 2006).

In yeast, H2A.Z was correlated with global gene activation as it was found in nucleosomes located within two thirds of active gene promoters (Guillemette and Gaudreau, 2006). In addition, it configures chromatin structure to poise genes

for transcriptional activation (Guillemette et al., 2005). Interestingly, a synergistic combination between H2A.Z and H4K16ac has been described at active gene loci (Shia et al., 2006). Particularly, H4K16ac was found to be necessary for H2A.Z incorporation near telomeres; synergistic attendance of both H2A.Z and H4K16ac was found to be essential for preventing the ectopic propagation of heterochromatin (Shia et al., 2006). H2A.Z and H4 mutants which cannot be acetylated were incompatible with life (Babiarz et al., 2006), which demonstrates how essential H2A.Z and H4K16 acetylation are for living organisms.

H2A.Z has also been shown to prevent the spreading of silent chromatin into proximal euchromatin telomeres (Rong, 2008). In addition, a close relationship between H2A.Z and H3K9me3 has been described during heterochromatin formation in vertebrate (Bulynko et al., 2006) and mammalian cells (Greaves et al., 2007). Consistently, in the metazoan genome, the affinity of HP1 binding to nucleosomal arrays was increased by 2-fold when H2A was replaced with H2A.Z (Fan et al., 2007). Together, H2A.Z maintains heterochromatin formation and gene silencing through promoting H3K9me3 and its modulators.

H2A.Z also has a role in transcriptional regulation, as it was found in association with functional gene regulatory elements (Barski et al., 2007, Gevry et al., 2007). H2A.Z was also found in association with active p53 during apoptosis in mammalian balstocysts (Rodriguez et al., 2007), which emphasises its role in gene transcription. In addition, studying H2A.Z in nucleosome core particles (NCPs) revealed a role in contributing to different biophysical properties of

nucleosomes (Placek et al., 2005) that regulate promoters and enhance transcription of genes (Jin and Felsenfeld, 2007).

H2A.Z has also been proposed to have a function in the DNA damage response. In yeast, H2A.Z was released from the p21 promoter upon DNA damage, followed by recruitment of TIP60 (see below) to activate p21 transcription (Gevry et al., 2007). It is worth mentioning that both H2A.Z and TIP60 were recruited to DNA double strand break sites (DSP) (Kawashima et al., 2007, Kalocsay et al., 2009).

H2A.Z undergoes dynamic redistribution at gene promoters which has been found to be necessary for cell fate transitions (Creyghton et al., 2008). H2A.Z has also been described as a critical element in cellular differentiation in human hematopoietic stem cells (Creyghton et al., 2008) and marine invertebrates cells (Arenas-Mena et al., 2007).

As mentioned above, H2A.Z is subjected to post translational modifications including acetylation. In chickens, ChIP-Seq studies revealed that a triacetylated form of H2A.Z is enriched at the 5' end of active genes, while the non-acetylated form was absent from both active and inactive genes during interphase. Conversely, at mitosis H2A.Z acetylation was erased, the non-acetylated form was predominant (Bruce et al., 2005). In yeast, acetylation of H2A.Z at lysine 14 was linked to genome-wide gene activity (Millar et al., 2006), consistent with the hypothesis that the acetylated form marks active genes (Bruce et al., 2005). In mammalian cells, deacetylation of H2A.Z is catalysed by SIRT1,

and in yeast this is achieved by Sir2 (the yeast homologue of SIRT1). Sir2 deacetylates H2A.Z at lysines (K) 4, 7, 11, 13, 15, 115 and 121 (Chen et al., 2006, Dryhurst et al., 2004). Interestingly, the acetylation status of H2A.Z regulates its turnover by the proteasome. H2A.Z deacetylation at K115 and K121 promotes its degradation via the ubiquitin/proteasome-dependent pathway (Chen et al., 2006, Seligson et al., 2009). Consistent with this, yeast genetic studies identified a role for H2A.Z in preventing Sir-dependent gene repression (Venkatasubrahmanyam et al., 2007), revealing a feedback control between H2A.Z acetylation and SIRT1. However, H2A.Z alone is not sufficient to establish an active chromatin structure (Arimbasseri and Bhargava, 2008); rather it acts as a chromatin based transcriptional memory mark for recently repressed genes to keep these localised to the nuclear periphery to promote their rapid reactivation (Brickner et al., 2007, Brickner, 2009).

A recent study has demonstrated that both histone PTMs and DNA sequences influence H2A.Z occupancy in nucleosomes, indicating that both genetic and epigenetic signals regulate H2A.Z targeting to distinct chromatin loci (Gervais and Gaudreau, 2009). For example, H3 and H4 acetylation status promotes H2A.Z deposition in yeast (Raisner et al., 2005). In addition, in human primary hematopoietic stem cells (HSCs), increased levels of H2A.Z were noted at the promoter of some genes in association with specific histone modifications during cellular differentiation (Cui et al., 2009).

1.2.10 Tumour Suppressor p53: Post Translational Modifications (PTMs) and its Role in Cancer

The transcription factor p53 is referred to as the “guardian of the genome”, and functions as a tumour suppressor protein protecting cells against a range of physiological stresses, including oncogene activation, radiation, mitotic stress, ribosomal stress and chemical insults (Lane, 1992). Upon cellular stress, p53 is activated, and undergoes a complex set of nuclear interactions to regulate the transcription of a variety of genes involved in growth arrest, repair, apoptosis, senescence or altered metabolism (Vousden and Lane, 2007). p53 has an additional cytoplasmic role in controlling cell cycle and apoptosis, through its interaction with mitochondrial associated proteins like Bcl-2 and Bax (Galluzzi et al., 2008). Because of its involvement in a wide range of cellular events, loss of p53 expression or functional abnormalities have been linked to human cancer (Goh et al.). For example, the p53 gene is mutated in 50% of human tumours (Oren, 1999), making it the most susceptible gene for alterations. However, it is likely that all cancers harbour mutations that result in aberrant p53 function.

p53 is subjected to numerous post translational modifications as shown in Figure 1.7, including phosphorylation, ubiquitination, acetylation, methylation and sumoylation (Meek and Anderson, 2009). Phosphorylation of p53 at Serine (S) and threonine (T) sites occurs within the N-terminal transactivation domain and the C-terminal regulatory domain (Dai and Gu, 2010). Following cellular stress, p53 is phosphorylated by several kinases like ATM, ATR, ChK1/2, such phosphorylation of p53 leads to stabilization of the p53 tetramer and enhanced

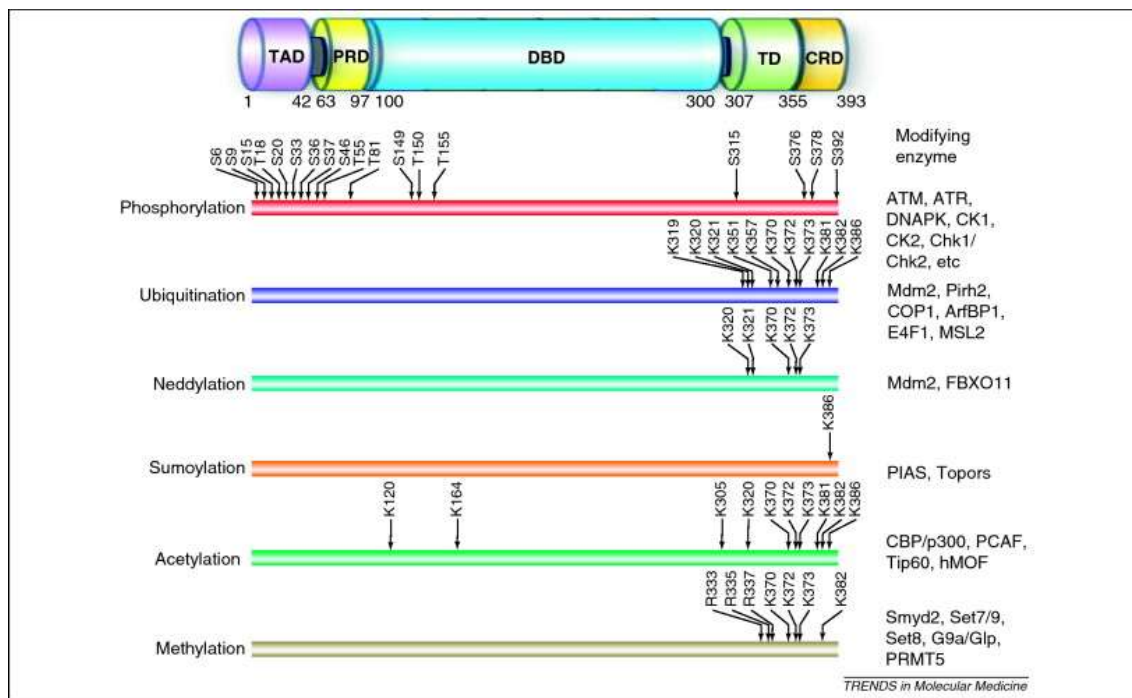
DNA binding and activity (Kruse and Gu, 2009). Phosphorylation at specific sites has been linked to specific p53 function; for example, p53 phosphorylation at S46 is critical for p53 mediated induction of pro-apoptotic genes (Taira et al., 2007) and phosphorylation at S392 is required for p53 stabilization (Matsumoto et al., 2006).

Ubiquitination which denotes the covalent conjugation of one or more ubiquitin molecules to a protein substrate requires the consecutive function of three enzymes: an E1 ubiquitin-activating enzyme, an E2 ubiquitin-conjugating enzyme and an E3 ubiquitin-ligating enzyme. The ubiquitination of p53 plays a key role in its cytoplasmic translocation (Lee and Gu, 2009) and is essential for p53 proteasomal degradation (Marine and Lozano, 2010).

p53 is also subjected to methylation at arginine and lysine residues by PRMT5 and several lysine methyltransferases (e.g. SET7/9), respectively (Sims and Reinberg, 2008). Interestingly, these modifications can alter the specificity of p53 for its target genes (Jansson et al., 2008, Chuikov et al., 2004). p53 methylation can be either activating or repressing depending on the site of methylation (Dai and Gu, 2010, Shi et al., 2007, Huang et al., 2006); and the number of covalent post translational modifications at the same site (Dai and Gu, 2010, Huang et al., 2007). Recently, it has been reported that p53-binding protein 1 (53BP1) accumulation at DSBs requires H4K20 methylation by the histone methyltransferase MMSET in a process involving γ H2A.X DNA damage response pathway (Pei et al., 2011), suggesting a functional link between p53 and histone methylation.

Acetylation of p53 is generally associated with increased transcriptional activity of p53. Acetylation enhances p53 stability by competing with ubiquitination and inhibiting the formation of MDM2/MDM4 repressive complexes on target gene promoters. In addition, it enhances p53 transcription activity by stimulating cofactor recruitment (Dai and Gu, 2010).

Nine acetylation sites in p53 have been described, six lysine residues in the C-terminal regulatory domain (K370, K373, K381, K382 and K386) are acetylated by CBP/p300, one in the tetramerization domain (K320) acetylated by PCAF and two in the DNA binding domain (K120, K164) which appear to be targeted by MYST family acetyltransferases and CBP/p300, respectively (Meek and Anderson, 2009). Acetylation at the C-terminal domain has been shown to enhance p53 binding to DNA sequences and promote p53 transcriptional activity and stability (Feng et al., 2005, Kruse and Gu, 2009). Acetylation of p53 at K320 by PCAF is linked to p53-related cell cycle arrest via enhanced transcription of the p21 gene (Knights et al., 2006a). Acetylation of the K120 residue, which is located in the DNA binding domain is induced by TIP60 and hMOF and found crucial for p53-dependent apoptosis (Tang et al., 2006a, Li et al., 2009c, Sykes et al., 2006), whereas acetylation of K164 by CBP/p300 (Tang et al., 2008) has been described as a critical step for p53-dependent transcription of apoptosis related genes (Xu et al., 2009b).

Figure 1.7: p53 PTMs.

Overview of p53 domain structure, sites for covalent PTMs and the enzymes responsible for each modification are shown on the right side. TAD, transactivation domain; PRD, proline rich domain; DBD, DNA-binding domain; TD, tetramerization domain; CRD, C-terminal regulatory domain. Reproduced with permission from the copyright holder (Elsevier).

Involvement of PTMs in p53 activation

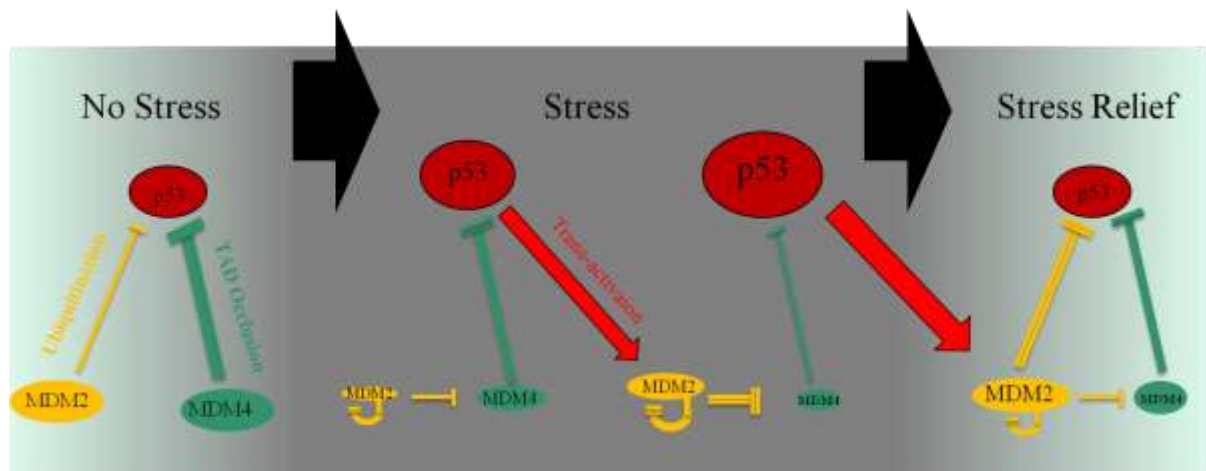
Cellular exposure to stress signals leads to marked elevation in p53 protein within a relatively short time. The rapid p53 elevation is achieved by enhanced translation of p53 mRNA, (Oren, 1999). Interestingly, p53 is a very labile protein whose half-life in some cells is measured in minutes (Rogel et al., 1985). Upon cellular stress, acetylation of p53 causes an accumulation of p53 and an increase in the protein half-life (Feng et al., 2005, Kruse and Gu, 2009). p53 activation enhances its gene specific, transcriptional activity, which relies on its ability to bind defined sequence elements within target genes (Oren, 1999). Once the cellular stress ceases, inhibition of p53 synthesis takes place through p53 binding to its own mRNA and p53 binding activity is also negatively regulated (Oren, 1999).

p53-Mdm2-MdM4 Loop

Mdm2 inhibits p53 function, in a negative feedback loop mechanism (Chen et al., 1994). Upon cellular stress, p53 binds specifically to the Mdm2 gene and stimulates Mdm2 transcription (Oren, 1999). Mdm2 protein binds p53, represses its transcriptional activity and enhances p53 export into the cytoplasm prior to complete elimination through proteolytic degradation (Oren, 1999, Alarcon-Vargas and Ronai, 2002). Interestingly, Mdm2 also possesses a self-ubiquitination property, upon cellular stress, Mdm2 is subjected to self-ubiquitination and degradation (Alarcon-Vargas and Ronai, 2002).

In mice, inactivation of the Mdm2 gene resulted in early embryonal lethality, which is reversed by simultaneous inactivation of p53 (Grier et al., 2006). Mdm2 is amplified in approximately 7% of human cancers (Alarcon-Vargas and Ronai, 2002); high expression levels of Mdm2 in tumours led to inhibition of p53 and thereby promoted cancer formation without a need for p53 gene alteration (Oren, 1999). In a cell line model, blocking the binding sites of p53 by monoclonal antibodies or competitor peptides results in a dramatic stabilization and accumulation of p53 in non-stressed cells (Oren, 1999). Notably, PTMs of p53 were found to remarkably oppose the Mdm2-induced inhibitory effects on p53. Upon cellular stress, phosphorylation and acetylation of p53 were reported to abolish Mdm2 association with p53 (Alarcon-Vargas and Ronai, 2002, Feng et al., 2005, Kruse and Gu, 2009).

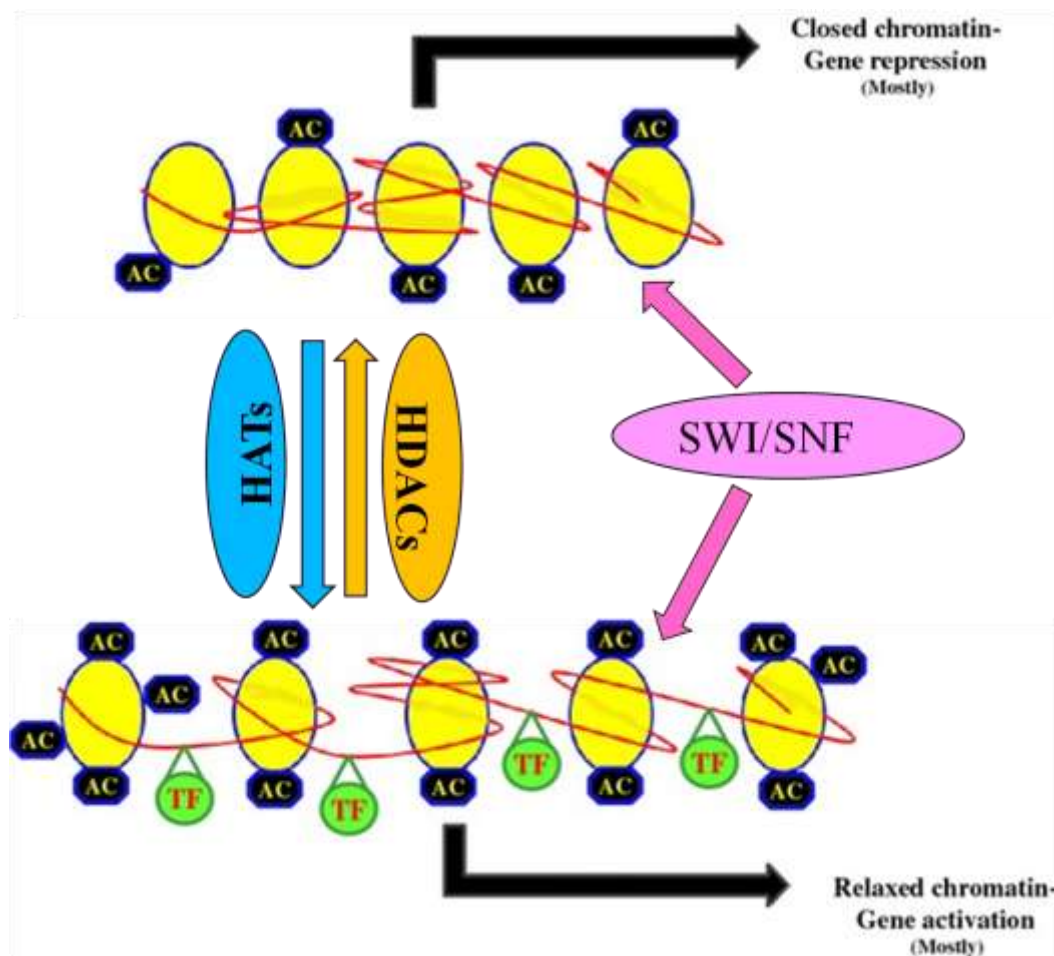
Toledo (2007) has described a mechanism (Fig. 1.8) for p53 regulation that involves p53, Mdm2 and MdM4. Under normal conditions in unstressed cells, p53 protein is kept at low levels as a consequence of Mdm2-mediated degradation and MdM4-mediated p53 transactivation domain (TAD) inactivation. During cellular stress, Mdm2 degrading activity is shifted to itself and MdM4, leading to depletion of both Mdm2 and MdM4 proteins, this builds up p53 protein levels and activity, resulting in enhanced p53 transcriptional activity. As soon as the cellular stress is relieved p53 returns to the basal pre-stress level (Toledo and Wahl, 2007).

Figure 1.8: Mdm2, MdM4 and p53 Regulatory Loop.

Schematic representation of p53, Mdm2 and MdM4 relationship. Under normal condition p53 protein is in low levels under the control of Mdm2 and MdM4. Upon cellular stress, Mdm2 activity is shifted to MdM4 and itself, leading to depletion of both Mdm2 and MdM4 proteins that build up p53 protein levels and activity. This leads to an increase in p53 transcription and enhancement of its activity (including Mdm2 transcription). As soon as cellular stress is relieved p53 levels returns to the basal pre-stress level. Adapted from Toledo (2007).

1.2.11 Histone Acetyltransferases (HATs)

HAT enzymes transfer acetyl groups from acetyl coenzyme A (acetyl-CoA) onto the ε -amino group of lysine (K) residues on histones. This neutralizes their net positive charge and diminishes their ability to bind to negatively charged DNA. This helps to maintain a more opened chromatin configuration, providing accessibility for specific transcription factors and the general transcription machinery (Glozak and Seto, 2007).

Figure 1.9: Histone Acetylation Status of Chromatin

Schematic representation of the potential interplay between SWI/SNF, HATs, and HDACs in relationship to chromatin assembly, histone acetylation and transcriptional regulation. HATs induce relaxed chromatin which facilitates transcriptional factors (TF) access to chromatin. HDACs abrogate acetylation (AC) and render chromatin unfavourable for TF. SWI/SNF ensures continuous oscillation of nucleosomes between a functional and disrupted structure. HATs target the disrupted nucleosome; fix the nucleosome in an inactive conformation favourable for TF. Conversely, recruitment of HDACs removes the AC, which subsequently is assembled back to functional nucleosomes by SWI/SNF. Where

yellow circle, histone protein; red thread, DNA; AC, acetylation; TF, transcription factors.

Histone Acetyltransferase families

A number of HAT families have been described including the GNAT superfamily (such as GCN-5, PCAF), MYST (such as MOZ, MOF, MORF, TIP60, Hbo1), p300/CBP, the basal transcription factor TFIIIC etc (Heery and Fischer, 2007, Roth et al., 2001). To date, numerous links between HAT deregulation and cancer have been reported. In the next part, I will discuss a number of well characterised HATs which display altered activity in cancer.

CBP and p300 are large multidomain proteins that interact with a wide range of nuclear proteins. Knockout studies have shown that they have distinct functions in haematopoiesis in mice (Kasper et al., 2002). CBP and p300 show a high degree of conservation and contain a large central HAT domain (Liu et al., 2008). This domain can target all four core histones and many non histone proteins including p53 as described previously above. Reciprocal translocations involving the CBP and p300 genes are associated with haematopoietic malignancies. This includes the MOZ-CBP fusion protein, which causes acute myeloid leukaemia (Troke et al., 2006). Similarly, missense mutation and loss of heterozygosity at the p300 gene locus have been reported in colorectal and breast cancer (Giles et al., 1998, Gayther et al., 2000). Mutations in the gene encoding CBP that inactivates its HAT activity results in ‘Rubinstein-Taybi syndrome’ (RTS), a developmental disorder characterised by mental retardation and facial anomalies (Roelfsema and Peters, 2007). Patients suffering from this syndrome

have a >300 fold increased risk of cancer (Iyer et al., 2004). Simultaneous mutations of CBP and p300 have been reported in colorectal, gastric, hepatocellular and breast cancers (Iyer et al., 2004). Thus these HATs have a clear role in maintaining cancerous growth of mammalian cells. Interestingly, small molecule inhibitors that block the HAT function of CBP/p300 (HATi) have been described (Balasubramanyam et al., 2003, Eliseeva et al., 2007).

TIP60 (Tat interactive protein, 60 kDa) the first member described in the MYST family was originally identified as a protein interacting with the HIV tat gene product (Kamine et al., 1996). It was reported in association with the yeast and mammalian NuA4 subunits coactivator complex (Doyon et al., 2004). A broad range of functions has been described for TIP60 in both yeast and human cells (Doyon et al., 2004, Roth et al., 2001, Thomas and Voss, 2007). Early studies showed that TIP60 is a transcriptional co-activator (Cao and Sudhof, 2001, Hattori et al., 2008). Importantly, it has a key role in DNA damage response (Sun et al., 2011, Squatrito et al., 2006, Sun et al., 2005, Jha et al., 2008), and repair of DNA double strand breaks (DSBs) (Murr et al., 2006, Stante et al., 2009, Kusch et al., 2004). Interestingly, at DSBs sites, TIP60 was reported to bind to H3K9me3 (Fischle, 2009); triggering histone acetylation (Xu and Price, 2011) and activating DNA DSBs repair (Fischle, 2009). TIP60 also has a critical role in apoptosis (Ikura et al., 2000, Tyteca et al., 2006, Xu et al., 2009a, Tang et al., 2006a). It enhances p53 dependent expression of apoptosis-related genes such as BAX (Xu et al., 2009a), through acetylation of p53 within the DNA-binding domain at lysine 120 (Tang et al., 2006a). In addition, TIP60 has an important role in androgen receptor (AR) signalling. AR acetylation was reported by p300, PCAF

and TIP60 *in vivo* (Fu et al., 2004). This was found to promote AR transcriptional activity and enhance prostate cancer progression (Halkidou et al., 2003, Lavery and Bevan, 2011).

hMOF (Human Male absent On the First) is another member of the MYST family (Thomas and Voss, 2007). It was first described in Drosophila where it was reported to enhance the transcription of X-linked genes in males through H4K16 acetylation; its loss of function was related to male-specific lethality (Hilfiker et al., 1997a, Akhtar and Becker, 2000). In contrast, in human cells, the inactive X chromosome is hypoacetylated at H4K16 (Jeppesen and Turner, 1993). Knock down of hMOF in HeLa and HepG2 cells caused a dramatic reduction of H4K16ac (Taipale et al., 2005). hMOF has a role in DNA damage response; in HeLa cells, knocking down of hMOF by RNA interference led to an accumulation of cells in the G2 and M phases of the cell cycle (Taipale et al., 2005). Low levels of hMOF were additional characteristic of aggressive breast cancer and medulloblastomas tumours; correlated with poor overall survival (Giangaspero et al., 2006, Pfister et al., 2008).

MOZ (monocytic leukemia zinc-finger) and its paralog MORF (MOZ related factor) proteins are also members in MYST family (Yang and Ullah, 2007a). Both proteins have intrinsic histone acetyltransferase activity and are important for proper development of murine hematopoietic and bone/neurogenic progenitors, respectively (Yang and Ullah, 2007b). MOZ was first described in acute myeloid leukemia as a protein lacking the carboxy-terminal domains fused with CBP, as a result of an in-frame fusion of the MOZ and the CBP gene (Borrow et al., 1996). Moreover, in our lab, we found that MOZ-TIF2 fusion

protein has an inhibitory effect on p53 transcriptional activity, mainly through a CBP-dependent pathway (Kindle et al., 2005). MORF gene mutations were also observed in acute myeloid leukemia and/or benign uterine leiomyomata (Yang and Ullah, 2007a). MOZ/MORF complexes are crucial for acetylation of chromatin substrates *in vivo* and essential for DNA replication to occur during S phase (Doyon et al., 2006). Although the MYST domains of MOZ and MORF target H4 for acetylation, knockout studies reveal the ablation of MOZ results in reduction of H3K9/K14 acetylation (Voss et al., 2009). Thus, the substrate specificity of the *in vivo* complexes containing MOZ and MORF are likely to be different to the isolated MYST domain.

HATs acetylates other proteins

In addition to histones, other nuclear proteins also serve as targets for the lysine acetyltransferases described above including many transcription factors such as p53, β -catenin, GATA and HMGI(Y) (Kruse and Gu, 2009, Wolf et al., 2002, Sterner and Berger, 2000). This can have profound effects on the stability, subcellular localisation, DNA binding or cofactor binding properties of these proteins. For example, acetylation of p53 (as described previously in section 1.2.10) at specific lysines can alter its DNA binding or transactivation functions of this protein, and thus affects p53-dependent cell-cycle arrest and apoptosis.

1.2.12 HATs Inhibitors

HAT enzymes have important roles in the function of normal cells; however they are also clearly important in the growth of tumours. Thus there has been considerable interest in the development of small molecule inhibitors of these enzymes as possible leads for therapeutic intervention. A number of compounds

showing HAT inhibitor activity have been isolated from natural sources, small molecule screens or by chemical synthesis (Heery and Fischer, 2007). These include lysyl-CoA, H3-CoA, γ -butyrolactones, isothiazolones, Spd-CoA, anacardic acid, curcumin, CTK7A, C646, garcinol, plumbagin, EGCG, and gallic acid (Selvi et al., 2010). While lysyl-CoA and similar compounds are thought to act as competitive inhibitors which compete with Acetyl-CoA for the active site, most of the other compounds are likely to be non-competitive inhibitors that act allosterically. In the next section, I focus on two natural compounds used in this study, curcumin and garcinol.

Curcumin (Diferuloylmethane) is a polyphenol, first isolated in 1815 and crystallized in 1870 (Ravindran et al., 2009). It is the major yellow pigment extracted from turmeric, an ingredient used in curries. It is derived from the *Curcuma longa* Linn (a perennial herb originally cultivated in tropical regions of Asia) from which the rhizome is selected and dried to obtain the turmeric (Ammon and Wahl, 1991, Somasundaram et al., 2002).

Curcumin is used as a constituent of many foods, for its colour and flavouring properties (Lin et al., 2000). For generations, extracts from curcumin have been used in India and Southeast in herbal medicines; according to tradition, in the treatment of inflammation, skin wounds, hepatic and biliary disorders, cough, and coryza, as well as certain tumours. Interestingly, the incidence of most cancers is low in parts of the world where the dietary intake of curcumin is high (Ravindran et al., 2009); the consumption of an adult may reach up to ≥ 200 mg of curcumin/day (7.8 $\mu\text{mol/kg}$ of body weight) (Commandeur and Vermeulen,

1996). In the western world (depending on diet) only half of this amount was detected in daily intake; for example, in France, an intake of $\geq 3.4 \mu\text{mol/kg/day}$ has been recorded (Verger et al., 1998).

The anticarcinogenic properties of curcumin have been verified through inhibition of tumour initiation and promotion (Ravindran et al., 2009). For example, curcumin was found to cause cell apoptosis through altering cell membrane curvature and increasing cellular permeabilization (Barry et al., 2009, Epand et al., 2002) and, also, to inhibit cell proliferation, invasion, metastasis and angiogenesis (Ravindran et al., 2009).

Curcumin was found to induce growth arrest of several tumour cell lines including colorectal, oesophageal, bladder, pancreatic, ovarian and other cell lines, highlighting a potential chemotherapeutic potential (Chauhan, 2002, O'Sullivan-Coyne et al., 2009, Park et al., 2006, Sahu et al., 2009, Weir et al., 2007). Most tumour cell lines treated with curcumin arrested in G2/M (Dugas-Breit et al., 2005, Kutala et al., 2006, Liu et al., 2007, O'Sullivan-Coyne et al., 2007, Weir et al., 2007, Zheng et al., 2004). However, other cell lines like melanoma, prostatic and mantle cell lymphoma were arrested in G1 (Carneiro et al., 2010, Chen et al., 2008b, Shishodia et al., 2005). With regard to breast cancer cell lines, curcumin treatment opposed tumour cell proliferation of both MCF-7 and MDA-MB-231 cells through down regulation of angiogenic factor transcription, which occur in both ER dependent in independent patterns (Shao et al., 2002). In a mouse model, curcumin was reported to reduce MDA-MB-231

tumour metastasis and subsequent apoptosis (Bachmeier et al., 2007). In MCF-7 cells, Curcumin was found to improve chemotherapeutic outcome with tamoxifen and mitomycin C (De Gasperi et al., 2009, Zhou et al., 2009). Curcumin treatment was also found to elicit p53-dependent apoptosis (Choudhuri et al., 2005). The apoptotic cells were mainly arrested in G2 and showed an increase in p53 expression, correlating with a release of cytochrome C from mitochondria, the essential requirement for apoptosis (Choudhuri et al., 2005).

Curcumin was reported to inhibit histone acetylation by p300 and CBP both *in vitro* and *in vivo* (Balasubramanyam et al., 2004b). Furthermore, it was not active against PCAF at similar concentrations. It is unknown whether curcumin can inhibit the activity of MYST domain proteins. The phenolic nature of the curcumin molecule suggests that it may be very reactive, and thus not very specific (Aggarwal and Harikumar, 2009). Consistent with this curcumin inhibits other enzymatic activities such as kinases (Zhou et al., 2011). Thus the general beneficiary properties of curcumin in targeting rapidly proliferating cells such as cancer cells may be related to inhibition of a range of cellular activities.

Garcinol is a naturally occurring polyisoprenylated benzophenone, isolated from *Garcinia indica* or kokum fruit (indigenous to southern parts of India). Garcinol was reported to be highly cytotoxic to HeLa cells, causing a down regulation of the majority of genes as demonstrated by gene expression microarray analysis (Balasubramanyam et al., 2004a). Interestingly, an inhibitory effect on both PCAF and p300 was illustrated (Balasubramanyam et al., 2003). This inhibition was later reported to occur via a non-competitive allosteric

mechanism (Arif et al., 2007). In order to find more potent, less toxic inhibitors, several garcinol derivatives based on isogarcinol, the product of intramolecular cyclisation of garcinol, were synthesized. Among 50 isogarcinol derivatives, only three have been found highly specific for HAT activity of p300 (Mantelingu et al., 2007b); LTK-13, LTK-14 and LTK-19, which specifically inhibit p300 HAT activity but not PCAF HAT activity (Arif et al., 2009). Recent results from our laboratory indicate that garcinol is also a potent inhibitor of MYST domain proteins (Messmer et al., in preparation). Garcinol and two of its derivatives isogarcinol and LTK14 were kindly provided by Prof. Tapas Kundu for use in this study.

1.2.13 Histone Deacetylases (HDACs)

Shortly, after the identification and cloning of HDACs, it was established that HDACs were recruited to promoters to repress transcription, thereby counteracting the activating effects of HATs (De Ruijter et al., 2003). In a simplified model, recruitment of HDACs causes decreased histone acetylation that (re-compacts) the chromatin and diminishes access by the transcription machinery, thereby transcriptional repression, although the exact mechanisms remain to be established.

Types of HDACs

Histone deacetylases are classified into four groups based on their homology to yeast histone deacetylases (Willis-Martinez et al., 2009) (Table 1.4). **Class I** histone deacetylases: HDAC1, HDAC2, HDAC3 and HDAC8, are homologous to yeast RPD3. **Class IIa** histone deacetylases: HDAC4, HDAC5, HDAC7 and HDAC9. **Class IIb** includes HDAC6 and HDAC10 which share homology with yeast Hda1 (De Ruijter et al., 2003). **Class III:** HDACs are NAD⁺ dependent and commonly referred to as sirtuins (Yang and Seto, 2008). This group comprises SIRT 1-7 which are homologues of yeast Sir2 (Ozdag et al., 2006). HDAC11 (**Class IV**) has only partial homology with I and II classes, so is considered as a separate type (Yang and Seto, 2008). HDACs have been studied extensively due to their important role in cellular function and tumour progression. In the next section I will review those members of HDAC family which were included in my study.

Table 1:4: Classes of Human HDACs

Class	Description	Yeast Homologue
I	HDAC1, HDAC2, HDAC3 and HDAC8	RPD3
IIa	HDAC4, HDAC5, HDAC7, HDAC9	Hda1
IIb:	HDAC6 and HDAC10	Hda1
III	SIRT 1-7	Sir2
IV	HDAC11 (closely related to Class I and II)	

HDAC1/HDAC2

HDAC1 is a class I histone deacetylase (Cai et al., 2000, Willis-Martinez et al., 2009). In a mouse model, knockout of HDAC1 caused hyperacetylation of histones H3 and H4, where loss of function was not compensated by the overexpression of HDAC2 and HDAC3, suggesting they have distinct functions (Lagger et al., 2002). HDAC1 has a critical role in controlling gene transcription and proliferation in embryonic stem cells (Zupkovitz et al., 2006, Lagger et al., 2002) and transcriptional repression in HeLa cells (Hassig et al., 1998). In association with SUV39H1, it has an important role in permanent chromatin silencing in drosophila (Czermin et al., 2001) and controls cellular senescence of melanoma cells (Bandyopadhyay et al., 2007). HDAC1 is essential to development, as gene deletion is seen to result in death in utero and perinatal death in mice (Montgomery et al., 2007).

HDAC2 is also a class I histone deacetylase (Willis-Martinez et al., 2009). It has an important role in controlling acetylation of histones and signalling proteins that control transcription (Okazaki et al., 2000, Ashburner et al., 2001, Kramer, 2009) including steroid hormone receptors (Bicaku et al., 2008). Knockdown of HDAC2 resulted in congenital cardiac abnormalities and neonatal death in a mouse model (Montgomery et al., 2007, Zimmermann et al., 2007), which suggested a critical role in embryonic development. However, HDAC2 seems not to be essential for life, as HDAC2-mutant mice exhibit low birth weight but survive into adulthood (Zimmermann et al., 2007).

In relation to the transcription factor p53, over expression of HDAC1 in melanoma cells was found to impair p53-dependent apoptosis (Bandyopadhyay et al., 2004). Similarly, HDAC2 was reported to inhibit p53 expression (Kramer, 2009). Moreover, knockdown of HDAC2 was reported to enhance p53 induced cellular senescence (Harms and Chen, 2007). This proposes an important role for both HDAC1 and HDAC2 in regulating tumour cell immortality.

Immunodetection of HDAC1 and HDAC2 in tissue samples revealed an ubiquitous expression in normal glandular cells of gastric and colorectal tissue and the nuclei of stromal and inflammatory cells (Weichert et al., 2008a, Weichert et al., 2008b) as well as the nuclei of normal prostatic and mammary gland tissue (Weichert, 2009). In regards to human tumour tissues, HDAC1 and HDAC2 were found to be highly expressed in haematological, gastric, colorectal and prostatic tumours (Marquard et al., 2008, Weichert et al., 2008a, Weichert et al., 2008b, Weichert et al., 2008c). In addition, high levels of HDAC1 was found in more than half of pancreatic tumours studied (Miyake et al., 2008). Importantly, high levels of HDAC2 were described as an independent poor prognostic marker in oral, prostatic, ovarian, endometrial and gastric cancer (Itoh et al., 2008, Chang et al., 2009, Weichert, 2009).

With regard to breast tissue, HDAC1 was detected in normal luminal but not basal cells. High levels of HDAC1 were noted in 40 % of breast cancer cases (Krusche et al., 2005) and linked to enhanced MCF-7 cells proliferation (Kawai et al., 2003).

1.2.14 HDAC inhibitors and Cancer

A number of natural compounds and chemical derivatives showing inhibitory activity against HDACs have been described. HDAC inhibitors can prevent histone deacetylation resulting in global histone hyperacetylation (Tanyi et al., 1999). Thus, they are considered a promising new class of cancer therapeutic agents. However, little is known about the non-histone targets of HDAC inhibitors and their roles in gene regulation (Hu and Colburn, 2005). Suberoylanilide hydroxamic acid (SAHA) for example, is a potent inhibitor of histone deacetylase that causes growth arrest, differentiation, and/or apoptosis of many tumour types *in vitro* and *in vivo* (Butler et al., 2002), such as HCT116 colon cells (Lobjois et al., 2009). SAHA was also described to improve the anti-tumour immune response of multipotent mesenchymal stromal cells (MSC) (Kruchen et al., 2010) and colon cell lines to 5-fluorouacil (Budillon et al., 2005). With regard to breast cancer, Munster *et al.*, (2001) found that SAHA caused an inhibition of MCF-7 cell proliferation and an accumulation of cells in G1 or G2/M in a dose-dependent manner. Moreover, withdrawal of SAHA led to re-entry of cells into the cell cycle and reversal to a less differentiated phenotype. Other HDACi like trichostatin A (TSA) and valproic (VPA) acid have been used as potential cancer therapeutic agents. Both TSA and valproic acid were reported to inhibit tumour cell proliferation and shift cells into apoptosis in prostatic, neuroblastoma, and leukemia cell models (Fortson et al., 2011, Poljakova et al., 2009, Sasaki et al., 2008). In addition, applying TSA or VPA treatment for H157 human lung cancer cell line cells was reported to sensitise the cells for etoposide mediated cell death (Hajji et al., 2009).

SIRT1

SIRT1 (silent mating-type information regulation 2 homologue 1) is a class III histone deacetylase; it is a mammalian homolog of the *Saccharomyces cerevisiae* chromatin silencing factor Sir2. SIRT1 deacetylates histone and non-histone proteins in a nicotinamide adenine dinucleotide (NAD⁺)-dependent manner (Denu, 2005, Cheng et al., 2003). SIRT1 has a wide range of biological functions including growth regulation, stress response, tumourgenesis, endocrine signalling, and extending cellular lifespan (Kim and Um, 2008, Rahman and Islam, 2011, Wang et al., 2011, Domloge et al., 2005). SIRT1 also has a role in facultative heterochromatin formation (Vaquero et al., 2004, Vaquero et al., 2007), through regulating the histone methyltransferase SUV39H1 (as described in H3k9me3, H4K20me3 and their modulators in section 1.2.8).

One of the main roles of SIRT1 is the deacetylation of H4K16. Cells deficient in SIRT1 were reported to have high H4K16ac levels (Hajji et al., 2009, Vaquero et al., 2006). Although SIRT1 is cytoplasmic during most of the cell cycle, it was reported to shift to the nucleus during the G2/M transition phase with concomitant global attenuation of H4K16 acetylation (Vaquero et al., 2006). Moreover, inhibition of SIRT1 was found to reactivate silenced genes (Pruitt et al., 2006), suggesting an important role for SIRT1 in gene silencing; and a possible therapeutic approach of SIRT1 targeting (Noshio et al., 2009).

SIRT1 also functions to regulate p53. SIRT1 was reported to deacetylate p53, inhibiting its transcriptional activity (Kim et al., 2007) and antagonizing

promyelocytic leukemia protein (PML)/p53-induced cellular senescence and apoptosis (Langley et al., 2002, Han et al., 2008). Knockdown of SIRT1 resulted in hyperacetylation of p53 in mice (Cheng et al., 2003) and induced apoptosis and growth arrest in human epithelial cancer cells (Ford et al., 2005b).

SIRT1 protein has been detected at high levels in cancer cells, such as the prostate cell lines (DU145, LNCaP, 22Rnu1, and PC3) in contrast to normal prostate epithelium (Ford et al., 2005a, Jung-Hynes et al., 2009). Interestingly, knockdown of SIRT1 resulted in apoptosis of epithelial cancer cells, but not the non-cancerous epithelial cells (Ford et al., 2005a). Sirtinol treatment (SIRT1 inhibitor) caused an inhibition of growth and sensitization for camptothecin and cisplatin in human prostate cells (Kojima et al., 2008). With regard to SIRT1 detection in tissues, high levels of SIRT1 were detected in malignant ovarian and prostate tumours compared to normal glandular tissue (Jang et al., 2009, Jung-Hynes et al., 2009). SIRT1 expression also correlated with shorter overall survival in diffuse large B-cell lymphoma (Jang et al., 2008).

SIRT1 expression and activity are controlled by a regulatory network of proteins, that function on multiple levels (Kwon and Ott, 2008). Upon cellular starvation, SIRT1 transcription is induced by p53 (Nemoto et al., 2004). SIRT1 deacetylase activity is enhanced by active regulator of SIRT1 (AROS), a binding partner identified in yeast two-hybrid screens, and potentiates deacetylation of p53 (Kim et al., 2007). In contrast, Deleted in Breast Cancer 1 (DBC1) is a negative regulator for SIRT1 (Kim et al., 2008, Zhao et al., 2008, Anantharaman and Aravind, 2008).

DBC1 (Deleted in Breast Cancer 1)

Deleted in Breast Cancer (DBC1) was first described by Hamaguchi *et al.* (2002) as DBC2, after its ancestor DBC1 (Deleted in Bladder Cancer 1) (Habuchi et al., 1998), as a tumour suppressor gene mapped to 9q32-33 (Habuchi et al., 1998, Nishiyama et al., 1999a, Nishiyama et al., 1999b). DBC1 was identified as a candidate tumour suppressor gene at a homozygous deletion region of human chromosome 8p21 (Hamaguchi et al., 2002). DBC1 function was first attributed to the urokinase-plasminogen pathway (Louhelainen et al., 2006) but was later shown to function through modulation of sirtuin deacetylase activity (Anantharaman and Aravind, 2008). Kim *et al.* (2008) identified DBC1 as a negative regulator, that directly interacted with SIRT1 both *in vivo* and *in vitro* (Kim et al., 2008). In the same year, Zhao *et al.* (2008) also identified DBC1 as a negative regulator for SIRT1 in human cells and they showed DBC1- mediated repression of SIRT1 that leads to increasing levels of p53 acetylation and upregulation of p53-mediated function (Zhao et al., 2008).

DBC1 may acts as a tumour suppressor as it enhances the function of the hyperacetylated p53 and FOXO through inhibiting SIRT1 deacetylase activity (Kim et al., 2008, Zhao et al., 2008). SIRT1 and its modulator DBC1 were targets for study in gastric and breast cancer (Cha et al., 2009, Sung et al., 2010). In 177 gastric cancers tumour tissue microarrays were IHC stained for SIRT1 and DBC1, expression of both SIRT1 and DBC1 was significantly associated with reduced overall survival and shorter relapse-free interval by univariate analysis (Cha et al., 2009).

1.3 Aims of This Thesis

This thesis presents research carried out on two fronts to address molecular mechanisms of histone and p53 modifications in cancer: two related topics

Aim 1 – Histone and p53 PTMs and their modulators in breast cancer

The first aim was to perform immunohistochemical analyses to detect the comparative levels of histone and p53 PTMS in 880 primary breast tumours, and to correlate this with data on expression levels of the enzymes and other regulatory proteins that control the deposition of these signals. The focus of this study centred on acetylation of H4K16, an important histone modification that we and others have shown is perturbed in cancer cells. Due to the role of the H4K16 regulatory pathway in controlling p53 acetylation, the extent of selected p53 modifications in the same tumour set was also determined. These data were then correlated with archived data from the tumour set on other biomarkers, histopathological variables and patient survival data.

AIM 2 -To Manipulate Global Histone and p53 PTMs in tumour cells using HAT inhibitor compounds

The second aim was to assess the effects of small-molecule inhibitors of acetyltransferases on the proliferation and survival of breast cancer cell lines, and to examine whether global levels of histone and p53 PTMs can be manipulated by chemical intervention. We focussed on the natural HATi compounds curcumin and garcinol, as well as garcinol derivatives. This approach included immunofluorescence staining of breast cancer cells lines, colony formation

assays, western blots and cell cycle analyses and assessment of DNA damage responses. This part of the project was designed to provide insight into the effects of HATi compounds on cancer cells and their mechanisms of action.

MATERIALS AND METHODS

2.1 General

All general laboratory chemicals were analytical grade, supplied by Sigma or Fisher Chemical Company Ltd. unless otherwise stated.

2.2 Breast Tumour Tissue

2.2.1 The Tissue Microarrays (TMAs)

A tissue microarray (TMA) comprised consecutive series of 880 cases of primary breast cancer tumours. The tumours belong to patients diagnosed from 1986 to 1998 included in the Nottingham Tenovus Primary Breast Carcinoma Series. The age of the patient ranged from 18 to 73 years (the mean is 55 years). At the time of resection, tumours were incised and immediately placed in formalin to obtain optimum tissue fixation. Conventional Haematoxylin and Eosin (H&E) staining, followed by pathological examination according to national and international standard were done. Data on histological grade, Histological types, tumour size, tumour stage, lymph node stage, NPI, vascular invasion were routinely assessed and recorded in a data base (<http://smrsp2.nottingham.ac.uk/distiller/login.php>).

The histological tumour types of the breast cancer TMA cohort comprised 449 invasive ductal carcinomas/NOS type, 182 tubular mixed carcinomas, 25 medullary carcinomas, 83 lobular carcinomas, 28 tubular carcinomas, 8 mucinous carcinomas, 6 cribriform carcinomas, 4 papillary carcinomas, 29 mixed no special type and lobular carcinomas, 23 mixed no special type and special type carcinomas, and 6 miscellaneous tumours. Clinical, histopathological and biological data for all these anonymised cases were available from a database

managed by Dr. Andrew Green, Nottingham Breast Unit. This study was approved by the Nottingham Research Ethics Committee 2 under the title of “Development of a molecular genetic classification of breast cancer”.

2.2.2 Construction of the Tissue Microarray Blocks

Tissue microarray slides prepared from paraffin-embedded blocks were provided by Dr. Des Powe and Dr. Abd El-Rehim as previously described (Rakha et al., 2006, Abd El-Rehim et al., 2004a, Abd El-Rehim et al., 2004b). The TMAs were constructed by sampling a representative site from each breast cancer tumour. Each TMA block is formed of 150 cores derived from 150 invasive breast cancer block. The orientation of the cores within the array is crucial for the proper evaluation of the experiment. The design and orientation of each breast cancer TMA are also listed in the data base. A manually-operated tissue puncher/Array (Beecher Instrument, Silver Spring, MD, USA) was used for TMA construction (Kononen et al., 1998, Camp et al., 2000, Rimm, 2001).

2.2.3 Immunohistochemistry (IHC) Staining and Data Analysis

Chemical/Solution

- Xylene
- Ethanol
- Tris buffered Saline
- Hydrogen Peroxide
- Normal Swine serum

- Copper sulphate
- Haematoxylin (Dako)
- Envision kit (Dako)

Staining optimization

Breast cancer tissue microarrays were prepared and immunohistochemically stained with a number of antibodies, which were initially tested and optimized using TMA sections including malignant breast tissue and normal kidney tissue to check for the exact pattern of staining in both normal and malignant tissue and to insure that the staining contains a varied spectrum ranging from high, medium, low, and totally negative intensity. The final antibodies dilutions after optimization are detailed in Appendix 1.

Protocol for IHC staining: ABC Method – Sequenza

Tissue sections were placed in the 60°C incubator for 10 minutes. The sections were dewaxed by immersing in 2 sequential xylene baths for 5 minutes each; rehydrated by immersing in a series of 3 alcohol baths (about 10 seconds in each). Sections were then washed well in running tap water. An antigen retrieval step was performed by placing the section in a plastic bucket containing citrate Buffer-Saline pH 6.0 (N.B. EDTA at pH 8.00 could also be used as an alternative antigen retrieval). The sections were micro-waved for 10 minutes at high power, followed immediately by 10 minutes on 50% power. The following steps were done at RT. Sections were immediately flooded with running tap water to stop the retrieval

process until they cooled down. Then, slides were loaded onto sequenza plates and placed in sequenza trays; ensuring the slides did not dry out. Sequenza reservoirs were filled to the middle with Tris Buffered Saline (TBS) pH 7.6 to rinse the slides. Blocking of endogenous peroxidase activity was done by applying a 0.3% solution of hydrogen peroxide in methanol for 10 minutes, followed by washing well with TBS. 200 μ l of Normal Swine Serum (NSS) (diluted 1/5 in TBS) was applied to each slide and incubated for 10 minutes; followed by incubation with 100 μ l of primary antibody (optimally diluted in NSS/TBS) to each slide for 45 minutes. The sections were washed well in TBS. Slides were incubated with 100 μ l of biotinylated secondary (C) antibody (diluted 1/100 in NSS/TBS) for 30 minutes at RT. The slides were washed again in TBS followed by incubation with 100 μ l of preformed AB Complex (AB) for 55 minutes at RT. AB was prepared at least 30 minutes prior to use to ensure adequate binding of the 2 components - diluted 1/100 in NSS/TBS). Another wash with TBS; followed by applying 200 μ l of freshly prepared liquid Diaminobenzidine (DAB) solution for 8-10 minutes (prepared by diluting 20 μ l of liquid DAB chromogen per ml of substrate buffer). Another wash with TBS; followed by incubation with 200 μ l of copper sulphate solution for 8-10 minutes at RT. Last wash in TBS; followed by adding 100 μ l of freshly filtered haematoxylin for 2 minutes only. Then, the slides were washed well in tap water. The slides were removed from sequenza plates and placed face up into a cover slipping rack, rinsed in running tap water, dehydrated in alcohols, cleared in xylene and finally mounted with DPX.

Protocol for IHC staining: Envision kit (Dako) Method – Sequenza

Tissue sections were placed in the 60°C incubator for 10 minutes. Sections were dewaxed by immersing in 2 sequential xylene baths for 5 minutes each; rehydrated by immersing in a series of 3 alcohol baths (about 10 seconds in each). Sections were washed well in running tap water. An antigen retrieval step was performed here (see above). The following steps were done at RT. Slides were loaded onto the sequenza plates and placed in sequenza trays; ensuring the slides do not dry out. Sequenza reservoirs were filled to the middle with Tris Buffered Saline (TBS) pH 7.6 to rinse the slides. Blocking endogenous peroxidase activity step was done; followed by washing well with TBS. Blocking unspecific antibody binding site was done by adding 200µl NSS (diluted 1/5 in TBS) to each slide for 10 min; followed by 100µl of primary antibody for 30 minutes. Slides were washed with TBS; 100µl of Envision A applied for 30 minutes at RT from dropper bottle. Another wash in TBS; 100µl of freshly prepared Envision C solution were applied for 6 minutes at RT (C is prepared 1/50 C to B Substrate buffer). Slides were washed well in TBS for 5 min; 100µl of freshly filtered haematoxylin applied for 6 minutes. Slides were washed well in tap water; removed from sequenza plates and placed in a rack in the water; dehydrated in alcohols; and cleared in xylene; mounted with DPX.

Scoring of IHC reactivity.

TMAs were scored using high-resolution digital images (NanoZoomer; Hamamatsu Photonics, Welwyn Garden City, UK), at X20 magnification, using a web-based interface (Distiller; Slidepath Ltd., Dublin, Ireland). Unsuitable TMA

cores, which were lost, fragmented or rolled out were excluded. IHC scoring was performed by the modified Histo-score (H-score)(McCarty et al., 1985), which involves semi-quantitative assessment for both the intensity and percentage of staining. The H-score is calculated as 0 X negative % + 1 X weak % + 2 X moderate % + 3 X strongly stained %. The range of possible scores is between 0-300. This method is superior to using either the conventional intensity or percentage scoring scheme.

2.2.4 Statistical analysis

Ordinary statistics

Statistical analysis was done using SPSS 15.0 statistical software (SPSS INC., Chicago, IL, USA). Data were dichotomized into high and low groups based on median H-score. Identical analysis on continuous non-categorical data was performed, which showed similar results, suggesting that dichotomization had not weakened the evidence for an association in this instance. Standard cut-offs were used for the well established prognostic variables, previously published on the same patient series (Abd El-Rehim et al., 2005, Elsheikh et al., 2009). All factors were used as dichotomous covariates with the exception of grade, NPI and phenotypic groups proposed by Nielsen et al. (2004) that were categorized into three groups. Distribution of the expression level of all the markers used in our study with other variables was analyzed using Pearson Chi-square statistic. Mann-Whitney-Wilcoxon test was used for two-level variables and Kruskal-Wallis for more than two-level variables. To assess the correlation of each of the biomarkers with tumour clinicopathological variables, biological and histone PTMs markers,

the interval by interval Pearson's r and Kendall's tau-b correlation coefficient tests were performed for categorical data; and Spearman test was applied on continuous data. All p values were two-sided. Given that 16 different biomarkers were assessed in this study, the chance of getting type 1 errors was increased. We therefore applied a Bonferroni correction, increasing the significance threshold of p in χ^2 test from 0.05 to 0.003 (by dividing the p value on the number of the studied biomarkers).

Survival analysis was evaluated using Kaplan-Meier curves and log-rank tests. Median follow-up was defined as follow-up period for those patients still alive and disease-free at their latest hospital visit. Differences between survivals were calculated using a log rank test. Cox proportional hazard model (Cox, 1972) determined the influence of the markers used in the study, when adjusted to conventional clinicopathological prognostic variables, on breast cancer specific survival (BCSS) and/or disease free survival (DFS). Post hoc tests were used in the situation where we obtained a significant omnibus F-test, with a factor that consists of three or more means, and additional exploration of the differences among means is needed to provide specific information, on which means are significantly different from each other (any correlation with grade, stage and NPI).

Clustering of tissue microarray data

Cluster analysis of histone and p53 PTMs marks were done with two clustering algorithm: K-means and the partitioning around medoids (PAM) (arc software)

kindly performed by Dr. Daniel Soria. Both methods run for clusters ranging from 2 to 20 clusters. Six validity indices tests were followed to determine the best number of clusters. The used indices are Calinski and Harabasz, Hartigan, Scott and Symons, Marriot, TraceW, and TraceW-1B. The number of groups considered in each index was chosen according to the rules previously reported (Wiley, 1990).

2.3 Cell Culture

2.3.1 Reagents

DMEM and RPMI media, L-glutamine, penicillin/streptomycin, foetal bovine serum (FBS) and Trypsin- EDTA were purchased from GIBCO, Invitrogen Corporation. Phosphate Buffer Saline (PBS) tablets were purchased from Oxoid Ltd.

2.3.2 Cell Line Maintenance

The cell lines indicated in Table 2.1 were grown in the appropriate media in sterile plasticware (TPP, Helena Biosciences, Tyne and Wear) at 37 °C, in a humidified atmosphere containing 5% CO₂. Cells were grown to confluence in 7.5 cm² flasks, 10 or 20 cm² dishes. Cells were grown in 5, 10 and 20 ml of culture media and passaged at 100% confluency for a maximum of 30 passages; after which they were discarded. For passaging cells, medium was aspirated; cells were washed twice with sterile PBS at room temperature. 1-4 ml 1x trypsin/0.5 mM EDTA (ethylenediamine tetra-acetic acid) (GIBCO) was added for 1 min and

incubated at 37 °C prior to being aspirated. Cells were then resuspended in an appropriate volume of culture medium.

Table 2:1: Mammalian Cell Lines Used in the Study.

Cell line	Origin	Growth medium
MCF-7	Human Invasive ductal Carcinoma	DMEM + 2 mM L-Glutamine + 1% Penicillin/streptomycin + 10%FCS
MDA-MB-231	Human invasive Lobular carcinoma	DMEM + 2 mM L-Glutamine + 1% Penicillin/streptomycin + 10%FCS
MRC-5	Human embryonic lung fibroblast	DMEM + 2 mM L-Glutamine + 1% Penicillin/streptomycin + 10%FCS
Saos2	Human Osteosarcoma, p53- null	RPMI-1640 + 2 mM L-Glutamine + 1% Penicillin/streptomycin + 10%FCS
U2OS	Human Osteosarcoma	DMEM + 2 mM L-Glutamine + 1% Penicillin/streptomycin + 10%FCS
HEK293	Human embryonic Kidney	RPMI-1640 + 2 mM L-Glutamine + 1% Penicillin/streptomycin + 10%FCS

The table is showing the origin of cell lines used in the study and the composition of their growing media. DMEM, Dulbecco's modified eagle medium (GibcoBRL); RPMI-1640, Roswell Park Memorial Institute 1640 medium (GibcoBRL).

2.3.3 Freezing Down Cells for Liquid Nitrogen Stocks

A near 100% confluent 10ml dish (containing $4-6 \times 10^6$) was used to make stocks for storage. The cells were washed twice with 5ml 1xPBS, harvested by adding 2ml 1x trypsin for one minute at 37°C. Trypsin was aspirated; cells were resuspended in 10 ml media, centrifuged for 5min at 1500 rpm. The supernatant were removed; the cells were again resuspended in 1ml culture media containing 10% DMSO, 40% FCS and 50% DMEM. The date; identity of cell line; passage number were recorded. The cells were gradually frozen by incubation at-20 for 1hr and -80°C overnight. Finally, the cells were transferred to liquid nitrogen for long term storage.

2.3.4 Thawing Cells from Liquid Nitrogen Stocks

Cells were immediately thawed by immersion in 37 °C water bath for 5 minutes. 9 ml of media was added, cells were centrifuged and resuspended in 10 ml full cultural media. Cells were allowed to attach overnight (37°C, 5% CO₂) before media was replaced and cells were passaged as described above.

2.3.5 Harvesting adherent cells

Adherent cells were dislodged from tissue culture dishes using a cell scraper. Tissue culture media containing cells was aspirated and centrifuged (5 min, 1500 rpm) at 4°C. The supernatant was discarded and the pellet was resuspended in 5 ml 1x PBS; centrifuged again (5 min, 1500 rpm) at 4°C twice, the supernatant was discarded and pellet was incubated in 100 µl lysis buffer on ice for 30 min.

Following vigorous vortexing, the lysed cells were transferred to clean labelled tubes, and frozen at -20 °C.

An alternative method for cell harvesting was performed as follow: cells were washed twice with 5 ml 1x PBS; were incubated with 1x trypsin at 37°C for 1 min. Trypsin solution was aspirated and cells were resuspended in 5m 1x PBS; centrifuged (5 min, 1500 rpm) at 4°C. The supernatant was discarded and the pellet was incubated in 100µl Lysis buffer on ice for 30 min. Following vigorous vortexing, the lysed cells were transferred to clean labelled tubes and frozen at -20°C.

2.4 Biochemical Techniques

2.4.1 Solutions and Buffers

- **4x SDS-PAGE sample buffer:** 200 mM Tris-HCl pH6.8, 40% (v/v) glycerol, 2% (w/v) SDS, 5% (v/v) β -mercaptoethanol, 0.4% (w/v) bromophenol blue. N.B. 400 mM dithiothreitol sometimes was used in replacement for (β -mercaptoethanol).
- **10-x SDS-PAGE running buffer:** 250 mM Tris-HCL, 2.5 M glycine, 1% (w/v) SDS
- **SDS-PAGE stacking gel:** 1ml volume: 680 µl H₂O, 170 µl 30% acrylamide mix (National Diagnostic, Hull), 130 µl 1M Tris-HCL pH 6.8, 10 µl 10% (w/v) SDS, 10 µl 10% (w/v) ammonium persulphate (APS), 1 µl TEMED (N,N,N'N'-Tetramethyl-ethylendiamine)

- **SDS-PAGE resolving gel:** different concentrations of acrylamide were used (as illustrated in Table 2.5) according to the molecular weight of the proteins to be detected.
- **High glycine transfer buffer:** 48 mM Tris-HCL, 380 mM glycine, 0.1% (w/v) SDS, 20% (v/v) methanol
- **RIPA Lysis buffer:** 50mM Tris-HCl pH7.4, 150 mM NaCl, 1% NP-40, 0.25% Na-deoxycholate, 1mM PMSF, 1x Complete mini protease inhibitor tablet (Roche) per 10 ml, 1x Pierce phosphatase inhibitor
- **PBST:** Phosphate buffer saline, 0.02% Tween-20
- **ECL detection reagents.**

Solution A Stock: 0.296 gm p-coumaric acid (Sigma) in 20 ml DMSO

Solution B Stock: 0.89g Aminophthalhdrazide (Luminol) (Sigma) in 20 ml DMSO

Table 2:2: Solution Compositions for preparing Resolving Gels for Tris-glycine SDS-Polyacrylamide Gel Electrophoresis.

% of acrylamide in Resolving Gel		6%	8%	12%	15%
Protein Size for separation (kDa)		150-300	100-250	30-100	10-50
Components	H ₂ O (μl)	2,600	2,300	1,600	1,100
	30% acrylamide mix (μl)	1,000	1,300	2,000	2,500
	1.5 M Tris-HCl pH 8.8 (μl)	1,300	1,300	1,300	1,300
	10%(w/v) SDS (μl)	50	50	50	50
	10% (w/v) (APS) (μl)	50	50	50	50
	TEMED	4	3	2	2
Volume (μl) required for 5ml resolving gel					

Recipes for preparation of 5ml resolving gel for gels with different acrylamide contents. Where SDS, Sodium dodecyl sulphate; APS, Ammonium persulphate; TEMED, N, N, N, 'N-tetramethylethylenediamine. Appropriate molecular weight ranger (in kilo Daltons) for different acrylamide concentrations is also shown.

2.4.2 Antibodies

Antibodies used in the study are detailed in Appendix 1

Validating the Specificity of the Antibodies Used in the Study

The anti-H3K18ac, H3K9me3 and H4K20me3 antibodies used in this work have passed the test used in an assessment of histone –modification antibody quality study (Egelhofer et al., 2011). The test included western blot analyses to test the antibody cross reactivity with unmodified histone in nuclear or whole-cell extracts, dot blot and chip-chip/seq tests. In addition, the specificity of H2A.Z antibody was confirmed. As shown in Appendix 2B the antibody targeted the histone variant H2A.Z but not the H3/H4core histone (Appendix 2B).

2.4.3 Total Protein Assay

The protein concentration of cell-free extracts was measured using Bio-Rad protein assay reagent according to the manufacturer’s instructions. Briefly, 2 µl of sample was mixed with 200 µl protein assay reagent and 798 µl dH₂O in a cuvette and incubated at RT for 15 min. The reaction between protein and copper in the alkaline solution and the Folin reagent is reduced by the copper-treated protein leads to colour development. Then, its absorbance was measured at 595 nm (A_{595 nm}). Protein concentration was determined by measuring against diluted BSA standards of known concentration.

2.4.4 Protein Separation and Transfer to Nitrocellulose

SDS PAGE electrophoresis was carried out according to standard protocols. Samples were prepared by mixing 1 volume 4X loading buffer with 3 volumes of protein extract; Samples were boiled for 5 min at 100 °C, followed by centrifugation at 8000 rpm for 30s immediately prior to loading. 50µg of each sample and 5µl of marker were loaded on 6-15% SDS-PAGE gels. Gels containing samples were electrophoresed in Biorad Protean II system in 1x SDS-PAGE running buffer at 150 V. The separated protein samples are transferred by a wet transfer apparatus (Bio-Rad Laboratories), onto nitrocellulose paper (Hybond P; Amersham Biosciences UK Limited) by wet blotting for 90 minutes in running buffer (formed of 1x methanol; 1x high glycine transfer buffer; and 3x distilled water) at constant current at 100 V, the duration may extend to over night at 30 V for large proteins.

2.4.5 Western Blotting and Immunodetection

Nitrocellulose membranes were stained in Ponceau S solution (Sigma) (0.1% (w/v) Ponceau S in 5% (v/v) acetic acid in dH₂O) for 5 min and then washed in distilled H₂O to monitor the efficiency of protein transfer. The following incubation steps were done at RT on a rocking platform. Nitrocellulose membranes were incubated in 20 ml blocking buffer (5% dried milk in 1x PBS) for 10 minutes, to block non-specific antibody binding sites. After removal of the blocking buffer, primary antibody diluted in milk was added (in a sealed bag) for a duration ranging from 1 hour at room temperature to O/N at 4 °C, depending on the primary antibody. Membranes were washed 3 times (5minutes, rocking) in

0.5% tween in PBS (PBST) before adding Secondary HRP-conjugated antibody (in a concentration ranging from 1:5000 to 1:20,000) in sealed bags for one hour. Excess /unbound secondary antibody was washed by three washes with PBST. Protein:antibody immunocomplexes were detected by ECL detection. The membrane was incubated for one minute face down in 10 ml ECL developer (22 µl solution A, 50 µl Luminol, 6 µl H₂O₂, 1ml of 1M Tris pH 8.5, 9 ml dH₂O). Excess reagent was drained and the membrane was wrapped in saran wrap. The membrane was placed in x-ray film cassette, exposed (10 sec-5 min) to autoradiograph film or chemiluminescence was measurement with Las 4000[®] (Fujifilm).

2.4.6 Immunocytochemistry and Fluorescence Microscopy

Mammalian cells were seeded into 2 ml cultural media (as described in table 2.1) in 24 well plates containing coverslips and cultured in a 5% CO₂ incubator. If required for the experiment, chemical reagents such as HAT inhibitors, etoposide or vehicle (DMSO) were added to the medium at least 3 hours after seeding to ensure proper cell attachment. After 24 hr, coverslips were washed gently twice with PBS and then fixed with PBS containing 4% paraformaldehyde for 10 min at RT. The following incubation steps were done at RT. Cells were then washed five times with PBS. After removing PBS, cells were permeabilised by incubation with 0.2% Triton- X100 in PBS for 2 min at RT, and washed again five times with PBS. Non-specific interactions were blocked by incubation with 3% BSA in PBS for 30min. Cells were incubated with primary antibody for 1 hr, then washed again five times with PBS. Cells were incubated with Alexa fluor[®] fluorophore-

conjugated secondary antibody (1:500 Alex-594 in 3% BSA) for 30 min. Then cells were washed again five times with PBS. To stain nuclei, cells were incubated with 0.5 μ g/ml Hoechst 33258 in PBS. Finally, the slides were washed five times in PBS. The coverslips were taken out using a non-toothed forceps and needle, and excess PBS was dried by touching the coverslip on a piece of tissue. The coverslips were inverted on mounting media (10 μ l of 90% glycerol in PBS). Excess mounting media underneath the slide was dried out with a piece of tissue; slide edge was sealed by nail polish.

A Zeiss LSM 510 META confocal microscope was used to image the mammalian cells. Flourescence from the 488, 594 secondary antibodies were detected using 488, 543nm laser excitation at 2% power and the long pass 505 filter for emission. The Hoechst counter stain for DNA was measured using a mercury bulb. The lenses used were 40x/1.3, 63x/1.4 oil lenses (Zeiss).

2.4.7 Bivariate Flow Cytometric Analysis of the Cell Cycle

Bromodeoxyuridine (BrdU), an analogue of the DNA base thymidine, is used in this protocol for effective analysis of the cell cycle. BrdU competes with thymidine for uptake during DNA synthesis. Thus, only cells that have been actively synthesising DNA during the time that BrdU is present will be positive for it. Therefore, the percentage of cells in G₀/G₁, S and G₂/M can be determined by simultaneous staining for BrdU (using a labelled Ab) and DNA content (using propidium iodide).

- 1x PBS

- 10 mM BrdU Stock Solution
- 70 % ethanol (ice-cold)
- 2M HCl
- PBST-BSA (PBS with 0.1 % Tween20 and 0.1% BSA)
- FITC conjugated Mouse anti-BrdU antibody (BD Biosciences)
- Propidium iodide solution (1 mg/ml) prepared in water
- Ribonuclease A solution 1mg/ml prepared in water

Cells were incubated with 20 μ M BrdU at 37 °C. Media was removed and kept in same tube as cells (for analysing apoptotic cells), washed with 4ml 1x PBS solution and then incubated with 4ml trypsin to detach cells. Trypsin was aspirated; 10ml media were added. Cells were centrifuged at 2000 rpm for 5 min. Cells were washed once with 20 ml cold 1 x PBS. Cells were fixed in 400 μ l ice-cold 70 % ethanol (with gentle vortexing) for 30 min on ice or overnight in the fridge. Another spinning at 1900 rpm for 5 min, followed by washing twice with 2 ml cold PBS. Cells were incubated with 400 μ l 2 M HCl for 20 min at RT with frequent mixing. 2 ml 1x PBS solution was added followed by spinning at 1900 rpm for 5 min, and then washed twice with 2 ml PBST-BSA. 20 μ l FITC-conjugated anti-BrdU antibody were added directly to 100 μ l PBST-BSA, left for 60 min at RT (in the dark). Cells were washed once with 2 ml 1x PBS (if another antibody was used in combination with anti-BrdU, the samples were incubated for 30 min with a secondary antibody covering the far red spectrum e.g. Alexaflour-633 or Alexaflour-647 followed by washing once with PBS). Cells were resuspended in 500 μ l 1x PBS; 10 μ l ribonuclease A was added for 15 min; and finally 1 μ l PI was added to each tube. 1 hour after PI incubation measurement

was carried out using a FACS Aria flow cytometer, FACS Diva software (BD Biosciences); analysis of results was done with the WinMDI package (<http://facs.scripps.edu>).

2.4.8 Colony formation study

MCF-7 cells (20,000 cells) were seeded in 6 cm² ml dishes, left for 6 hrs to attach. Cells were then treated for 24 hours with either Garcinol (20 µM), or LTK14 (20 µM) alone or in combination with Etoposide (5 µM). After washes, cells were incubated for an additional 12 days to allow colony formation. The cultured cells were fixed in methanol and stained by 10% Giemsa in PBS. The number and size of colonies were estimated using Image J software. Unpaired t test was used to measure data pooled from three independent experiments.

2.5 Bacterial Manipulations

2.5.1 Reagents, cells, media, supplements

Bacterial strain: *E. coli* DH5α (Stratagen, Texas, USA) bacterial strain was used for plasmid transformations and maxi DNA preparations.

Bacterial Cell Culture media: Luria Bertani medium (LB): 10g/L Tryptone (OXOID Ltd), 5g/L yeast extract (OXOID Ltd), 10 g/L NaCl (Fisher Scientific) was prepared in deionised water pH 7.0 and sterilised by autoclaving at 121°C for 20 minutes (min). For LB agar, 15 g bacto-agar (OXOID Ltd) was added to 1 litre of LB medium prior to sterilization. For LB agar plate 20-25 ml molten agar medium (55°C) were poured into each Petri dish. Solidified agar plates were dried

under UV in a laminar flow hood for 20 min to eliminate excess moisture and stored at 4 °C.

Sterile antibiotics were added to liquid LB or molten LB agar medium at ~55 °C as required, at the following concentrations.

Ampicillin (100µg/ml) 1,000x stock solution: 100mg/ml in 50% ethanol.

Antibiotics were sterilised by filtration through a 0.2 µm filter (Millipore).

2.5.2 Culture of *E. coli* DH5 α

DH5 α cells were streaked for single colonies on LBA plates (containing antibiotic if required) and grown overnight at 37 °C. After 24hrs, 5-10ml LB in a sterile Erlenmeyer flask was inoculated with a single colony and cultured at 37 °C.

2.5.3 Preparation of *Escherichia coli* (*E. coli*) competent cells.

The Calcium chloride/Rubidium chloride method was used for making *E. coli* DH5 α competent for DNA transformation. A single colony from a fresh streak of cells was used to inoculate 5ml LB. After overnight growth at 37 °C the culture was diluted at 1:100 ratio in LB medium at 37 °C, until it reached an optical density (at 600 nm) of 0.5. The log phase cells were incubated on ice for 10 minutes in a pre-chilled 50 ml falcon tube. Cells were harvested by centrifugation at 2400 rpm for 10 minutes at 4 °C. The supernatant was removed, the cell pellets were gently resuspended in 20 ml ice cold Buffer 1 (on ice). Centrifugation was repeated (2400 rpm for 10 minutes at 4 °C); the pellet was resuspended in 2 ml

ice-cold Buffer B and the cell suspension combined. Prior to storing at -80 °C, 200µl competent cells aliquots in Microfuge tubes were snap frozen on dry ice.

Buffer 1: (30 mM KCl; 100mM RbCl; 10mM CaCl₂, 50 mM MgCl₂, 15% glycerol; adjust to pH 5.8 using 0.2 M glacial acetic acid)

Buffer 2: (10 mM MOPS; 75 mM CaCL₂, 10 mM RbCl, 15% glycerol; adjust to pH 6.5 using 1M filter sterilised KOH).

2.5.4 Plasmid DNA Transformation into *E. coli* cells

Plasmid DNA was used to transform competent DH5α *E. coli* cells as follows. Firstly, the competent host cells were removed from -80°C and thawed on ice. For each of the transformations, 1 µl of plasmid DNA was mixed with a 100 µl volume of cell suspension, and incubated on ice for a further 45 minutes. The cells were heat shocked in a water bath at 42°C for 2 minutes before returning to ice for 2 min. 400µl of LB was added aseptically and the transformed cells incubated at 37°C for 1 hour on a shaking incubator. Transformation mixes were spun at 13,000 rpm for 1 minute to pellet the cells, 400µl of supernatant was removed and the pellet resuspended in the remaining media. The bacteria were spread onto LB agar plates containing the appropriate antibiotic and incubated overnight at 37°C.

The plasmids used in this study were wild type and mutant full length p53 cloned into pcDNA3 as described in (Rodriguez et al., 2000), kindly provided by Professor Ronald Hay (University of Dundee), as shown in Table 2.2.

Table 2:3: Plasmids Used in the Study.

Plasmid	Source
pcDNA3	Invitrogen
p53	Professor Ronald Hay, University of Dundee
p53K372-3R	Professor Ronald Hay, University of Dundee
p53K381-2R	Professor Ronald Hay, University of Dundee
p53K386R	Professor Ronald Hay, University of Dundee
p53K6R	Professor Ronald Hay, University of Dundee

2.6 Molecular biology techniques

2.6.1 Plasmid Purification from *E.coli*

For large-scale preparation of plasmid DNA, 200ml cultures were inoculated with 1/100 fold dilution of suspended cells and left to replicate overnight at 37°C, 250 rpm. To isolate the plasmid DNA from these cells the QIAGEN Plasmid Maxi Kit protocol was used with the following amendments: To precipitate plasmid DNA, centrifugation was carried out at 7000 rpm for 15 min and after addition of isopropanol; the pellet was washed with 75% ethanol; dried by vacuum evaporation and finally resuspended in sterile water.

2.6.2 Determination of Nucleic Acid Concentration

The concentrations and purity of plasmid DNA preparations were determined using the Nanodrop ND-1000 UV-Vis Spectrophotometer. A260/A280 values were also calculated and were useful indicators of sample purity. For uncut DNA plasmids, 1µg was then run on a 0.8% agarose gel to allow estimation of the ratio of supercoiled to nicked DNA.

2.6.3 Sequencing of Plasmid DNA

Plasmid DNA for sequencing was sent to Geneservice Ltd (MRC, Medical solutions plc, Nottingham, UK). Samples were sequenced using Big Dye V3.1 chemistry and an AB13730xl Automated Sequencer.

2.6.4 Calcium Phosphate-Mediated Transfection of Adherent Cells

Adherent SaOs2 (p53 deficient) cells were seeded at 1-2x10⁶ cells/ plate 24 hours prior to transfection. 50-80% subconfluent cells were transfected by using the calcium phosphate coprecipitation method (CalPhos™ Mammalian Transfection Kit- Clontech, Basingtoke, UK). 1-3 hr prior to transfection cells were washed with sterile 1X PBS and 10 ml of fresh medium added. Cells were transfected with 10µg of pcDNA3 (p53, p53K372-3R, p53K381-2R, p53K386R and p53K6R) expression vectors. Expression of p53 proteins was confirmed by western blots using anti-p53 antibody. For each condition, a DNA mastermix containing sterile water, DNA and 12.5% (v/v) 2M calcium solution was prepared; added dropwise to an equivalent volume of 2X Hepes Buffered Saline (HBS) while vortexing. Solutions were incubated at room temperature (RT) for 20 min. 200µl was subsequently added dropwise to the 10 ml of medium present in the plate. After 16 hours of incubation at 37°C, cells were washed twice with 1X PBS; then maintained in DMEM for another 24 hours. Cells were then washed with 1X PBS and harvested in PBS for subsequent protocols, e.g. wetern blots.

2.6.5 Data bank analysis

The NCBI databases and BLAST program was used for DNA and protein sequence verifications.

2.6.6 RNA interference

RNA interference (RNAi) is a post-transcriptional process used to induce temporary gene silencing. Where a double-stranded RNA molecules triggers a sequence specific mRNA degradation of homologous single-stranded target RNAs and the translated products (Tuschl and Borkhardt, 2002). Interference of RNA initiates by the conversion of dsRNA into 21-23 nucleotide fragments by the RNase III enzyme, Dicer. These short RNA nucleotide fragments are called small interfering RNAs (siRNAs), containing two nucleotide single-stranded overhangs at the 3' end and bearing 5'-monophosphate and 3'- hydroxyl groups which are crucial for the degradation of the target RNAs complementary to the siRNA sequence. Then, the siRNAs incorporated into the RNA-induced silencing complex (RISC), in an ATP-dependent step (in this step siRNA duplex is unwound into single strands), that guide the RISC to recognize and cleave the target RNA (Schwarz et al., 2002). In this study, we silenced SUV420H2 gene using siSUV420H2 (Dharmacon). INTERFERinTM (Polyplus Transfection) was used as the transfection reagent. 2,000,000 MCF-7 cells per 6 cm² dishes were plated 24 hrs prior to transfection. The following steps were done at room temperature. 1.1 µl siRNA was mixed with 399 µl DMEM media, followed by adding 15 µl INTERFERin with continuous vortexing for 10 min. The culture media was removed from the plate and replaced with fresh media, to which the mix was added. The final concentration of siRNA oligos in each plate was 5 nM. As a control reaction for the experiment, cells were subjected to transfection with scrambled siRNA in order to detect cellular effects caused by the transfection event or delivery process. After 24 hrs, garcinol treatment was added for 24

hours, followed by western blotting for detecting the levels of H4K20me3 in the MCF-7 cells.

**EVALUATION OF HISTONE PTMs IN
BREAST TUMOURS**

3.1 Evaluation of the H4K16ac Regulatory Axis as a Novel Biomarker Set in Breast Tumours

In a previous study, we assessed the occurrence of global histone PTMs in an archived set of 880 paraffin-embedded breast tumour biopsies using immunohistochemistry of tissue microarrays (TMAs). This study revealed that global histone PTM levels in breast tumours correlate with tumour phenotypes, prognostic factors, and patient outcome (Elsheikh et al., 2009). ‘Low’ levels (below the median) of 7 different histone PTMs were associated with advanced stage tumours, and correlated with a significantly poorer long term survival. Similar observations have been reported in prostate tumours (Seligson et al., 2005), renal cell carcinoma (Mosashvilli et al., 2010, Liu et al., 2010) and bladder cancer (Dudziec et al., 2011). Thus, it has been suggested that assessment of histone PTM levels may be a useful prognostic indicator predictive of clinical outcome in solid tumours (Seligson et al., 2005, Elsheikh et al., 2009). This is consistent with the findings that H4K16ac and H4K20me3 PTMs are very low or absent in most cancer cell lines, and are thus considered hallmarks of cancer (Fraga et al., 2005). In contrast these marks are readily detected in normal tissues or non-transformed cells (Jones et al., 2008). As our previous study indicated decreased H4K16 acetylation in even early stage tumours (Elsheikh et al., 2009), we reasoned that this might be one of the early epigenetic changes to occur in tumour cells. Thus, it was decided to use TMAs to determine the expression of the H4K16ac regulatory axis, i.e. the enzymes that control H4K16 acetylation status and their cofactors. Therefore, the hypothesis under investigation here is that factors that regulate H4K16 acetylation might also be altered in their expression

or function in breast tumours, and might therefore be useful cancer biomarkers or offer new leads to discover novel therapeutic targets.

3.1.1 Enzymes that Regulate H4K16 Acetylation: The H4K16ac Axis

Axis

A number of *in vitro* studies have revealed that MYST domain proteins such as hMOF, TIP60, MOZ/MYST3 and MORF/MYST4 are capable of acetylating histone H4 at K16 (Troke et al., 2006), although there is still some controversy in the field regarding whether all of these enzymes can regulate this PTM *in vivo*. The human homolog of the Drosophila MOF (males absent on the first) protein has been suggested to be responsible for the majority of H4K16 acetylation *in vivo* under normal growth conditions (Taipale et al., 2005). In support of this, hMOF knock down by siRNA in HeLa and HepG2 cells showed a strong reduction in H4K16 acetylation, with inhibitory effects on the cell cycle (Taipale et al., 2005). The Drosophila MOF is a component of the male specific lethal (MSL) and non-specific lethal (NSL) complexes and is required for dosage compensation in flies (Hilfiker et al., 1997b). However, its role in mammalian cells remains unclear. Nonetheless, it has been shown that down-regulation of hMOF in mammalian cells results in a global decrease in H4K16 acetylation (Taipale et al., 2005). In addition, another study showed that ablation of hMOF led to a decreased expression of the tumour suppressor gene TMS1, accompanied by changes in nucleosome positioning within its promoter. Interestingly, this silencing of TMS1 was reversed by re-expression of hMOF (Kapoor-Vazirani et al., 2008). Similarly, ablation of MOF in mouse fibroblasts was associated with

G2/M arrest, aberrant chromosomal segregation and defective repair of DNA damage (Li et al., 2011). As hMOF has been shown to be downregulated or deleted at a high frequency in breast tumours or medulloblastomas (Pfister et al., 2008), we considered this protein as a possible central player in the H4K16ac regulatory axis.

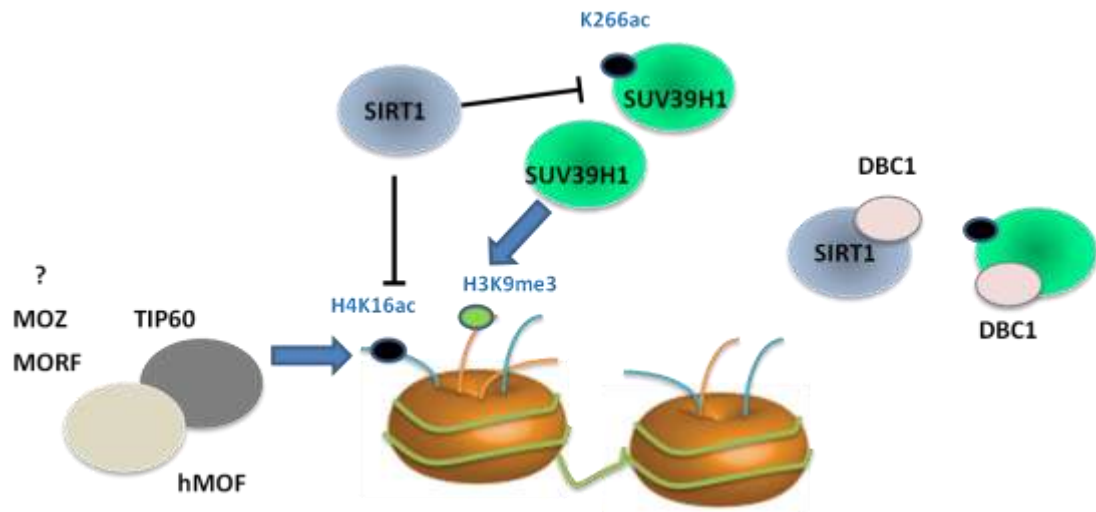
Other MYST proteins have also been shown to acetylate H4. The MYST domain of TIP60 can acetylate H4K16 (Kimura and Horikoshi, 1998), although this is likely to be in response to cell stress such as DNA damage. Consistent with this, in Chapter 5, I will show that treatment of cells with DNA damaging agents led to increased TIP60 expression and concomitant H4K16 acetylation. The MOZ and MORF (or MYST3 and MYST4) proteins have also been reported to acetylate H3 and H4 at several sites including H4K16 (Kitabayashi et al., 2001). Data from our lab has shown that the MYST domain of MOZ can acetylate H4 at K16 (Collins et al., in preparation). However, some studies have suggested full-length MOZ acetylates H3 preferentially when associated with the ING5 protein complex (Doyon et al., 2006). This suggests that the MYST domain substrate preference may be modulated by other domains in MOZ/MYST3 or by cofactors. Indeed, recent results from our group have discovered a second H3 acetyltransferase activity in MOZ/MYST3 (Deeves et al., in preparation). Nonetheless, there is clear evidence that H4K16 may be a target for MOZ and TIP60 under some conditions.

Deacetylation of H4K16 has been reported to be catalyzed by the Class III NAD-dependent HDAC SIRT1 (Vaquero et al., 2006). SIRT1 is negatively

regulated by a cofactor termed Deleted in Breast Cancer (DBC1) which blocks its HDAC function (Zhao et al., 2008, Kim et al., 2008). Thus loss of DBC1, which is frequently deleted in breast tumours, would in theory result in increased activity of SIRT1 and thus hypoacetylation of H4K16. Thus DBC1 was also considered a possible factor within the H4K16ac regulatory axis (Fig. 3.1).

DBC1 has also been reported to block the activity of the histone methyltransferase SUV39H1 (Li et al., 2009e). SUV39H1 is responsible for H3K9 trimethylation (Rea et al., 2000), which is a histone PTM associated with transcriptional silencing and DNA repair (Tachibana et al., 2005). and localises to transcriptionally silent heterochromatin (Bhaumik et al., 2007). The N-terminus of SUV39H1 interacts with the heterochromatin protein HP1 β , (Melcher et al., 2000). The presence of H3K9me3 in chromatin stabilises the recruitment of heterochromatin proteins (HP1 α - γ), which bind this PTM via the chromo domain to promote silencing (Bannister et al., 2001). The activity of the SET domain of SUV39H1 is impaired by acetylation of K226, although it is not clear which acetyltransferases mediate this modification. In contrast SIRT1 can remove the acetyl group from K226, thus acting as a positive regulator of SUV39H1 and promoting deposition of H3K9me3 in chromatin. The negative regulator DBC1 blocks the activity of SUV39H1, by binding to its catalytic domain (Li et al., 2009e). Moreover, SIRT1 deacetylates SUV39H1 at its catalytic SET domain, resulting in increased activity, higher levels of the H3K9me3 modification and impaired localization of heterochromatin protein1 (Vaquero et al., 2007) (Fig. 3.1).

Thus, MOF, TIP60, DBC1, SUV39H1 and possibly MOZ/MYST3 are all potentially part of the H4K16 regulatory axis which crosstalk to other PTMs such as H3K9me3 and H4K20me3. We therefore decided to explore the expression of hMOF, DBC1, TIP60, SUV39H1 as well as the incidence of H3K9me3 in breast tumours and correlate this within previous data on histone PTMs and archived information on other clinico-pathological factors.

Figure 3.1: The H4K16ac Axis.

hMOF, TIP60 and possibly other MYST domain histone acetyl transferases acetylate H4K16, whereas SIRT1 deacetylates H4K16; The SET domain of the methyl transferase SUV39H1 is negatively regulated by acetylation at K266, although the HAT that catalyses this unknown; SIRT1 can also deacetylates SUV39H1 at K266, thus stimulating its ability to trimethylate H3K9 (H3K9me3) a repressive mark in chromatin; the regulatory protein Deleted in Breast Cancer (DBC1) can bind and inhibit both SIRT1 and SUV39H1.

3.1.2 TMA profiling of the H4K16ac Regulatory Axis in Breast Tumours

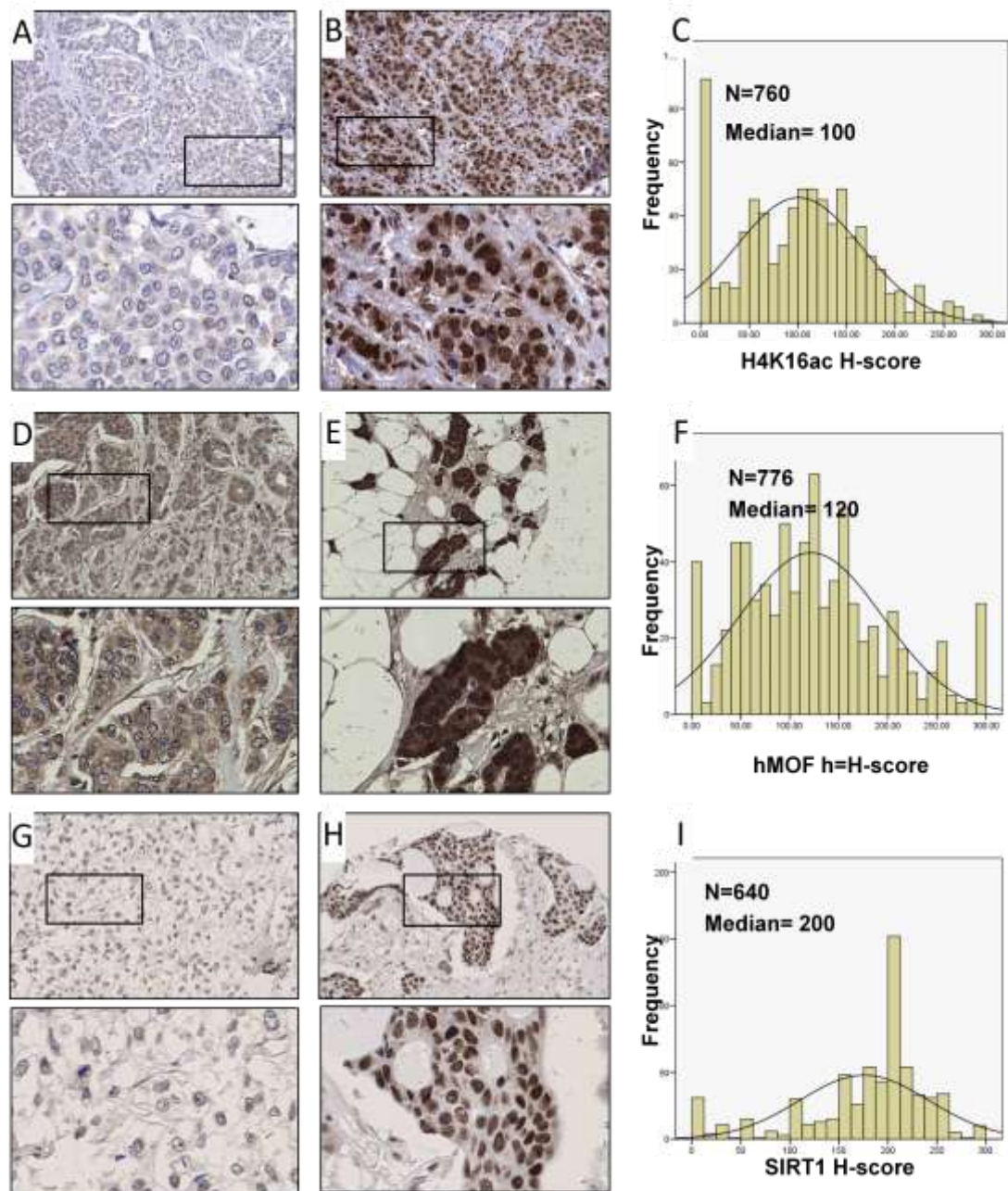
Tissue microarrays representing core sections from 880 breast tumour cores were provided by the Nottingham Breast Unit. The TMAs were stained for the presence of four chromatin regulators (hMOF, SIRT1, DBC1 and SUV39H1) as well as H3K9me3 and H4K16ac. The antibodies used are described in Appendix 1, and all were optimized by IHC staining of optimization slides (TMA slides that lost numerous tissue cores) with different primary antibody dilutions, which further increased/decreased according to the staining outcome. The final antibody dilution and method for antigen retrieval (Appendix 1) were determined when the staining outcome, and the majority of the tissue cores showing some level of staining. IHC staining was performed as described in Materials and Methods (Section 2.2.3). Any damaged samples were discounted. A standard H-score system was used for evaluating the staining intensity for all marks (Elsheikh *et al.*, 2009).

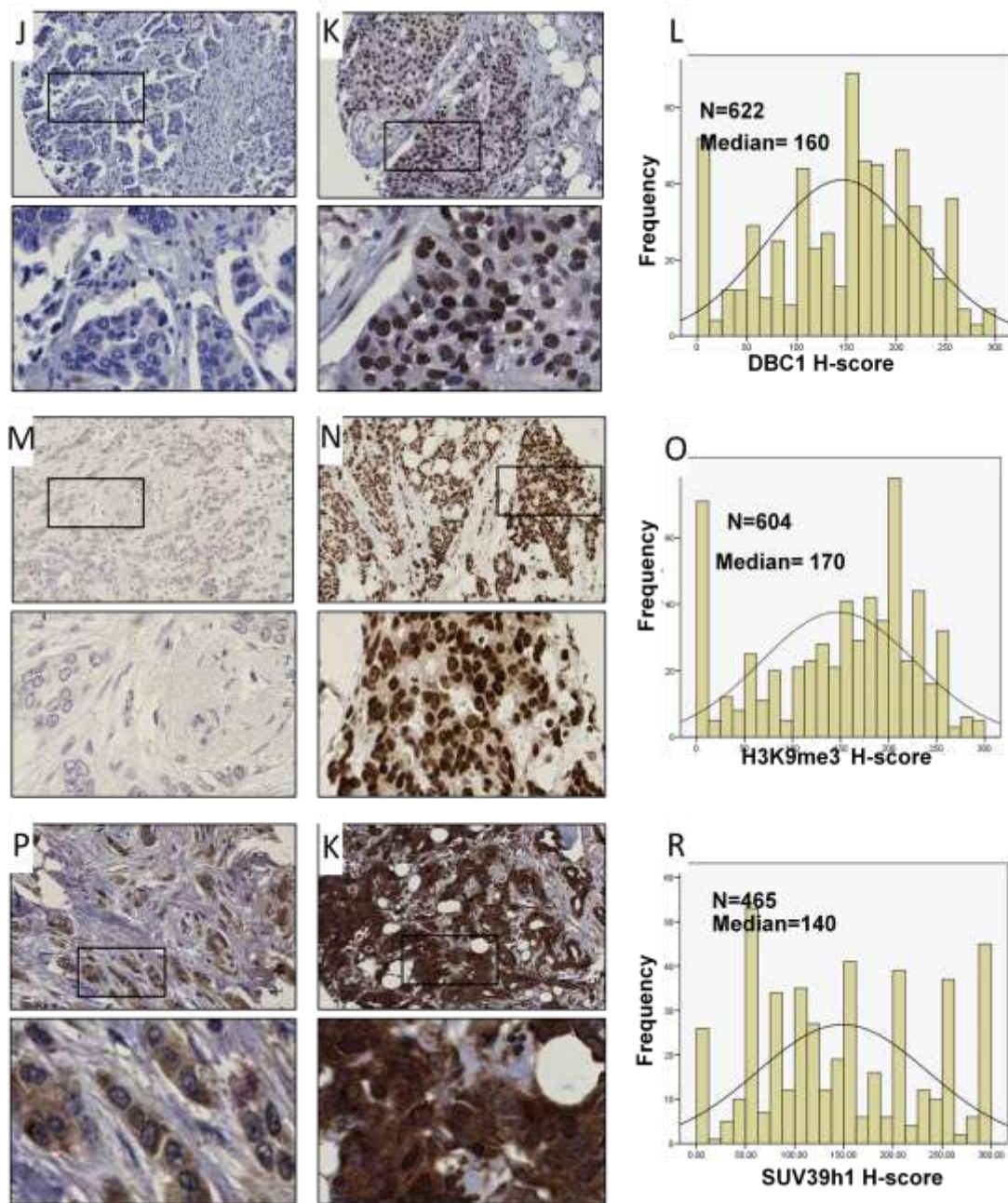
Two antibodies were used to detect H4K16ac in TMAs (Abcam, ab1762) and (Upstate, 06762). Data from the first antibody was reported in El Sheikh *et al.*, (2009), while data obtained with the second antibody (Upstate) is reported here. The specificity of this antibody was verified using dot blot assays with H4 1-22 peptides acetylated at K5, K8, K12 and K16, or unacetylated H4 (personal communication; Sian Deevies). Immunoreactivity for the above biomarkers was generally detected in the nuclei of the examined tissue; except for SUV39H1, which showed additional cytoplasmic reactivity. H-score was done according to only the nuclear reactivity. Representative examples of breast cancer tumour

tissue cores presenting with low or high levels of staining for each antibody are shown in Figure 3.2 left and central column. Histograms illustrating the frequency for H-score for each mark plotted against the number of cases are shown in Figure 3.2, right column. The histone PTM H4K16ac gave a zero score in more than 10% of tumours (90 out of 760 cases) although the median H-score was 100. This is consistent with our previous data using another H4K16ac antibody as reported in El Sheikh *et al.* (2009), and is consistent with other reports of a reduction of this histone PTM in breast and medulloblastoma tumours (Pfister *et al.*, 2008). Interestingly, 40 cases were also recorded as H-score =zero for hMOF, the primary acetyltransferase for H4K16 in cell line studies. Similarly, DBC1 expression absent in around 10% of tumours, and 90 tumours also had zero H-score for the global levels of H3K9me3. In contrast, fewer tumours were negative for SIRT1, which may be indicative of its essential role in cells (Fig. 3.2).

For further analysis of the distribution of the H4K16ac regulatory axis, IHC staining levels were studied with respect to various tumour clinicopathological and biological parameters. To facilitate comparison, the data was categorised into low or high detection levels. The median H-score was used to categorise data into ‘low’ (Below or equal the median) or ‘high’ level staining (Above the median), as described in previous studies from the Nottingham Breast Unit (Habashy *et al.*, 2008a, Habashy *et al.*, 2009, Zhang *et al.*, 2009, Aleskandarany *et al.*, 2010).

Figure 3.2: Detection of the H4K16ac Regulatory Axis in Breast Cancer TMAs as determined by IHC.





Representative examples of breast tumour tissue cores presenting with low (left hand column) or ‘high’ H-scores (central column) for expression of the H4K16ac regulatory axis. H4K16ac (A, B); hMOF (D, E); SIRT1 (G, H); DBC1 (J, K); H3K9me3 (M, N); and SUV39H1 (P, K). The right hand column (C, F, I, L, O, R) shows the combined H-scores for each biomarker in this tumour set. Original magnification is x20, further magnifications are presented below.

H4K16ac Regulatory Axis in Relationship to Breast Cancer Histologic Tumour Types

H-score data was used to categorise tumours as ‘high’ or ‘low’ level detection for each of the H4K16-related biomarkers. The numbers for each category in relation to tumour type is shown in Table 3.1. No striking associations were apparent, although for most tumour types the numbers in the study are too low for meaningful statistical analysis. However, we noted a tendency for association of several of the biomarkers tested with lobular tumour type. 48 out of 77 (62%) of hMOF stained lobular tumours were ‘High’ score, which also had a tendency (73%) to score high for H4K16ac. In contrast, 43 out of 61 (70%) of SIRT1-stained lobular tumours were ‘low’ score. Invasive duct carcinoma/NOS type tumours scored tended to have lower levels of H4K16ac axis members. Medullary type tumours also tended to have lower levels of H4K16ac axis members, although fewer tumours were of this type were present in the sample. DBC1 levels did not show considerable variation among different tumour histopathological types. Furthermore, all mucinous tumour cases examined (6 cases) had high levels of both H3K9me3 and SUV39H1.

H4K16ac Regulatory Axis in Relationship to Breast Cancer Phenotypic Groups

Concerning breast cancer tumour phenotypes proposed by Nielson and colleagues (Nielsen et al., 2004), significant differences in H4K16ac and its regulator, the hMOF expression levels were noted where the *p* value in χ^2 test were below 0.003 (*p*<0.003 (Table 3.2). In particular, H4K16ac and hMOF tend to be low in

the poor prognostic HER2 type ($p=0.002$ and $p<0.001$). This proposes an association between low levels of H4K16ac regulatory axis components and tumour types associated with poor prognosis.

Similar results were obtained when correlating the data with breast cancer tumour phenotypes proposed by Abd El-Rehim and colleagues (Abd El-Rehim et al., 2005), (Table 3.3). Considerable differences were noted in the H4K16ac regulatory axis (Table 3.3). H4k16ac and hMOF levels were found predominantly low in HER2 tumours. All other marks except H3K9me3 were also low in HER2. In addition, hMOF and SIRT1, the H4K16ac regulators, tended to be low in basal tumours, especially those expressing normal p53. SUV39H1, the H3K9 methylation regulator, also tended to be low in basal-p53 normal tumours. On the other hand, although H3K9me3 levels did not show considerable differences among HER2 or basal tumours, significant differences in H3K9me3 and its regulator SUV39H1 levels were noted among luminal type B tumours (Tumour class characteristics is shown in Fig. 1.2).

Table 3:1: H4K16ac Regulatory Axis detection levels in Relationship to Tumour Histo-Pathological Types.

	H4K16ac		hMOF		SIRT1		DBC1		H3K9me3		SUV39H1	
	LD	HD	LD	HD								
Invasive Ductal/NOS Type	212	162	255	131	207	117	176	140	177	140	131	97
Invasive papillary	1	2	3	0	1	2	1	2	0	3	1	1
NST& Lobular	13	13	6	12	12	9	10	12	8	9	9	4
NST& Special	10	11	9	12	5	9	6	10	8	5	9	4
Classical lobular	29	48	21	56	43	18	33	27	21	34	15	32
Tubular	9	14	11	13	8	9	8	9	7	9	4	8
Tubular mixed	70	91	76	83	81	47	58	70	65	59	47	54
Medullary	14	6	16	6	14	5	10	8	15	3	10	5
Mucinous	2	5	2	5	3	1	2	2	0	6	0	5
Cribiform	4	2	4	2	1	3	2	3	1	1	2	1
Miscellaneous	2	1	3	1	2	1	2	1	1	0	2	1
Total	721		735		598		592		572		442	

LD, low detection; HD, high detection; NOS, no other specified.

Table 3:2: H4K16ac Regulatory Axis detection levels in Relationship to Tumour Phenotype groups of Breast Cancer as defined by Nielsen *et al* (Nielsen et al., 2004).

Nielsen classes of breast cancer (Nielsen et al., 2004)	H4K16ac			hMOF			SIRT1		
	LD	HD	p	LD	HD	p	LD	HD	p
Class			0.002			<0.001			0.775
HER2	41	24		52	16		42	19	
Luminal	182	224		189	222		202	126	
Basal-like	43	29		57	17		34	22	
Total	543			553			445		
Nielsen classes of breast cancer (Nielsen et al., 2004)	DBC1			H3K9me3			SUV39H1		
	LD	HD	p	LD	HD	p	LD	HD	p
Class			0.846			0.088			0.009
HER2	31	25		22	25		23	17	
Luminal	162	177		179	169		123	131	
Basal-like	38	21		47	26		31	12	
Total	454			468			337		

LD, low detection; HD, high detection; all *p* values are calculated by χ^2 test. Bonferroni correction test was applied and reduced the (*p*) value of significance to 0.003.

Table 3:3: H4K16ac Regulatory Axis detection levels and Phenotype groups of Breast Cancer as defined by Abe El-Rehim *et al* (Abd El-Rehim *et al.*, 2005).

Abd El-Rehim classes of breast cancer	H4K16ac		hMOF		SIRT1		DBC1		H3K9me3		SUV39H1	
	LD	HD	LD	HD	LD	HD	LD	HD	LD	HD	LD	HD
Luminal A	16	21	11	26	18	17	18	12	12	20	12	15
Luminal B	16	16	17	16	15	9	14	13	17	9	14	5
Luminal N	40	47	45	42	42	36	41	37	29	49	35	30
HER2	20	10	23	7	16	8	18	9	9	16	12	6
Basal-p53 altered	11	9	12	7	7	6	10	6	10	5	9	1
Basal-p53 normal	13	14	22	4	14	8	11	13	11	11	13	6
Not classified	58	59	69	53	63	37	55	44	48	46	44	30
Total	350		356		296		301		292		232	

LD, low detection; HD, high detection.

Correlation of H4K16ac Regulatory Axis with Clinicopathological Factors

Complete clinical and follow-up data for 835 of the 880 patient samples. Analysis of the data revealed a number of significant correlation with the biomarkers tested in this study (Table 3.4 and 3.5). In particular, tumour grade tended to correlate negatively with H4K16ac and hMOF ($p<0.001$ and $p<.001$ respectively). Low grade tumours were more likely to express high levels of H4K16ac and its regulators. Conversely, high-grade tumours were found to be less likely to express H4K16ac and its regulatory axis. In contrast, SIRT1 expression did not appear to correlate with tumour grade (Table 3.4).

Regarding Nottingham Prognostic Index (NPI), there was a tendency towards high H4K16ac detection in the good and moderate prognostic groups and low scores for this PTM in the poor prognostic group. Generally, H4K16ac was negatively correlated with NPI ($p=0.011$). Consistent with that, high hMOF expression was detected in more than half of the tumours within a good prognosis group and it tended to be low in a considerable part of the moderate and poor prognostic groups ($p<0.001$) (Table 3.4). A significant difference in SUV39H1 levels was also noted among various NPI categories. High SUV39H1 levels were found to be negatively correlated with NPI ($p<0.001$); where 58% (n=161) of the tumours of the good NPI category were found to be high in SUV39H1, 71% (n=56) of the poor category were low in SUV39H1 (Table 3.5).

A negative correlation was found for hMOF expression in large tumours ($>5\text{cm}$), as 63% scored as low for hMOF, although this was not observed for

H4K16Ac. Conversely, SIRT1 showed a trend toward positive correlation with tumour size ($p=0.03$), where big tumours ($>5\text{cm}$) tended to express higher SIRT1 levels (Table 3.4) which is consistent with a role for SIRT1 in proper growth and development in mice embryo (Cheng et al., 2003). High SUV39H1 levels negatively correlated with tumour size ($p=0.017$), where big tumours ($>5\text{cm}$) tended to express low SUV39H1 levels (Table 3.5), which was consistent with the identification of growth retardation in a mouse model when SUV39H1 was over expressed (Czvitkovich et al., 2001).

Correlation with other cancer biomarkers

Comparison of H-scores for our biomarker set to a range of other cancer biomarkers (14 biomarkers) for the 880 tumours detected a number of significant correlations (Table 3.5). The biomarkers showing significant correlation with H4K16ac, hMOF and SIRT1 are reported in Figure 3.4 whereas correlation data for H3K9me3, DBC1 and SUV39H1 are shown in Table 3.6. I have reported all significant correlations, but due to the large volume of data, I will summaries the main point we can extract from our data.

High scores for H4K16ac and hMOF expression were significantly associated with high levels of luminal cytokeratins CK7/8 and CK19 and low levels of basal cytokeratin 5/6 and CK14 (Table 3.4). This is consistent with the data in Table 3.2 showing a tendency for luminal tumours to have high scores for H4K16ac and hMOF; and the tendency for basal tumours to have low scores for both biomarkers. Steroid hormone receptors i.e. estrogen, progesterone and

androgen receptors which are usually good prognostic indicators in breast tumours, also correlated with high levels of hMOF and H4K16ac, in contrast to SIRT1 which did not show a correlation with steroid receptor status. Similarly forkhead-box A1 (FOXA1), previously described as a growth repressor in breast cancer (Habashy et al., 2008b), and BRCA1, the tumour suppressor gene BRCA1 (Lee et al., 2010) showed a tendency to positive correlation with high H4K16ac and hMOF (Table 3.4). In addition, both hMOF and H4K16 Ac showed a negative correlation with c-MYC (Cheng et al., 2006) and the mutated form of p53.

Table 3:4: H4K16ac, hMOF and SIRT1 Detection Levels in relationship to Tumour Clinicopathological Parameters; Biological factors.

Parameter	H4K16ac				hMOF				SIRT1			
	Total	LD	HD	p	Total	LD	HD	p	Total	LD	HD	p
Age	722			0.237	736			0.388	599			0.272
≤50		123	129			145	113			133	84	
>50		244	226			262	216			245	137	
Grade	722			<0.001	736			<0.001	599			0.015
I		63	95			73	88			69	59	
II		106	130			104	137			132	57	
III		198	130			230	104			177	105	
Stage	720			0.876	734			0.505	597			0.994
1		110	238			262	226			247	144	
2		90	82			102	75			95	55	
3		34	35			41	28			35	21	
NPI	720			0.011	734			<0.001	597			
Good		110	143			114	145			127	70	0.759
Moderate		198	172			221	155			201	117	
Poor		57	40			70	29			49	33	
Size	722			0.086	736			<0.001	599			0.03
< 5cm		224	235			239	233			256	132	
> 5cm		143	120			168	96			122	89	
LN Metastasis	720			0.417	734			0.144	597			0.528
Negative		241	238			262	226			247	144	
Positive		124	117			143	103			130	76	
ER receptor	668			0.001	680			<0.001	555			0.272
Low		126	88			160	60			122	66	
High		207	247			217	243			227	140	
PR receptor	658			0.017	671			<0.001	549			0.195
Negative		169	138			211	99			162	88	
Positive		163	188			164	197			182	117	
AR receptor	618			<0.001	631			<0.001	517			0.229
Negative		159	101			174	86			138	75	
Positive		157	201			170	201			186	118	
P53 (Altered)	664			0.030	676			<0.001	552			0.344
Negative		237	245			247	242			247	150	
positive		105	77			123	64			100	55	
CK7/8	693			0.005	708			<0.001	581			0.503
Negative		145	107			163	93			128	75	

Positive		208	233			228	224			237	141	
CK18	593			0.407	602			0.012	505			0.026
Negative		92	91			112	69			108	46	
positive		212	198			217	204			213	138	
CK19	690			0.037	702			0.003	575			0.200
Negative		79	57			90	45			77	38	
positive		272	282			303	264			286	174	
CK5/6	699			0.013	713			<0.001	584			0.074
Negative		260	273			275	267			295	160	
Positive		98	68			123	48			74	55	
CK14	676			0.051	691			<0.001	567			0.179
Negative		266	267			282	261			291	165	
positive		83	60			109	39			65	46	
c-MYC	340			0.001	343			0.045	276			0.010
Low		145	99			160	88			131	72	
High		39	57			71	24			35	38	
nBRCA1	504			<0.001	512			<0.001	430			0.016
Low		137	79			140	79			130	62	
High		110	178			137	156			136	102	
FOXA1	581			<0.001	591			<0.001	486			0.141
Low		176	132			214	98			169	100	
High		117	156			130	149			125	92	
FHIT	438			0.016	445			0.019	372			0.484
Low		133	112			142	112			131	82	
High		84	109			87	104			99	60	
EGFR	483			0.008	494			0.265	460			0.063
Low		203	196			216	191			228	143	
High		30	54			50	37			63	26	

LD, low detection; HD, high detection; LN, lymph node; ER, estrogen receptor, PR, progesterone receptor; AR, androgen receptor; all *p* values are calculated by χ^2 test. Bonferroni correction test was applied and reduced the (*p*) value of significance to 0.003.

DBC1, the negative regulator for SIRT1 exhibited striking associations with other biomarkers. Although DBC1 has been previously reported functionally interact with estrogen receptor (Trauernicht et al., 2007) and androgen receptors (Milne et al., 2007), no significant correlations in expression for these proteins were detected. We did note a tendency for ‘high’ DBC1 in low grade tumours (Table 3.5).

Low expression of SUV39H1 was associated with poor prognostic index (NPI), large tumour size, low expression of steroid receptors and was negatively correlated with luminal cytokeratins CK18 and CK19. SUV39H1 showed a positive association with FOXA1 and tumour suppressor FHIT; and inverse correlation with the poor prognostic marker FGFR (Haugsten et al., 2010). In addition, SUV39H1 and its product H3K9me3 levels were found to score lower in Grade III tumours (Table 3.5).

**3.5: H3K9me3, DBC1 and SUV39H1 Detection Levels in relationship to
Tumour Clinicopathological Parameters; Biological factors.**

Clinico-Pathological data	DBC1				H3K9me3				SUV39H1			
	Total	LD	HD	p	Total	LD	HD	p	Total	LD	HD	p
Age	593			0.302	573			0.231	442			0.516
≤50		114	98			103	100			82	75	
>50		195	186			201	169			148	137	
Grade	593			0.005	573			0.035	442			<0.002
I		51	78			59	67			47	60	
II		103	84			87	91			65	78	
III		155	122			158	111			118	74	
Stage	590			0.638	572			0.545	440			0.263
1		197	188			208	173			143	145	
2		77	71			70	70			61	51	
3		33	24			25	26			25	15	
NPI	590			0.057	572			0.156	440			<0.001
Good		93	107			95	100			67	94	
Moderate		165	146			172	131			122	101	
Poor		49	30			36	38			40	16	
Size	593			0.108	573			0.494	442			0.017
< 5cm		185	185			199	175			135	146	
> 5cm		124	99			105	94			95	66	
LN Metastasis	590			0.312	572			0.157	440			0.100
Negative		197	188			208	173			143	145	
Positive		110	95			95	96			86	66	
ER receptor	551			0.127	534			0.107	417			<0.001
Low		100	79			99	76			89	44	
High		187	185			181	178			132	152	
PR receptor	550			0.038	529			0.014	411			0.006
Negative		145	113			140	99			110	71	
Positive		141	151			141	149			110	120	
AR receptor	512			0.076	497			0.003	386			0.008
Negative		124	95			125	86			98	60	
Positive		146	147			132	154			112	116	
p53 (Altered)	553			0.098	529			0.080	409			0.162
Negative		198	199			191	182			155	145	
positive		88	68			91	65			63	46	
CK7/8	576			0.306	555			0.111	430			0.096
Negative		114	99			111	84			87	64	

Positive		185	178			184	176			141	138	
CK18	42			0.048	481			0.506	378			0.008
Negative		84	62			74	67			71	39	
positive		169	177			177	163			135	133	
CK19	753			0.343	547			0.029	424			0.028
Negative		60	50			63	38			51	29	
positive		240	223			229	217			176	168	
CK5/6	580			0.191	558			0.148	431			0.081
Negative		227	217			221	205			168	161	
Positive		76	60			76	56			58	44	
CK14	561			0.130	536			0.066	415			0.524
Negative		242	204			213	205			172	152	
positive		55	60			70	48			48	43	
c-MYC	275			0.546	258			0.066	210			0.098
Low		99	109			116	71			101	60	
High		32	35			36	35			25	24	
nBRCA1	428			0.004	412			<0.001	331			<0.001
Low		115	79			110	75			100	44	
High		108	126			95	132			82	105	
FOXA1	481			0.206	464			<0.001	355			<0.001
Low		140	124			157	100			131	72	
High		106	111			93	114			62	90	
FHIT	372			0.024	359			0.240	292			0.014
Low		120	90			109	102			95	72	
High		75	87			70	78			54	71	
EGFR	397			0.321	389			0.508	238			0.021
Low		169	161			165	152			112	114	
High		37	30			38	34			10	2	

LD, low detection; HD, high detection; LN, lymph node; ER, estrogen receptor, PR, progesterone receptor; AR, androgen receptor; all *p* values are calculated by χ^2 test. Bonferroni correction test was applied and reduced the (*p*) value of significance to 0.003.

Relationship to histone marks and their modulators

H4K16ac regulatory axis levels showed a correlation with most histone PTMs and modulators used in this study. Remarkably, high levels of H4K16ac were positively correlated with eight (H3K9ac, H3K18ac, H4K12ac, H4K16ac (abcam), H3K4me2, H3K9me3, H4R3me2 and H3K56ac) histone PTMs marks with highly significant *p* values (*p*<0.001) as shown in Table 3.6. Interestingly, high levels of a number of those histone PTMs, including H4K16ac (abcam antibody) have been already reported in association with favourable prognosis in breast cancer (Elsheikh et al., 2009). In addition, high levels of H4K16 correlated with high levels of histone acetyltransferase TIP60, hMOF and MORF and with high levels of the methyltransferase SUV39H1 (*p*<0.001). Strikingly, the DNA damage marker, H3K56ac (Masumoto et al., 2005, Vempati et al., 2010) was also correlated with high level of H4K16ac in a highly significant *p* value (*p*<0.001).

High levels of hMOF correlated with all histone PTMs marks studied in this work (Table 3.6). Specifically, with high levels of the active gene marks H3K9ac (Lindeman et al., 2010); the transcriptional activation mark H3K4me3 (Ruthenburg et al., 2007); H3K18ac; H4K12ac and as expected with H4K16ac (*p*<0.001). The positive correlation with histone acetylation marks other than H4K16 could be explained by either redundancy in hMOF activity or due to enhanced expression of other HATs. The DNA damage mark H3K56ac was positively correlated with hMOF which is consistent with the role for hMOF in the DNA damage response (Taipale et al., 2005). hMOF was also correlated with high levels of most HATs in our study, such as TIP60 and MORF (*p*=0.015 and *p*<0.001 respectively). Consistent with our hypothesis, although the *p* values were

not significant, hMOF levels were negatively correlated with HDACs (HDAC1, HDAC2 and SIRT1) levels. hMOF was found positively correlated with the repressed gene mark H3K9me3 (Derks et al., 2009, Snowden et al., 2002) and with the high levels of H3K9me3 modulator, the histone methyltransferase SUV39H1 (Bhaumik et al., 2007) ($p=0.01$ and 0.001 respectively). hMOF was found positively correlated with, H4K20me3 and H4R3me2 histone methylation marks, which might be a sign of histone PTMs cross talk, which is consistent with the reported ordered and interdependent deposition of acetylation and arginine methylation during histone PTMs during gene transcription (Daujat et al., 2002).

SIRT1 levels were correlated with a number of histone acetylation and methylation marks used in the study (Table 3.6). Although the differences in SIRT1 levels among some of them were not statistically significant, high levels of SIRT1 were positively correlated with the repressed gene marker H3K9me3 (Tachibana et al., 2005) which is consistent with the role of SIRT1 in inducing gene repression (Pruitt et al., 2006, Noshio et al., 2009); and H3K4me3 ($p=0.003$), the active gene mark (Tserel et al., 2010). Regarding HATs, differences in SIRT1 levels were not significant among any of them except MORF ($p=0.003$). As expected, SIRT1 was positively correlated with HDACs. Where, SIRT1 positively correlated with both HDAC1 and HDAC2 ($p=0.012$; 0.018 respectively), which is consistent with their deacetylase activity. Interestingly, DBC1 the negative regulator for SIRT1 was found positively correlated with SIRT1 in highly significant value ($p<0.001$).

Table 3:6: H4K16ac, hMOF and SIRT1 Detection Level and Histone PTMs and their Modulators.

Histone and Histone Modulators	H4K16ac				hMOF				SIRT1			
	Total	LD	HD	p	Total	LD	HD	p	Total	LD	HD	p
H3K9ac	500			<0.001	511			<0.001	428			0.151
Low		165	96			185	82			152	80	
High		83	156			119	125			118	78	
H3K18ac	506			<0.001	516			<0.001	431			0.017
Low		159	99			188	74			156	77	
High		93	155			119	135			112	86	
H4K12ac	484			<0.001	494			<0.001	414			0.017
Low		172	104			194	83			158	79	
High		70	138			100	117			99	78	
H4K16ac (Abcam)	519			<0.001	528			<0.001	444			0.106
Low		220	143			238	135			203	117	
High		42	114			66	89			70	54	
H4K16ac (Millipore)					741			<0.001	558			0.028
Low						247	133			187	101	
High						173	188			153	117	
H3K4me2	489			<0.001	498			<0.001	421			0.039
Low		169	95			181	83			155	81	
High		78	147			117	117			105	80	
H4K20me3	462			0.002	474			0.009	408			0.065
Low		52	27			56	23			54	25	
High		182	201			221	174			192	137	
H3K9me3	531			<0.001	543			0.010	519			0.001
Low		199	83			174	112			185	93	
High		75	174			130	127			127	114	
H4R3me2	554			<0.001	563			0.003	470			0.003
Low		189	134			211	117			197	95	
High		86	145			123	112			97	81	
H3k56ac	569			<0.001	584			<0.001	467			0.415
Low		194	102			196	107			148	97	
High		109	164			124	157			131	91	
MORF	491			0.001	504			<0.001	474			0.003
Low		143	105			151	101			168	76	
High		104	139			113	139			129	101	

TIP60	545			0.162	194			0.015	166		0.332
Low		155	50			72	19			49	36
High		137	68			66	37			43	38
hMOF	741			<0.001					566		0.259
Low		247	173							189	128
High		133	188							156	93
SUV39H1	411			0.001	423			0.001	393		0.324
Low		135	80			140	81			135	78
High		91	105			98	104			119	61
HDAC1	513			<0.001	524			0.420	475		0.012
Low		150	109			155	115			161	83
High		106	148			149	105			128	103
HDAC2	559			0.078	568			0.016	547		0.018
Low		134	154			126	120			161	79
High		109	162			195	127			178	129
SIRT1	558			0.082	566			0.259			
Low		146	120			189	128				
High		142	150			156	93				
DBC1	318			0.065	331			0.463	308		<0.001
Low		104	69			103	73			131	35
High		74	71			89	66			79	63

LD, low detection; HD, high detection; all p values are calculated by χ^2 test.

Bonferroni correction test was applied and reduced the (p) value of significance to

0.003.

High DBC1 levels were correlated with high levels of SIRT1; histone acetylation and methylation marks as shown in Table 3.7, which is consistent with its inhibitory role for the SIRT1 deacetylase activity (Kim et al., 2008).

A remarkable relationship between changes in H3K9me3 levels and the level of other histone PTMs and histone modulators was noticed. H3K9me3 levels correlated with all histone acetylation and methylation marks studied in this work. Specially, with high H3K4me2 levels, which is consistent with their tendency for substantial decrease during transcription (Wang et al., 2001, Li et al., 2002, Nishioka et al., 2002a). The rest of positive correlations with histone PTMs might be explained via H3K9me3 central role in a variety cellular function, and its involvement in diverse pathways. In addition, although H3K9me3 has been previously described as a repressed gene mark (Tachibana et al., 2005); when H3K9me3 and other histone PTMS were explored in cancer cell lines derived from different tissues; Immunoprecipitation (IP) study revealed H3K9me3 association with active genes rather than being a repressive mark as previously described (Wiencke et al., 2008). Consistent with H3K9me3 role in DNA damage (Sun et al., 2009), high levels of H3K9me3 correlated with high levels of H3K56ac and hMOF levels ($p<0.001$ and 0.010). High H3K9me3 levels were also correlated with high expression level of MORF ($p<0.001$), but not TIP60. H3K9me3 was found positively correlated with all HDACs where the p values were ($p=0.004$, $p<0.001$ and $p= 0.001$ respectively) for HDAC1, HDAC2 and SIRT1. This is really consistent with their role in inducing global gene repression (Wang et al., 2009b). As expected H3K9me3 expression level has been found

positively correlated ($p<0.001$) with its positive regulator, the histone methyltransferase SUV39H1 (Bhaumik et al., 2007); this is really consistent with the SUV39H1 role in inducing gene repression (O'Carroll et al., 2000, Rea et al., 2000, Bhaumik et al., 2007).

High SUV39H1 levels were found correlated with high level of all histone acetylation and methylation marks (Table 3.7). This suggests a close biological relationship between those histone marks and SUV39H1, or the involvement in same cellular pathways. For example, the positive correlation with the DNA damage mark H3K56ac ($p=0.011$) is consistent with SUV39H1 role in DNA damage response (Zhu et al., 2007). With regard to HATs, differences in SUV39H1 levels were significant among number of HATs. For example, SUV39H1 levels positively correlated with both MORF and hMOF levels ($p<0.001$ and $p=0.001$). But did not with high TIP60, although TIP60 was previously reported to attach to H3K9me3 during the repair of DNA double-strand break (Fischle, 2009). Consistently with the literature (Macaluso et al., 2003, Macaluso et al., 2006), high levels of SUV39H1 correlated with high HDAC1 levels ($p=0.042$), which consistent with their interaction *in vivo* in Drosophila and their involvement in the permanent silencing of transcription in particular areas of the genome (Czermin et al., 2001). Similarly, HDAC2 levels were also correlated with high SUV39H1 ($p=0.007$).

Table 3:7: H3K9me3, DBC1 and SUV39H1 Detection Level and Histone PTMs and their Modulators.

Histone and Histone Modulators	DBC1				H3K9me3				SUV39H1			
	Total	LD	HD	p	Total	LD	HD	p	Total	LD	HD	p
H3K9ac	425			0.004	417			<0.001	329			0.004
Low		135	94			133	80			109	64	
High		89	107			88	116			75	81	
H3K18ac	454			0.004	420			<0.001	329			<0.001
Low		131	92			142	73			113	59	
High		91	110			77	128			71	86	
H4K12ac	410			0.011	396			<0.001	311			<0.001
Low		134	101			148	69			113	64	
High		79	96			63	116			57	77	
H4K16ac (Millipore)	585			0.189	531			<0.001	411			0.001
Low		169	144			199	75			135	91	
High		136	136			83	174			80	105	
H3K4me2	414			0.012	407			<0.001	318			<0.001
Low		132	97			141	75			115	56	
High		85	100			72	119			63	84	
H4K20me3	394			0.048	390			<0.001	301			0.043
Low		40	26			48	19			34	17	
High		159	169			158	165			131	119	
H3K9me3	461			0.514					400			<0.001
Low		131	119							144	73	
High		110	101							73	110	
H4R3me2	474			0.131	452			<0.001	355			0.010
Low		160	130			172	97			129	80	
High		91	93			71	112			71	75	
H3k56ac	534			0.137	462			<0.001	382			0.011
Low		151	125			150	102			120	79	
High		128	130			90	120			88	95	
MORF	428			0.043	467			<0.001	388			<0.001
Low		124	97			144	98			118	83	
High		98	109			88	137			77	110	
TIP60	526			0.110	442			0.083	361			0.386
Low		141	120			116	92			91	74	
High		128	137			114	120			104	92	

hMOF	593			0.304	543			0.010	423			0.001
Low		178	160			174	130			140	98	
High		128	127			112	127			81	104	
SUV39H1	382			0.489	400			<0.001				
Low		110	101			144	73					
High		88	83			73	110					
HDAC1	434			0.009	475			0.004	364			0.042
Low		131	99			145	100			110	81	
High		92	112			107	123			83	90	
HDAC2	477			0.290	531			<0.001	405			0.007
Low		105	102			138	89			107	72	
High		145	125			138	166			106	120	
SIRT1	308			<0.001	519			0.001	393			0.324
Low		131	79			144	96			135	119	
High		35	63			134	145			78	61	
DBC1					461			0.514	382			0.489
Low						131	110			110	88	
High						119	101			101	83	

LD, low detection; HD, high detection; all *p* values are calculated by χ^2 test.

Bonferroni correction test was applied and reduced the (*p*) value of significance to 0.003.

H4K16ac regulatory axis and patient outcome

Our previous study identified H3K18 acetylation status as a significant independent prognostic indicator of patient survival (El Sheikh et al., 2009). A priority of this study was to determine whether components of the H4K16 regulatory axis show a correlation with patient outcome in breast cancer, and might therefore represent useful biomarkers in assessment of the disease. We therefore assessed the components of the H4K16 axis for their effects on patient outcome. Kaplan Meier curves analysing the whole breast cancer TMA cohort revealed that tumours scoring high for either H4K16ac, hMOF or SUV39H1 associated (Fig. 3.3) with increased breast cancer specific survival (BCSS) and longer disease free survival after surgical excision of the tumour (DFS). In contrast, no association with patient outcome was observed for SIRT1, DBC1 or H3K9me3 levels. Multivariate analysis using the Cox proportional regression model (Cox, 1972) showed that the prognostic effects of H4K16ac, SUV39H1 or hMOF were dependent on other key prognostic factors in breast cancer including histological grade, tumour size and tumour stage (Table 3.8). hMOF appears to be a good indicator of patient outcome and correlates well with H4K16 acetylation status (Table 3.6) . However, unlike other histone PTMs, H3K9me3 did not show an association with patient outcome, in contrast to its regulator SUV39H1. However, these results were a stimulus to undertake cluster analyses to determine if these markers together could give improved prognostic value.

Analysing the whole cohort of breast cancer TMA with respect to revealed that three out of six marks (H4K16ac, hMOF and SUV39H1) were found associated with both favourable breast cancer specific survival (BCSS) and longer

disease free survival (DFS). In particular, the ‘high’ H4K16ac group tended to live longer than the low-H4K16ac ($p=0.030$). In addition, ‘high’ H4K16ac was also associated with longer disease-free interval after tumour excision as compared to the low H4K16ac group ($p=0.020$) (Fig. 3.3).

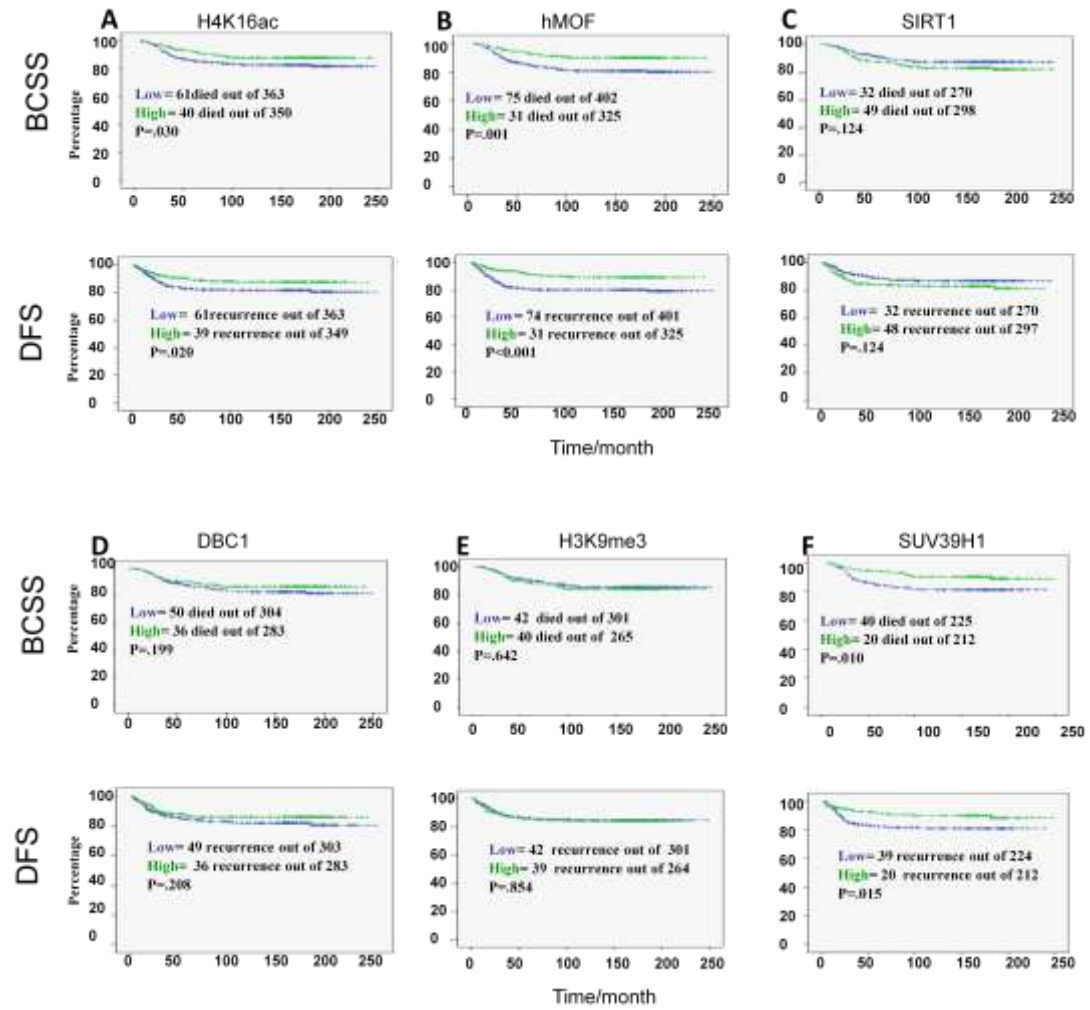
With regard to hMOF, high detection levels of hMOF showed highly significant associations with favourable BCSS and DFS ($p=0.001$). This is consistent with the importance of hMOF protein level as a marker for good tumour outcome and patient survival.

Kaplan Meier curves revealed a trend towards low level expression of SIRT1 in association with longer BCSS and DFS, although the differences were not statistically significant. A similar trend was observed for high expression of DBC1, the negative regulator for SIRT1 although again the association was not statistically significant.

Although trimethylation of H3K9 showed no association with patient outcome, the methyltransferase responsible for this PTM i.e. SUV39H1 appears to be a favourable prognostic indicator. High level expression of SUV39H1 was significantly associated with both longer BCSS and DFS ($p=0.010$ and $p=0.015$ respectively).

Multivariate analysis by using Cox proportional regression model (Cox, 1972) showed that the prognostic effect of H4K16ac regulatory axis members on survival was dependent on other key prognostic factors in breast cancer including

histological grade, tumour size, tumour stage and lymph node stage. However, the diverse association between the members of H4K16ac regulatory axis and patient outcome was a stimulus for further assessment of this pathway in breast tumours.

Figure 3.3: H4K16ac Regulatory Axis and Patient Outcome.

Kaplan-Meier curves for levels of H4K16ac regulatory axis in breast cancer TMA with respect to Breast cancer specific survival (BCSS) and disease free survival (DFS). The green and blue colours represent in order high and low detection group for each marker, the Y axis represent survival probability, X axis represent time relapse in months.

Table 3:8: Cox proportional Hazard Model Showing Hazard Ratios for BCSS and DFS conferred by H4K16ac, hMOF, SUV39H1 and clinicopathological variables

A

BCSS			
Variable	Hazard Ratio	95% CI	p
Tumour size (cm)	0.633	0.310 to 1.009	0.054
Tumour stage	1.439	1.310 to 2.689	0.001
Grade	2.215	1.428 to 4.070	0.001
H4K16ac (high)	0.556	0.539 to 1.674	0.859
hMOF (high)	0.577	0.598 to 2.147	0.701
SUV39H1	0.521	0.943 to 3.230	0.076

B

DFS			
Variable	Hazard Ratio	95% CI	p
Tumour size (cm)	0.632	0.292 to 0.974	0.041
Tumour stage	1.44	1.338 to 2.795	<0.001
Grade	2.213	1.415 to 4.054	0.001
H4K16ac (high)	0.557	0.607 to 1.927	0.790
hMOF (high)	0.576	0.947 to 3.218	0.712
SUV39H1	0.520		0.074

A, H4K16ac, hMOF and SUV39H1 are dependent of other prognostic factors in breast cancer with respect to breast cancer specific survival (BCSS); **(B)**, and disease free survival (DFS); CI, confidence interval ; p, χ^2 p value.

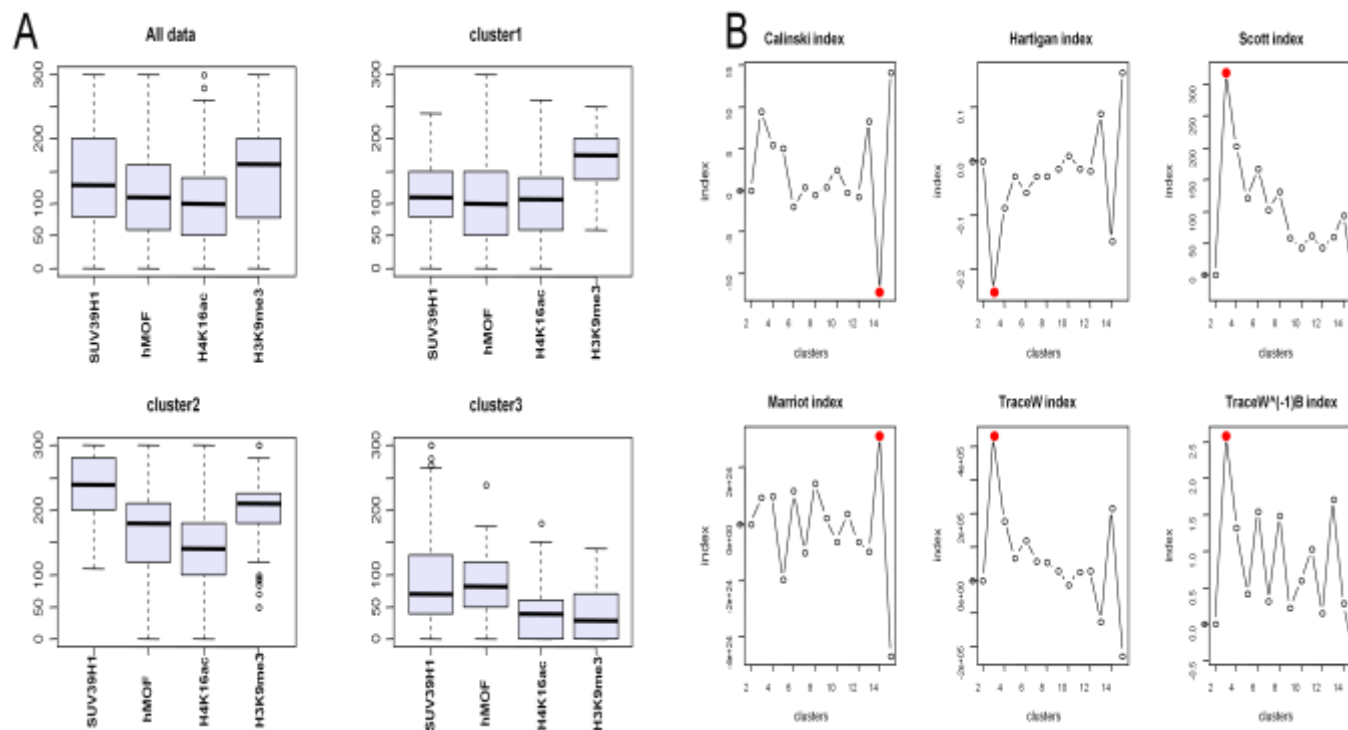
Cluster analysis of H4K16ac regulatory axis

To explore the relationship between individual components of the H4K16ac regulatory axis with regard to patient survival, an unsupervised cluster analysis was performed. This work was performed with the assistance of Dr. Daniel Soria, (School of Computer science, Nottingham University). Two different algorithms were used for cluster analysis: the K-means and the partitioning around medoids (PAM) methods. Both methods run for clusters ranging from 2 to 20 clusters. Six validity indices tests were followed to determine the best number of clusters. The used indices are Calinski and Harabasz, Hartigan, Scott and Symons, Marriot, TraceW, and TraceW-1B. The number of groups considered in each index was chosen according to the rules previously reported (Wiley, 1990).

Initial attempts to perform, cluster analysis on all markers i.e. H4K16ac, hMOF, SIRT1, DBC1, H3K9me3 and SUV39H1 was unsuccessful due to lower number of samples scored for DBC1. Therefore, DBC1 was discarded from the analysis. Cluster analysis with the remaining 5 markers yielded 4 common cluster groups, obtained from 301 cores stained for each marker. However, SIRT1 distribution among the cluster groups had no striking effect. So, SIRT1 was also discarded from the cluster; which retained 46 more cores. Finally, the established cluster groups (N=347) were based only on four marks: H4K16ac, hMOF, H3K9me3 and SUV39H1 distributed on three common cluster groups. The cluster numbers yielded in K-means algorithms was found consistent in 4 (Hartingen, Scott, TraceW, and TraceW-1B) out of the 6 validity indices tests (Fig. 3.4). Moreover, the cluster numbers obtained by PAM algorithms were validated by the 6 validity indices tests (Fig. 3.5). Remarkably, cluster 2 which is characterized

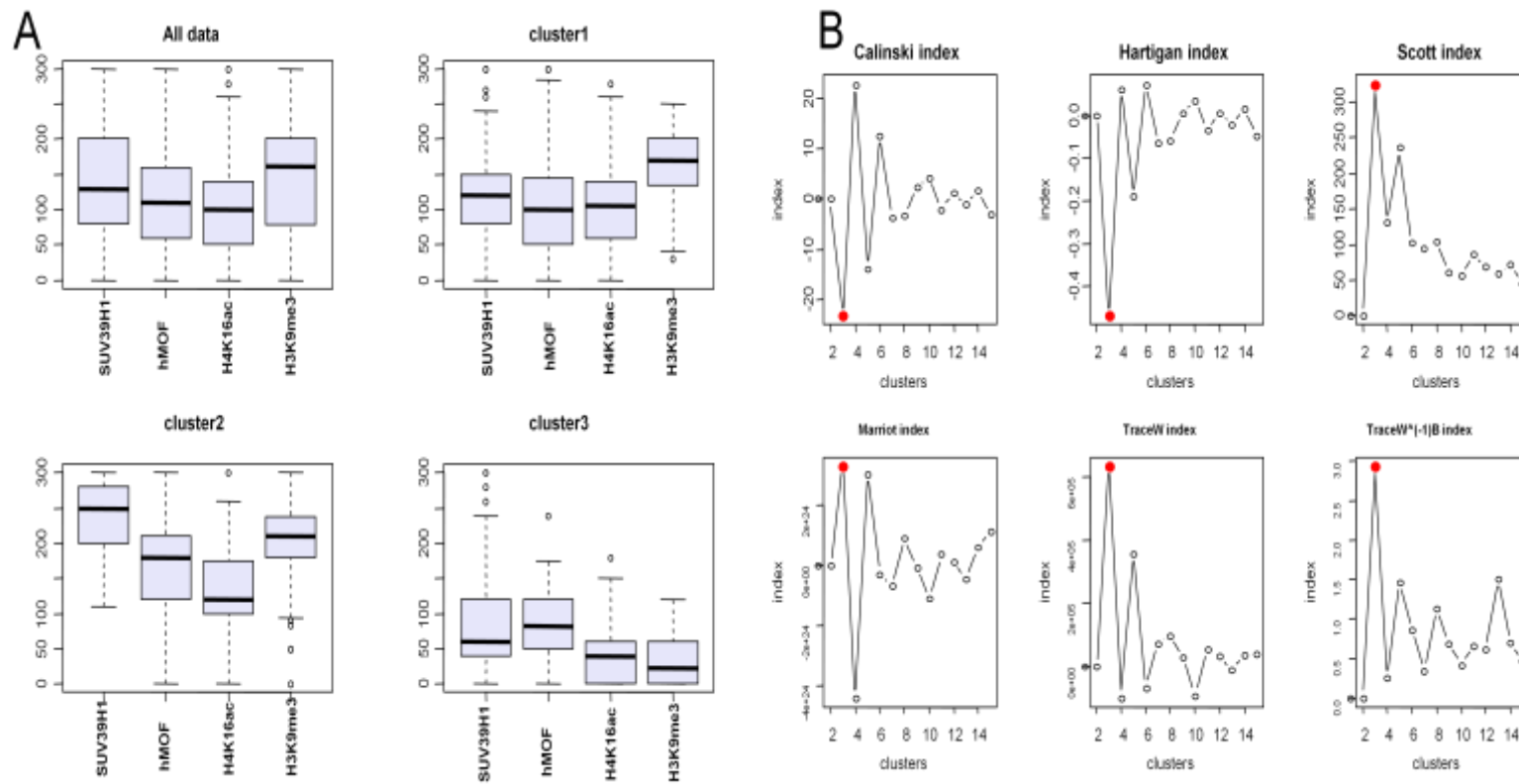
by high level of SUV39H1, hMOF and H4K16ac was found to be correlated with low tumour grades and better survival (Fig. 3.6), consistent with the hypothesis these markers may be useful indicators in breast tumours.

Figure 3.4: K-means Clustering Algorithm for Breast Cancer Tumour TMA in Regards to H4K16ac Regulatory Axis detection Levels and Validity Indices tests.



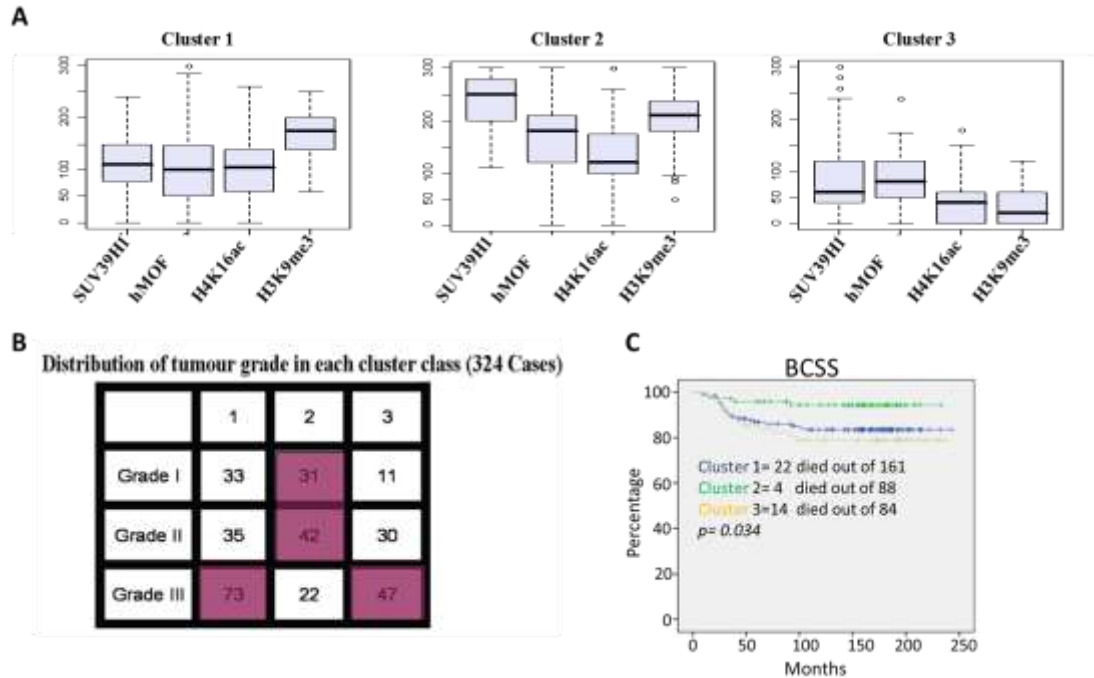
A, Boxplots for H4K16ac, hMOF, H3K9me3 and SUV39H1 grouped by K-means algorithm; **B**, Four out of six validity indices tests indicate 3 clusters.

Figure 3.5: PAM Clustering Algorithm for Breast Cancer Tumour TMA in Regards to H4K16ac Regulatory Axis Detection Levels and Validity Indices Tests.



A, Boxplots for H4K16ac, hMOF, H3K9me3 and SUV39H1 grouped by K-means algorithm; **B**, All validity indices tests indicate 3 clusters.

Figure 3.6: Common Clustering of H4K16ac Regulatory Axis, Cluster 2 Correlates with Favourable Tumour Grade and Better Survival.



A, Boxplots for H4K16ac, hMOF, H3K9me3 and SUV39H1 grouped by common clusters, Cluster 2 is characterized by high levels of H4K16ac, hMOF and SUV39H1 in comparison to other two clusters; **B**, Cluster 2 correlates with the favourable grades I and II, cluster 1 and 3 correlate with ominous grade III; **C**, unadjusted Kaplan-Meier curves for H4K16ac regulatory axis common clusters is showing cluster 2 correlating with favourable patient outcome.

Summary of Findings: The H4K16ac Regulatory Axis in Breast tumours

In this Chapter we examined expression levels in breast tumours of proteins or histone PTMs that are functionally related to H4K16 acetylation. The H-score data for each tumour was categorised as high or low and correlated with tumour histological/phenotypic types, clinicopathological factors, and tumour biological markers. In addition, we examined the relationship of the H4K16 axis with patient outcome. The data indicates hMOF, the factor that contributes to the establishment of H4K16 acetylation, tends to correlate with this PTM, as might be expected from the proposed functional relationship. Moreover, tumours that score high for H4K16ac tend to also have high levels of H3K56ac as well as other ‘active’ markers H3K18ac, and also H4K20me3. In general H4K16ac and its positive regulators tend to show an association with favourable tumour grade, tumour type and other favourable clinicopathological markers. Most importantly, cluster analysis using hMOF, SUV39H1, H3K9me3 and H4K16ac defined a patient group that had shown significantly improved post-operative survival and lower recurrence of the disease.

H4K16ac has been variously implicated as a marker of active genes and DNA repair, but also has a role in establishment of gene repression. The acetylation of histone H4K16 specifically disrupts the formation of higher-order chromatin structures (Shogren-Knaak et al., 2006). The opened chromatin configuration provides accessibility for specific transcription factors and the general transcription machinery (Glozak and Seto, 2007). In yeast, H4K16ac is a prerequisite for the methylation of H3K79 by the DOT methyltransferase (Altaf et al., 2007). Together with H3K56ac, these PTMs repel the recruitment of the Sir3

repressor and thus halt the spread of repressive heterochromatin into active genes (Oppikofer et al., 2011). However, H4K16ac is also important to establish repressive chromatin. In yeast, recent evidence indicates that acetylated H4K16 repels the recruitment of Sir3 to chromatin, but, stimulates recruitment of Sir2-4 dimers. Subsequent deacetylation of H4K16 by Sir2-4 can then promote recruitment of the Sir2-3-4 holocomplex (Oppikofer et al., 2011). The understanding of this pathway in human cells is less advanced, therefore it is possible that other Sirtuin proteins may be involved, and their expression in breast tumours should be investigated.

Acetylation of H4K16 is a critical step during cell replication; particularly, it has been observed during S-phase just prior to H4K20 di-methylation in early replicating chromatin domains. This epigenetic label then persists on the chromatin throughout mitosis and become deacetylated during early G1-phase (Fidlerova et al., 2009). Knock down of hMOF activity, the H4K16ac regulator, in a HeLa cell line cells, resulted in accumulation of cells in the G2 and M phases of the cell cycle (Taipale et al., 2005). Both H4K16ac and H3K56ac have been implicated in repair of DNA damage (Raisner and Madhani, 2008) and have been seen to be enriched in γ H2A.X foci along with TIP60 (Kusch et al., 2004) (Rossetto et al., 2010), a MYST domain acetyltransferase that can also acetylate H4K16 (Miyamoto et al., 2008).

It is therefore intriguing that H4K16 acetylation appears reduced in most cancer cell lines and in tumour tissues in TMA studies, particular in those tumours with poorest prognosis. This may reflect a global increase in repressive

chromatin needed to silence tumour suppressor genes and apoptotic gene pathways. It might also indicate a failure in the DNA damage repair and genome maintenance processes, or indicate more rapid turnover of this PTM in proliferating tumour cells, due to enhanced activity of NAD-dependent HDACs. As H4K16 acetylation is globally attenuated in G2/M (Vaquero et al., 2006), low level may indicate a high proportion of tumours cells undergoing mitosis. 'Clippases' have been identified in yeast that can remove histone N-terminal tails (Best and Carey, 2010, Bannister and Kouzarides, 2011). Deregulation of such enzymes in tumours might lead to global loss of histone N-terminal tails (and their associated PTMs) and failure of genome regulation as observed in many tumour cells. Resolving these mechanisms will be the goals of future studies.

hMOF is the major enzyme responsible for H4K16ac establishment in normal cells (Kapoor-Vazirani et al., 2008, Gupta et al., 2008). Ablation of hMOF results in defective cell cycle progression, reduced transcription of certain genes and impaired DNA damage response after irradiation (Rea et al., 2007). Optimisation of hMOF antibody concentration to be used in IHC staining revealed that the working concentration was 1/8. This is relatively high concentration suggesting low antibody sensitivity. Our results demonstrate that low level hMOF expression is associated with poorly differentiated high grade tumours.

SIRT1 has a wide range of biological functions, as it participates in growth regulation, stress response, tumourgenesis, endocrine signalling and control of cellular lifespan (Kim and Um, 2008). It functions by promoting gene silencing (Noshio et al., 2009) and thus inhibition of SIRT1 can reactivate silenced

genes (Pruitt et al., 2006), suggesting it as an attractive therapeutic target (Noshio et al., 2009). SIRT1 coordinates facultative heterochromatin formation (Vaquero et al., 2004) through its ability to deacetylate H4K16 and SUV39H1 during heterochromatin formation (Hajji et al., 2009, Vaquero et al., 2006, Vaquero et al., 2007). While SIRT1 has been reported to be cytoplasmic during most of the cell cycle, it shifts to the nucleus during the G2/M transition phase, corresponding with global attenuation of H4K16 acetylation in mammalian fibroblasts (Vaquero et al., 2006). Mouse embryonic fibroblasts (MEFs) deficient in SIRT1 exhibit increased levels and mislocalised H4K16ac during S phase (Vaquero et al., 2006). We did not detect a strong association of nuclear SIRT1 expression in tumours with patient outcome, tumour grade, tumour phenotype or other biomarkers. However, this highlights the importance of screening for proteins that regulate SIRT1 activity, such as the negative regulator Deleted in Breast Cancer (DBC1) (Kim et al., 2008; Zhao et al., 2008b; Anantharaman and Aravind, 2008).

DBC1 and SIRT1 expression in breast tumours showed a positive correlation consistent with a recent study that showed elevated level of both SIRT1 and DBC1 in breast cancer (Sung et al., 2010). Previous studies have reported associations of DBC1 and SIRT1 expression in breast tumours, although using far fewer cases than in this study, i.e. 28 tumours (Sung et al., 2010) or 110 tumours (Lee et al., 2011). Sung *et al.* (2010) reported higher SIRT1 and DBC1 protein levels in breast tumour tissue compared to their matched normal tissue; Lee *et al.*, (2011) reported a positive correlation between SIRT1 and DBC1 in breast tumour tissue. In addition, our results indicated that most tumours express SIRT1 possibly reflecting its vital role in tissue growth and development, and the

hazardous effects of SIRT1 over expression in ovarian and prostate tumours (Jang et al., 2009, Jung-Hynes et al., 2009). SIRT1 levels were found highly expressed in malignant ovarian epithelial tumours and prostate cancer. In addition, it was associated with poor prognosis in large B cell lymphoma and gastric carcinoma (Jang et al., 2008, Cha et al., 2009). When SIRT1 and DBC1 levels were assessed in fresh frozen breast cancer tissue; the study revealed that their over expression in breast cancer tumour tissue was correlated with both favourable and unfavourable clinicopathological factors, suggesting their pleiotropic functions as a potential tumour promoter and tumour suppressor in tumourgenesis (Sung et al., 2010). Although, the study was done on smaller sized population (28 cases); it could explain the conflict in our results that showed high grade tumours tending to express low SIRT1 levels; however, smaller tumours (<5cm) tend to express low SIRT1 level. Thus, the role of SIRT1 in breast tumours remains unclear.

The DBC1 protein (Hamaguchi et al., 2002) is reported to be a key negative regulator of SIRT1 (Zhao et al., 2008, Kim et al., 2008). DBC1-mediated repression of SIRT1 leads to increased p53 acetylation and upregulation of p53-mediated function (Zhao et al., 2008) and is thus considered to function as a tumour suppressor (Kim et al., 2008, Zhao et al., 2008). When SIRT1 and DBC1 expression levels were explored in gastric carcinoma by TMA in 177 gastric tumours, DBC1 positive tumours correlated with SIRT1 positive tumours; DBC1 was found to be significantly correlated with advanced tumour stage, shorter overall survival and disease-free survival (Cha et al., 2009). In addition, Lee *et al.* (2011) reported that high DBC1 and SIRT1 levels in breast cancer

tissue were associated with advanced tumour grade, shorter survival and distant metastatic relapse in breast cancer tissue, suggesting them as significant prognostic indicators for breast carcinoma patients.

A previous study by the Breast Cancer Pathology Research Group at Nottingham University using the same breast tumour archive analysed the relationship between tumour type, epithelial cell lineage, hormone and growth factor receptors Abd El-Rehim *et al.* (2005). This study identified six classes of breast tumour using cluster analyses. Soria *et al.* (2010) validated these data with different clustering algorithms and identified novel breast cancer sub-groups. Elsheikh *et al.* (2009) used cluster analysis to show that breast tumours can be separated into biologically and prognostically distinct groups depending on their histone modification pattern. However, the histone PTMs examined in that study were chosen at random as opposed to having a biological or functional basis. In this study cluster analysis of components of the H4K16ac regulatory axis showed that breast cancer tumours can be classified into biologically and prognostically distinct groups, where high levels of H4K16ac, hMOF and SUV39H1 group were correlated with favourable tumour grade and breast cancer specific survival. Our findings suggest that SUV39H1, in particular has prognostic value, although one of its targets 3meH3K9 did not show an association with survival. Thus, methylation of H3 may be subject to redundancy in that other enzymes may also target this residue. Alternatively, SUV39H1 may have other functions outside of H3 methylation which are important for tumour suppression.

3.2 : Histone Variants in Breast Cancer

Histone variants perform specialised functions in the cell, and are increasingly topical as important regulators of nuclear processes. In particular variants of the H2A histone have recently been identified as performing specific functions within chromatin as outlined in Chapter 1 (1.2.9). However relatively few studies have assessed whether histone variants such as H2A.Z and macroH2A expression levels are altered in tumours. For this reason we next turned our attention to study the expression of these histones in breast tumours. This study was performed in collaboration with Prof. Stefan Dimitrov, University of Grenoble, who provided specific antibodies for the study.

.

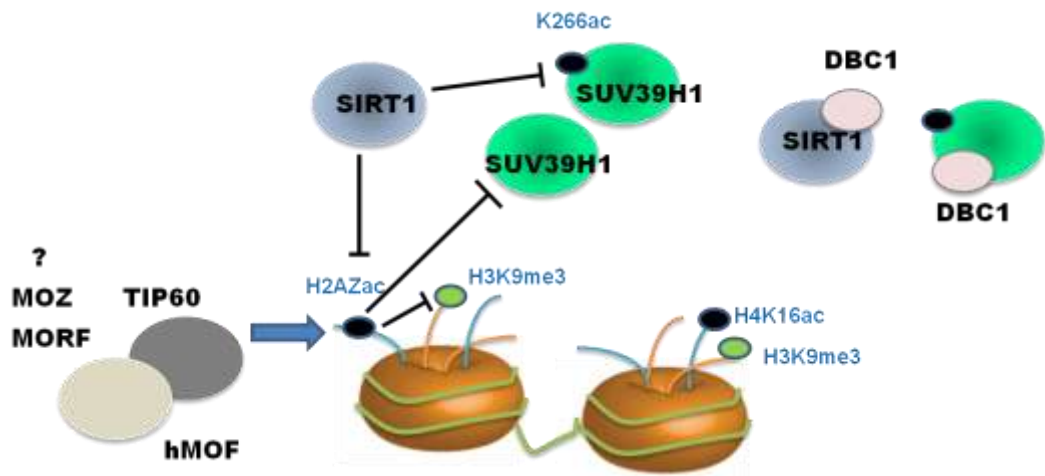
Macro H2A is involved in a number of cellular functions including nucleosomal remodelling (Angelov et al., 2003), inactive X chromosome (Costanzi and Pehrson, 1998), transcription repression (Angelov et al., 2003, Doyen et al., 2006, Ouararhni et al., 2006), and heterochromatin formation in association with heterochromatin markers (histone H3K27me2 and H327me3) (Araya et al., 2010). In addition, it has a potential role in tumour progression. Knocking down of mH2A in melanoma cells resulted in significantly increased proliferation and migration *in vitro* and growth and metastasis *in vivo* (Kapoor et al., 2010).

H2A.Z has been described as a marker for active genes, although like most regulatory proteins it can have both positive and negative roles in gene regulation (Marques et al., 2010). In yeast, H2A.Z replaces H2A at active genes and is inserted into chromatin by Swr1 and Swr1-like complexes, where it induces

biophysical changes in the nucleosome (Placek et al., 2005). In addition to roles in transcription initiation and elongation, H2A.Z is required for heterochromatin integrity (Rangasamy et al., 2003), guarding against heterochromatin propagation (Shia et al., 2006). H2A.Z has also a role in DNA damage repair (Ahmed et al., 2007, Gevry et al., 2007) and for recruitment of transcription factors (Fu et al., 2008, Draker and Cheung, 2009, Lemieux et al., 2008). Acetylation of H2A.Z were linked to genome-wide gene activity in yeast (Millar et al., 2006), chicken (Bruce et al., 2005) and mammalian cells (Chen et al., 2006). Genome wide studies have found that acetylated H2A.Z is enriched at the boundaries of active and poised genes (Valdez-Mora 2011).

Deacetylation of H2A.Z in mammalian cells is catalysed by SIRT1, which regulates H2A.Z turnover via ubiquitin/proteasome-dependent pathway (Chen et al., 2006, Seligson et al., 2009) (Fig. 3.7). Conversely, H2A.Z was found to prevent SIR-dependent gene repression in yeast (Venkatasubrahmanyam et al., 2007), suggesting a feedback relationship between H2A.Z acetylation and SIRT1. H2A.Z was reported to inversely localize with H3K9me3 and its modulators SUV39h1 at heterochromatin loci (Bulynko et al., 2006). In summary, H2A.Z plays a pivotal role in gene regulation and its acetylation has functional links with the H4K16ac pathway.

In this next section, I assess the levels of mH2A, H2A.Z and the acetylated form of H2A.Z (H2A.Zac) in breast tumours and explore their association with clinicopathological parameters, other biomarkers and patient outcome.

Figure 3.7: Histone PTMs, HATs and HDACs Relationship

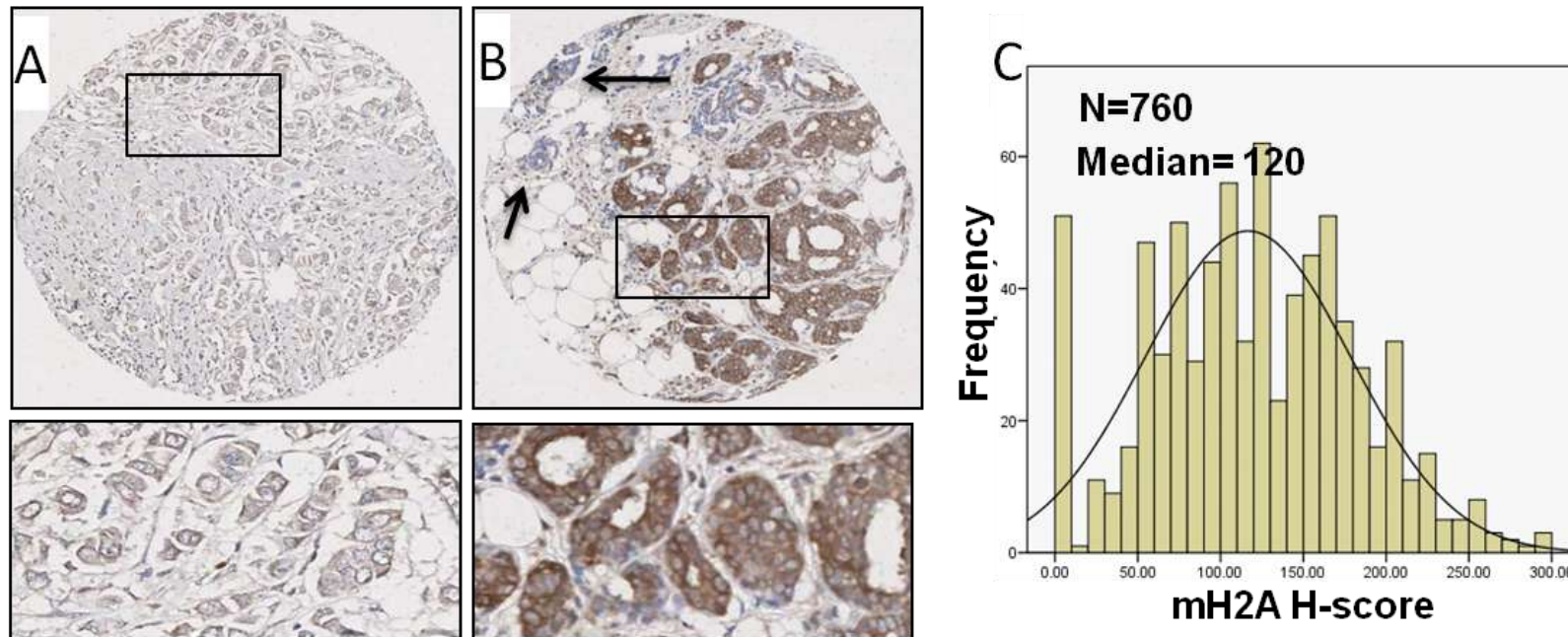
H2A.Z inversely localizes with H3K9me3 and its modulators SUV39h1 at heterochromatin loci. H2A.Z is subjected to acetylation/deacetylation by Histone acetyltransferases (HATs). Deacetylation of H2A.Z in mammalian cells is catalysed by SIRT1, which regulates H2A.Z turnover via ubiquitin/proteasome-dependent pathway. At the same time, H2A.Z prevents SIRT1-dependent gene repression.

3.2.1 Detection of Histone Variants in Breast Tumour TMAs

The TMA set used in the previous section was also IHC stained for the presence of histone variants mH2A, H2A.Z and the pan-acetyl form of H2A.Z. The antibodies used were provided by Prof. Stefan Dimitrov (U. Grenoble). Working dilutions and the method of antigen retrieval are described in Appendix 1. The staining patterns observed were close to homogeneous in most of the examined cores; with variation in staining intensity between different cases (Fig. 3.8, 3.9 and 3.10A and B). Evaluation of the stained cores showed immunoreactivity in all tumour cells for both mH2A and H2A.Z (Fig. 3.8 and 3.9). Positive reactivity was also noted in the nuclei of myoepithelial, stromal and inflammatory cells (Fig. 3.8 and 3.9). However, cores stained for H2A.Zac showed an attenuated immunoreactivity in myoepithelial, stromal and inflammatory cell nuclei relative to tumour cells (arrows in Fig.3.10). H-scoring for all cores stained revealed 760, 774 and 600 valid cores for mH2A, H2A.Z and H2A.Zac respectively. Histograms illustrating the frequency for H-score for each mark plotted against the number of cases are shown in Figure 3.8C, 3.9C and 3.10C. Fifty cores were totally negative for mH2A. However, only ten cores were negative for both H2A.Z and H2A.Zac.

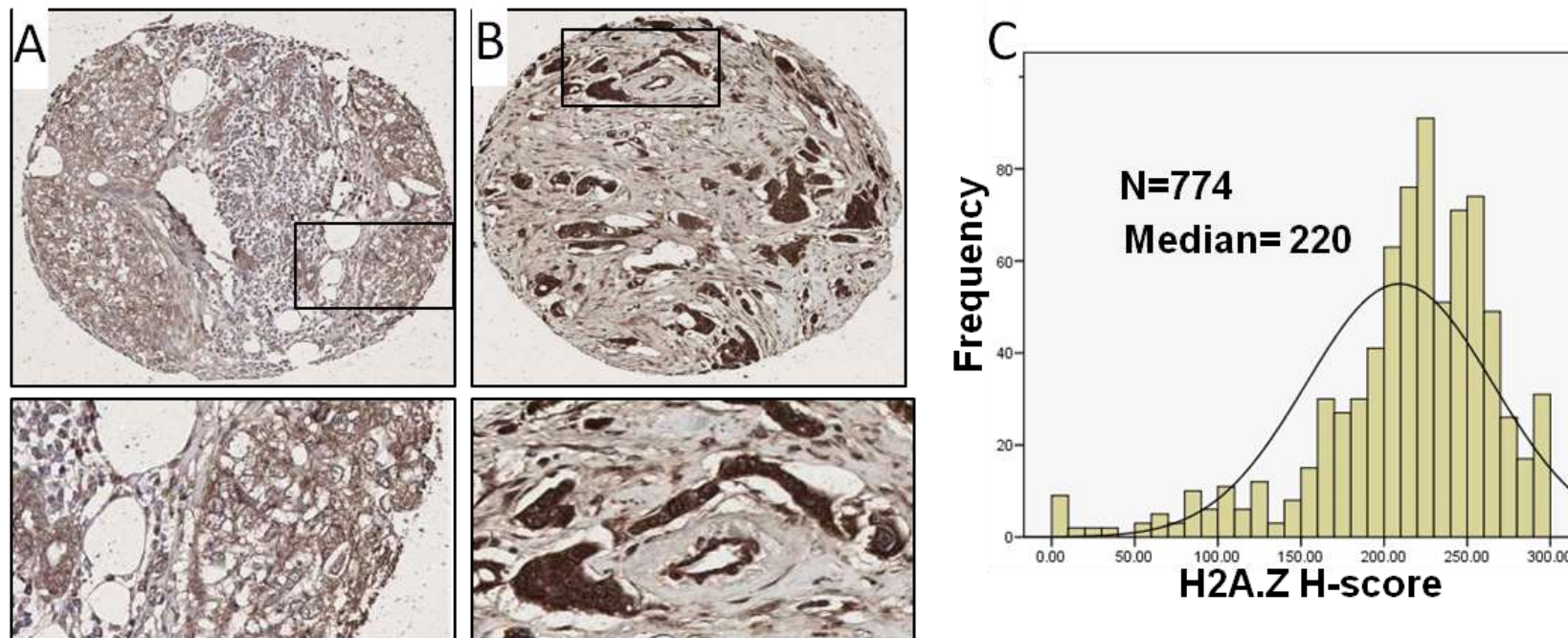
As in the previous section, H-score data was used to dichotomize the tumour cores into two groups (low and high) according to the median values (Fig. 3.8C). Any H-score between zero and the median value was considered to be in the low detection group, any score above median to 300 was considered among the high detection group.

Figure 3.8: Detection of mH2A in Breast Cancer TMAs as determined by IHC



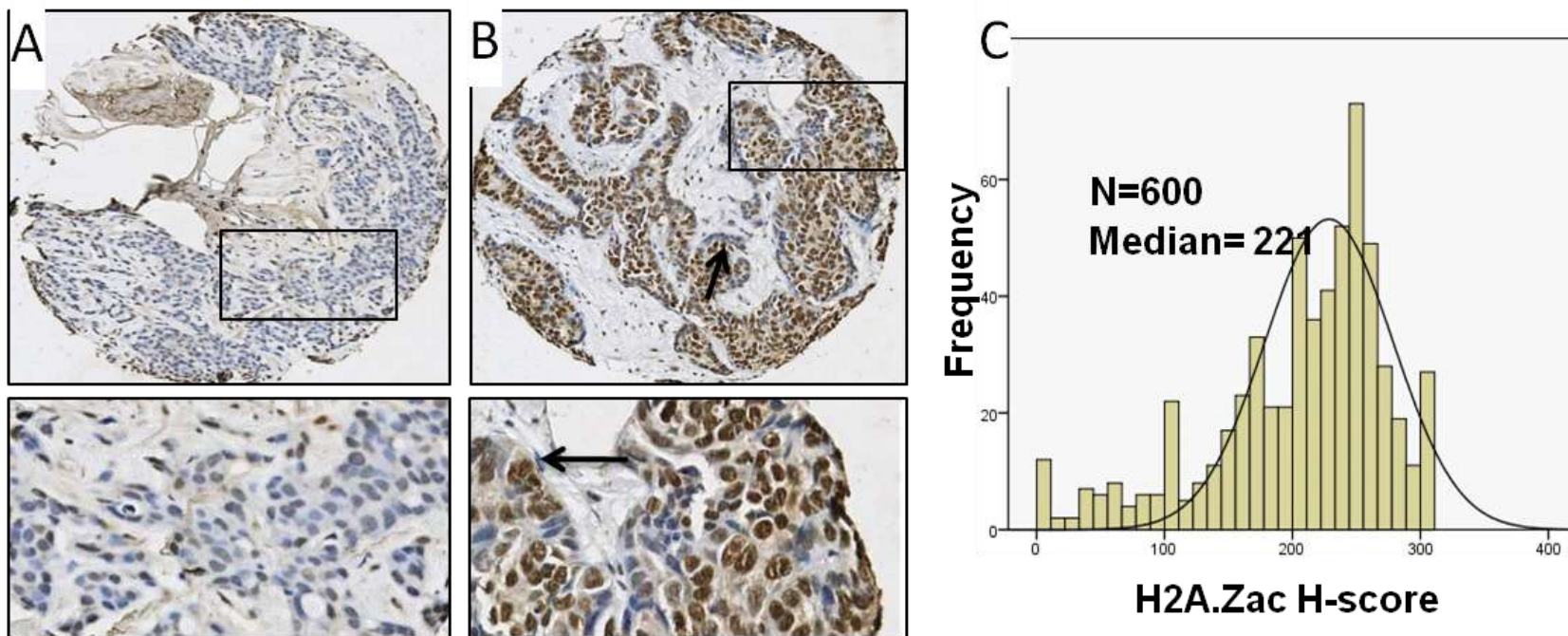
Breast tumour tissue cores presenting with low level (**A**) or high level (**B**) of mH2A; distribution of H-scores of breast cancer cores stained for mH2A (**C**). Non- tumourous tissue is low for mH2A (arrows). Original magnification is X20.

Figure 3.9: Detection of H2A.Z in Breast Cancer TMAs as determined by IHC



Breast tumour tissue cores presenting with low level (**A**) or high level (**B**) of H2A.Z; distribution of H-scores of breast cancer cores stained for H2A.Z (**C**). Original magnification is X20.

Figure 3.10: Detection of H2A.Zac in Breast Cancer TMAs as determined by IHC



Breast tumour tissue cores presenting with low level (A) or high level (B) of H2A.Zac; distribution of H-scores of breast cancer cores stained for H2A.Zac (C). Myoepithelial cells are low in H2A.Zac staining (Arrows). Original magnification is X20.

Histone Variants in Relationship to Breast Cancer Histologic Tumour Types

The data indicated associations of H2A variants with tumour histopathological types (Table 3.9). Low detection levels of mH2A and H2A.Z were seen among invasive ductal/ NOS and medullary tumours, where 233 out of 378 (62%) and 233 out of 383 (61%) invasive duct/ NOS tumours were low for mH2A and H2A.Z respectively. In medullary tumours, 17 out of 22 (77%) and 18 out of 21 (86%) scored low for mH2A and H2A.Z respectively. In addition, low H2A.Z levels were encountered among the well differentiated tubular and mucinous tumours, for example 16 out of 32 (69%) tubular type tumours and 6 out of 7 (86%) of mucinous tumour tumours were low in H2A.Z. In contrast, classical lobular tumours were more likely to exhibit high expression levels of both mH2A and H2A.Z i.e. 43 out of 73 (59%) of lobular tumours scored high for mH2A; 47 out of 80 (59%) stained ‘high’ for H2A.Z. Interestingly, H2A.Zac detection levels did not show considerable variation among most tumour histopathological types, with the exception of mucinous and cribriform tumours, which tended to express low level of H2A.Zac. Indeed, 5 out of 6 cases of mucinous tumour and 3 out of 4 cases of cribriform tumour low in H2A.Zac.

Histone Variants in Relationship to Breast Cancer Phenotypic Groups

Significant differences in both mH2A and H2A.Z levels were observed ($p<0.001$) with regard to Nielsen’s tumour phenotypes. The poor prognostic markers HER2 and basal tumour types were characterized by low levels of both mH2A and H2A.Z (Table 3.10). These results suggest an association between low detection levels of both marks with specific classes of breast cancer characterized by poor

prognosis. In regards to H2A.Zac, no statistically significant differences were observed among Nielson classes.

Corresponding to breast cancer tumour phenotypes proposed by Abd El-Rehim and colleagues (Abd El-Rehim et al., 2005), considerable differences were noted among basal tumours stained for mH2A H2A.Z and H2A.Zac. Both basal groups tended to express low levels for mH2A, H2A.Z and H2A.Zac irrespective of whether p53 was normal or altered (Table 3.10). In addition, 14 out of 24 (58%) of HER2 tumours were found tending to show low levels of H2A.Zac. These results show further association between Low detection levels of histone variants with poor prognostic breast cancer classes.

Table 3:9: Histone Variants detection levels in Different Tumour Histopathological Types.

	mH2A		H2A.Z		H2A.Zac	
	LD	HD	LD	HD	LD	HD
Invasive Ductal/NOS Type	233	145	232	151	141	161
Invasive papillary	2	2	2	1	3	0
NST& Lobular	15	10	10	16	12	8
NST& Special	14	5	8	12	8	6
Classical lobular	30	43	33	47	23	30
Tubular	8	13	16	7	11	7
Tubular mixed	84	80	76	85	68	63
Medullary	17	5	18	3	8	6
Mucinous	2	5	6	1	5	1
Cribriform	5	0	4	2	3	1
Miscellaneous	2	1	2	2	1	3
Total	721		734		569	

LD, low detection; HD, high detection; NOS, no other specified.

Table 3:10: Histone Variants detection levels and Phenotype groups of Breast Cancer as defined by Nielsen and Colleagues (Nielsen et al., 2004).

Nielsen classes of breast cancer (Nielsen et al., 2004)	mH2A				H2A.Z				H2A.Zac			
	Total	LD	HD	p	Total	LD	HD	p	Total	LD	HD	p
Neilson Groups				<0.001	596			<0.001	425			0.717
HER2		45	21			36	20			24	33	
Luminal		209	199			218	230			150	166	
Basal-like		54	18			71	21			30	22	

LD, low detection; HD, high detection; all p values are calculated by χ^2 test. Bonferroni correction test was applied and reduced the (p) value of significance to 0.003.

Table 3:11: Histone Variants detection levels and Phenotype groups of Breast Cancer as defined by Abe El-Rehim and Colleagues (Abd El-Rehim et al., 2005).

Abd El-Rehim classes of breast cancer	mH2A		H2A.Z		H2A.Zac	
	LD	HD	LD	HD	LD	HD
Luminal A	20	17	15	22	12	22
Luminal B	16	14	13	20	15	11
Luminal N	50	40	47	42	33	52
HER2	15	12	16	14	14	10
Basal-p53 altered	14	6	12	3	10	5
Basal-p53 normal	24	2	16	6	15	8
Not classified	74	48	43	45	56	46
Total	352		314		309	

LD, low detection; HD, high detection

Expression of H2A Variants Correlates with Breast Cancer

Clinicopathological Factors and Biological markers

Analysis of histone variants expression in relationship to clinicopathological variables revealed a number of significant differences and correlations (Table 3.12). In particular, high mH2A levels were negatively correlated with tumour grade ($p<0.001$); where, 220 out of 323 (68%) of grade III tumours tended to show low level of mH2A, and 86 out of 158 (54%) of grade I showed high levels of mH2A. Consistent with that, mH2A levels were also found to negatively correlate with NPI ($p=0.009$), in that moderate and poor categories scored low for mH2A. However, no significant pattern of mH2A expression was detected in relation to patient age, tumour size or nodal metastasis (Table 3.12).

High levels of H2A.Z were also negatively correlated with tumour grade ($p<0.001$); where 211 out of 331 (64%) of grade III tumours tended to show low levels of mH2A. However, no significant differences in H2A.Z level were detected among different patient age, NPI categories, tumour stage or tumour size.

Concerning acetylated H2A.Z levels, advanced tumour stage was found to positively correlate with H2A.Zac ($p=0.002$), as, 64% of stage 3 tumours were high in H2A.Zac. High H2A.Zac levels were also significantly correlated with poor NPI ($p=0.009$) and nodal metastasis status ($p<0.001$). However, no correlation was observed for H2A.Zac with patient age, tumour grade or tumour size.

Histone Variants Correlate with Breast Cancer Biological Markers

Our analysis also indicated other statistically significant associations for H2A variants in relationship to other biological markers in breast tumours (Table 3.12).

Remarkably, high levels of both mH2A and H2A.Z, (but not H2A.Zac) were positively correlated with steroid receptors. Interestingly, H2A.Z has been reported to be an estrogen regulated gene (Hua et al., 2008) and to be important for estrogen receptor alpha signalling in breast cancer cells (Svotelis et al., 2009b).

Tumours with high scores for mH2A and H2A.Z were found more likely to express luminal cytokeratins, whereas, tumours negative for CK7/8 and CK18 showed low mH2A levels ($p=0.010$ and 0.001 respectively); and low H2A.Z levels ($p<0.001$, $p<0.001$ and $p=0.001$ respectively). On the other hand, both variants were inversely correlated with basal cytokeratin, i.e. CK5/6 positive tumours, whereas H2A.Z levels showed a tendency to be low in p53 altered tumours. These results again suggest an association between the low levels of H2A variants levels with poor prognostic tumour types such as basal tumour. Conversely, mH2A showed a positive association with FOXA1 ($p<0.001$), a breast tumour growth repressor (Habashy et al., 2008b).

Table 3:12: Relation between Histone Variants Detection levels and Clinico-pathological Parameters and Biological Factors.

Parameter	mH2A				H2A.Z				H2A.Zac1			
	Total	LD	HD	p	Total	LD	HD	p	Total	LD	HD	p
Age	722			0.028	735			0.034	570			0.029
≤50		155	94			216	150			112	90	
>50		258	215			192	177			172	196	
Grade	722			<0.001	735			<0.001	570			0.377
I		72	86			83	76			73	61	
II		121	120			114	131			91	90	
III		220	103			211	120			120	135	
Stage	719			0.311	733			0.056	567			0.002
1		276	205			286	203			206	169	
2		90	78			84	91			55	78	
3		45	25			38	31			21	38	
NPI	719			0.009	733			0.141	567			0.007
Good		127	128			132	128			112	90	
Moderate		220	145			220	156			144	145	
Poor		64	35			56	41			26	50	
Size	722			0.450	735			0.116	570			0.208
< 5cm		261	193			251	216			188	179	
> 5cm		152	116			157	111			96	107	
LN Metastasis	733			0.018	719			0.465	567			<0.001
Negative		286	203			276	205			206	169	
Positive		122	122			135	103			76	116	
ER receptor	669			<0.001	681			<0.001	532			0.403
Low		149	61			153	68			89	88	
High		233	226			225	235			173	182	
PR receptor	663			0.003	673			<0.001	528			0.527
Negative		196	111			201	116			120	123	
Positive		188	168			175	181			141	144	
AR receptor	621			<0.001	631			<0.001	494			0.108
Negative		189	69			170	94			109	103	
Positive		181	182			171	196			128	154	
CK7/8	695			0.010	707			<0.001	557			0.142
Negative		159	93			169	87			104	92	
Positive		238	205			225	226			173	188	
CK18	595			0.001	604			<0.001	475			0.211
Negative		119	55			120	65			71	67	

positive		231	190			208	211			158	179	
CK19	691			0.004	703			0.001	552			0.500
Negative		92	43			94	44			52	51	
positive		306	250			300	265			224	225	
CK5/6	701			0.016	713			<0.001	559			0.008
Negative		295	241			278	265			196	224	
Positive		107	58			118	52			82	57	
CK14	679			0.509	690			0.013	548			0.045
Negative		312	221			294	248			204	223	
positive		85	61			96	52			69	52	
p53 (Altered)	671			0.043	678			0.001	531			0.271
Negative		269	219			256	239			189	197	
positive		115	68			119	64			66	79	
c-MYC	337			0.005	342			0.265	301			0.111
Low		156	87			145	60			108	116	
High		45	49			102	35			44	33	
nBRCA1	507			0.005	514			0.180	395			0.042
Low		144	80			120	101			73	109	
High		149	134			146	147			105	108	
FOXA1	576			<0.001	592			0.398	456			0.015
Low		199	112			176	137			115	147	
High		126	139			153	126			106	88	
FHIT	437			0.010	443			0.018	339			0.338
Low		146	99			140	112			81	110	
High		92	100			86	105			67	81	
EGFR	400			0.019	491			0.143	383			0.015
Low		196	167			215	191			152	164	
High		27	10			51	34			22	45	

LD, low detection; HD, high detection; NPI, Nottingham Prognostic Index; LN,

lymph node; ER, estrogen receptor, PR, progesterone receptor; AR, androgen

receptor; all *p* values are calculated by χ^2 test. Bonferroni correction test was

applied and reduced the (*p*) value of significance to 0.003.

Correlation of H2A Variants with Histone PTMs and their Modulators

H2A variant scores were found to correlate with a range of other histone PTMs and their modulators (Table 3.13). MacroH2a was positively associated with histone acetylation and methylation PTMs, as well as the acetyltransferases MORF, hMOF and CBP. In addition, mH2A was also positively correlated with SUV39H1, but showed no apparent association with deacetylases such as HDAC1, HDAC2 or SIRT1.

With regard to H2A.Z, high detection levels were correlated with high levels of mH2A and several histone PTMs marks (Table 3.13), all of which tend to be associated with favourable outcome (El Sheikh et al., 2009). Interestingly, the positive correlations with all active gene marks H4K16ac, H4K20me3 are consistent with the role of H2A.Z in gene activation; e.g. in yeast where H2A.Z and H4K16ac were present in nucleosomes at the promoters of active genes (Guillemette and Gaudreau, 2006, Shia et al., 2006). Furthermore, high H2A.Z levels were also correlated with high expression levels of the DNA damage mark H3K56ac (Vempati et al., 2010) ($p<0.001$) as well as hMOF and CBP ($p<0.001$ for both).

With regard to the acetylated form of H2A.Z (Table 3.13), few significant correlations were observed (after application of Bonferroni correction), with the exception of a positive correlation with TIP60 expression. Interestingly, H2A.Z is implicated in the repair of DNA double strand break (DSB) (Kawashima et al., 2007, Kalocsay et al., 2009), and TIP60 is required for H2A.Z incorporation into nucleosomes (Svotelis et al., 2009a).

Table 3:13: Correlation between Histone Variants Levels and Histone PTMs and their Modulators.

Histone and Histone Modulators	mH2A				H2A.Z				H2A.Zac			
	Total	LD	HD	p	Total	LD	HD	p	Total	LD	HD	p
mH2A					728			<0.001	541			0.435
Low						248	167			159	171	
High						148	165			104	107	
H2A.Z									541			0.014
Low										159	142	
High										103	137	
H3K9ac	500			<0.001	511			0.113	395			0.056
Low		184	80			152	113			90	120	
High		105	131			127	119			95	90	
H3K18ac	507			<0.001	515			<0.001	400			0.511
Low		183	74			162	100			93	114	
High		118	132			117	136			86	107	
H4K12ac	486			<0.001	492			<0.001	378			0.254
Low		193	89			173	103			92	122	
High		84	120			92	124			77	87	
H4K16ac (Millipore)	718			<0.001	747			0.417	408			0.021
Low		258	109			211	169			127	168	
High		151	200			200	167			62	51	
H3K4me2	488			<0.001	498			0.006	385			0.146
Low		185	79			158	109			91	124	
High		103	121			110	121			82	88	
H4K20me3	465			<0.001	474			0.001	363			0.545
Low		67	12			55	24			26	34	
High		205	181			198	197			132	171	
H3K9me3	536			<0.001	541			0.495	432			0.004
Low		194	94			158	127			96	134	
High		129	119			143	113			111	91	
H4R3me2	556			<0.001	563			0.087	439			0.213
Low		215	113			189	139			122	149	
High		108	120			121	114			83	85	
H3k56ac	584			<0.001	586			<0.001	478			0.054
Low		222	80			189	114			133	122	
High		115	167			135	148			99	124	

MORF	502			<0.001	504			0.342	395			0.032
Low		175	79			140	117			80	120	
High		125	123			140	107			97	98	
TIP60	554			0.485	193			0.057	425			<0.001
Low		158	116			61	30			124	96	
High		160	120			56	46			76	129	
hMOF	728			<0.001	755			<0.001	534			0.104
Low		270	138			279	145			159	158	
High		141	179			139	192			96	121	
CBP	720			<0.001	708			<0.001	516			0.318
Low		251	149			249	143			145	142	
High		157	163			143	173			110	119	
SUV39H1	421			<0.001	421			0.190	363			0.009
Low		158	64			121	99			78	118	
High		98	101			101	100			88	79	
HDAC1	515			0.039	523			0.447	404			0.326
Low		156	107			152	118			106	109	
High		129	123			140	113			88	101	
HDAC2	558			0.104	567			0.130	447			0.079
Low		150	92			130	116			82	113	
High		178	138			186	135			124	128	
SIRT1	562			0.108	566			0.020	449			0.089
Low		209	131			179	168			123	152	
High		124	98			133	86			90	84	
DBC1	327			0.087	594			0.016	274			0.153
Low		111	66			185	122			72	72	
High		82	68			147	140			56	74	

LD, low detection; HD, high detection; all *p* values are calculated by χ^2 test.

Bonferroni correction test was applied and reduced the (*p*) value of significance to

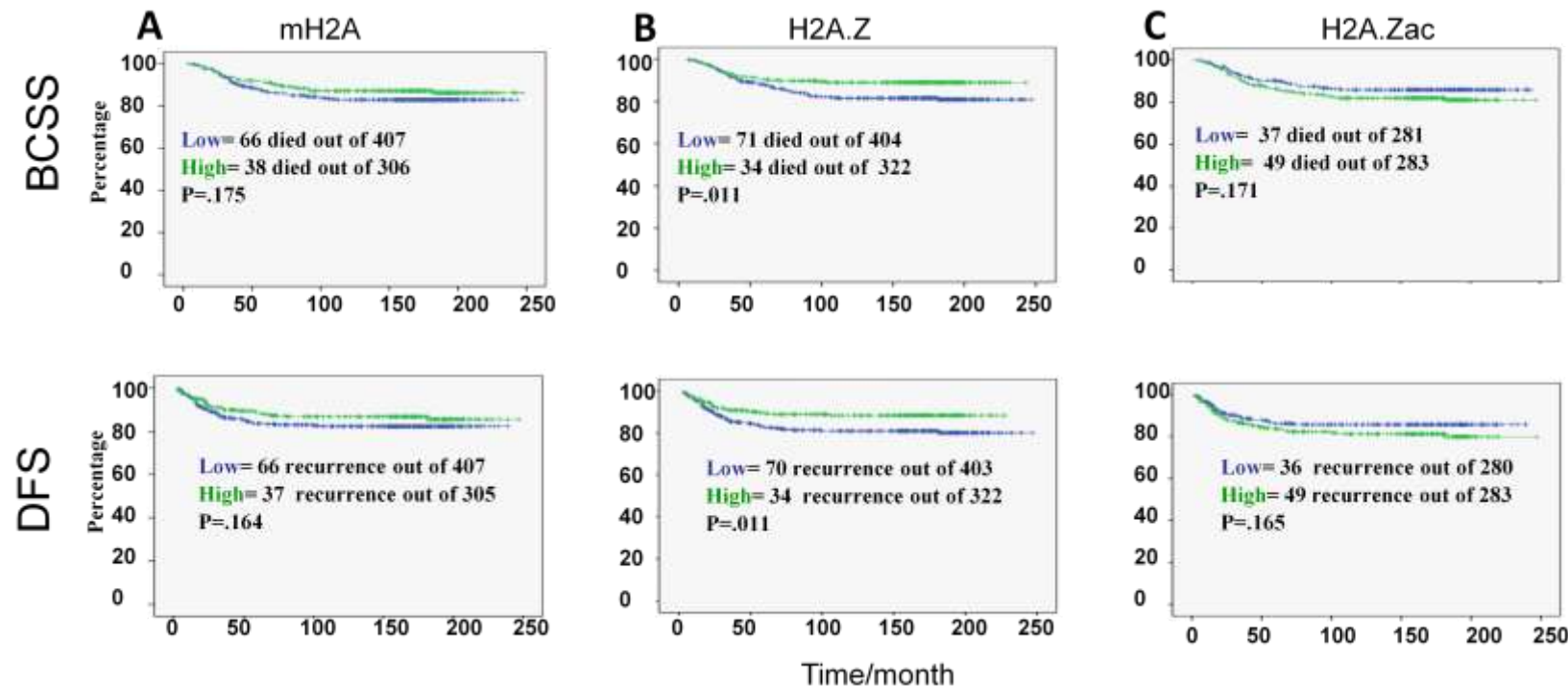
0.003.

H2A variants and patient outcome

Kaplan Meier curves correlating H2A variants to patient outcome were generated as described earlier and are illustrated in Figure 3.11. Patients presenting with high scores for H2A.Z showed improved survival breast cancer specific survival (BCSS) and longer disease free survival (DFS) ($p=0.011$ for both); which is consistent with the association of higher H2A.Z expression with favourable prognostic indicators. However acetylated H2AZ showed a reverse relationship, with a marginally poorer survival for high scoring patients. Although the results were not statistically significant ($p=0.171$ and $p=0.165$ for BCSS and DFS respectively), they are consistent with the observation that high H2A.Zac correlates with advanced tumour stage, poor NPI and tumour tendency for nodal metastasis. Patients who showed high detection levels of mH2A at time of diagnosis tended to have marginally better breast cancer specific survival (BCSS) and longer disease free survival (DFS) in comparison to low score mH2A-group. However, the differences between the two groups were not statistically significant.

Multivariate analysis by using Cox proportional regression model (Cox, 1972) showed that only the prognostic effect of H2A.Z was independent of other key prognostic factors in breast cancer including histological grade, tumour size and tumour stage (Table 3.10). Taken together, we conclude that mH2A and H2A.Z show a trend to being markers of more favourable outcome in breast cancer, whereas high levels of acetylated H2A.Z may be indicative of worse prognosis.

Figure 3.11: High H2A.Zac level correlates with better patient survival.



Kaplan-Meier curves for levels of histone variants in Breast Cancer TMA with respect to breast cancer specific survival (BCSS) and disease free survival (DFS). The green and blue colours represent in order high and low detection groups for each marker, the Y axis represent survival probability, X axis represent time relapse in months.

Table 3:14: Cox proportional Hazard Model Showing Hazard Ratios for BCSS and DFS conferred by H2A.Z and clinicopathological variables

A

BCSS			
Variable	Hazard Ratio	95% CI	p
Tumour size (cm)	0.535	0.352 to 0.813	0.003
Tumour stage	2.226	1.733 to 0.2.860	<0.001
Grade	2.368	1.665 to 3.368	<0.001
H2A.Z (high)	0.625	0.411 to 0.951	0.028

B

DFS			
Variable	Hazard Ratio	95% CI	p
Tumour size (cm)	1.902	1.245 to 2.906	0.003
Tumour stage	2.238	1.738 to 2.883	<0.001
Grade	2.338	1.639 to 3.333	<0.001
H2A.Z (high)	0.609	0.399 to 0.928	0.021

A, H2A.Z prognostic effect is independent of other prognostic factors in breast cancer with respect to breast cancer specific survival (BCSS); **(B)**, and disease free survival (DFS); CI, confidence interval ; p, χ^2 p value.

Summary of Findings: The Histone H2A Variants in Breast tumours

As described in the introduction, H2A variants appear to participate in many aspects of cellular function. mH2A was previously reported in association with malignant tumours progression and metastasis (Kapoor et al., 2010) whereas H2A.Z over expression was reported to promote cellular proliferation in ER negative breast cancer cells (Svotelis et al., 2010) and independently increased the prognostic power of biomarkers currently in clinical use (Hua et al., 2008). Hence we tried to explore their immunoreactivity in a large set of breast cancer TMA (880) to point out their relation with conventional clinical and histopathological breast cancer variables and tumour outcome. Optimisation of Histone H2A variant antibodies concentration to be used in IHC staining revealed that the working concentration for H2A.Zac was 1/5. This is relatively high concentration suggesting low antibody sensitivity. However, the antibodies were highly specific according to tests supplied by our collaborator S Dimitrov, and western blots comparing detection of H2AZ but not core histones (Appendix 2B).

The data indicate that ‘high’ levels of mH2A show an association with other favourable prognostic markers good tumour outcome biomarker, whereas low mH2A levels were correlated with the ominous high grade tumours and poor NPI categories. This appears to be consistent with reports that mH2A can suppress melanoma tumour cell growth, whereas knock down of mH2A results in enhanced tumour growth and metastasis (Kapoor et al., 2010). However we did not detect a significant association of mH2A with patient outcome, thus it is unlikely to be a very useful marker in this disease.

The data also revealed negative association of H2A.Z in relation to tumour grade which is consistent with the reported role of H2A.Z in relation to cellular differentiation. However, the positive correlation between H2A.Z and nodal metastasis was not consistent with H2A.Z being a biomarker for good tumour outcome. With regard to H2A.Zac, high levels were correlated with advanced tumour stage, poor NPI, older age group and nodal metastasis, proposing it as a biomarker of poor tumour outcome. Thus, global H2A.Z acetylation may increase during tumour progression.

The expression levels of H2A variants revealed an association with specific tumour classes, as determined by expression of biomarkers such as luminal and basal cytokeratins and HER2. High levels of both mH2A and H2A.Z were correlated with luminal type tumours and luminal type specific cytokeratin. Conversely, they showed a negative correlation with basal type-specific cytokeratins.

Interestingly, high levels of mH2A and H2A.Z correlated with high levels of ER, PR and AR receptors levels, which may be consistent with H2A.Z essential role in transcription of ER α -dependent genes (Svotelis et al., 2009b, Gevry et al., 2009) and the induction of H2A.Z expression by ER α (Hua et al., 2008). H2A.Z and mH2A also correlated with high levels of several tumour suppressor genes, transcription factors and cell cycle regulators. For example, high mH2A levels were correlated with the tumour suppressor gene BRCA1 (Lee et al., 2010) the growth suppressor FOXA1 (Habashy et al., 2008b) and FHIT, a tumour suppressor protein (Syeed et al., 2010). Conversely, p53-altered tumours

were associated with low levels of H2A.Z ($p=0.001$). However, it is not clear whether these apparent associations have any functional basis.

Interestingly, whereas fewer significant associations were reported for H2A.Zac, this marker tended to display opposite associations to mH2A or H2A.Z. For example, high levels of H2A.Zac were negatively correlated with the tumour suppressor nBRCA1 and FOXA1 expression. In addition, high levels of H2A.Zac correlated with EGFR expression, a poor prognostic biomarker in breast cancer (Abd El-Rehim et al., 2004b).

With regard to core histone PTMs, mH2A and H2A.Z showed a significant positive association, with the exception of H4K16ac. This may possibly reflect functional associations of H2A variants and core histone PTMs. For example, mH2A has been reported to function in transcription repression (Ouararhni et al., 2006), and to be functionally associated with H3K9me3 (Tachibana et al., 2005) and its modulator SUV39H1 (Bhaumik et al., 2007).

High H2A.Z levels were positively correlated with H3K18ac, H4K12ac, H3K4me3 and H4K20me3, all of which are good prognostic indicators in breast tumours (Elsheikh et al., 2009). Although H2A.Z has been shown to colocalise with H4K16ac at the promoters of active genes (Guillemette and Gaudreau, 2006, Shia et al., 2006) we did not detect a significant correlation of H2A.Z expression with H4K16ac. However, it is unclear whether changes in H2A.Z occupancy at active promoters reflect changes in the overall cellular levels of H2A.Z or a relocalisation to active genes. Thus there may not be a relationship between

H2A.Z levels and H4K16 acetylation. Increased H2A.Z levels have also been correlated with the DNA damage response (Pillus, 2008, Gevry et al., 2007) and H2A.Z has been implicated in repair of DNA double strand breaks (DSB) (Kawashima et al., 2007, Kalocsay et al., 2009). Acetylation of H2A.Z by Tip60, another protein induced in response to DSBs, is required for incorporation of H2AZ into nucleosomes (Svotelis et al., 2009a). DNA damage also results in increased acetylation of H3K56 (Masumoto et al., 2005, Vempati et al., 2010) and H4K16 at sites of DNA damage (Krishnan et al., 2011), although the HATs responsible for this are not yet clear. In this study we found that H2A.Z expression in breast tumours was positively correlated with H3K56 acetylation levels ($p < 0.001$). Moreover, a strong positive correlation between acetylated H2A.Z and TIP60 was observed. We also detected significant positive correlations with the H2A.Z deacetylase SIRT1 (Chen et al., 2006, Seligson et al., 2009) and DBC1, the SIRT1 negative regulator (Kim et al., 2008). These findings may support the functional relationship between TIP60, SIRT1 and DBC1 in regulating the acetylation of H2A.Z and its incorporation into nucleosomes at active genes or DSBs.

Assessing the relationship of H2A variants to patient survival, I would like to highlight two points. First, high detection level of H2A.Z in breast cancer tumours appears to be moderately associated with good prognosis in regard to both BCSS and DFS. H2AZ expression was found to be an independent predictor of survival and to provide significant prognostic information independent of conventional prognostic variables like tumour grade, tumour stage and size. However, this result contrasts with a study using a smaller number (500 cases) of

breast tumour samples that reported high H2A.Z levels as a poor prognostic factor in breast cancer, although enhanced H2A.Z expression by estrogen have been reported (Hua et al., 2008). The reason for this discrepancy is unknown, but might be explained by differences in the preparation of samples, or the antibody used. Second, H2A.Zac levels differs from H2A.Z in relationship to the correlation with clinicopathological factors, biological variables and patient survival that further support the impact of PTMs on H2A.Z functions.

**EVALUATION OF p53 PTMs AND
THEIR MODULATORS IN BREAST
CANCER**

4.1 p53 Post Translational Modifications (PTMs)

4.1.1 Acetylation of p53 in breast cancer

The tumour suppressor protein p53 is probably functionally compromised in most tumours, either directly through p53 gene mutations, or indirectly through alterations to regulatory systems that are required for p53 function. Post translational modifications of p53 are now known to be important in the regulation of its functions both in the nucleus and the cytoplasm. In this chapter, I investigated whether acetylated forms of p53 can be detected in breast tumours using TMA, and used this approach to assess whether we can detect altered p53 acetylation in breast cancer.

Acetylation of p53 at lysine 120 (K120ac) has been shown to be catalysed by TIP60/hMOF (Tang et al., 2006a, Li et al., 2009c), which was found to be required for p53 proapoptotic function (Tang et al., 2008), such as BAX expression (Xu et al., 2009a). This modification occurs within the p53 DNA binding domain and has been reported to alter the ability of p53 to bind DNA (Sykes et al., 2006), it has also a well defined cytoplasmic function other than its conventional nuclear function (Green and Kroemer, 2009). Acetylation of the C-terminal activation domain is generally considered to promote the transcriptional activity of p53 (Dai and Gu, 2010), such as acetylation of K373 which is driven by CBP/p300 and reversed by HDAC1 (Meek and Anderson, 2009). Acetylation of K373 leads to hyperphosphorylation of p53 NH₂-terminal residues and enhances the p53 activity toward the apoptotic pathway (Knights et al., 2006b). Furthermore, CBP/p300 HATs were reported to acetylate p53 at lysine 386

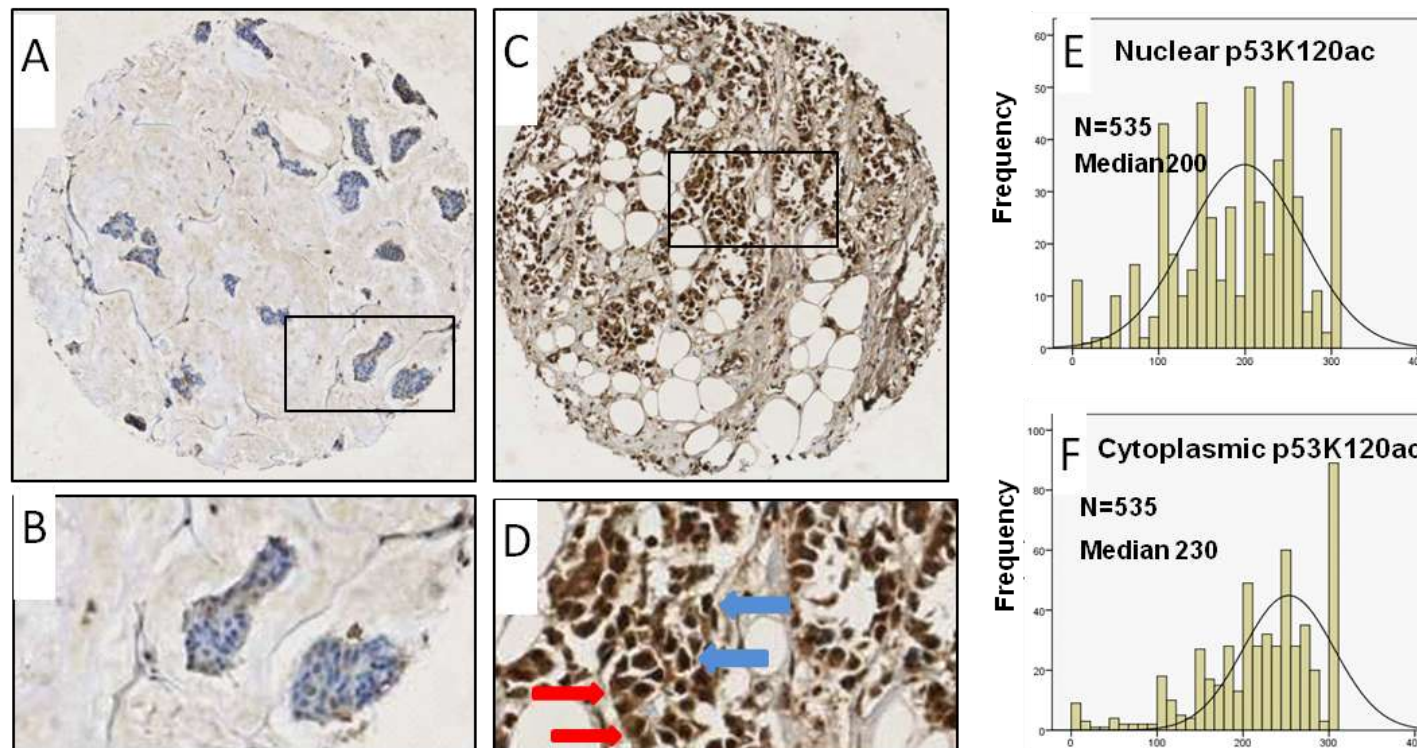
(K386) which was reported to enhance p53 sequence-specific binding to DNA and its transcriptional activity in tissue culture system. Finally, acetylation augments p53 stability through the mutual exclusion of acetylation and ubiquitination, which is involved in p53 turnover by the proteasome (Feng et al., 2005). In the next section, an evaluation of p53 acetylation at three different lysine residues (K120, K373 and K386) in breast tumours is presented.

4.1.2 Detection of p53 Acetylation in Breast Tumour Tissue

The breast cancer TMA cohort (880 tumour cores) was IHC stained (Materials and Methods, section 2.2.3) with commercial anti-acetyl p53 antibodies targeting specific p53 acetylation sites at K120, K373 and K386. The working concentration and antigen retrieval methods used for each antibody are listed in Appendix 1. IHC staining with the three antibodies revealed immune reactivity in breast tumour, stromal myoepithelial and inflammatory cells; which vary in pattern and intensity. The reactivity was mainly nuclear for p53K373ac and p53K386ac stained tissue cores with p53K373 solely nuclear and p53K386 showing nuclear with some cytoplasmic background (Fig. 4.2 and Fig.4.3). p53K120ac stained tumour cores showed strong nuclear and cytoplasmic reactivity but for some tumours staining was almost exclusively cytoplasmic (Fig. 4.1A, B, C and D). As acetylation of p53 at K120 has a well defined cytoplasmic function, assessment for cytoplasmic p53K120 immunoreactivity was also evaluated alongside the nuclear staining. As described in the previous chapter scoring of the immunoreactivity of the three p53 acetylation marks was done by modified H-score. The valid breast cancer tissue cores were further categorised

into low and high detection groups according to the H-score median values. As before, where H-score values between zero and the median were considered to be in low detection group (LD) and values above the median to 300 were considered in the high detection group (HD). Histograms showing frequency of H-score plotted against the number of cases are shown in Figure 4.1, right column. Strikingly, the intensity of immunoreactivity for nuclear p53K120ac differs from the cytoplasmic compartment, which was reflected in the distribution of frequency in both histograms (Fig. 4.1E and F).

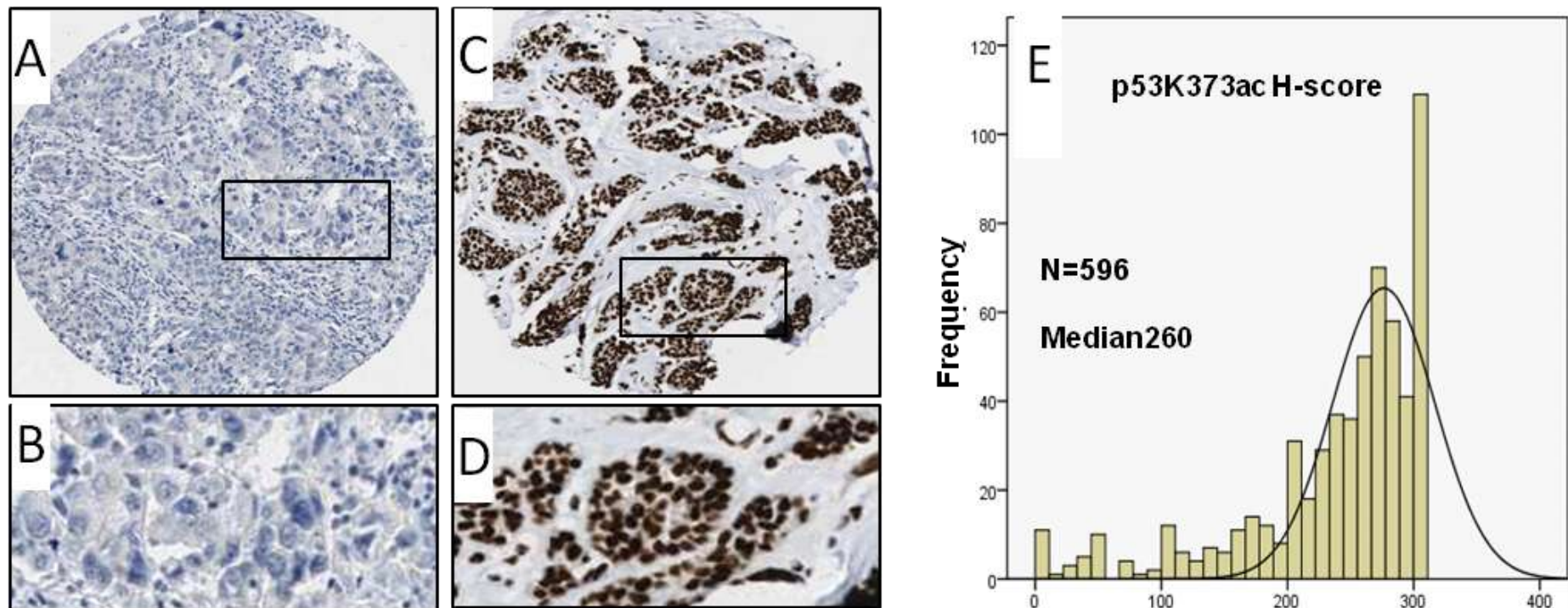
Figure 4.1: Detection of p53K120 Acetylation Mark in Breast Cancer as determined by IHC.



Breast tumour tissue cores presenting with low (**A**) and high (**C**) levels for p53K120ac; further magnifications are presented below (**B** and **D**).

Both nuclear (blue arrows) and cytoplasmic staining (red arrows) for p53K120ac were observed (**D**). Original magnification is X20. Distribution of nuclear (E) and cytoplasmic (F) H-score of breast cancer TMA stained for p53K120ac.

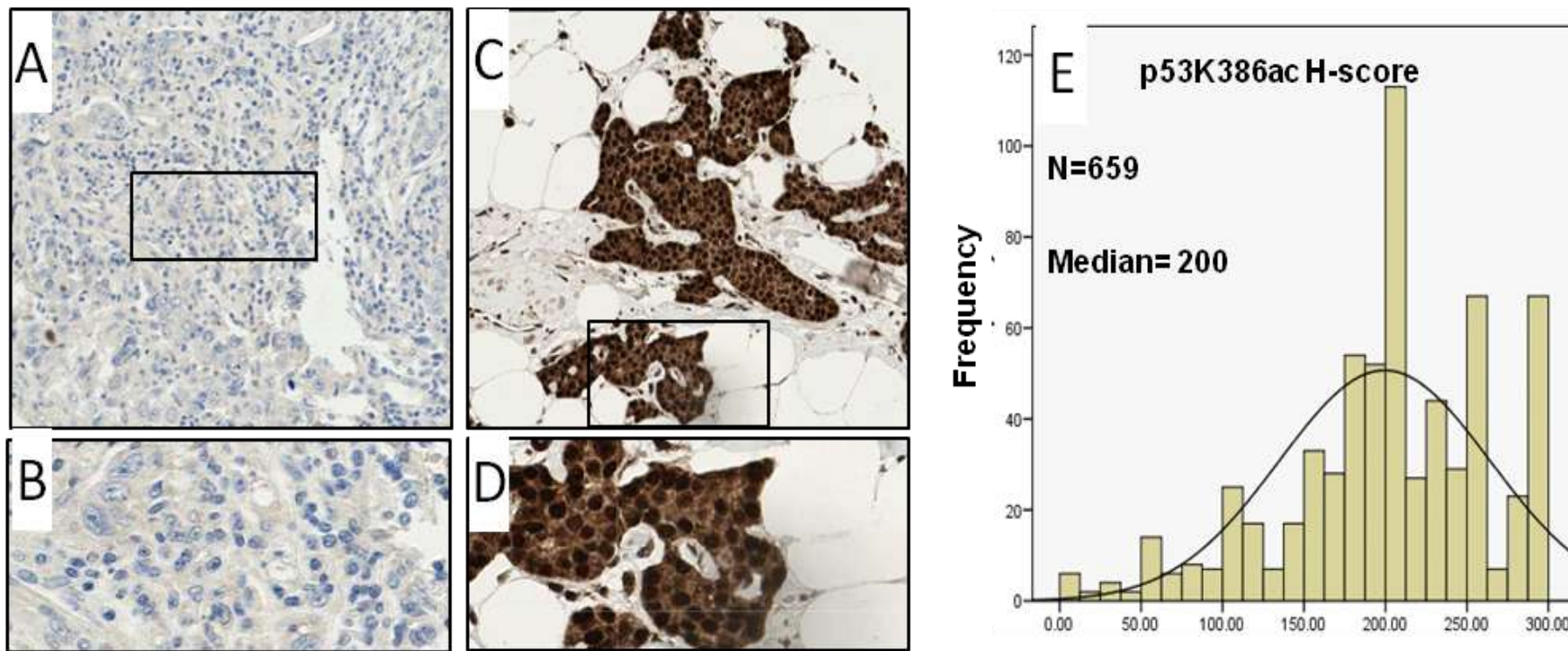
Figure 4.2: Detection of p53K373 Acetylation Mark in Breast Cancer as determined by IHC.



Breast tumour tissue cores presenting with low (A) and high (C) levels for p53K373ac; further magnifications are presented below (B and D).

Original magnification is X20. Distribution of H-score of breast cancer TMA stained for p53K373ac (E).

Figure 4.3: Detection of p53K386 Acetylation Mark in Breast Cancer as determined by IHC.



Breast tumour tissue cores presenting with low (**A**) and high (**C**) levels for p53K373ac; further magnifications are presented below (**B** and **D**).

Original magnification is X40. Distribution of H-score of breast cancer TMA stained for p53K386ac (**E**).

p53 PTMs Detection Levels in Relationship to Breast Cancer Histological Types

p53 acetylation marks were found to vary among different tumour histopathological types as shown in (Table 4.1). In particular, low levels of nuclear p53K120ac were observed in invasive duct, invasive papillary, medullary and mucinous and cribriform tumours; while, 8 out of 10 (80%) of tubular tumours expressed high levels of nuclear p53K120ac. Concerning cytoplasmic p53K120ac, low levels have been noted among 28 out of 47 (60%) of classical lobular, 11 out of 16 (69%) of medullary and 3 out of 4 (75%) of mucinous tumours.

With regard to p53K373ac, conversely to cytoplasmic p53K120ac, high levels have been noted in 44 out of 59 (75%) of lobular tumours. Both tubular and cribriform tumours also tended to show high levels of p53K373ac. Where 11 out of 16 (69%) of tubular tumours and 3 out of 4 (75%) cribriform tumours were high for p53K373ac levels. However, almost all (15 out of 16 tumours) medullary and all mucinous (3 cases) tumours were low in p53K373ac levels.

p53K386ac levels have been also shown to vary considerably among tumour histopathological types, high levels have been noted in 42 out of 68 (64%) of lobular, 14 out of 20 (70%) of tubular and most mucinous (5 out of 6) and cribriform (4 cases) tumours. However, low levels were observed in 14 out of 19 (74%) of medullary tumours and more than half (57%) of invasive ductal/NOS tumours.

These results illustrate that tumour histological types differ in their p53 acetylation levels. Moreover, medullary tumours always tend to show low levels of p53 acetylation. Finally, high levels of p53K373ac and p53K386ac have been observed in well differentiated tumours; however, p53K120 acetylation levels did not correlate with tumour grade regardless of the staining was nuclear or cytoplasmic.

p53 PTMs in Relationship to Breast Cancer Phenotypic Groups

Regarding breast cancer tumour phenotypes proposed by Nielson *et al* (Nielsen et al., 2004), significant differences in nuclear p53K120ac levels were noted ($p<0.001$). Low nuclear p53K120ac levels were observed in 67% of HER2 and 72% of basal subtypes, whereas, no significant differences were observed among luminal type tumours. Similar trends were obtained from nuclear levels of both p53K373ac and p53K386ac ($p<0.001$ for both) as shown in Table 4.2. Remarkably, high levels of nuclear p53K386ac were observed in 208 out of 281 (74%) of luminal tumours. With regard to cytoplasmic p53K120ac, no significant differences were noted among Neilson phenotypes. The tendency for bad prognostic HER2 and basal tumours to show low detection levels of nuclear p53 acetylation marks and loss of H4K16 acetylation may indicate dysfunction of HATs in those tumours. This data suggests that nuclear p53 acetylation may be a useful indicator of tumour type. Conversely, cytoplasmic p53K120ac does not seem related to breast cancer phenotypic groups.

With regard to p53 acetylation levels in tumour classes proposed by Abd El-Rehim *et al* (Abd El-Rehim et al., 2005), nuclear p53K120ac levels were low in both luminal N class and both HER2 and basal classes. Cytoplasmic p53K120ac levels were also low in both luminal N and HER2 classes; however, 10 out of 16 (60%) of p53-altered (mutated) class showed tendency towards high p53K120ac. This suggests a difference in the subcellular distribution of p53K120ac in different tumour classes, especially in relation to p53 mutations. With regard to p53 acetylation at K373 and K386, high levels of both marks were observed in luminal A and N classes; however, low levels were seen in basal classes (Table 4.3).

Table 4:1:p53 PTMs Detection Levels in Relationship to Tumour Histopathological Types.

Histopathological type	p53K120ac (N)		p53K120ac (C)		p53K373ac		p53K386ac	
	LD	HD	LD	HD	LD	HD	LD	HD
Invasive Ductal/NOS Type	162	114	136	140	174	129	184	139
Invasive papillary	3	1	3	1	1	2	2	1
NST& Lobular	13	7	11	9	12	8	6	11
NST& Special	6	8	6	8	10	6	11	4
Classical lobular	24	23	28	19	15	44	26	42
Tubular	2	8	5	5	5	11	6	14
Tubular mixed	53	56	48	61	50	69	61	77
Medullary	13	3	11	5	15	1	14	5
Mucinous	3	1	3	1	3	0	1	5
Cribiform	3	0	2	1	1	3	0	4
Miscellaneous	0	4	2	2	4	0	2	0
Total	507		507		563		615	

LD, low detection; HD, high detection; NOS, no other specified.

Table 4:2: p53 PTMs detection levels in Relationship to Tumour Phenotype Groups of Breast Cancer as defined by Nielsen and Colleagues (Nielsen et al., 2004).

Nielsen classes of breast cancer (Nielsen et al., 2004)	p53K120ac (N)				p53K120ac (C)				p53K373ac				p53k386ac			
	Total	LD	HD	p	Total	LD	HD	p	Total	LD	HD	p	Total	LD	HD	p
Neilson Groups	373			<0.001	373			0.484	422			<0.001	505			0.003
HER2		31	15			22	24			36	22			31	14	
Luminal		135	142			132	145			135	174			73	208	
Basal-like		36	14			30	20			41	14			46	33	

LD, low detection; HD, high detection; all *p* values are calculated by χ^2 test. Bonferroni correction test was applied and reduced the (*p*) value of significance to 0.003.

Table 4:3: p53 PTMs Detection Levels and Phenotype Groups of Breast Cancer as defined by Abe El-Rehim and Colleagues (Abd El-Rehim et al., 2005).

Abd El-Rehim classes of breast cancer	p53K120ac (N)		p53K120ac (C)		p53K373ac		p53K386ac	
	LD	HD	LD	HD	LD	HD	LD	HD
Luminal A	14	15	12	17	11	17	12	22
Luminal B	16	10	13	13	13	14	15	11
Luminal N	44	25	41	28	29	50	33	52
HER2	16	6	14	8	12	14	14	10
Basal-p53 altered	10	6	6	10	11	5	10	5
Basal-p53 normal	14	9	13	10	15	8	15	8
Not classified	44	37	43	38	41	44	56	46
Total	266				284			309

LD, low detection; HD, high detection; N, nuclear; C, cytoplasmic.

p53 PTMs Correlate with Breast Cancer Clinicopathological factors

Statistical analysis of p53 acetylation marks in relationship to breast cancer clinicopathological variables revealed a number of significant results (Table 4.4). In particular, high nuclear p53K120ac levels negatively correlated with NPI ($p=0.001$); where, 70% of stage 3 tumours and 69% of poor prognostic NPI group were low in p53K120ac levels. Consistently, low p53K120ac levels correlated with nodal metastasis ($p=0.014$). However, cytoplasmic localisation of p53K120ac did not correlate with NPI. With regard to p53 acetylation at K373, high levels inversely correlated with tumour grade ($p<0.001$), where grade I and II (favourable grades) were more likely to show high levels of p53K373ac; conversely, 60% of grade III tumours were low in p53K373ac. Similarly, high levels of p53K386ac were inversely correlated with tumour grade ($p<0.001$); where, grade I and II were more likely to express high levels of p53K386ac; conversely 61% of grade III tumours were low in p53K386ac levels. In addition, high levels of p53K386ac inversely correlated with NPI categories ($p<0.001$); where 60% of tumours in the good category were showing high levels of p53K386ac and 59% of tumours in the poor category were showing low levels of p53K386ac. These results may consider p53 acetylation being favourable prognostic indicators.

p53 PTMs Correlate with Breast Cancer Biological Markers

Complementary to the abovementioned work, a set of correlations between p53 acetylation and a group of breast cancer biological markers were also assessed (Table 4.4). In particular, high levels of nuclear p53K120ac significantly

correlated with well known markers for good outcome, such as high ER receptor expression and high levels of FOXA1 expressions ($p<0.001$ for both) which suggests it as a potentially active form of p53.

Concerning acetylation at K373, high levels significantly correlated with luminal type-specific markers, the cytokeratins CK7/8 and CK18 ($p<0.001$, and $p=0.001$ respectively) and high levels of the hormone receptors estrogen, progesterone and androgen where the p value was <0.001 in all of them. Low levels of p53K373ac correlated with the basal type tumour marker CK5/6 ($p<0.001$), which consistent with the low p53K373ac levels in basal type tumour classes as shown in Table 4.2 and Table 4.3 . In addition, a number of favourable outcome related-tumour biological markers also correlated with high levels of p53K373ac such as, the transcription factor c-MYC and the tumour suppressor genes BRCA1 (Lee et al., 2010) and EGFR; moreover, high levels the p53 dependent apoptotic marker BCL2. However, these results were not statistically significant. Collectively, these results suggest p53K373ac as a potential marker for good outcome in breast cancer.

With regard to p53 acetylation at K386, high detection levels were also - like K373- found to significantly correlate with luminal type-specific markers the cytokeratins CK7/8 and CK18 ($p<0.001$ and $p<0.001$ respectively), and high levels of the hormone receptors estrogen, progesterone and androgen with highly significant p values ($p<0.001$ for all). In relationship to favourable outcome related-tumour biological markers, high p53K386ac levels also correlated with high levels of the tumour suppressor genes BRCA1 ($p=0.001$) and BCL2 levels

($p=0.007$). Together, these results are consistent with the hypothesis that active i.e. acetylated p53 correlated with biological markers for good outcome, inversely correlated with markers of poor prognosis in breast cancer tumours and has a close relationship with steroid hormone signaling and apoptosis.

Table 4:4: Relation between p53 PTMs Detection levels and Clinico-pathological Parameters and Biological Factors.

Parameter	p53K120ac (N)				p53K120ac (C)				p53K373ac				p53K386ac			
	Total	LD	HD	p	Total	LD	HD	p	Total	LD	HD	p	Total	LD	HD	p
Age	507			0.014	507			0.040	564			0.309	616			0.230
≤50		114	69			102	81			106	93			116	102	
>50		168	156			153	171			185	180			198	200	
Grade	507			0.020	507			0.950	564			<0.001	616			<0.001
I		52	57			54	55			55	70			55	92	
II		83	78			80	81			77	99			87	102	
III		147	90			121	116			159	104			172	108	
Stage	504			0.031	504			0.032	561			0.218	614			.619
1		170	158			154	174			195	169			87	129	
2		73	50			64	59			63	76			180	140	
3		37	16			35	18			32	26			46	32	
NPI	504	75	90	<0.001	504			0.128	561			0.317	614			<0.001
Good		155	112			75	90			90	99			87	129	
Moderate		50	22			135	132			155	138			180	140	
Poor		43	29			43	29			45	34			46	32	
Size	507			0.149	507			0.089	564			0.477	616			0.055
< 5cm		164	142			146	160			184	171			196	208	
> 5cm		118	83			109	92			107	102			118	94	
LN Metastasis	504			0.014	504			0.029	561			0.131	614			0.199
Negative		170	158			154	174			195	169			201	204	
Positive		110	66			99	77			95	102			112	97	
ER receptor	471			<0.001	471			0.051	527			<0.001	575			<0.001
Low		113	43			88	68			118	62			113	65	

High		151	164			151	164			150	197			178	219	
PR receptor	472			0.094	472			0.534	523			<0.001	567			<0.001
Negative		131	88			110	109			152	97			148	101	
Positive		135	118			127	126			113	161			139	179	
AR receptor	435			0.073	435			0.073	484			<0.001	533			<0.001
Negative		119	75			119	75			140	70			130	88	
Positive		130	111			130	111			107	172			139	176	
p53 (Altered)	470			0.023	470			0.529	524			0.149	567			0.041
Negative		180	156			170	166			185	191			199	212	
positive		86	48			68	66			81	67			89	67	
c-MYC	259			0.225	259			0.008	299			0.043	284			0.233
Low		93	89			66	116			133	86			118	91	
High		44	33			41	36			39	41			38	37	
CK7/8	494			0.419	494			0.390	550			0.011	597			<0.001
Negative		99	83			89	93			118	86			129	79	
Positive		174	138			158	154			164	182			76	213	
CK18	428			0.076	428			0.122	480			0.001	520			<0.001
Negative		79	47			69	57			90	59			100	54	
positive		165	137			145	157			148	183			65	201	
CK19	491			0.356	491			0.379	547			0.006	589			0.010
Negative		60	44			50	54			65	38			64	39	
positive		213	174			195	192			217	227			238	248	
CK5/6	497			0.059	497			0.331	554			<0.001	599			0.094
Negative		198	173			184	187			196	221			225	227	

Positive		78	48			66	60			88	49			83	64	
CK14	484			0.076	484			0.050	537			0.011	575			0.165
Negative		214	154			193	175			202	208			225	221	
positive		58	58			50	66			78	49			72	57	
nBRCA1	368			0.026	368			0.288	400			0.007	447			0.001
Low		107	62			85	84			100	83			113	82	
High		105	94			107	92			91	126			106	146	
FOXA1	412			<0.001	412			0.326	458			0.024	498			0.005
Low		146	84			110	120			145	122			155	118	
High		81	101			92	90			85	106			101	124	
FHIT	304			0.379	304			0.041	340			0.182	396			0.004
Low		98	74			94	78			90	96			124	104	
High		72	60			58	74			66	88			68	100	
EGFR	340			0.451	340			0.010	378			0.015	421			0.502
Low		158	122			133	147			162	150			178	168	
High		35	25			39	21			24	42			38	37	
BCL2	216			0.111	216			0.404	232			0.014	279			0.007
Low		77	61			67	71			84	67			103	74	
High		36	42			40	38			32	49			43	59	

N, nuclear; C, cytoplasmic; LD, low detection; HD, high detection; NPI, Nottingham Prognostic Index; LN, lymph node; ER, estrogen receptor; PR, progesterone receptor; AR, androgen receptor; all *p* values are calculated by χ^2 test. Bonferroni correction test was applied and reduced the (*p*) value of significance to 0.003.

The Relationship between p53 PTMs, Histone PTMs and Their Modulators

High levels of nuclear p53K120ac showed a positive correlation with the histone variants mH2A ($p<0.001$) and several histone PTM marks (Table 4.5). Specifically, high levels of the histone methylation marks H3K4me3 and H3K9me3 (0.002 and 0.008 respectively) and the H3K9 methyltransferase SUV39H1 ($p=0.01$) was observed. This may be consistent with the colocalization of p53 and SUV39H1 in a complex capable of methylation of H3K9 (Chen et al., 2010).

Moreover, the observed association with the DNA damage mark H3K56ac ($p<0.001$) may reflect the relationship between acetylation of p53 at K120 and its role in the DNA damage response (Li et al., 2009b). With regard to HATs, high levels of hMOF, which has been previously reported to acetylate p53 at K120 (Li et al., 2009c), correlated with high levels of nuclear p53K120ac ($p= 0.006$). In addition, high MORF levels also correlated with high levels of nuclear p53K120ac ($p<0.001$). Unpublished data from our group has shown that the MOZ related protein MORF can acetylate p53 at K120 (HM Collins, M Mesmer, data not shown). Conversely, low levels of nuclear p53K120ac correlated with high levels of the histone deacetylase HDAC2 ($p=0.010$), although the p value was not statistically significant after Bonferroni correction. With regard to DBC1, the SIRT1 negative regulator, high levels of DBC1 positively correlated with nuclear p53K120ac ($p<0.001$), which may be consistent with SIRT1-mediated p53 deacetylation (Zhao et al., 2008).

Cytoplasmic detection of p53K120ac was found to correlate positively with high levels of mH2A ($p<0.001$). In contrast to the nuclear fraction, cytoplasmic p53K120ac negatively correlated with the histone methylation mark H3K9me3 ($p<0.001$), which may indicate differential functions of the nuclear and cytoplasmic fractions of p53K120ac, although how this might occur is unknown.

A number of significant correlations were observed for p53K373ac levels among histone variants, histone PTMs and histone modulators (Table 4.5). High levels of p53K373ac correlated with high levels of mH2A ($p<0.001$); histone acetylation and methylation marks ($p<0.001$), which may be consistent with p53K373ac role in genome transcription (Knights et al., 2006b). Knights *et al.*, (2006b) reported that acetylation of p53 at K373 enhances p53 phosphorylation at NH2-terminal residues and improves p53 interaction with gene promoters. In addition, high levels of p53K373ac correlated with high levels of H3K56ac ($p<0.001$); which was previously described to localize at DNA repair foci after DNA damage (Masumoto et al., 2005, Vempati et al., 2010, Yuan et al., 2009) and is consistent with p53 and H3K56ac colocalization at DNA damage sites (Vempati et al., 2010). With regard to HATs, high levels of p53K373ac correlated with high levels of MORF ($p<0.001$); The histone acetyltransferase MOZ or MORF genes have been described to be associated with the nuclear receptor coactivators TIF2, p300 or CBP. In our lab MOZ-TIF2 was previously described to inhibit p53 gene transcription through impairment of CBP function (Kindle et al., 2005). In addition, high levels of hMOF correlated with high p53K373ac levels ($p<0.001$); which is consistent with the role of hMOF p53 acetylation and ATM activation in response to DNA damage response (Rea et al., 2007).

Concerning HDACs, high levels of p53K373ac correlated with high levels of both SIRT1, the p53 deacetylase (Hasegawa and Yoshikawa, 2008) and DBC1 ($p<0.001$ and $p=0.007$ respectively). These results may be consistent with the previously reported deregulation of the p53-SIRT1-DBC1 regulatory loop (Tseng et al., 2009) in breast cancer. With regard to SUV39H1, high levels correlated with p53K373ac high levels ($p=0.002$). Interestingly, SUV39H1 and p53 form a complex capable of H3K9 methylation (Chen et al., 2010).

Finally, significant differences in p53K386ac levels also correlated with histone variants, histone PTMs and histone modulator levels (Table 4.5). Like p53K373ac, high p53K386ac levels also correlated with mH2A with a highly significant value ($p<0.001$) and remarkably there was significant correlation between p53K386ac and all histone acetylation and methylation marks. This may reflect the activity of HATs that target both histone and p53 acetylation. Like p3K373ac, high levels of p53K386ac positively correlated with high levels of H3K56ac the DNA damage marker (Masumoto et al., 2005, Vempati et al., 2010, Yuan et al., 2009) in highly significant value ($p<0.001$). High levels of p53K386ac also correlated with high levels of the histone acetyltransferases MORF and hMOF ($p<0.001$ in both), the p53 acetylators (Dai and Gu, 2010, Meek and Anderson, 2009). High p53K386ac levels also positively correlated with both SIRT1 and HDAC1 ($p<0.001$ and $p=0.022$ respectively) which may be consistent with their suppression of p53-dependent apoptosis in post neuronal cells (Hasegawa and Yoshikawa, 2008) and promoting Mdm2-dependent p53 degradation (Ito et al., 2002). With regard to SUV39H1, high levels positively

correlated with high levels of p53K386ac ($p<0.001$) consistent with their colocalization in a complex responsible for H3K9 methylation (Chen et al., 2010).

Interestingly, high levels of p53K386ac correlated with high levels of nuclear p53K120ac and p53K373ac ($p=0.005$, $p<0.001$ respectively). However, cytoplasmic p53K120 levels negatively correlated with nuclear p53K373 with a highly significant p value ($p<0.001$), which may indicate a varied p53 function dependent on either the site or localization of its PTMs. Taken together, our data shows that monitoring p53 acetylation status may be a useful prognostic indicator in breast cancer and may also reveal how changes in p53 acetylation occur during tumour progression indicating this may be important for the advance of the disease.

Table 4:5: p53 PTMs in Relation to Histone PTMs and their Modulators.

Parameter	p53K120ac (N)				p53K120ac (C)				p53K373ac				p53K386ac			
	Total	LD	HD	p	Total	LD	HD	p	Total	LD	HD	p	Total	LD	HD	p
mH2A	478			<0.001	478			0.249	526			<0.001	579			<0.001
Low		179	97			135	141			191	120			202	132	
High		90	112			106	96			76	139			93	152	
H2A.Z	478			0.010	478			<0.001	533			0.051	587			0.498
Low		156	99			154	101			160	132			164	158	
High		112	111			85	138			114	127			134	131	
H2A.Zac	453			0.334	453			0.005	515			0.004	467			0.124
Low		121	98			122	97			149	101			103	116	
High		135	99			101	133			126	139			131	117	
H3K9ac	360			0.016	360			0.509	406			<0.001	447			<0.001
Low		126	73			101	98			133	86			141	86	
High		83	78			81	80			70	117			97	123	
H3K18ac	370			0.326	370			0.104	415			<0.001	450			<0.001
Low		117	78			92	103			144	73			144	87	
High		100	75			95	80			62	136			93	126	
H4K12ac	356			0.096	356			0.184	391			<0.001	428			<0.001
Low		128	81			101	108			142	51			151	87	
High		79	68			79	68			80	118			77	113	
H4K16ac (Millipore)	469			0.185	469			0.006	523			<0.001	576			<0.001

Low		136	116			110	142			182	92			177	120	
High		127	90			121	96			92	157			116	163	
H3K4me2	356			0.002	356			0.539	397			<0.001	439			<0.001
Low		125	66			95	96			133	79			147	83	
High		82	83			82	83			67	118			86	1230	
H4K20me3	342			0.032	342			0.553	376			<0.001	415			0.001
Low		38	16			28	26			45	19			50	21	
High		161	127			149	139			131	181			167	177	
H3K9me3	400			0.008	400			<0.001	440			<0.001	554			<0.001
Low		120	109			97	132			153	82			185	102	
High		111	60			105	66			72	133			97	170	
H4R3me2	407			0.018	407			0.350	449			<0.001	485			0.002
Low		148	97			124	121			160	113			169	117	
High		80	82			78	84			66	110			91	108	
H3k56ac	432			<0.001	432			0.251	480			<0.001	500			<0.001
Low		144	81			117	108			158	92			163	104	
High		98	109			100	107			80	150			91	142	
MORF	385			<0.001	385			0.169	409			<0.001	511			<0.001
Low		131	65			106	90			107	99			181	83	
High		88	101			92	97			89	114			92	155	
hMOF	476			0.006	476			0.181	534			<0.001	588			<0.001
Low		167	107			143	131			184	132			196	131	

High		99	103		96	106		87	131		102	159	
SUV39H1	358			0.010	358		0.306	381		0.002	442		<0.001
Low		123	77		96	104		118	87		148	80	
High		77	81		81	77		75	101		87	127	
HDAC2	414			0.215	414		0.010	453		0.207	566		0.149
Low		100	84		81	103		107	90		131	116	
High		135	95		129	101		128	128		154	165	
SIRT1	409			0.366	409		0.366	445		<0.001	552		<0.001
Low		143	99		143	99		163	112		157	100	
High		95	72		95	72		68	102		136	159	
DBC1	418			<0.001	418		0.039	456		0.007	499		0.087
Low		132	78		113	97		134	107		143	119	
High		96	112		93	115		94	121		114	123	
p53k120ac (N)							488		0.309	438			0.005
Low								144	133		144	107	
High								104	107		83	104	
p53k120ac (C)							488		<0.001	438			0.220
Low								104	139		110	111	
High								144	101		117	100	
p53k373ac										478			<0.001
Low											154	91	
High											92	141	

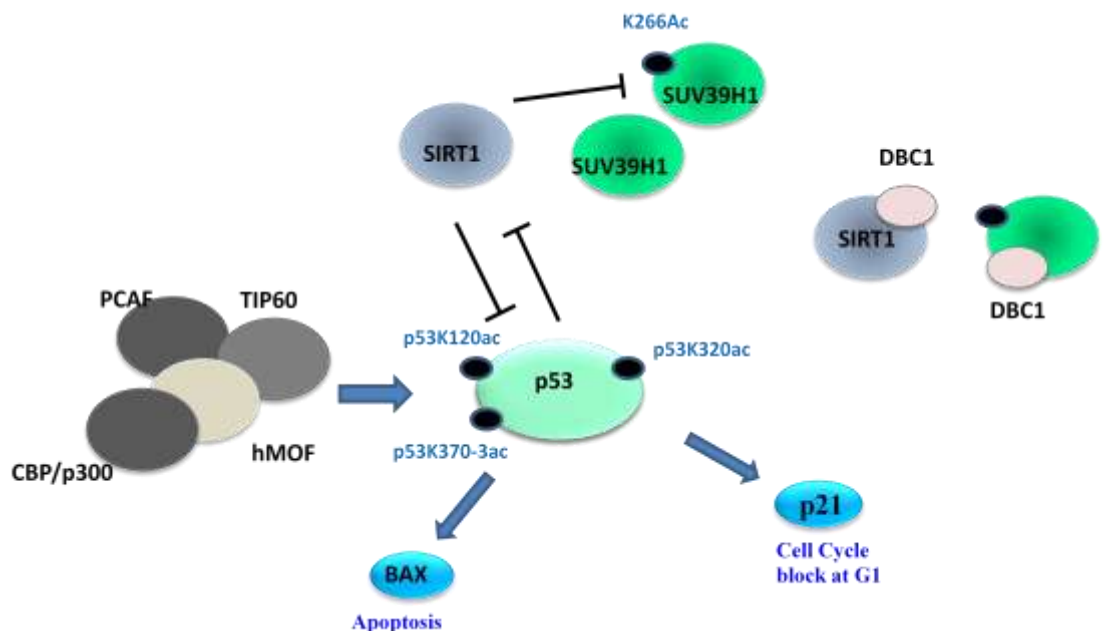
N, nuclear; C, cytoplasmic; LD, low detection; HD, high detection; NPI, Nottingham Prognostic Index; all *p* values are calculated by χ^2 test.

Bonferroni correction test was applied and reduced the (*p*) value of significance to 0.003.

4.2 *p53 Acetylation Modulators*

In previous section we explored breast cancer TMA immunoreactivity for p53 acetylation at (K120, K373 and K386). Those acetylation sites are catalysed by a number of modulators (Fig. 4.4); some of these modulators have been evaluated in the breast cancer TMA in the following section. TIP60, CBP and HDAC1 staining patterns and intensities, their relationship with various tumour types, clinicopathological factors, and biological markers are determined. In addition, exploring their relationship to both (p53 and histone) PTMs and histone PTMs modulators.

Figure 4.4: p53 PTMs, HATs and HDACs and their effects on Cell Cycle Progression.



p53 is acetylated at several lysine residues by histone acetyltransferases, such as hMOF, TIP60, CBP/p300, and possibly others; deacetylated by histone deacetylases such as SIRT1, which reduces p53 transcription activity and enhance p53 degradation. Acetylated p53 represses SIRT1 gene transcription. Acetylation of p53 at K120, and K373 facilitates p53 binding to pro-apoptotic genes. Acetylation at K320 facilitates p53 binding to cell cycle repression gens.

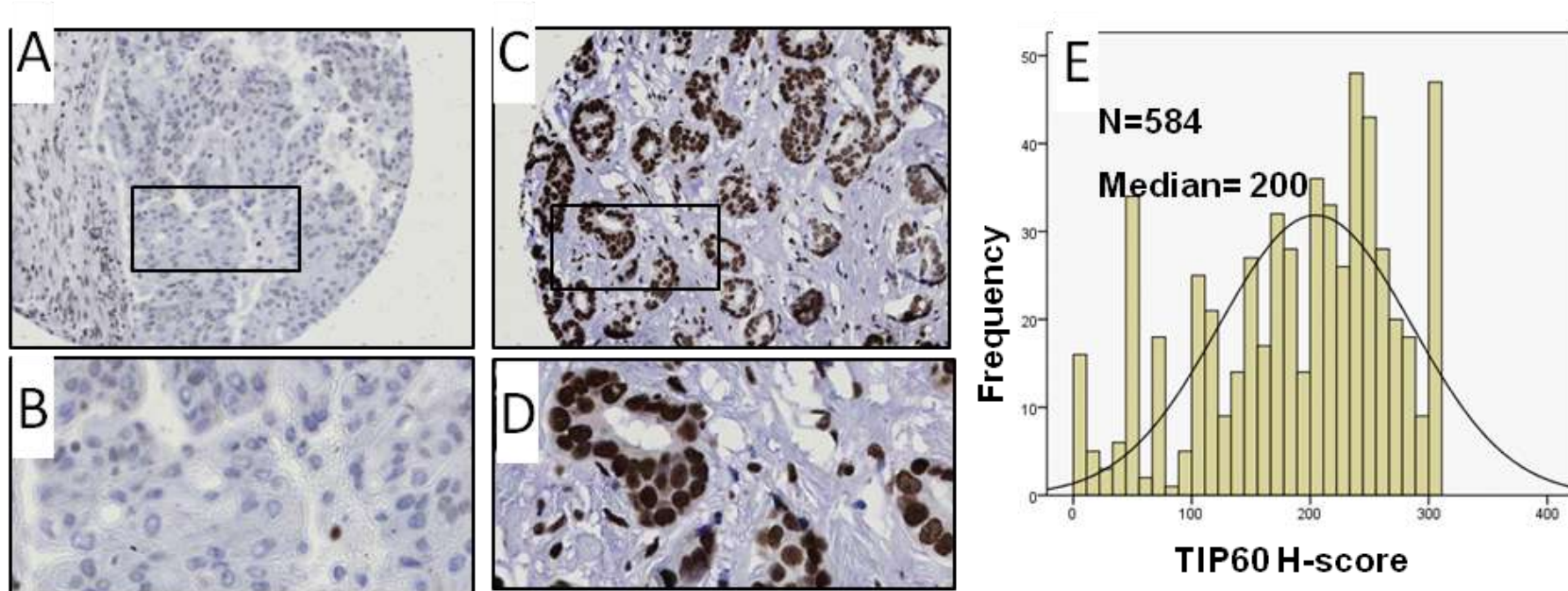
4.2.1 Detection of p53 Acetylation Modulators in Breast Tumour

TMA

We IHC stained the whole set of breast cancer TMAs (880 cases) as previously described in the Materials and Methods with antibodies against TIP60, CBP and HDAC1 (Antibody details are listed in Appendix 1) to assess their patterns and intensities in breast cancer tissue. The working dilution and method of antigen retrieval are also listed in Appendix 1. The TIP60 staining pattern was almost homogeneous in most of the cores examined. Immunoreactivity for TIP60 was confined to the nuclei of tumour cells. Positive reactivity to a lesser extent was also observed in stromal, myoepithelial and inflammatory cells. A range of staining intensities from totally negative to highly stained breast cancer cores was observed (Fig. 4.5A and B). As for CBP staining, the pattern of immunoreactivity was near to homogeneous in most of the tumour cores and the intensity ranged from low to high levels. CBP immunoreactivity was mainly seen in the nuclei but also occasionally in the cytoplasm of tumour cells. Stromal cells were usually devoid of staining (Fig. 4.6A and B). An assessment of HDAC1 staining revealed a homogeneous pattern of immunoreactivity confined to the nuclei of tumour cells and sometimes in the cytoplasm. Stromal cells, myoepithelial cells and lymphocytes were usually devoid of staining as shown in Figure 4.7A and B.

H-scores for TIP60, CBP and HDAC1 were dichotomized according to the median and the H-score distributions are illustrated in Figure 4.5E, 4.6E and 4.7E.

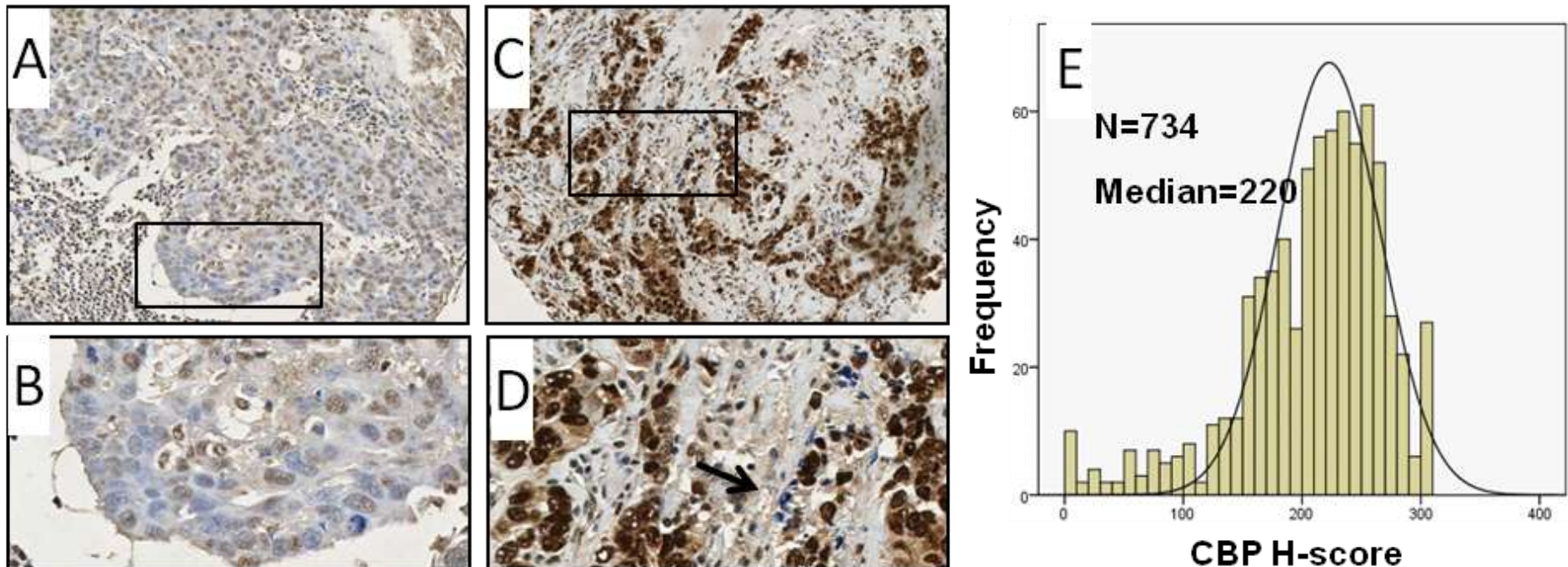
Figure 4.5: Detection of TIP60 in Breast Cancer TMAs as determined by IHC staining.



Breast tumour tissue cores presenting with low (A) and high (C) levels for TIP60; further magnifications are presented below (B and D).

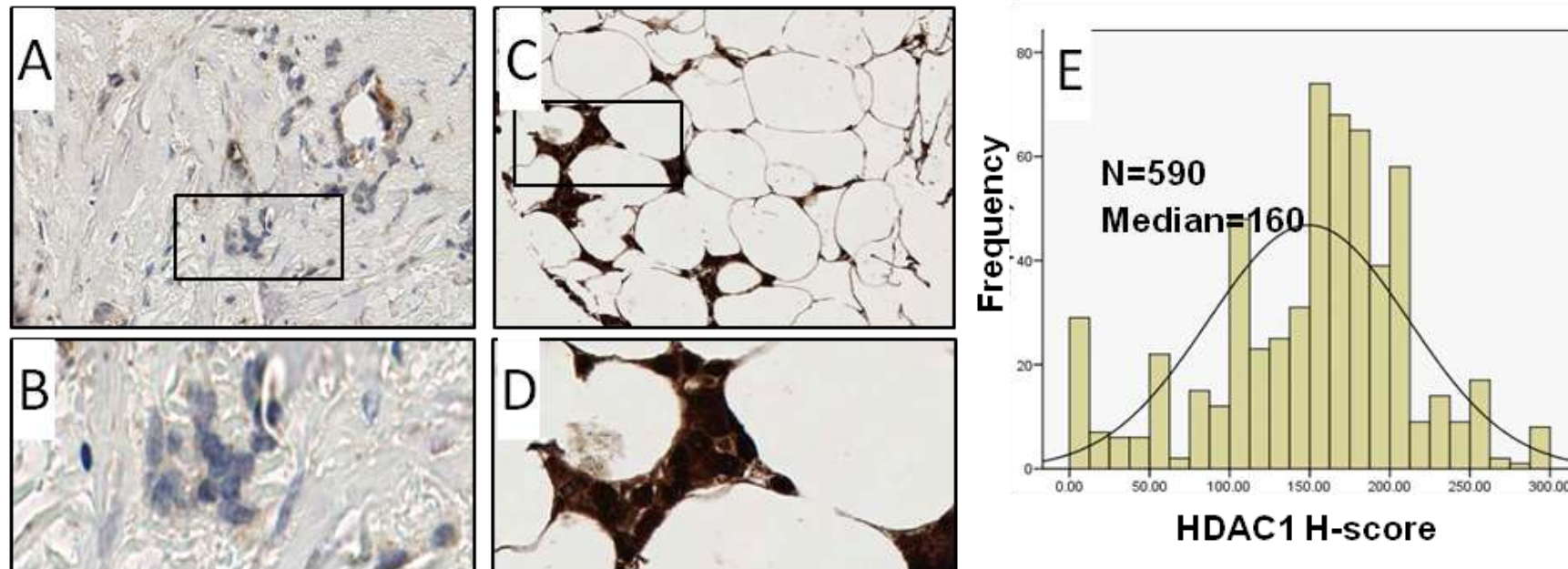
Original magnification is X40. Distribution of H-score of breast cancer TMA stained for p53K386ac (E).

Figure 4.6: Detection of CBP in Breast Cancer TMAs as determined by IHC staining.



Breast tumour tissue cores presenting with low (A) and high (C) levels for CBP; further magnifications are presented below (B and D). Stromal cells are ‘low’ for CBP (arrow in D). Original magnification is X40. Distribution of H-score of breast cancer TMA stained for p53K386ac (E).

Figure 4.7: Detection of HDAC1 in Breast Cancer TMAs as determined by IHC staining.



Breast tumour tissue cores presenting with low (**A**) and high (**C**) levels for HDAC1; further magnifications are presented below (**B** and **D**).

Original magnification is X40. Distribution of H-score of breast cancer TMA stained for p53K386ac (**E**).

p53 Acetylation Modulators in Relation to Breast Cancer Histopathological Types

p53 acetylation modulators showed considerable variation among tumour histopathological types (Table 4.6). Invasive duct/NOS type tumours did not show considerable variation except those stained for CBP where 219 out of 366 (60%) of the tumours were low for CBP. Remarkably, NST & lobular tumour tended to be ‘high’ for both TIP60 and CBP. Where 14 out of 19 (74%) and 14 out of 24 (58%) of NST& lobular tumours were high for TIP60 and CBP. However, high TIP60 levels were seen in 33 out of 56 (59%) of lobular tumours. As for medullary tumours, considerable percentages were observed among the ‘low’ groups for TIP60, CBP and HDAC1. Interestingly, most mucinous tumours stained for CBP (8 cases) were ‘low’ for CBP.

p53 Acetylation Modulators in Relation to Breast Cancer Phenotypic Groups

Regarding the breast cancer tumour phenotypes proposed by Nielson and colleagues (Nielsen et al., 2004), statistical differences in CBP and HDAC1 levels ($p=0.022$, not significant; $p=0.003$ respectively) were noted. Low levels of CBP were noted in 57% of HER2-positive, and in 86% of basal subtypes. In addition, low levels of HDAC1 were also found in 66% of HER2-positive, and 63% of basal subtypes. However, TIP60 expression did not show significant association with Neilson breast groups. These results propose an association between both CBP and HDAC1 levels and poor prognostic tumour groups.

With regard to tumour classes proposed by Abd El-Rehim and colleagues (Abd El-Rehim et al., 2005, Soria et al., 2010) TIP60 levels tended to vary among luminal type tumours. High levels of TIP60 were noted in luminal A and N classes; where 63% of luminal A and 66% of luminal N tumours were high in TIP60 levels. Conversely, although not very different, 56% of luminal B tumours were low in TIP60 levels. CBP levels were also low in 63% of luminal B class. In addition, low levels of CBP were also noted in 71% of the HER2 and both basal classes. Similarly, low levels of HDAC1 were also noted in luminal B, HER2 and basal classes (Table 4.8). These suggest an association between low levels of both CBP and HDAC1 and poor prognostic tumour classes.

Table 4:6: The Detection level of p53 Acetylation Modulators in Different Tumour Histopathological Types.

Histopathological type	TIP60		CBP		HDAC1	
	LD	HD	LD	HD	LD	HD
Invasive Ductal/NOS Type	159	150	219	147	154	150
Invasive papillary	3	0	1	3	2	1
NST& Lobular	5	14	10	14	8	7
NST& Special	8	9	9	10	9	8
Classical lobular	23	33	39	33	32	28
Tubular	9	6	13	6	8	7
Tubular mixed	54	60	78	77	50	64
Medullary	13	4	14	8	10	4
Mucinous	3	2	7	1	3	1
Cribiform	2	2	2	3	1	1
Miscellaneous	1	1	0	3	3	1
Total	561		697		552	

LD, low detection; HD, high detection; NOS, no other specified.

Table 4:7: The Detection level of p53 Acetylation Modulators and Phenotype Groups of Breast Cancer as defined by Nielsen and Colleagues (Nielsen et al., 2004).

Nielsen classes of breast cancer (Nielsen et al., 2004)	TIP60				CBP				HDAC1			
	Total	LD	HD	p	Total	LD	HD	p	Total	LD	HD	p
Neilson Groups	425			0.069	531			0.022	448			0.003
HER2		35	21			39	29			31	16	
Luminal		138	173			197	198			153	177	
Basal-like		30	28			46	22			45	26	

LD, low detection; HD, high detection; all *p* values are calculated by χ^2 test. Bonferroni correction test was applied and reduced the (*p*) value of significance to 0.003.

Table 4:8: The Relationship of p53 Acetylation Modulators to Phenotype groups of Breast Cancer as defined by Abd El-Rehim and Colleagues (Abd El-Rehim et al., 2005).

Abd El-Rehim classes of breast cancer	TIP60			CBP			HDAC1		
	Total	LD	HD	Total	LD	HD	Total	LD	HD
Cluster Class	286			343			590		
Luminal A		12	20		14	19		15	16
Luminal B		14	11		20	12		13	7
Luminal N		24	47		51	38		32	32
HER2		14	14		20	8		16	11
Basal-p53 altered		6	11		13	5		8	9
Basal-p53 normal		10	13		20	7		13	9
Not classified		47	43		64	52		44	46

LD, low detection; HD, high detection.

p53 Acetylation Modulators in Relationship to Breast Cancer Clinico-pathological Factors

A number of correlations were found between p53 acetylation modulators and clinicopathological variables as shown in Table 4.9. High levels of CBP significantly correlated with advanced patient age ($p=0.001$). Conversely to CBP, although not statistically significant, high levels of TIP60 were noted in younger patients, smaller tumour size and low grade tumours (grade I and II), where 106 out of 184 (58%) of grade II tumours were more likely to show high TIP60 expression. Conversely, 146 out of 261 (56%) of grade III tumours showed low levels of TIP60.

p53 Acetylation Modulators Correlate with Breast Cancer Biological Markers

Correlations between TIP60, CBP and HDAC1 expression levels and different biological markers were also noted (Table 4.9). Remarkably, high levels of p53 PTM modulators correlated with high levels of steroid hormone receptors levels, especially CBP and HDAC1 which correlated with high estrogen receptor levels in highly significant p value ($p=0.001$). Similarly, high levels of TIP60 correlated with high levels of androgen receptors ($p=0.001$) for which it is reported to be coactivator (Brady et al., 1999). Conversely, low levels of TIP60 correlated with CK5/6, the basal tumour type marker ($p=0.005$). Analysis of HDAC1 immunoreactivity revealed that low levels of HDAC1 also correlated with high levels of CK5/6 ($p=0.029$). Conversely, high levels of HDAC1 were significantly correlated with high levels of CK7/8 the luminal type-specific marker ($p=0.002$). These results denote a close association between TIP60, CBP, HDAC1 and

hormonal receptors; and a tendency for low expression of those marks in basal-type tumours.

Table 4:9: The Relationship between detection levels of the p53 Acetylation Modulators and Clinico-pathological Parameters and Biological Factors.

Parameter	TIP60				CBP				HDAC1			
	Total	LD	HD	p	Total	LD	HD	p	Total	LD	HD	p
Age	561			0.050	698			0.001	552			0.051
≤50		90	110			155	86			106	84	
>50		190	171			238	219			174	188	
Grade	561			0.017	698			0.119	552			0.157
I		56	60			82	68			53	63	
II		78	106			119	111			84	92	
III		146	115			192	126			143	117	
Stage	558			0.112	695			0.953	549			0.899
1		30	28			259	203			185	175	
2		138	173			93	71			69	68	
3		35	21			40	29			25	27	
NPI	561			0.069	695			0.554	549			0.260
Good		89	97			133	108			85	100	
Moderate		142	156			200	158			151	134	
Poor		46	28			59	37			43	36	
Size	561			0.011	698			0.159	552			0.021
< 5cm		160	188			254	185			165	184	
> 5cm		120	93			139	120			115	88	
LN Metastasis	558			0.096	695			0.431	549			0.390
Negative		190	177			259	203			185	175	
Positive		87	104			133	100			94	95	
ER receptor	522			0.056	648			0.001	513			0.001
Low		91	75			134	74			105	68	
High		167	189			226	214			154	186	
PR receptor	520			0.007	642			0.005	503			0.189
Negative		137	108			183	115			123	108	
Positive		123	152			175	169			133	139	
AR receptor	486			0.001	601			0.034	478			0.179
Negative		121	94			154	98			104	86	
Positive		113	158			186	163			144	144	
P53 (Altered)	521			0.122	648			0.266	509			0.370
Negative		177	195			257	209			182	180	
positive		80	69			106	76			77	70	
c-MYC	246			0.059	327			0.228	259			0.210
Low		108	68			130	105			97	88	
High		51	19			46	46			34	40	

CK7/8	547			0.016	672			0.150	531			0.002
Negative		110	84			144	101			115	77	
Positive		165	188			23	195			157	182	
CK18	465			0.305	579			0.138	462			0.258
Negative		69	68			103	69			75	64	
positive		155	173			222	185			162	161	
CK19	542			0.517	669			0.008	525			0.092
Negative		54	53			87	45			57	41	
positive		218	217			289	248			214	213	
CK5/6	550			0.005	678			0.504	534			0.029
Negative		196	221			290	228			194	205	
Positive		80	53			89	71			205	56	
CK14	530			0.024	658			0.307	515			0.123
Negative		200	218			288	227			203	200	
positive		66	46			84	59			64	48	
nBRCA1	414			0.382	493			0.012	394			0.102
Low		87	102			137	78			95	73	
High		108	117			148	130			112	114	
FOXA1	453			0.369	558			0.459	448			0.526
Low		125	121			164	136			126	117	
High		101	106			139	119			106	99	
FHIT	352			0.336	427			0.532	428			0.453
Low		96	106			132	107			45	41	
High		67	83			104	84			174	168	
EGFR	377			0.030	465			0.475	369			0.183
Low		139	168			212	170			153	146	
High		41	29			47	36			31	39	

N, nuclear; C, cytoplasmic, LD, low detection; HD, high detection; NPI,

Nottingham Prognostic Index; LN, lymph node; ER, estrogen receptor; PR,

progesterone receptor; AR, androgen receptor; all *p* values are calculated by χ^2

test. Bonferroni correction test was applied and reduced the (*p*) value of

significance to 0.003.

The Detection Levels of p53 Acetylation Modulators Correlate with Histone PTMs and p53 Acetylation Marks

High levels of TIP60 in breast tumours correlated with high levels of H2A.Zac ($p<0.001$) and all histone acetylation marks except H4K16ac. Specifically, high levels of TIP60 correlated with high levels of the active gene marks H3K9ac (Lindeman et al., 2010), the transcription activation mark H3K4me3 (Ruthenburg et al., 2007), H3K18ac and H4K12ac and as shown in Table 4.10. Interestingly, high levels of the DNA damage mark H3K56ac (Masumoto et al., 2005, Vempati et al., 2010, Tjeertes et al., 2009) also correlated with high TIP60 levels. Perhaps consistent with the TIP60 role in the DNA damage response in cancer cells (Mattera et al., 2009). With regard to HATs, TIP60 levels correlated positively with hMOF ($p<0.001$) which is consistent with their role in acetylating p53 at K120 (Tang et al., 2006b, Li et al., 2009c). Concerning p53 acetylation marks, TIP60 levels correlated positively with p53 acetylation at K373 and K386 ($p=0.018$ and $p=0.008$ respectively). However, unexpectedly, TIP60 was not correlated with CBP which is responsible for those acetylation marks. Furthermore, we found TIP60 not statistically correlated with p53K120ac levels.

With regard to CBP, high levels significantly correlated with high levels of both mH2A and H2A.Z (where $p<0.001$ for both) and most histone acetylation marks considered in this study with the exception of H4K16ac. In particular, CBP levels positively correlated with the active gene mark H3K9ac (Lindeman et al., 2010). With regard to histone methylation, high CBP levels positively correlated with the favourable prognostic mark H4K20me3 (Van Den Broeck et al., 2008) with a highly significant p value ($p<0.001$) but not with any other methylation

marks. With regard to the relationship to p53 acetylation marks, high levels of CBP positively correlated with high levels of nuclear p53K120ac and p53K373ac ($p<0.001$ and $p=0.003$ respectively); which may be consistent with CBP localization with p53 in a complex structure during acetylation-related transcription activation (Eichenbaum et al., 2009). However, no significant correlation has been noted between CBP and p53K386 acetylation, suggesting a negligible role for CBP in inducing K386 acetylation if compared with hMOF.

Significant differences in HDAC1 levels were observed in relationship to histone PTMs, p53 PTMs and their modulators (Table 4.10). Specifically, high HDAC1 levels correlated high levels of H4K16ac ($p<0.001$); the repressed gene mark H3K9me3 and its modulator SUV39H1 ($p=0.004$ and $p=0.042$ respectively). Which may be consistent with the central role of HDAC1 in regulating gene activity (Renthal et al., 2008, Gurtner et al., 2008) and its involvement in heterochromatin formation (Zhou and Grummt, 2005, Bandyopadhyay et al., 2007). Concerning HATs, interestingly, high levels of HDAC1 also correlated with MORF ($p=0.001$); which may be consistent with HDAC1 and MORF being reported in a complex required for normal cell cycle progression through S phase. With regard to other HDACs included in the study, HDAC1 positively correlated with SIRT1 ($p=0.002$); which may be consistent with interaction of SIRT1 with mSIN3A/HDAC1 complex that mediates transcription repression (Binda et al., 2008). These results may suggest a role for HDAC1 in transcription regulation in breast cancer. For further confirmation, evaluation of the relationships between HDAC1 and p53 acetylation marks K120, K373 and K386 were analysed, this revealed a correlation with high p53

acetylation levels at K120 and K386 ($p=0.015$ and $p=0.022$ respectively). Although not statistically significant, it may be consistent with a cascade of events related to cell cycle regulation in response to DNA damage that includes p53 acetylation, HDAC1 recruitment, Cdc2 and cyclin B promoters' repression which are key regulators of the G2/M transition (Imbriano et al., 2005). Together, these propose a critical role for HDAC1 in regulating cell cycle progression and cell fate.

Collectively, our results revealed apparent associations between TIP60, CBP and HDAC1 with their biological targets, i.e. histone and p53 PTMs. However, we did not always detect associations between these enzymes and their experimentally defined targets. For example, our data suggest significant positive correlations between TIP60 and p53K373 and K386 acetylation but not with its proposed target p53K120ac. Similarly, high levels of CBP were associated with p53K120ac but not its target p53K386 acetylation. This may be due to the limitation of the IHC staining sensitivity or the H-scoring system. More likely it reflects the complexity of biological systems, as compared to in vitro experiments. It is not clear whether subtle changes in the global levels of the PTMs will be detected by this approach, or whether the expressed levels of the modulator enzymes are functional. Moreover there may be enzymatic redundancy between HAT enzymes with regard to their histone and p53 Lysine targets. There may also be indirect effects from other regulators that are not really clear yet. Despite these limitations, TMA staining data appears to be a useful approach to the discovery of cancer biomarkers.

Table 4:10: p53 PTM Acetylation Modulators Detection Levels in Relationship to Histone PTMs and their Modulators.

Histone and Histone Modulators	TIP60				CBP				HDAC1			
	Total	LD	HD	p	Total	LD	HD	p	Total	LD	HD	p
mH2A	554			0.485	720			<0.001	515			0.039
Low		158	160			251	157			156	129	
High		116	120			149	163			107	123	
H2A.Z	550			0.010	708			<0.001	523			0.447
Low		163	137			249	143			152	140	
High		110	140			143	173			118	113	
H2A.Zac	425			<0.001	516			0.318	404			0.326
Low		124	76			145	110			106	88	
High		96	129			142	119			109	101	
H3K9ac	397			0.016	487			<0.001	391			0.282
Low		119	103			159	98			103	101	
High		74	101			104	126			88	99	
H3K18ac	402			0.006	496			0.016	386			0.152
Low		109	93			149	101			102	95	
High		82	118			122	124			87	102	
H4K12ac	388			0.008	470			0.033	371			0.060
Low		118	105			158	110			107	96	
High		66	99			101	101			74	94	
H4K16ac (Millipore)	545			0.162	701			0.027	513			<0.001
Low		150	137			186	172			150	106	
High		123	135			204	139			109	148	
H3K4me2	387			0.020	477			0.143	375			0.012
Low		113	99			148	110			105	89	
High		74	101			114	105			76	105	
H4K20me3	374			0.439	450			<0.001	364			0.056
Low		31	33			56	21			32	22	
High		144	166			191	182			144	166	
H3K9me3	442			0.083	523			0.143	475			0.004
Low		116	114			146	133			145	107	
High		92	120			140	104			100	123	
H4R3me2	441			0.038	541			0.237	428			0.001
Low		144	123			171	146			142	108	
High		78	96			13	111			74	104	
H3K56ac	514			0.002	570			0.088	433			0.125

Low		148	123			168	129			126	100	
High		101	142			138	135			103	104	
MORF	405			0.059	480			0.012	419			0.001
Low		87	124			145	98			137	91	
High		96	98			116	121			86	105	
hMOF	553			<0.001	708			0.006	524			0.420
Low		176	130			239	163			155	149	
High		99	148			152	154			115	105	
CBP	545			0.467					499			0.236
Low		155	153							144	129	
High		121	116							111	115	
SUV39H1	361			0.386	409			0.261	364			0.042
Low		91	104			113	105			110	83	
High		74	92			106	85			81	90	
HDAC1	411			0.486	499			0.236				
Low		107	111			144	111					
High		96	97			129	115					
HDAC2	451			0.137	544			0.509	480			0.120
Low		89	109			133	102			107	95	
High		128	125			174	135			131	147	
SIRT1	445			0.309	543			0.055	475			0.002
Low		119	146			202	132			129	90	
High		86	94			111	98			115	141	
DBC1	526			0.110	591			0.042	286			0.277
Low		141	128			175	127			75	67	
High		120	137			146	143			70	74	
p53k120ac (N)	396			0.116	463			<0.001	366			0.015
Low		110	116			167	97			119	82	
High		92	78			85	114			78	87	
p53k120ac (C)	396			0.383	463			0.009	366			0.303
Low		98	98			141	94			102	82	
High		104	96			111	117			95	87	
p53k373ac	417			0.018	512			0.003	411			0.178
Low		116	93			160	102			114	95	
High		93	115			121	129			100	102	
p53k386ac	470			0.008	562			0.531	492			0.022
Low		128	110			164	125			148	114	
High		98	134			155	118			108	122	

N, nuclear; C, cytoplasmic; LD, low detection; HD, high detection; all *p* values are calculated by χ^2 test. Bonferroni correction test was applied and reduced the (*p*) value of significance to 0.003.

4.2.2 Tumour Outcome in relation to p53 Acetylation Marks and their Modulators

As p53 acetylation was found to be indispensable for the p53 proapoptotic function (Tang et al., 2008), we explored the impact of the levels of p53 acetylation marks and their acetylation modulators with regards to tumour outcome and patient survival.

As shown in the Kaplan Meier survival curves in Figure 4.8A and B, tumours showing high levels of p53K120ac (Nuclear and cytoplasmic) were slightly better than those showing low levels in relationship to BCSS and DFS. However, the *p* values were not statistically significant.

With regard to p53K373ac, high levels were found associated with better breast cancer specific survival (BCSS) (*p*=0.081). Where 36 out of 270 (13%) patients in p53K373ac high-level group died from breast cancer; while 54 out of 287 (19%) in p53K373ac low-level group died from breast cancer. High levels of p53K373ac also correlated with longer disease free survival (DFS) (*p*=0.046). 35 patients out of 270 (13%) in the high p53K373ac group presented with recurring of breast cancer; while 54 out of 287 (19%) in low p53K373ac presented with recurring breast cancer (Fig. 4.8C).

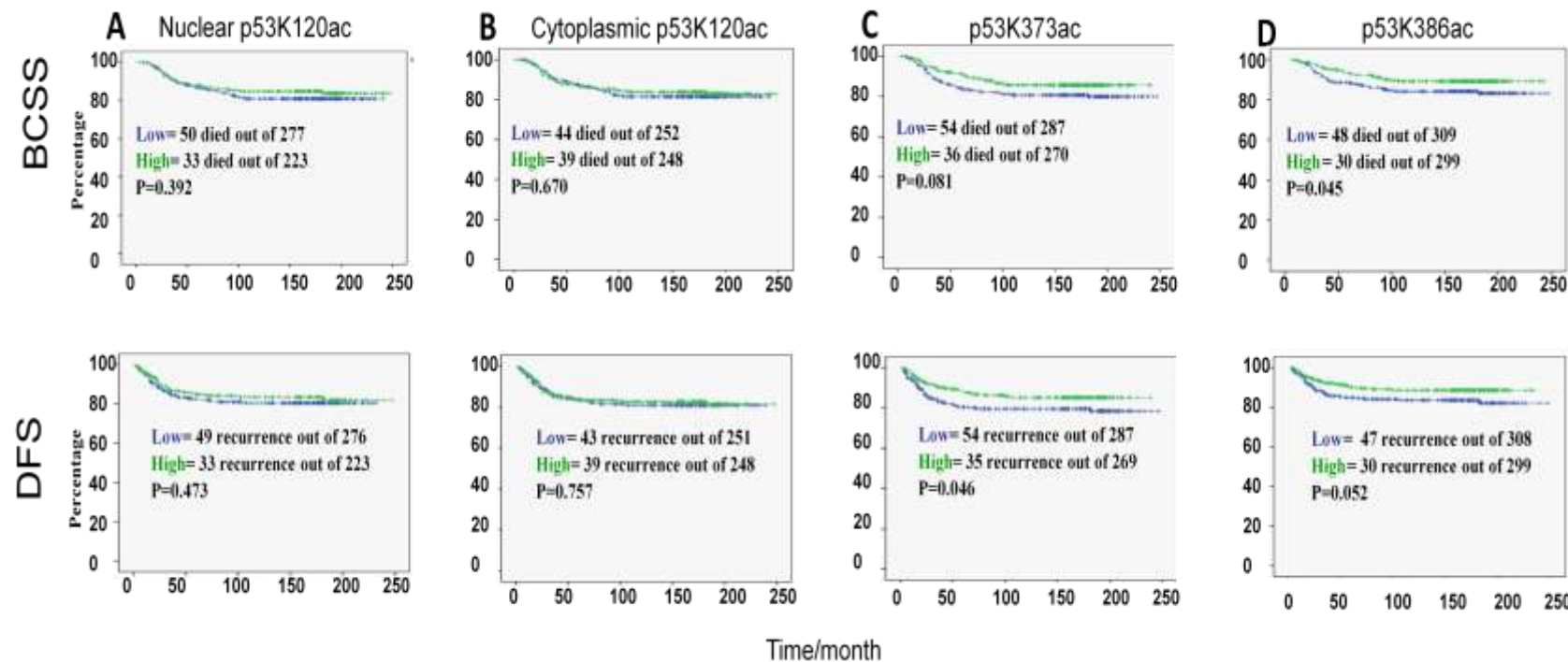
High levels of p53K386ac (Fig. 4.8D) correlated with better BCSS (*p*=0.045); where, 30 out of 299 (10%) patients in the high p53K386ac group died from breast cancer, while 48 out of 309 (15.5%) in the low p53K386ac group died from breast cancer. Regarding DFS, high levels of p53K386ac were also

associated with a favourable outcome ($p=0.052$); where 30 out of 299 (10%) patients in the high p53K386ac group had a recurrence of breast cancer; while, 47 out of 308 (15%) in low p53K373ac had a recurrence of breast cancer.

As TIP60 and CBP have been previously reported to acetylate p53 (Tang et al., 2006a, Li et al., 2009c, Meek and Anderson, 2009) the impact of both these markers and HDAC1 levels were also explored in relation to patient survival.

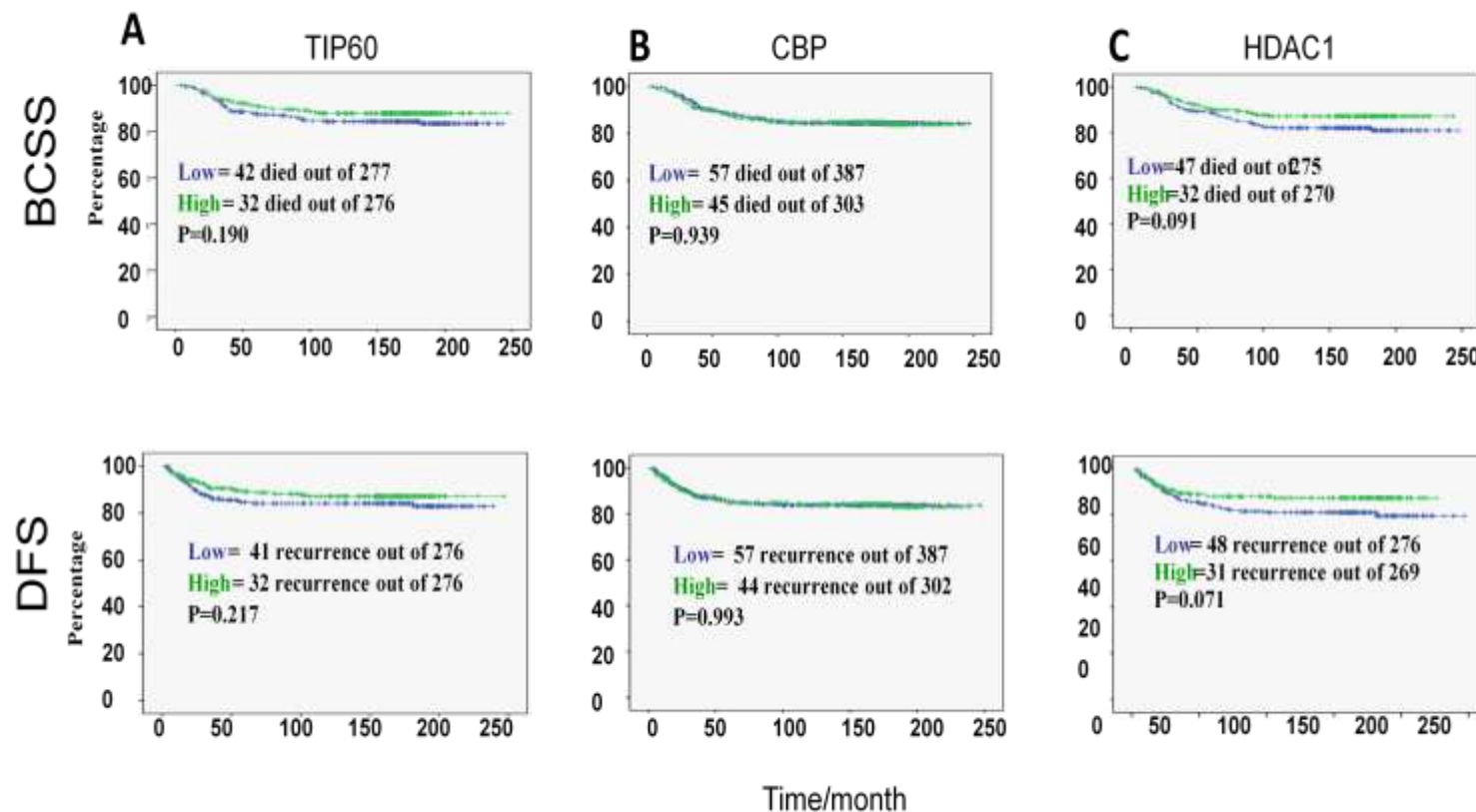
Analysis revealed trend for high levels of both TIP60 and HDAC1 with both BCSS and DFS (Fig. 4.9A and B). However the p values did not reach the values of significance for TIP60 ($p=0.19$ and $p=0.217$ respectively) or HDAC1 ($p=0.091$ and $p=0.071$ respectively). Unexpectedly, we found that CBP detection levels have no impact on patient survival as shown in Figure 4.9C Multivariate analysis using the Cox proportional regression model (Cox, 1972) showed that the prognostic effect of p53 acetylation marks and their modulators on survival was dependent on other key prognostic factors in breast cancer including histological grade, tumour size, tumour stage and lymph node stage.

As a number of significant statistical relationships have been noted between p53 acetylation marks and their modulators, we gathered data from those marks together to perform a cluster analysis. Further evaluation of association between the revealed cluster classes in relationship to tumour grades and patient survival was also explored.

Figure 4.8: Tumour outcome in Breast Cancer TMA stained for p53 Acetylation Marks and their Acetylation Modulators

Kaplan-Meier curves for the levels of p53 acetylation marks (A, B, C, D) in breast cancer TMA with respect to breast cancer specific survival (BCSS) and disease free survival (DFS). The green and blue colours represent in order the high and low detection groups for each marker, the Y axis represents survival probability, X axis represents time relapse in months.

Figure 4.9: Tumour outcome in Breast Cancer TMA stained for p53 Acetylation Modulators



Kaplan-Meier curves for the levels of p53 acetylation modulators (A, B, C) in breast cancer TMA with respect to breast cancer specific survival (BCSS) and disease free survival (DFS). The green and blue colours represent in order the high and low detection groups for each marker, the Y axis represents survival probability, X axis represents time relapse in months.

Table 4:11: Cox proportional Hazard Model Showing Hazard Ratios for BCSS and DFS conferred by p53K373ac and p53K386ac and clinicopathological variables

A

BCSS			
Variable	Hazard Ratio	95% CI	p
Tumour size (cm)	0.640	0.386 to 1.101	0.110
Tumour stage	1.450	1.633 to 3.073	<0.001
Grade	2.233	1.533 to 3.758	<0.001
p53K373ac	0.511	0.836 to 2.435	0.192
p53K386ac	0.520	0.711 to 2.083	0.474

B

DFS			
Variable	Hazard Ratio	95% CI	p
Tumour size (cm)	0.640	0.373 to 1.092	0.101
Tumour stage	1.450	1.654 to 3.174	<0.001
Grade	2.233	1.537 to 3.800	<0.001
p53K373ac	0.514	0.881 to 2.566	0.134
p53K386ac	0.518	0.698 to 2.030	0.522

A, p53K373ac and p53K386ac are dependent of other prognostic factors in breast cancer with respect to breast cancer specific survival (BCSS); **(B)**, and disease free survival (DFS); CI, confidence interval ; p, χ^2 p value.

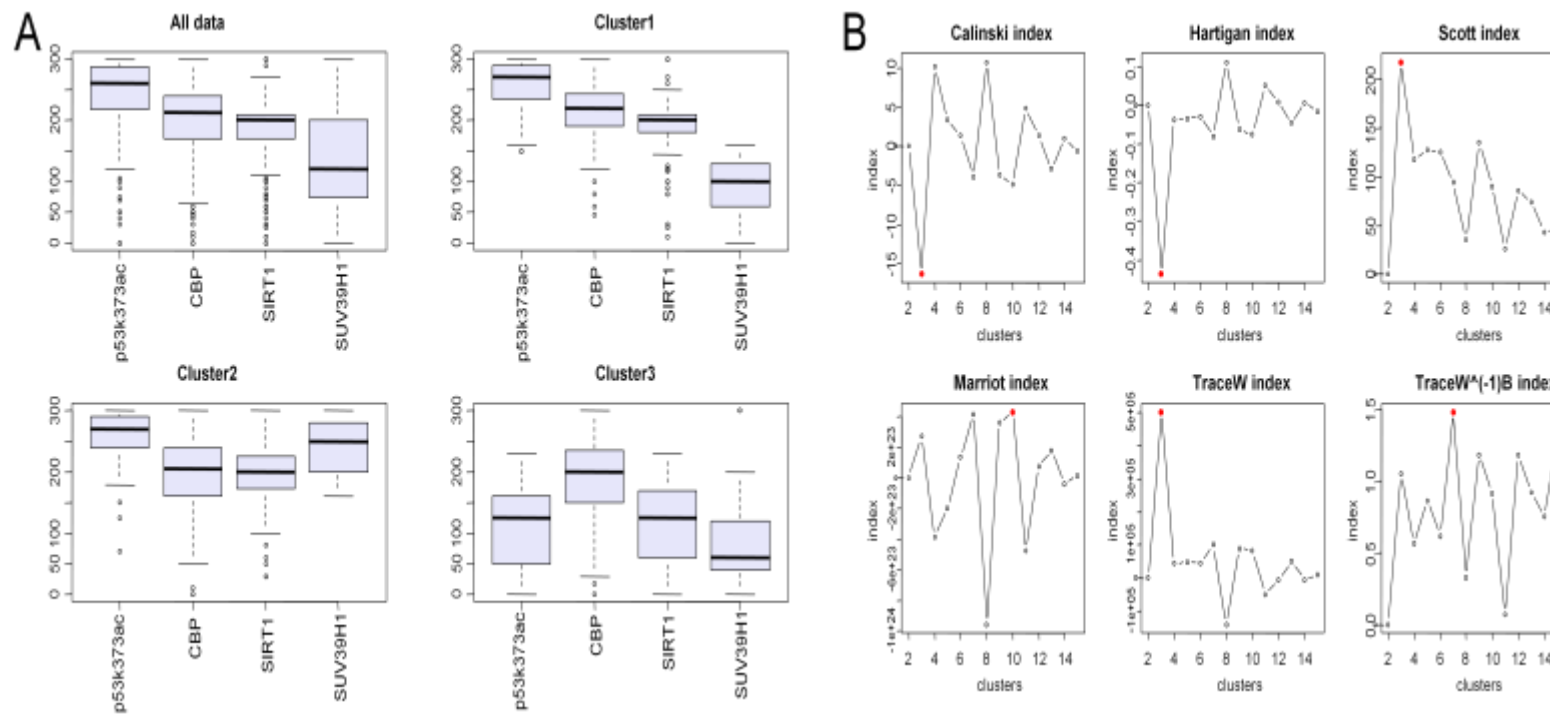
4.2.3 Cluster analysis of p53 PTMs and their regulators

p53K373ac, CBP, SIRT1 and SUV39H1 cluster analysis

Cluster analysis and validity indices tests were performed by Dr Daniel Soria, School of Computer Science, University of Nottingham. At first, the cluster analysis was applied to p53K373ac, CBP, SIRT1 and SUV39H1. CBP is responsible for p53 acetylation at K373 in association with p300 (Zhao et al., 2006), SIRT1 has been described to deacetylate p53 (Hasegawa and Yoshikawa, 2008) and SUV39H1 which has been described in a complex with p53 is capable of H3K9 methylation (Chen et al., 2010). The cluster analysis by K-means yielded 3 clusters (from 292 patients). The number of the clusters in the K-means algorithm was consistent in 3 (Calinski, Hartigan and Scott) out of the 6 K-means validity indices tests (Fig. 4.6A and B). In addition, 4 clusters were obtained from the PAM algorithm; two of them were merged yielding 3 clusters (Fig. 4.7). Three common clusters (containing 267 patients) were obtained after using data from both K-means and PAM algorithm to assign patients to the same clusters; where 267 cases were clustered into three common cluster groups, only 25 cases did not match (Fig. 4.10A). Analysis of the obtained common clusters revealed a remarkable association between cluster 2 (which is characterized by high levels of both p53K373ac and SUV39H1) and better BCSS (as illustrated in Fig. 4.10C) in a significant p value ($p=0.045$); Conversely, The cluster 1 and 3 (which are characterized by low levels of SUV39H1) correlated with poorer patient survival and showed more tendencies toward being among higher grade tumours (Fig.4.10B). CBP and SIRT1 levels showed no significant impact on the clustering. However, the role of both SUV39H1 and p53K373ac in segregating clusters was obvious. The results indicate a potentially role for p53K373ac as a

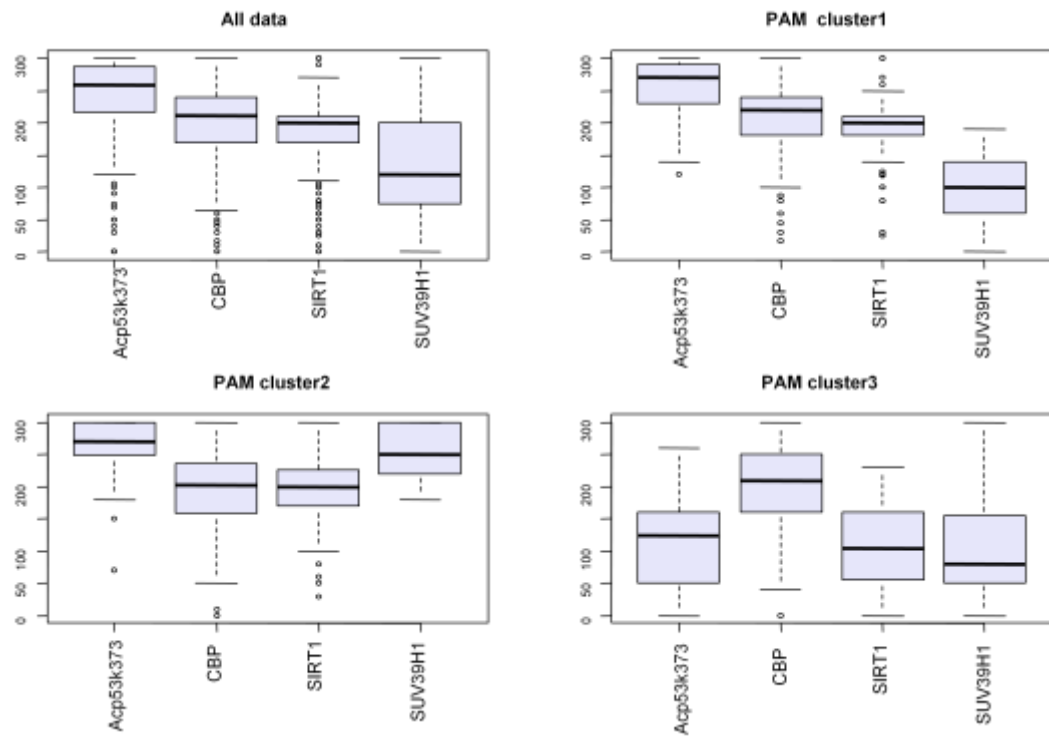
marker (in conjunction with the H4K16ac, hMOF and SUV39H1) for better tumour outcome and patient survival.

Figure 4.10: K-means Clustering Algorithm and Validity Indices tests for Breast Cancer Tumour TMA with Regard to p53K373ac, CBP, SIRT1 and SUV39H1 Detection Levels.



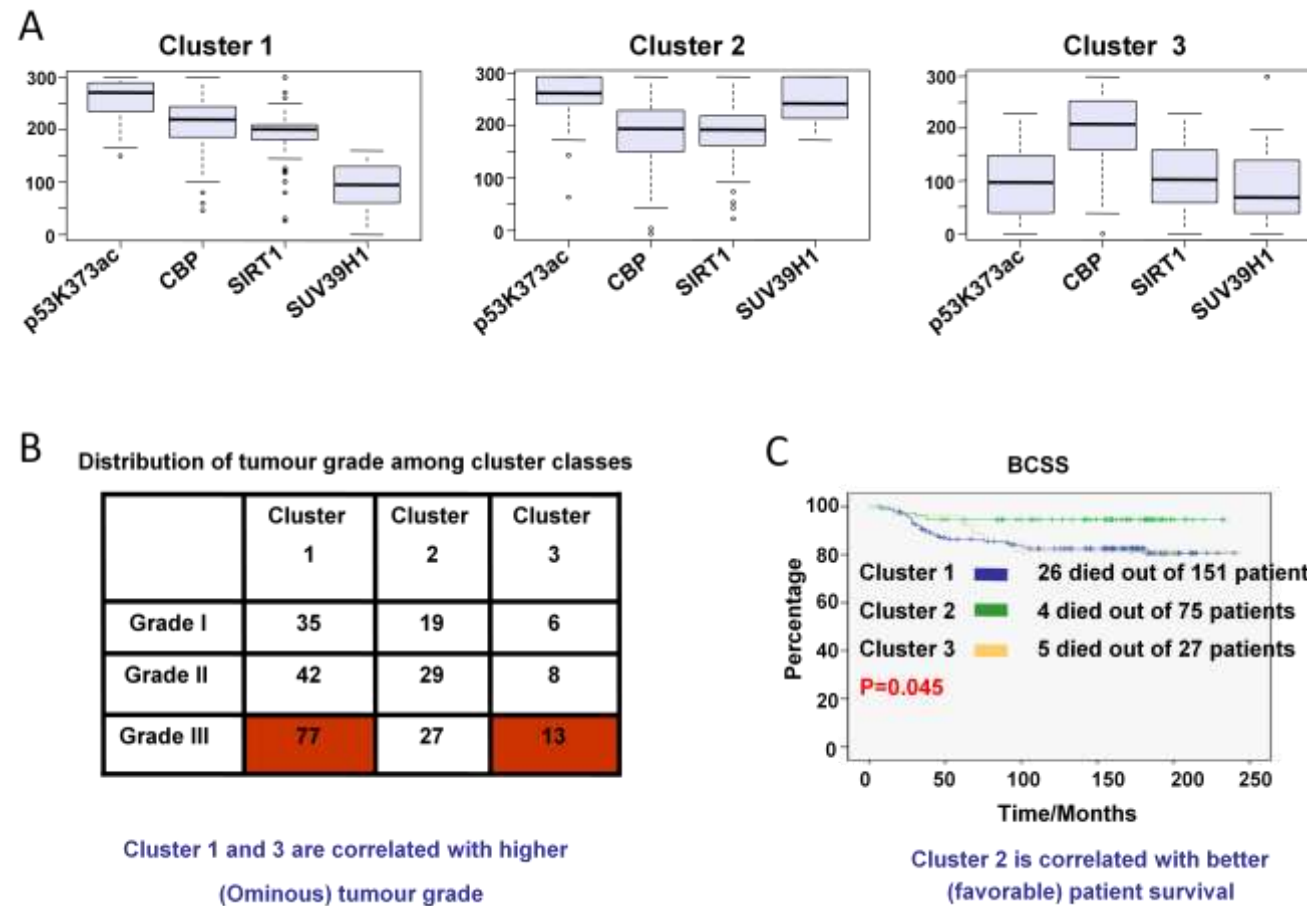
A, Boxplots for p53K373ac, CBP, SIRT1 and SUV39H1 grouped by K-means algorithm; **B**, Three out of six validity indices tests indicate 3 clusters.

Figure 4.11: PAM Clustering Algorithm for Breast Cancer Tumour TMA with Regards to p53K373ac, CBP, SIRT1 and SUV39H1 Detection Levels.



Boxplots for p53K373ac, CBP, SIRT1 and SUV39H1 grouped by PAM algorithm

Figure 4.12: Clustering of (p53K373, CBP, SIRT1 and SUV39H1), Correlation with Tumour Grade and Tumour Outcome.



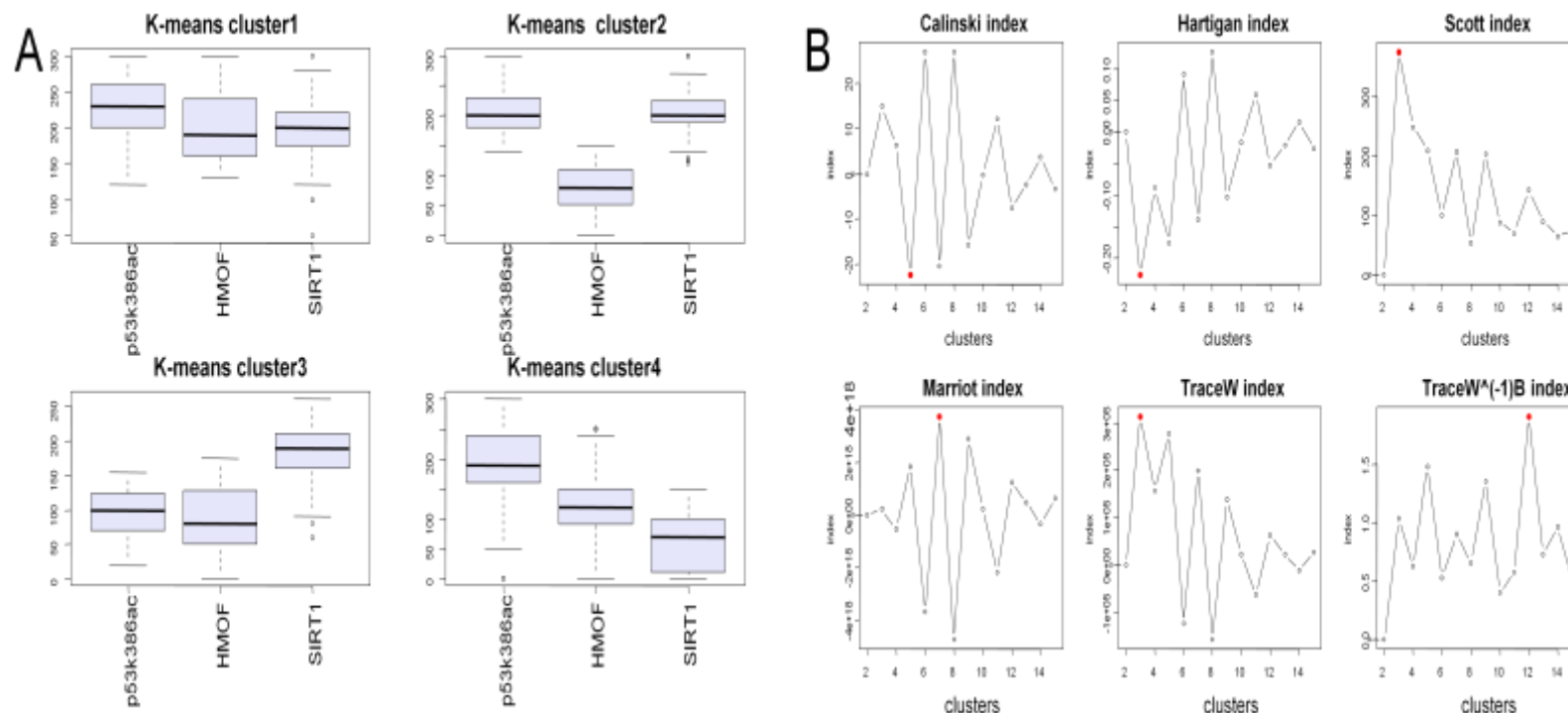
A, Boxplots for p53K373ac, CBP, SIRT1 and SUV39H1 grouped by common clusters, cluster 2 is characterized by high levels of both p53K373ac and SUV39H1 in comparison to the other two clusters; **B**, cluster 1 and 3 correlate with the ominous grade III; **C**, unadjusted Kaplan-Meier curves for p53K373ac, CBP, SIRT1 and SUV39H1 cluster groups are showing that cluster 2 correlates with favourable patient outcome.

p53K386ac, hMOF and SIRT1 cluster analysis

hMOF and SIRT1 have been previously described in regulating acetylation of p53 (Rea et al., 2007, Cheng et al., 2003). In addition, according to our results, both hMOF and p53K386ac correlated with favourable tumour outcome and patient survival. Therefore we decided to group the three biomarkers together in a cluster analysis. Initially, the cluster analysis was applied to 507 cases (valid cores for the three marks together) by both K-means and PAM algorithms; which yielded three clusters. However, the consensus was quite poor; the 3 groups obtained by K-means were quite different from the 3 groups obtained by PAM. In addition, the number of “NC” (not common/not matched cases) was quite high. So the cases were re-clustered into 4 groups (Fig. 4.13A, 4.14A), specially as 2 validity indices for PAM algorithm suggested 4 as the best number of clusters (Fig 4.14B). Reclustering showed an improved consensus where 365 cases were matching in the two algorithm; only 142 NC.

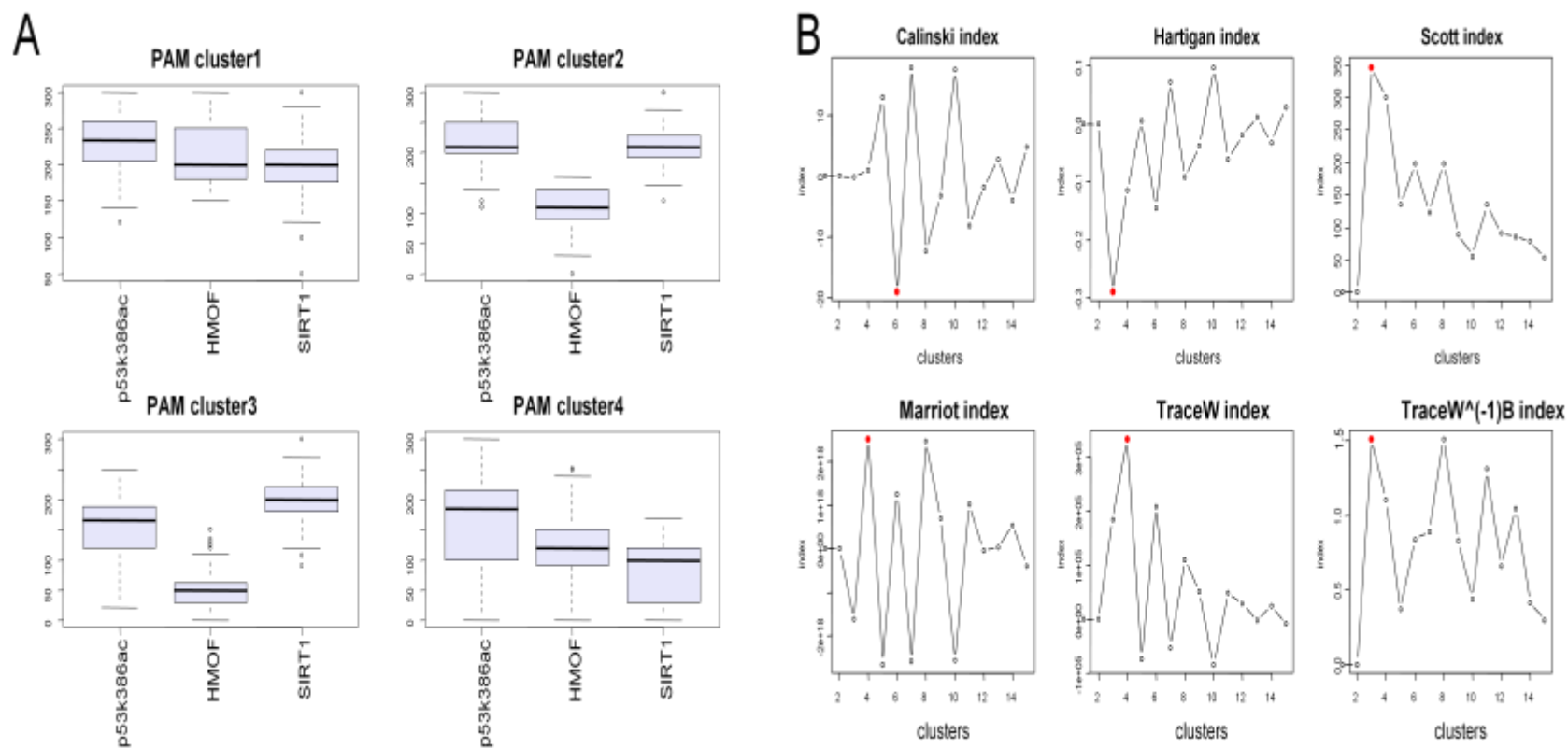
Among the obtained four common clusters (Fig. 4.15A), cluster 1 and 2 which are characterized by high levels of p53K386ac and high or moderate levels of hMOF were (as illustrated in Fig. 4.15B) correlated with better patient survival at statistically significant value ($p=0.026$). Conversely, cluster 3 and 4 correlated with poor patient survival. These clusters are characterized by low levels of both p53K386ac and hMOF (Cluster 3) or very low levels of SIRT1 (cluster 4). These results may suggest a potentially role for p53K386ac as a biomarker (in conjunction with the H4K16ac, hMOF, SUV39H1) for better tumour outcome and patient survival.

Figure 4.13: K-means Clustering Algorithm and Validity Indices tests for Breast Cancer Tumour TMA in Regards to p53K386ac, hMOF and SIRT1 Detection Levels.



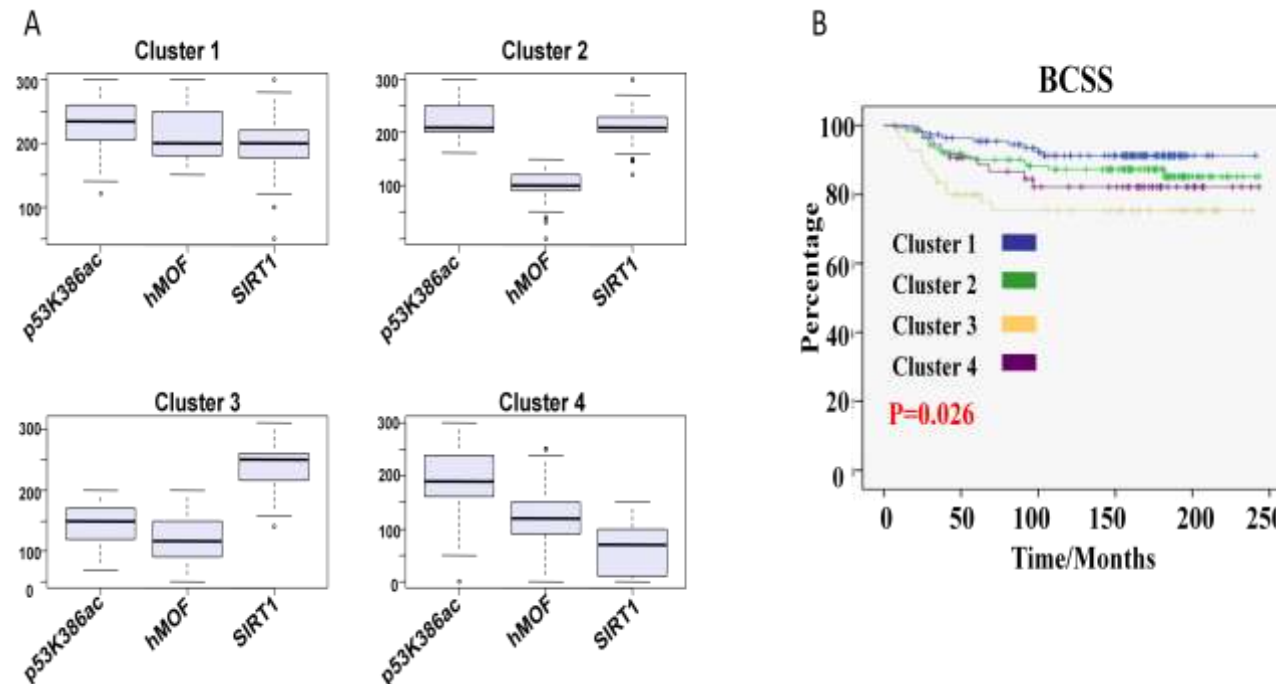
A, Boxplots for p53K386ac, hMOF and SIRT1 grouped by K-means algorithm; **B**, Three out of six validity indices indicate 3 clusters.

Figure 4.14: PAM Clustering Algorithm and Validity Indices tests for Breast Cancer Tumour TMA in Regards to p53K386ac, hMOF and SIRT1 Detection Levels.



A, Boxplots for p53K386ac, hMOF and SIRT1 grouped by PAM algorithm; **B**, Two out of six validity indices tests indicate 4 clusters.

Figure 4.15: Clustering of (p53K386ac, hMOF and SIRT1) and Tumour Outcome



A, Boxplots for p53K386ac, hMOF and SIRT1 grouped by common clusters, cluster 1 and 2 are characterized by high levels of p53K386ac and high or moderate levels of hMOF. Conversely, cluster 3 and 4 are characterized by low levels of both p53K386ac and hMOF (Cluster 3) or very low levels of SIRT1 (cluster 4); **B**, unadjusted Kaplan Meier curves for p53K3386ac, hMOF and SIRT1 cluster groups showing that cluster 1 and 2 correlate with favourable patient survival.

Summary of Findings: p53 acetylation marks and their modulators in Breast tumours

In this Chapter we examined global levels of p53 acetylation marks and proteins that regulate p53 acetylation in breast tumour tissue. The data indicated that low levels of p53 acetylation at K120, K373 and K386 tended to correlate with the poor tumour prognostic HER2 and basal tumour subtypes. Conversely, high levels of p53 acetylation at K373 and K386 correlated with favourable tumour grade, good NPI and positive hormonal receptors status including estrogen, progesterone and androgen receptors. In addition, high levels of p53 acetylation at K373 and K386 correlated with luminal tumour subtype specific markers such as CK7/8 and CK9 and inversely correlated with CK5/6, the basal subtype specific marker. Taken together, these results are consistent with the hypothesis that active i.e. acetylated p53 correlated with good tumour outcome related variables.

p53 acetylation markers also positively correlated with histone H2A variants and histone PTMs. High levels of p53K373ac and K386ac were correlated with the good tumour outcome markers H3K18ac, H4K16ac and H4K20me3, which previously reported to be lost in human cancer (Fraga et al., 2005) and high grade breast tumours (Elsheikh et al., 2009). Moreover, p53 acetylation marks positively correlated with the DNA damage response mark H3K56ac (Masumoto et al., 2005, Vempati et al., 2010, Yuan et al., 2009).

We also determined the levels of the histone acetyltransferases TIP60 and CBP, which previously reported to acetylate p53 at K120, K373 and K386 (Tang et al., 2006b, Meek and Anderson, 2009); and the histone deacetylase HDAC1

which reported to deacetylate p53 at K373 (Meek and Anderson, 2009). Our data identified a correlation between low levels of TIP60, CBP and HDAC1 with HER2 and basal tumours, the poor prognostic breast cancer. We also identified positive correlation between high levels of CBP and advanced patient age. In addition, CBP and HDAC1 positively correlated with high levels of estrogen receptors, whereas TIP60 correlated with positive androgen receptor expression.

Consistent with the histone variant TMA data, high levels of TIP60 correlated with high levels of acetylated H2A.Z and the histone acetyltransferase hMOF, CBP correlated with high levels of histone H2A variants, the mH2A and H2A.Z, and high levels of H3K9ac and H4K20me3, the good outcome markers in human tumours.

Kaplan Meier survival curves in Figure 4.8 identified high levels of p53 acetylation at K373 and K386 as markers for favourable patient survival. However, Cox regression test revealed that the prognostic effects of both p53K373ac and p53K386ac levels were dependent on key prognostic factors in breast cancer. With regard to TIP60 and HDAC1, high levels showed a trend towards favourable patient survival. Although they have been found not statistically significant (Fig. 4.9) we included those markers and HDAC1 in clustering analysis to identify their trend in breast cancer tumours. Our data identified that tumours characterized by high levels of p53K373ac, p53K386ac and SUV39H1 to correlate with favourable tumour grade longer patient survival.

Collectively, according to our results in this chapter, acetylation of p53 found to be correlated with better tumour outcome factors and longer patient survival, with a possible future application in medical practice, especially if explored in combination with SUV39H1.

**THE EFFECT OF THE HAT
INHIBITORs ON HISTONE AND p53
PTMs AND MCF-7 CELL CYCLE
PROLIFERATION**

In Chapters three and four we examined the levels of histone and p53 PTMs and their regulators in breast cancer TMAs by IHC staining. This revealed an association of several of these markers with patient survival, indicating that they may be useful individually or in combination as prognostic indicators. Interestingly, global loss of H4K16ac and H4K20me3 have been reported as hallmarks of human cancer, and loss of these PTMs have been detected in tumour suppressor genes (Fraga et al., 2005) and higher grade breast tumours (Elsheikh et al., 2009). Although it is not yet clear if histone/p53 PTMs are causal factors or a consequence of other changes driving tumourgenesis, they offer an attractive therapeutic target as they are amenable to reversal by small molecules. In the forthcoming chapter, I will present our results showing the influence of natural HAT inhibitor (HATi) treatment on these biomarkers in a cell model. We explored the effects of curcumin and garcinol HATi on histone and p53 PTMs levels and their effects on cell cycle progression and proliferation of MCF-7 cells.

5.1.1 HAT inhibitors Alter Histone H3 and H4 Acetylation

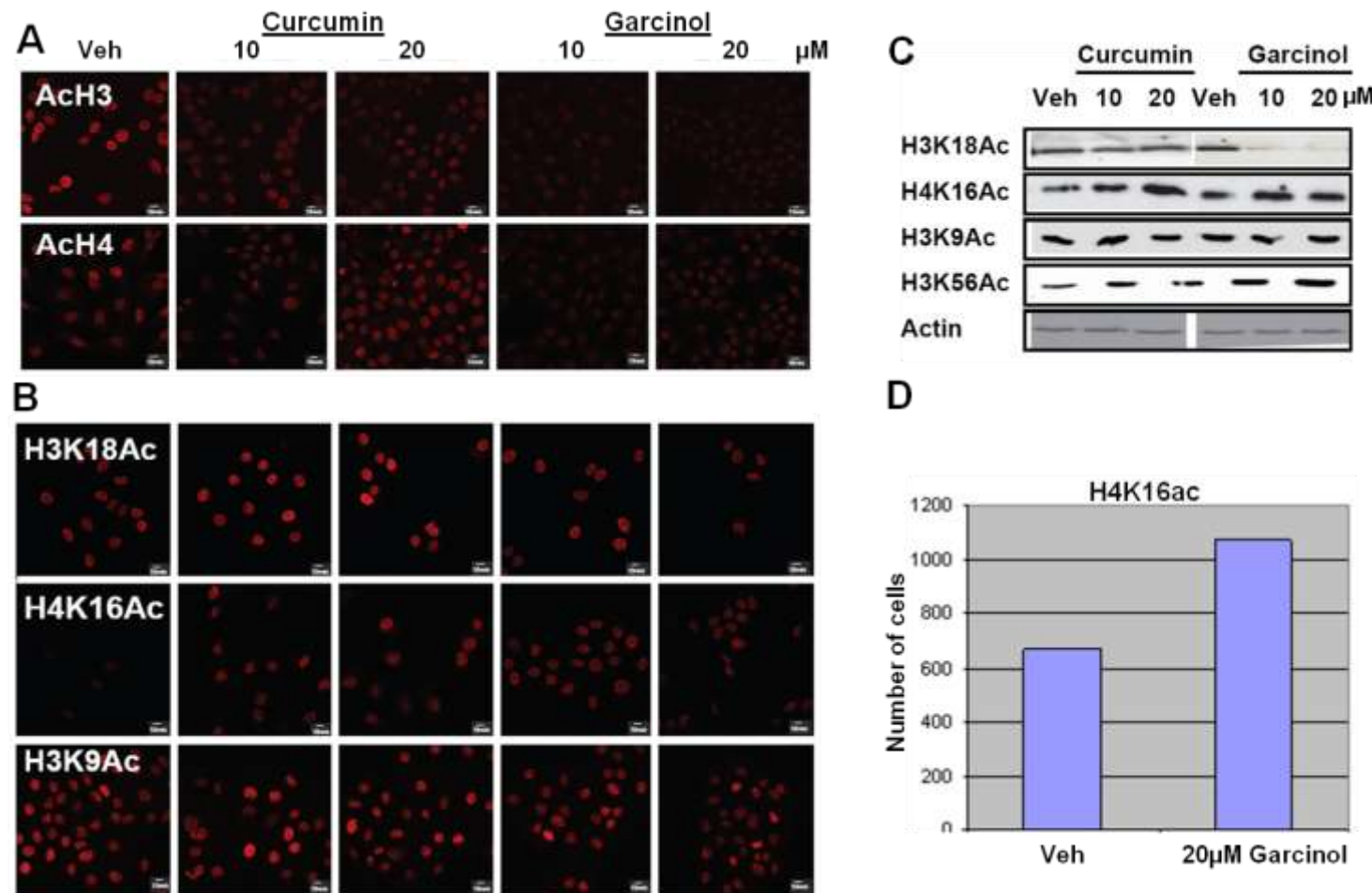
MCF-7 cells were treated with the HAT inhibitors, curcumin and garcinol for 24 hrs as described in section 1.2.12. Curcumin is a natural HATi compound previously reported to inhibit p300 and CBP acetyltransferase activity (Balasubramanyam et al., 2004b) and to induce growth arrest of several cell lines with a potential chemotherapeutic potential (Chauhan, 2002, O'Sullivan-Coyne et al., 2009, Park et al., 2006, Sahu et al., 2009, Weir et al., 2007). Garcinol is another natural HATi compound reported to be highly cytotoxic to HeLa cells and has an inhibitory effect on both PCAF and p300 (Balasubramanyam et al., 2003). These compounds were used at a concentration of 10 and 20 μ M as preliminary range finding experiments indicated cell toxicity effects in excess of 30 μ M. Cells

were then fixed and stained with antibodies specific for different histone PTMs and analysed by fluorescence microscopy using a Zeiss LSM510 confocal microscope as described in Materials and Methods (section 2.4.6). In addition, changes in histone PTMs were monitored by preparation of cell free extracts and western blotting as described in Section 2.4.5. A list of antibodies and dilutions used are detailed in Appendix 1. As shown in Figure 5.1A, curcumin and garcinol treatment caused a decrease in bulk acetylation of histones H3 and H4 as determined by pan-acetyl H3 and pan-acetyl H4 antibodies. Specifically, 10 µM curcumin treatments caused greater reduction in histone H3 and H4 acetylation than 20 µM treatment; suggesting differential and dose-dependent effects of HATi on histone modifications *in vivo* (this experiment was verified by two researchers). Concerning garcinol, the decrease in acetylation was found proportional with the concentration of treatment (Fig. 5.1A).

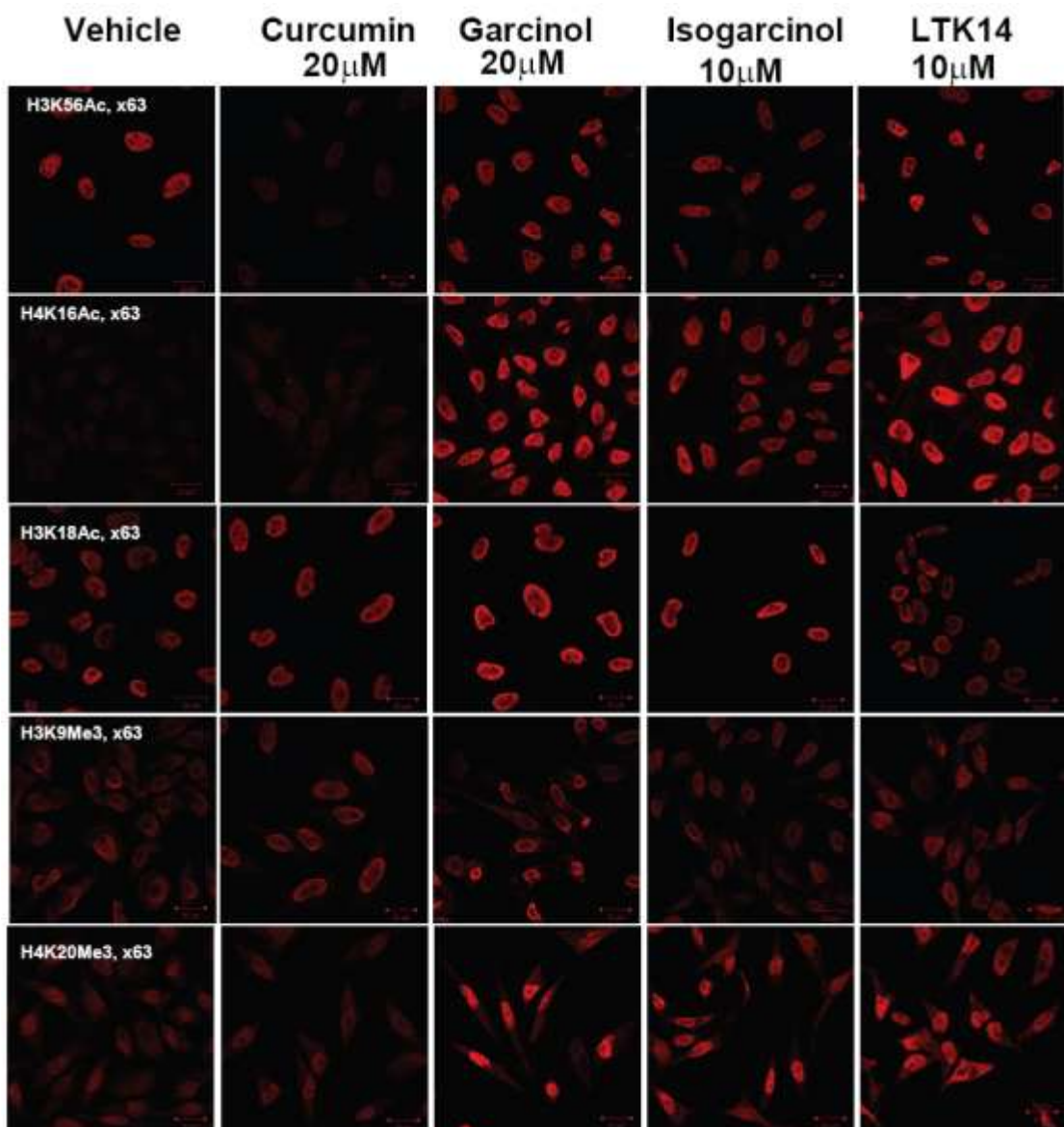
Looking at specific histone acetylation marks, H3K18ac, an indicator of actively transcribed genes and DNA synthesis, (Horwitz et al., 2008) was markedly decreased by garcinol as measured by both immunofluorescence and western blotting (Fig. 5.1B and C). However, no significant change in H3K18ac was observed after curcumin treatment (Fig. 5.1B and C). Interestingly, global levels of H4K16ac, which barely detectable in MCF-7 cells, were increased after both curcumin and garcinol treatment (Fig. 5.1B and C). Conversely, no detectable change in H3K9ac detection levels was observed after HATi treatment (Fig. 5.1B and C). We also noted that garcinol treatment caused a marked increase in the H3K56ac, the CBP/p300 dependent histone PTM that has been reported to be associated with DNA damage response (Das et al., 2009). This

result suggests a possible garcinol-induced DNA damage response in MCF-7 cells (Fig. 5.1C). Actin was used as a loading control (Fig. 5.1C). For further confirmation, we quantified garcinol-induced H4K16ac by flow cytometry analysis as described in Materials and Methods (section 2.6.8). After garcinol treatment, MCF-7 cell were fixed, permeabilised and probed with anti-H4K16ac antibody, followed by evaluation of MCF-7 cells for H4K16ac. The number of cells showing high levels of H4K16ac increased upon garcinol treatment (Fig. 5.1D). MRC-5 cells were also treated with 20 μ M curcumin or garcinol and 10 μ M isogarcinol or LTK14 for 24 hrs (Fig. 5.2). Isogarcinol and LTK14 are semi-synthetic products of intermolecular cyclisation of garcinol reported to have potent p300 inhibitory effect (Mantelingu et al., 2007b). MRC-5 treated with HATi also showed increased H4K16ac and H3K56ac levels after garcinol, isogarcinol and LTK14 treatment. However, in contrast to MCF-7 cells, MRC-5 cells showed a decrease in H4K16ac after curcumin and increased H3K18ac after garcinol treatment. Taken together, these results indicate that MCF-7 cells differ from the non-transformed MRC-5 cell line with regard to changes in global histone acetylation pattern after HATi treatment. In addition, in the MCF-7, garcinol can induce differential changes in the levels of histone PTMs; with potential impact on basic cellular function and behaviour. While the CBP-dependent acetylation mark H3K18ac was reduced, another target for this HAT i.e. H3K56ac appeared to be increased. This might suggest pleiotropic effects of garcinol, outside of its HAT inhibitory activity. Alternatively it may indicate that while H3K18 acetylation is regulated by CBP/p300, other HATs that are unaffected by garcinol can acetylate H3K56.

Figure 5.1: Differential Effects of HATi treatment on Histone H3 and H4 Acetylation.



A, Immunofluorescent staining for MCF-7 cells treated with vehicle (Ethanol), curcumin or garcinol in the concentration of 10 and 20 μ M for 24 hrs. Cells were stained with pan acetyl H3 and H4 following treatment; **B**, MCF-7 cells were also evaluated for H3K18ac, H4K16ac and H3K9ac levels; **C**, Western Blotting for histone PTMs levels in MCF-7 cells treated with vehicle (Ethanol), curcumin and garcinol in the same concentration used in **(A)** and **(B)**. Actin was used as a loading control; **D**, number of MCF-7 cells expressing high levels of H4K16ac after treatment with Vehicle (Ethanol) or Garcinol (20 μ M) for 24 hours. The total cell count was 4,000 cells.

Figure 5.2: Histone PTMs in MRC-5 Cells after HATi Treatment

Detection of histone PTMs by immunofluorescence staining of MRC-5 cells, the cells were treated for 24 hrs with vehicle (Ethanol), 20 μ M curcumin or garcinol and semi-synthetic derivatives of garcinol, the isogarcinol or LTK14 in a concentration of 10 μ M.

5.1.2 HATi treatment Alters Histone H3 and H4 Methylation

In addition to the effects on acetylation, we explored the effect of curcumin and garcinol treatment on histone methylation. H3K9me3, the repressed gene mark (Groner et al., 2010) was not altered after the treatment with curcumin or garcinol (Fig 5.3A and B). However, its regulator the methyltransferase SUV39H1 (Rea et al., 2000) which correlated with better breast cancer tumour outcome (as described in Chapter 3 and 4) was found to show increased expression after curcumin treatment (Fig 5.3B). This may be consistent with the anticarcinogenic properties of curcumin (Ravindran et al., 2009)), and is of interest with regard to our observation that low expression levels of SUV39H1 are associated with higher grade tumours.

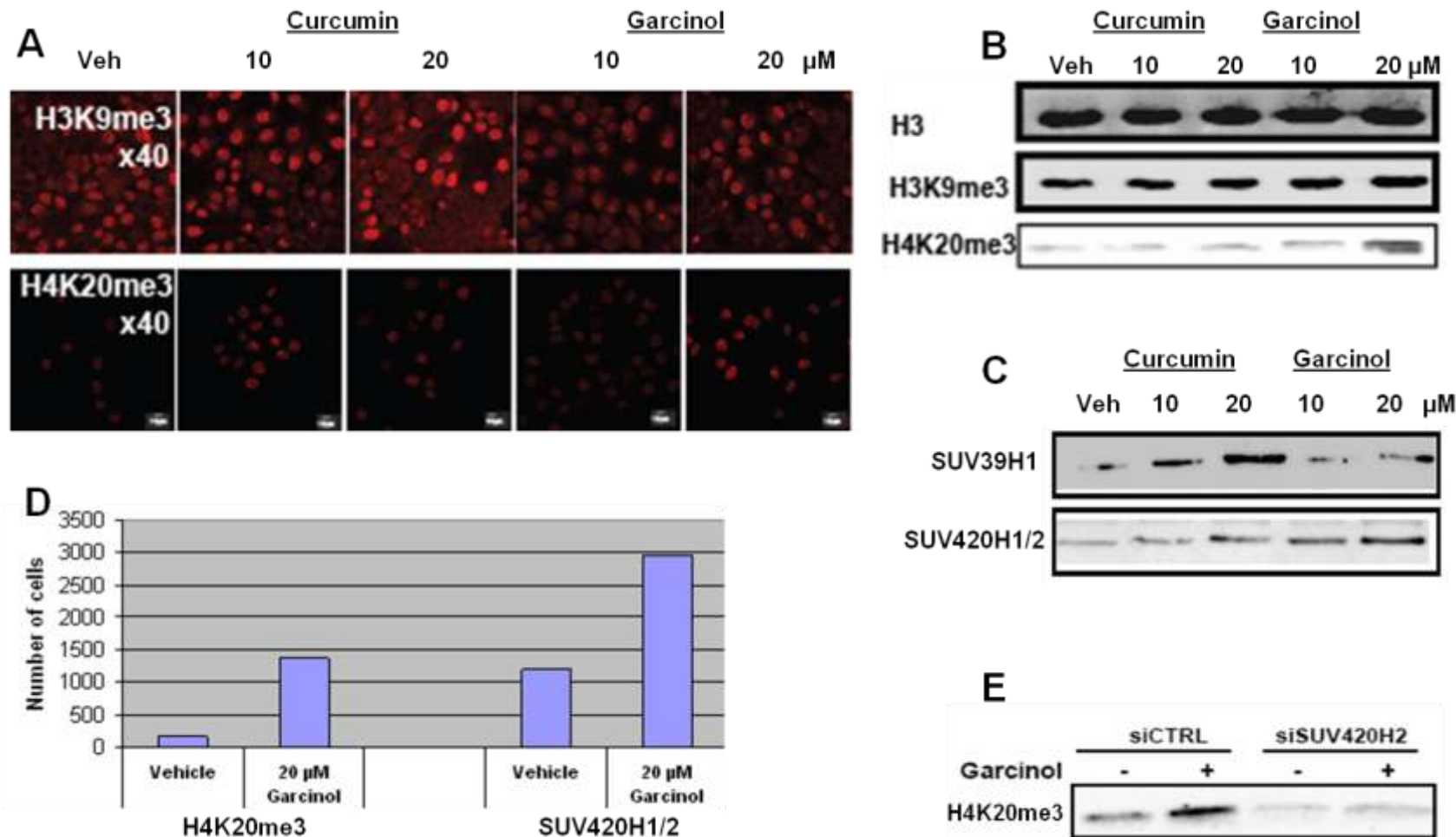
H4K20me3 levels are low or absent in cancer cell lines (Fraga et al., 2005) and to be a good outcome marker in breast and lung cancer (Elsheikh et al., 2009, Van Den Broeck et al., 2008). Remarkably, H4K20me3 was strongly induced by garcinol treatment in as shown by both immunofluorescence and western blotting (Fig. 5.3A and B). Consistent results for H3K9me3 and H4K20me3 in MRC-5 cells are shown in Figure 5.2. Thus we conclude that garcinol has unexpected effects on the histone methylation status of H4K20, another important marker in cancer cells.

Whereas monomethylation of H4K20 is catalysed by several methyltransferases such as SET8 (Fang et al., 2002) and PR-Set7 (Nishioka et al., 2002b), di and tri-methylation appear to be catalysed by SUV420H1/H2 respectively (Schotta et al., 2004, Schotta et al., 2008). As it seemed unlikely that

garcinol could act both as a direct inhibitor of selected acetyltransferase enzymes, and at the same time stimulate methyltransferase activity, we decided to assess the effects of garcinol on expression levels of chromatin modifying proteins. We therefore assessed the levels of the H4K20me3 methyltransferase SUV420H1 and SUV420H2 (Souza et al., 2009) in MCF-7 cells, before and after treatment. The antibody used is able to detect both SUV420H1 and H2 isoforms. As shown in Figure 5.3 SUV420 expression levels were markedly increased by garcinol, but not curcumin, as detected by western blots and flow cytometry analysis (Fig. 5.3C and D). After garcinol treatment, MCF-7 cell were fixed; permeabilised; probed with anti-H4K20me3 or SUV420H2 antibodies and followed by evaluation of MCF-7 cells for both biomarkers. The number of cells high for H4K20me3 and its regulator SUV420H2 were markedly increased by several fold upon garcinol treatment (Fig. 5.3D).

These results indicate that garcinol treatment of MCF-7 cells invokes in a strong induction of H4K20me3 and a concomitant increase in the methyltransferases SUV420H1 and SUV420H2. To determine whether these enzymes are responsible for the observed increase in K20 trimethylation, an siRNA knockdown experiment was performed in combination with garcinol treatment. The experiment was carried out with my colleague Dr HM Collins, who has previous experience in siRNA techniques. MCF-7 cells were transfected with siSUV420H2 or control scrambled siVector For 24 hours. Following that, cells were treated with garcinol for a further 24 hrs. As shown in Figure 5.3E knockdown of SUV420H2 but not the control siRNA prevented the induction of H4K20 trimethylation by garcinol. This indicates that increased expression of

SUV420H2 in response to garcinol is likely to be responsible for the observed increase in H4K20 trimethylation induced by this agent. As H4K20 methylation has been previously observed in DNA damage response (Greeson et al., 2008, Hsiao and Mizzen, 2010, Sakaguchi and Steward, 2007, Sanders et al., 2004), our results suggest that SUV420 enzymes may be upregulated following DNA damage stress.

Figure 5.3: HAT inhibitors Treatment Alters Histone Methylation.

A and **B**, MCF-7 cells were treated with vehicle or 10, 20 μ M curcumin or garcinol for 24 hrs. Cells were stained for methylation marks and assessed by immunofluorescence (**A**) and Western blotting (**B**), histone 3 (H3) levels were used as loading control; **C**, the number of MCF-7 cells expressing high levels of H4K20me3 and SUV240H1/2 after treatment with vehicle or 20 μ M garcinol for 24 hrs was assessed by FACS. The total cell count was 4,000 cells; **D**, siRNA of MCF-7 cells with scrambled siVector (siCTRL) or siSUV420H2, detection of H4K20me3 by western blotting following 24 hrs of garcinol treatment.

5.1.3 Effects of HATi on HATs and HDACs Expression

To gain insight into the possible mechanistic role of garcinol in upregulation of H4K16 and H3K56 acetylation, we examined the expression levels of candidate factors responsible for acetylation and deacetylation of these residues. The commercial antibodies used to detect HATs, HDACs and methyltransferases are described in Appendix 1.

hMOF which acetylates H4 at K16 both *in vivo* and *in vitro* (Taipale et al., 2005, Thomas et al., 2008) (Taipale et al., 2005, Thomas et al., 2008) was our first target. We did not observe any significant change in levels of hMOF present in MCF-7 cells after garcinol treatment as detected by western blots (Fig. 5.6B). Although the quality of hMOF immunodetection in breast cancer TMAs was acceptable (Fig 3.2D and E), we were also unable to assess changes in hMOF levels in cells due to poor quality of immunofluorescence staining for hMOF. However, TIP60, which was previously reported to acetylate H4K16 *in vivo* (Doyon et al., 2006) was found to be expressed at higher levels following garcinol treatment (Fig 5.6A and B); suggesting that the increase in H4K16 acetylation could be mediated by TIP60. There was insufficient time to test whether this increase could be prevented by siRNA knockdown of TIP60, although these experiments are currently in progress in the lab (Dr HM Collins). As TIP60 is known to be induced by DNA damage (Col et al., 2005), this is consistent with the notion that garcinol may cause DNA damage in MCF-7 cells. In contrast, garcinol did not alter the expression levels of SUV39H1 or SIRT1.

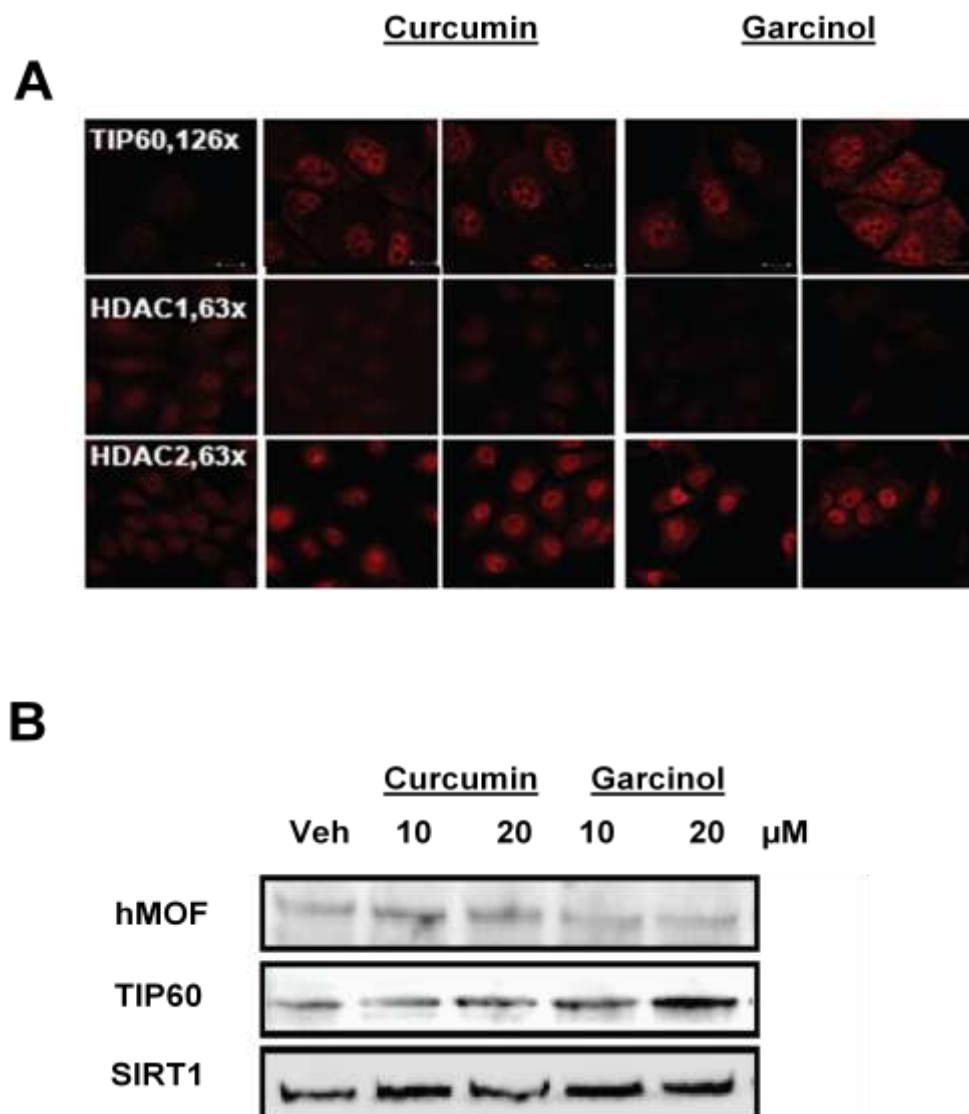
Treatment of MCF-7 cells with curcumin induced a strong increase in expression of the histone methyltransferase SUV39H1. However, this upregulation was not reflected in increased H3K9 trimethylation as might be expected (Fig 5.3A and B). Consistent data was observed for H3K9me3 in MRC-5 cells following garcinol treatment (Fig 5.2). However as outlined in Chapter 3, SUV39H1 activity is negatively regulated by acetylation, and it is therefore possible that upregulation of HATs in response to garcinol induced DNA damage target K266 acetylation in SUV39H1. We were unable to confirm this as a specific antibody for SUV39H1 acetylation was not available.

We also noted that garcinol and curcumin can induce changes in the cellular levels of HDACs. HDAC1 expression appeared to be suppressed by HATi treatments, whereas HDAC2 levels increased and SIRT1 was unaffected (Fig 5.6A and B). However, these changes remain to be confirmed by western blots. We also noted what appeared to be enhanced expression of CBP in MCF-7 and MRC-5 cells; however, as some of the staining observed was cytoplasmic we were unable to conclude whether this was a *bona fide* increase in CBP levels and subcellular localisation or an artefact. Thus results for CBP were largely inconclusive.

These results indicate that changes in histone PTMs induced by garcinol treatment are caused by changes in the expression levels of chromatin regulators, especially those that are implicated in the DNA damage response. Whether these changes are due to increased transcription, increased stability or changes in

activity remain to be established. These data emphasise the powerful effects natural products such as garcinol may have in the biology of cancer cells.

Figure 5.4: HAT inhibitors Induce Alterations in the Levels of Histone Acetylation Regulators.

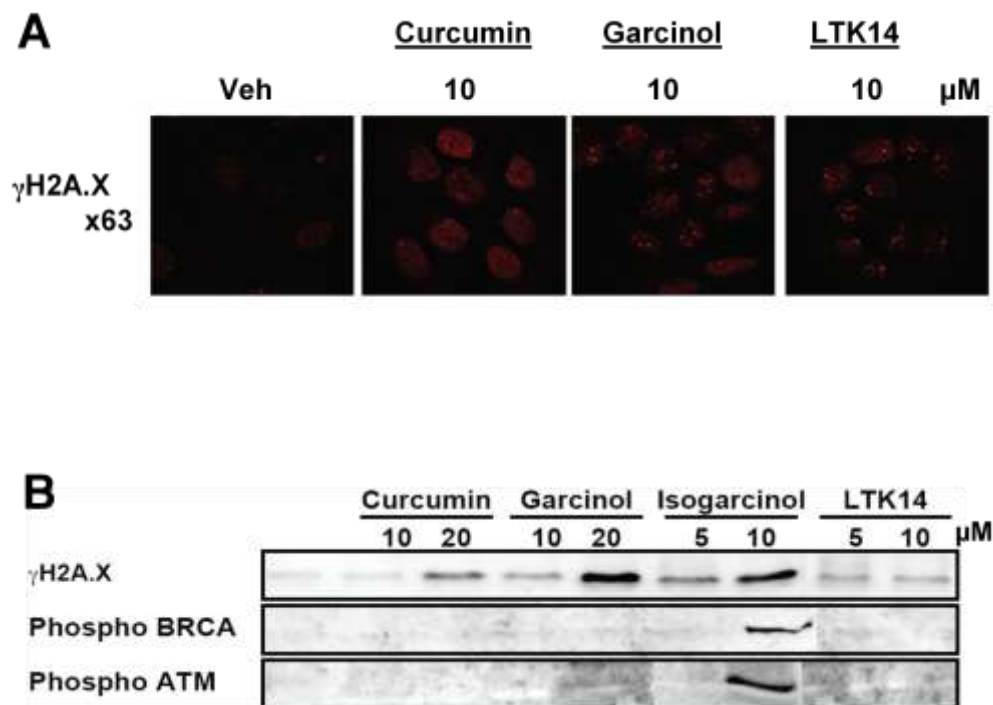


A, Immunoflourescence for the histone acetyltransferase TIP60; the histone deacetylases HDAC1, HDAC2 following treatment with vehicle (Ethanol), curcumin or garcinol in the concentration of 10 and 20 μM for 24 hrs; **B**, WB for hMOF, TIP60 and SIRT1 levels in MCF-7 cells following HATi treatment.

5.1.4 Garcinol induces DNA Damage *in vivo*

As evidence was emerging for the upregulation of DNA damage markers after exposure to garcinol, we examined a number of DNA damage markers in MCF-7 cells. MCF-7 cells were treated with 10, 20 μ M curcumin or garcinol; 5, 10 μ M isogarcinol or LTK14 (Mantelingu et al., 2007a) (Semi-synthetic derivatives of garcinol kindly provided by Prof. Tapas Kundu) and stained for γ H2A.X (Yoshida et al., 2003), phospho BRCA and phospho ATM (Gatei et al., 2000) as described in Material and Methods (Section 2.4.5 and 2.4.6). As shown in Figure 5.5A, treatment of MCF-7 cells with 10 μ M of curcumin, garcinol or the garcinol related compound LTK14 induced DNA damage foci as indicated by γ H2A.X staining. As seen in the Figure, γ H2A.X positive sites are markedly observed in the nuclei of MCF-7 cells. In comparison, to the control sample (left) that was treated with the vehicle (DMSO) only, signals for γ H2A.X were hardly detected. This result was confirmed by western blots showing that γ H2A.X is markedly upregulated following curcumin, garcinol and isogarcinol treatment. Similarly, other DNA damage markers, notably phospho BRCA and phospho ATM, were also elevated after isogarcinol treatment (Fig 5.5B). As shown later, isogarcinol is more potent and more cytotoxic than garcinol, and therefore increased ability to damage DNA in cells. The mechanism of DNA damage remains to be determined, whether it is due to direct genotoxic effects, or due to the induction of replication stress by indirect means. e.g. by blocking HAT activity required during DNA synthesis in S phase.

Figure 5.5: HATi Induces High Levels of DNA Damage Response Markers.



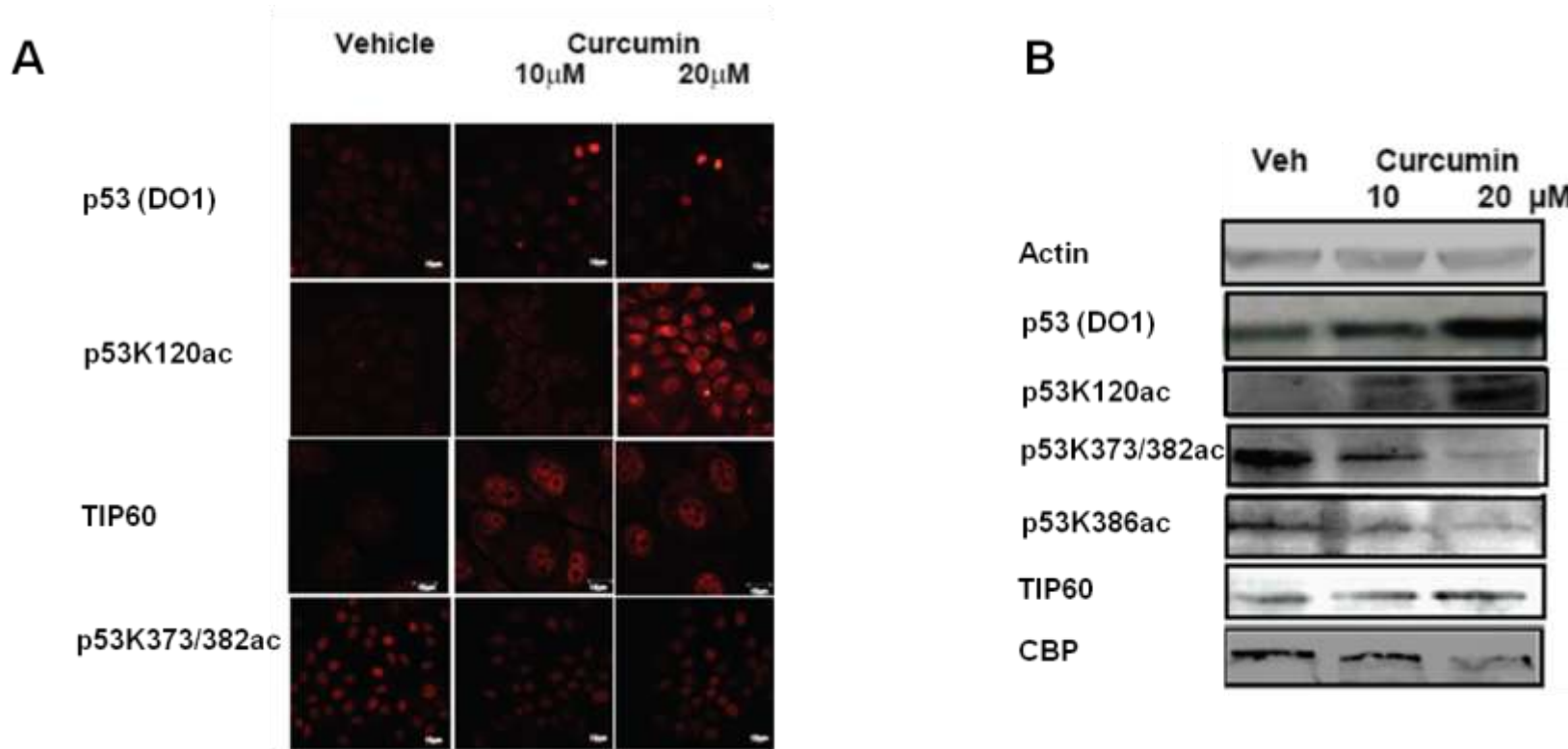
Detection of DNA damage marks in MCF-7 cells treated with vehicle (DMSO) or HATi for 24 hours, followed by **A**, immunoflourescence staining for γH2A.X and **B**, Western Blot for γH2A.X and phospho BRCA/ATM levels.

5.1.5 HATi Alters p53 Function

Upon cellular stress such as radiation, mitotic stress, chemical insults and DNA damage p53 is activated with multiple possible consequences including apoptosis, cell cycle arrest and senescence (Jackson et al., 2010). According to our results presented in chapter 4, hyperacetylation of p53 at K373 and K386 correlated with favourable prognosis and patient survival in breast cancer. In order to explore the possibility that HATi compounds alter p53 acetylation status, MCF-7 cells were treated with either curcumin or garcinol as described previously; followed by detection of p53 and p53 PTMs using commercially available antibodies (antibodies used are detailed in appendix 1).

Curcumin Alters p53 Expression and Acetylation

Treatment of MCF-7 cells with 10 and 20 µM curcumin caused an increase in p53 (Santa Cruz, DO1) detection levels in both immunofluorescence staining and western blotting (Fig 5.6A and B). This indicated that curcumin treatment induces some sort of cellular stress in MCF-7 cells. Acetylation at K120 was found markedly increased whereas acetylation of p53 at K373 and K386 was markedly diminished. These observations are consistent with the slightly elevated level of TIP60 after curcumin treatment which may increase K120 acetylation (Fig 5.6A and B). In contrast, expression analysis showed that the higher concentration of curcumin resulted in lower CBP levels, and thus correlates with the reduced levels of K373 and K386 acetylation (Fig 5.6A and B). Thus curcumin treatment of cells induces p53 expression and alters expression of HATs that regulate p53.

Figure 5.6: Curcumin Alters p53 Acetylation.

MCF-7 cells were treated with vehicle (Ethanol) or curcumin (10 and 20 μ M) for 24 hrs. **A**, Immunofluorescence staining; **B**, Western Blot, actin was used as loading control.

Garcinol Alters p53 Expression and Acetylation

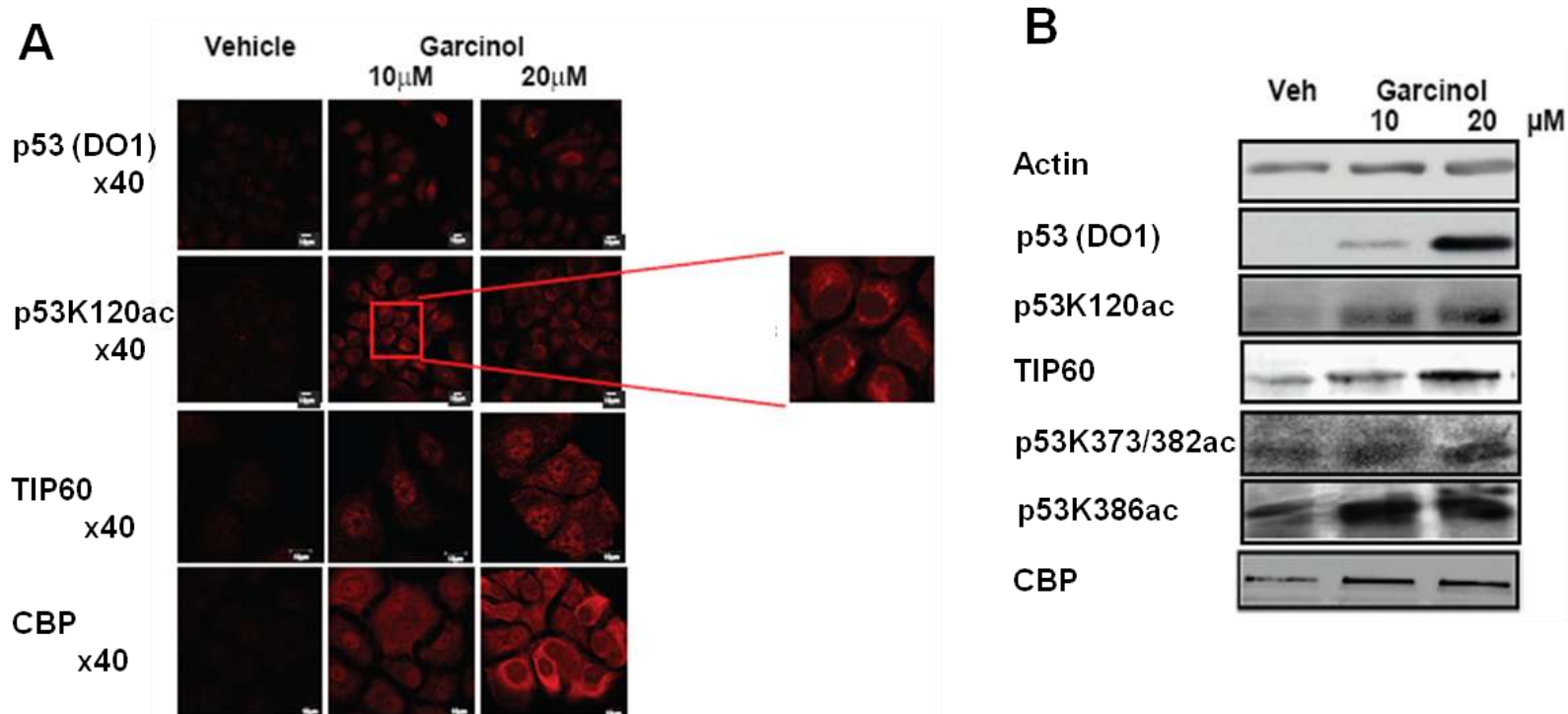
In order to discover whether garcinol treatment could also have any effect on the p53 PTM profile, MCF-7 cells were treated with 10 and 20 µM garcinol as previously described. Garcinol treatment was found to cause an increase in p53 detection levels in both immunofloourescence staining and western blot experiments. The level of p53 induced was even higher than for curcumin. Concerning p53 post translational acetylation at K120, K373/382 and K386; treatment with garcinol was found to upregulate K120ac which is consistent with the observed increase in TIP60 (Fig.5.7A and B). Remarkably p53K120ac was detected in the cytoplasm (Fig 5.7A); which is consistent with its positive immunoreactivity in breast cancer TMA described in Chapter 4. This result suggests that garcinol treatment can also affect the subcellular localisation of p53, which has been reported to have cytoplasmic functions, relocating to mitochondria during apoptosis (Galluzzi et al., 2008). However we did not confirm this by other methods, such as subcellular fractionation to separate nuclear and cytoplasmic compartments.

In contrast to curcumin, acetylation of p53 at K373 and K386 also appeared to be induced; curiously staining for CBP suggested a relocation of CBP to the cytoplasm (Fig 5.7A and B). Although other studies have detected cytoplasmic localisation of CBP under some conditions (Bellodi et al., 2006, Shi et al., 2009) these results would need to be confirmed by other antibodies targeting CBP.

For further confirmation, p53 acetylation levels were quantified by flow cytometry as previously described in Materials and Methods (Section 2.4.7). MCF-7 cells were treated with either vehicle (Ethanol) or 20 µM garcinol for 24 hrs. Levels of p53K120ac, p53K386ac and TIP60 were measured in each cell by Fluorescence Activated Cell sorting (FACS) machine. The results revealed an elevation in the number of cells showing high level of both p53K120ac and p53K386ac by more than 4 fold; which, was consistent with an increase by 50% in TIP60 (Fig. 5.8A). As both anti p53k120ac and anti BrdU antibodies were monoclonal mouse antibodies, I was unable to assess the changes in cell cycle profile in relationship to p53K120ac following garcinol treatment.

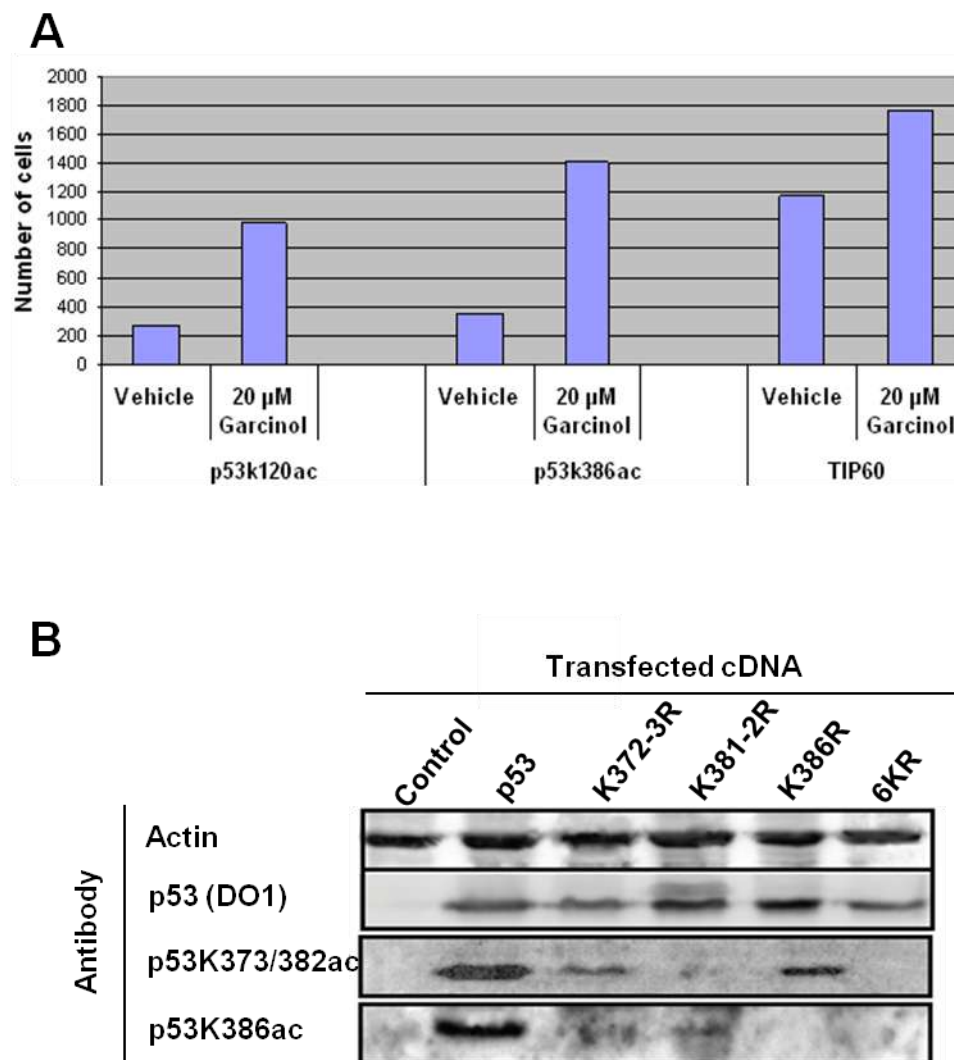
In order to validate the specificity of the used antibodies used for specific p53 PTMs, transfection by pcDNA mutant p53 at K372-3R, K381-2R, K386R and 6KR which contain mutated lysine residues 370, 372, 373, 381, 382, and 386 to arginine residues (Rodriguez et al., 2000) into SaOs2 cells, a p53 null cell line. The vectors were kindly provided by Prof. Ronald Hay. Figure 5.8B shows the immunodetection of p53 and p53 acetylation forms by this set of anti p53 antibodies. The results revealed that DO1 antibody was able to detect both wild type and all mutant forms of p53. The antibody against p53K373/ 382 was able to detect both wild type p53 and p53 mutant at K386R. Conversely, the antibody failed to detect mutant p53 at 6KR or K381-2R. In addition, the results also showed a remarkable reduced capacity to recognize p53 mutant at K372-3R. This suggests the specificity for the antibody against both lysine sites. In addition, the weak band at K372-3R was expected as the antibody should recognize K381 lysine acetylation. Concerning the antibody against p53K386ac which was used in

breast cancer TMA staining; the antibody managed to identify both wild type p53 and to lesser extent p53 mutant at K372-3R and K381-2R. Conversely, the antibody was unable to detect mutant p53 at K6R or K386R. This suggests that the antibody is highly specific against K386. On the other hand, the faint immunoreactivity band at K372-3 and K381-2R suggests lower sensitivity of p53K373/382ac and p53K386ac antibody if compared to p53 (DO1) antibody.

Figure 5.7: Garcinol Alters p53 Acetylation.

MCF-7 cells treated with 10 or 20 μ M garcinol (or vehicle) assessed for p53, TIP0 and CBP by Immunofluorescence staining (**A**) and Western Blot (**B**). Actin is used as loading control.

Figure 5.8: Cont. Garcinol Alters p53 Acetylation, Validation of p53 PTMs antibodies.

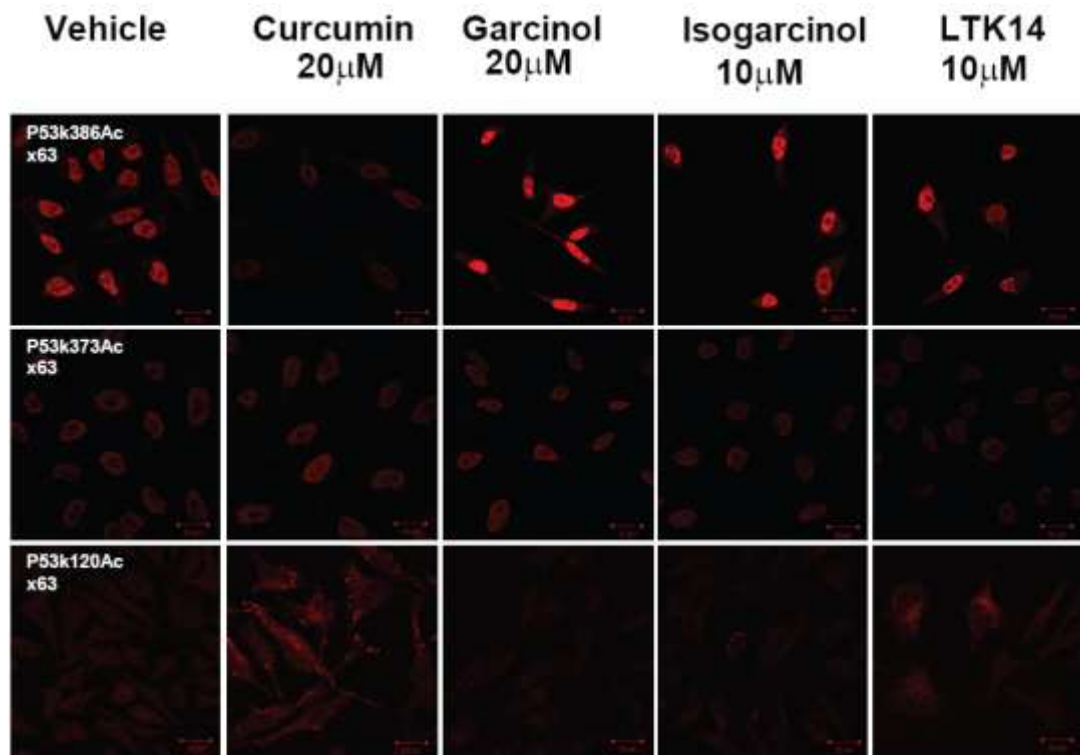


(A) Analysis of the level of p53K120ac, K386ac and TIP60 in MCF-7 cells by flow cytometry analysis following 20 μ M garcinol treatment. The total number of cells is 4,000 cells. D, validation of p53 acetyl antibodies assessed using the transfection of p53 mutants into the p53 null cell line (SaOs2).

HATi Alters p53 Acetylation Marks in Non-cancerous MRC-5 Cells

In order to discover any differences between cancerous and non-cancerous cells in the detection of p53 acetylation marks, acetylated forms of p53 at K120, 373/382 and 386 were also explored in the human embryonic fibroblast cells, MRC-5 after HATi treatment. HATi treatment of MRC-5 cells caused an alteration in p53 PTMs levels (Fig. 5.8). Consistent with the results obtained from MCF-7 cells, garcinol and its semi-synthetic derivatives isogarcinol and LTK14 caused enhanced detection levels of p53K386ac. However, HATi treatment did not appear to change p53K373ac levels. Remarkably, curcumin treatment caused increased p53K120ac detection level with marked shift of immunoreactivity into the cytoplasm. These results reinforce the finding using MCF-7 cells but show that similar effects are encountered in non-cancerous cells in culture.

Figure 5.9: HATi Treatment Alters p53 Acetylation at K386, K373 and K120 in MRC-5 Cells.



MRC-5 cells were treated with vehicle (DMSO), 20 μ M curcumin or garcinol; 10 μ M of isogarcinol or LTK14 for 24 hrs prior to Immunofluorescence staining for p53K386ac, p53K373/382ac, and p53K120ac (Magnification is x63).

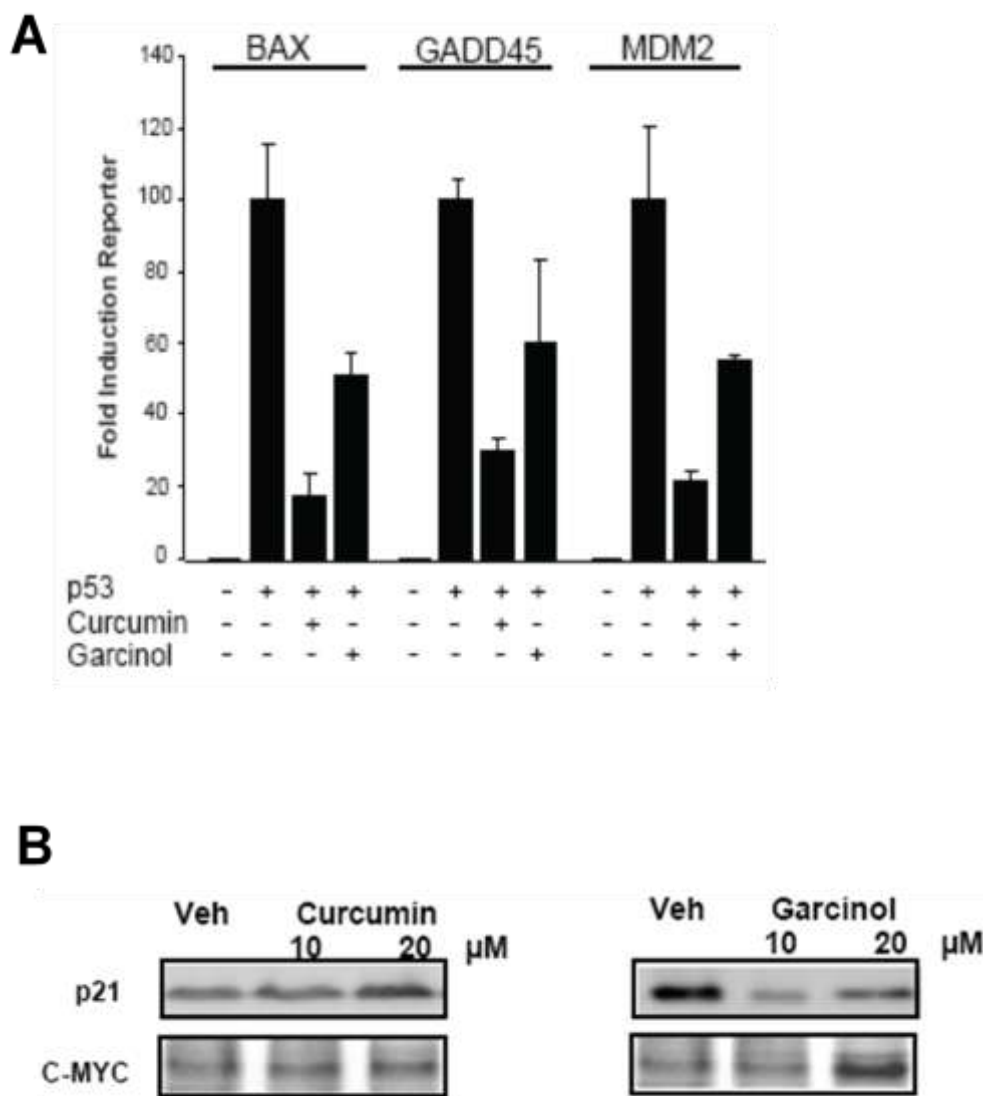
5.1.6 HATi Treatment Alters p53 Function

HATi Treatment Reduces p53 Transcriptional Activity

In order to explore how HATi treatment affects p53 function, the p53 dependent reporter assays were performed. The experiment was designed (personal communication with Dr Hilary Collins) to analyse the effect of curcumin or garcinol treatment on p53 transcriptional activity. SaOS2 cells were co-transfected with a luciferase reporter gene regulated by p53 binding sites derived from BAX, GADD45 and Mdm2 promoters as previously described (Collins *et al.*, 2006). The cells were also transfected with p53 expression vector or empty vector as a negative control to normalize for transfection efficiency. None of the three reporters was active in the absence of p53 conferring the absence of endogenous p53 in this cell line (Fig. 5.10). Exogenous p53 induced the reporter activities approximately 100-fold for each of the three reporters. However, curcumin treatment reduced reporter activities to 20%, 30% and 25% of the maximum activity for BAX, GADD45 and Mdm2 genes promoters. Similarly, garcinol also caused similar effects on the three reporters, showing a decrease to 50%, 60% and 55% of control (Fig. 5.10A). These effects are most likely through targeting p53-associated HATs including CBP and p300 (Collins, Abdelghany *et al.*, in preparation).

In order to understand the mechanism of cell cycle changes that takes place after HATi treatment, we evaluated the level of p21 protein, which is a major cell cycle regulator in the response to DNA damage (Cherrier *et al.*, 2009) and a direct target of p53 (Eldeiry *et al.*, 1993). HATi treatment for 24 hours induced a differential effect on p21 detection levels. Specifically, curcumin

caused an increase in the p21 level; however, garcinol caused the opposite effect (Fig. 5.10B). In addition, c-MYC level, a transcription factor acetylated by p300 (Zhang et al., 2005, Faiola et al., 2005) was found markedly increased following garcinol treatment. This is consistent with the loss of H3K18 acetylation which catalysed by p300 that required for the activation of S phase in quiescent fibroblast cells (Horwitz et al., 2008, Ferrari et al., 2008). However, curcumin treatment did not affect c-MYC levels. Therefore, this result may suggest a differential effect of HATi treatment on MCF-7 cells cell cycle regulatory proteins. As altered p21, and c-MYC levels and reduced p53 transcription activity could possibly affect cell cycle progression, we evaluated the effect of HATi treatment on the cell cycle progression in cancerous and non-cancerous cell lines.

Figure 5.10: HATi Treatment Alters p53 Transcriptional Activity.

A, The effect of curcumin and garcinol on p53 induction of the BAX, GADD45 and Mdm2 promoters in SaOS2 cells (personal communication with Dr Hilary Collins); **B**, WB for p21 and c-MYC in MCF-7 cells treated with vehicle (DMSO), 10 and 20 μ M curcumin or garcinol for 24 hrs.

HATi Treatment Alters Cell Progression Through Cell Cycle

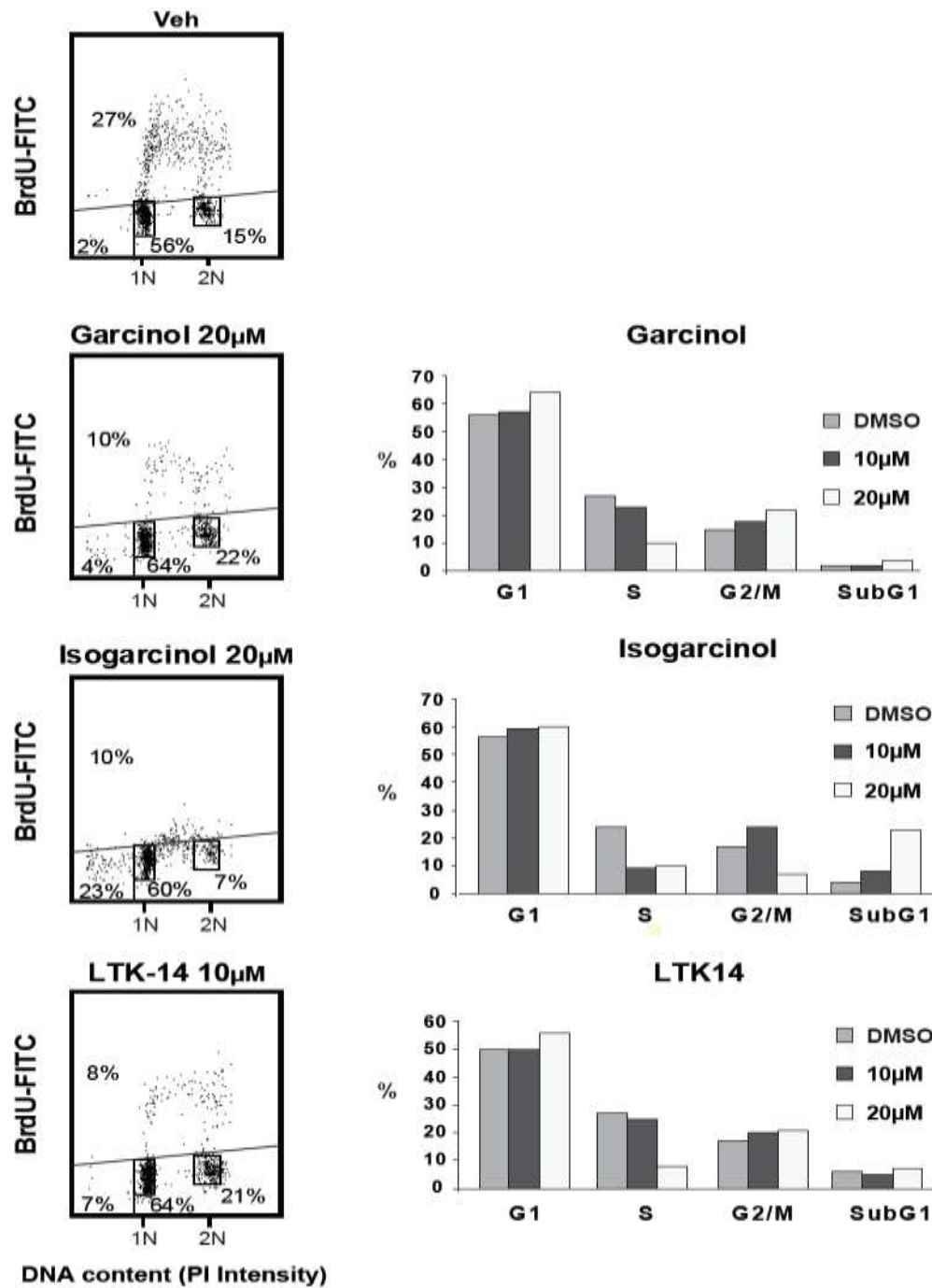
In order to explore the effect of HATi treatment on cell cycle progression; we analysed cell cycle changes in both MCF-7 and MRC-5 cells following treatment for 24 hrs. The cell cycle analyses were performed by bivariate flow cytometry as described in Material and Methods (Section 2.4.7).

Remarkably, MCF-7 cells showed a dramatic reduction in S phase population upon treatment with garcinol, isogarcinol or LTK14 molecules. This effect indicates a failure of HATi treated cells to progress through the step of DNA synthesis, which require H3K18ac and a functioning p300/CBP (Horwitz et al., 2008). In addition, both garcinol and LTK14 caused an increase in G1 and G2 populations. Interestingly, 10 µM isogarcinol caused an increase in G2 at low treatment concentration and became markedly cytotoxic to the cells at higher concentration (20 µM) with a marked build up in subG1, the apoptotic population (Fig. 5.11). The EC50 (half-effective concentration) of isogarcinol in MCF-7 cells was in the range of 4-8 µM. This proposes a fundamental different cytotoxicity between isogarcinol and LTK14 as reported in MTT assays (Collins, Abdelghany *et al*, in preparation). Concerning the effects of curcumin treatment, similar to the others, it caused a reduction in S phase population; and a pronounced increase in G2/M population (Fig. 5.12) which is consistent with results reported after treatment of HEPG2 cells with curcumin (Sahu et al. 2009).

In order to evaluate the effects of HATi treatment on cell cycle progression in non-cancerous cells; MRC-5 cells were treated with 20 µM curcumin, 10µM of isogarcinol and LTK14 for 24 hours (20 µM was not used due

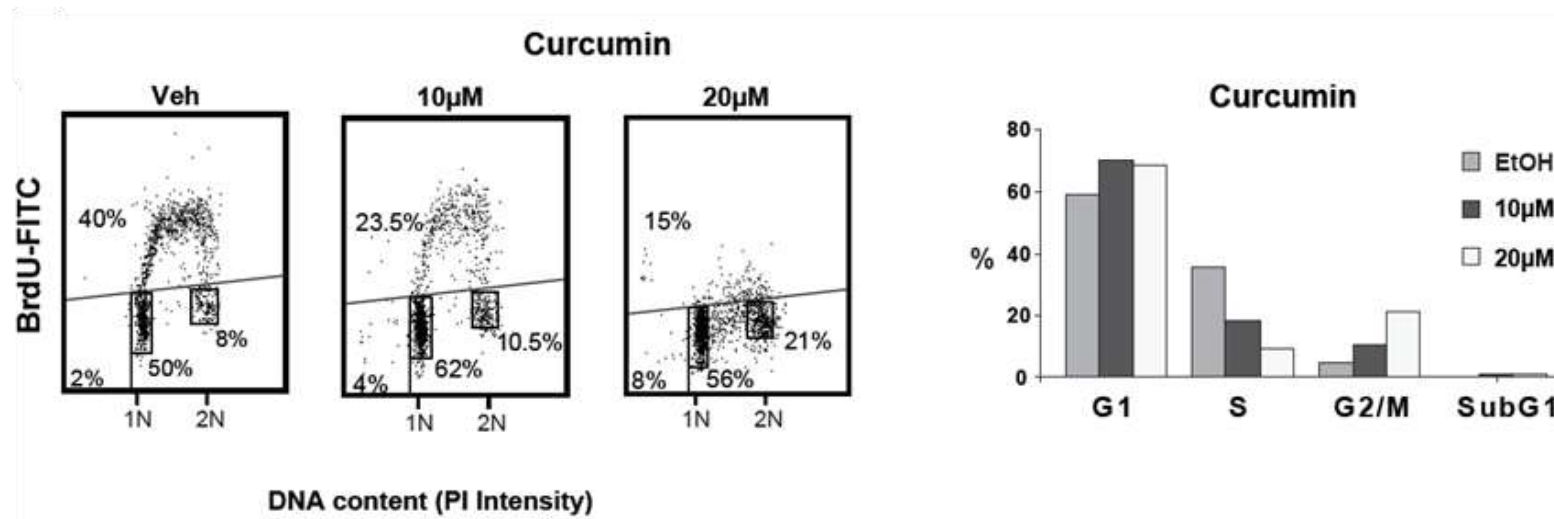
to its cytotoxic effects). Curcumin treatment for MRC-5 cells caused increased number of cells in the S and G₂/M phases of the cell cycle, and a reduced number of cells in G₁. However, surprisingly, isogarcinol and LTK14 treatment caused minimal changes in cell cycle progression (Fig 5.13). This suggests a differential effect of curcumin treatment on MCF-7 and MRC-5 cells. In addition, MCF-7 cells show marked sensitivity to isogarcinol (10 μM) treatment as compared to the non-cancerous MRC-5 cells.

Figure 5.11: Garcinol, Isogarcinol and LTK14 Treatment Impedes Proliferation of MCF-7 Cells by blocking S Phase.



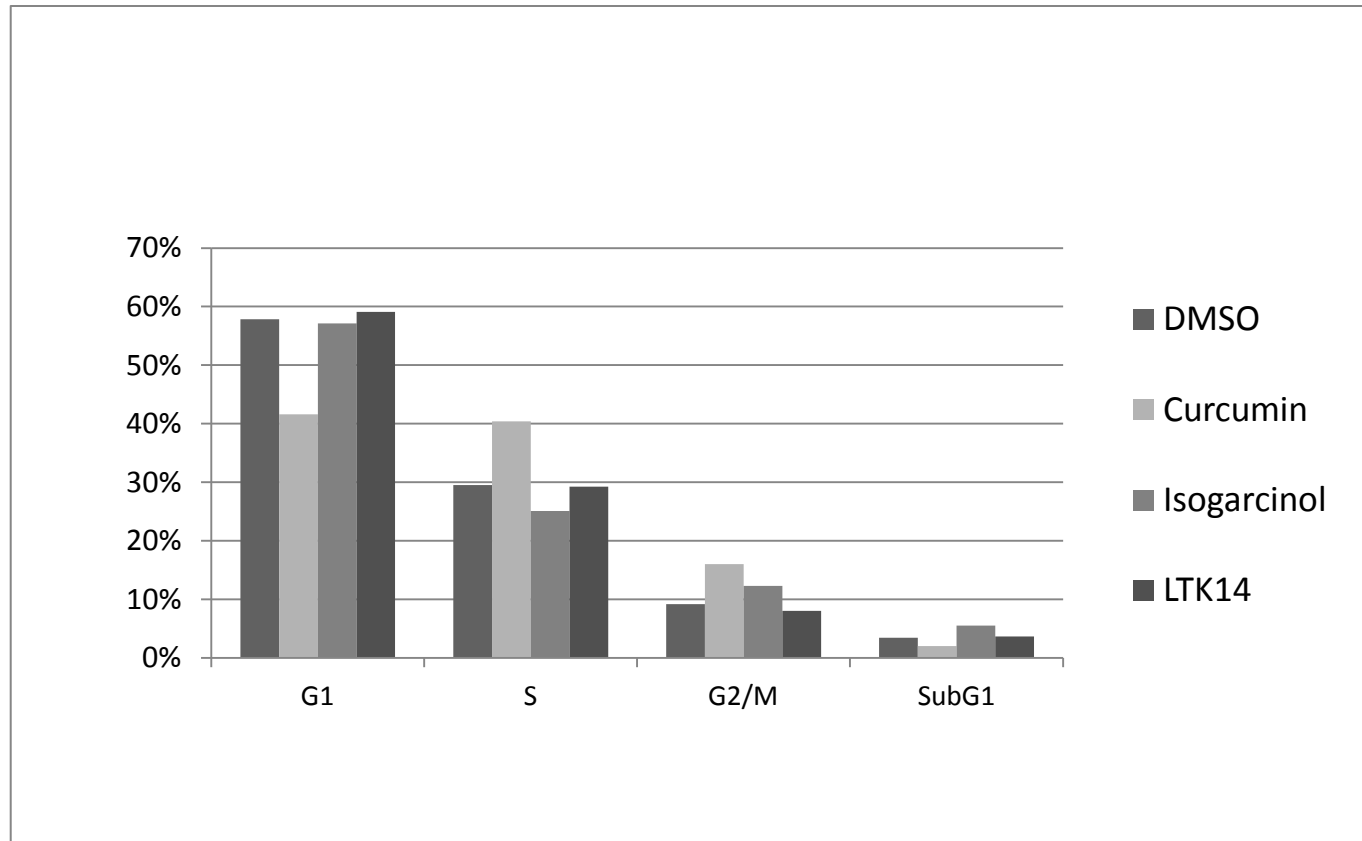
MCF-7 cells were treated with 10 and 20 µM garcinol, isogarcinol and LTK14 for 24 hours, followed by flow cytometry cell cycle analysis.

Figure 5.12: Curcumin Treatment Impedes Proliferation of MCF-7 Cells by blocking S Phase.



MCF-7 cells were treated with 10 and 20 µM curcumin for 24 hours, followed by flow cytometry cell cycle analysis.

Figure 5.13: Cell Cycle Changes in MRC-5 Cells upon HATi Treatment.

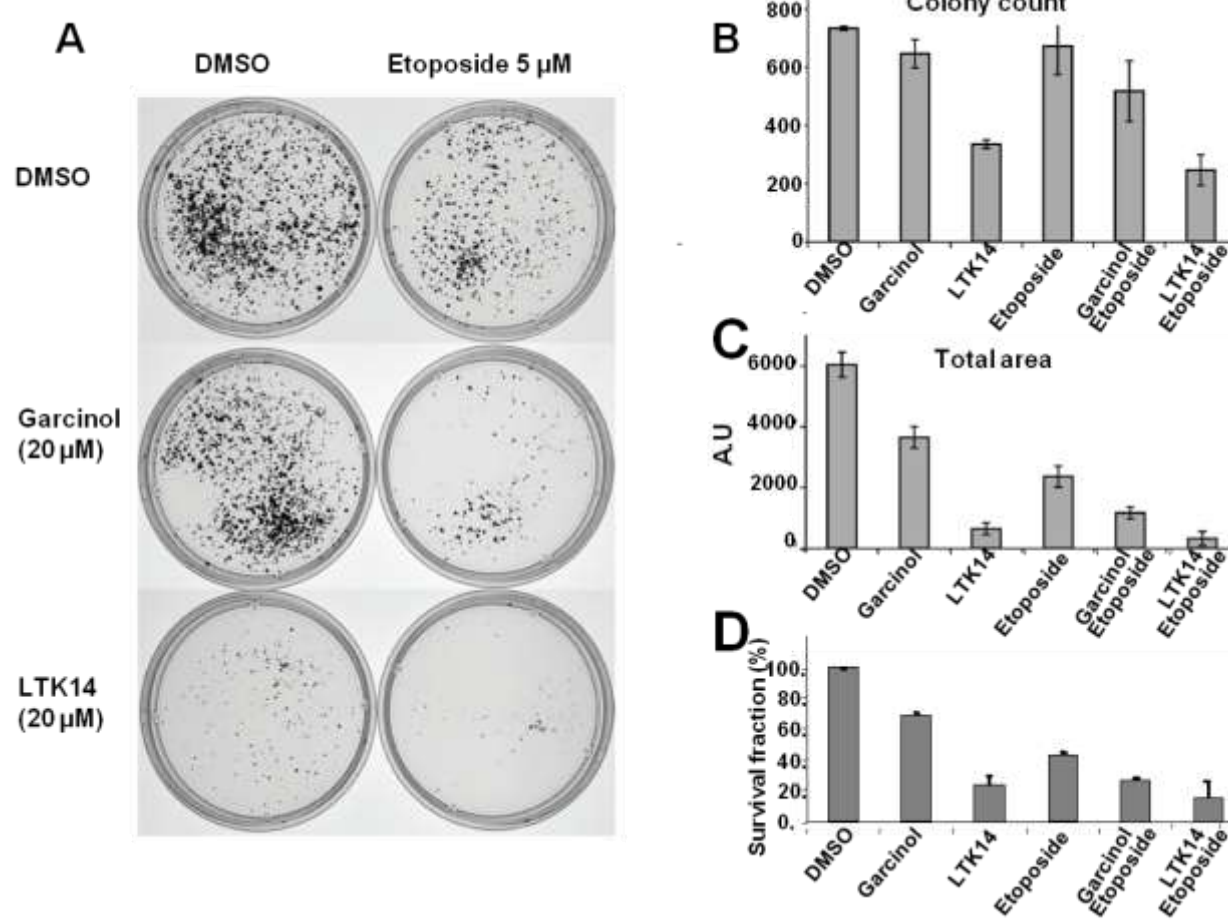


MRC-5 cells were treated with 20 μ M curcumin, 10 μ M isogarcinol and 10 μ M LTK14 followed by FACS cell cycle analysis.

5.1.7 HATi Treatment Sensitizes MCF-7 Cells to Etoposide and Reduces Colony Formation

To further study the long term effects of HATi treatment on cell proliferation we explored the effects of garcinol or LTK14 treatment on the ability of MCF-7 cells to form cell colonies. MCF-7 cells, which were the optimum choice for the experiment, were used. MCF-7 cells are known to resist ionizing radiation (Wang et al., 2009a, Essmann et al., 2004), however, they are chemotherapy sensitive (Janicke et al., 2001). The cells were treated with 20 μ M garcinol or LTK14 or in co-combination with (5 μ M) etoposide (Fig. 5.12A), a well-characterized and specific topoisomerase II inhibitor used clinically in chemotherapy (Hajji et al., 2008). Following 24 hrs of treatment, MCF-7 cells were incubated in fresh culture media for 12 days (Material and Methods section 2.4.8). The results revealed that garcinol alone or etoposide alone did not induce a marked reduction on colony count if compared with the effect when they were used in combination (Fig. 5.12B). In addition, garcinol treatment mainly caused an effect on colony total area, which measures colony size (at least 50 cells to be visible) (Fig. 5.12C). Combination of garcinol and etoposide treatment resulted in marked reduction in colony total area (Fig. 5.12C). LTK14 treatment caused a marked reduction in both colony total area and count (Fig. 5.12B and C). In addition, combined LTK14 and etoposide treatment enhanced the effect of etoposide on MCF-7 cells colony area (Fig. 5.12C) and MCF-7 survival fraction (Fig. 5.12 D).

Figure 5.14: Effects of HATi on MCF-7 Cells Proliferation.



MCF-7 cells were treated with garcinol, or LTK14 alone or in combination with etoposide for 24 hrs. After washing, cells were incubated for an additional 12 days to allow colony formation. The cultures was fixed with methanol and stained with Geimsa method, and the number of colonies were counted. **A**, MCF-7 cell colonies at day 12 after different treatments; **B**, count and total area of colonies, measurements were done by Image J software; **C**, survival fraction, which was calculated as the colony formation efficiency of the treated cells compared with control set to 100%. Data are pooled from three independent experiments. Column and error bars represent average and standard deviation.

5.1.8 Summary of Results: HATi Treatment can Reverse the Loss of Histone and p53 PTMs in Breast Cancer Cells.

In Chapters 3 and 4 and in previous work we established that histone and p53 PTM status, and the expression of their modulators in breast tumours, can be useful indicators of patient outcome. As these modifications are reversible, we explored whether small molecule inhibitors that target histone acetyltransferases might be able to alter histone p53 PTMs in MCF-7 cells, and to assess what implication this has on cancer cell proliferation. We therefore treated cells with curcumin, garcinol or synthetic garcinol derivatives. Our results confirmed that bulk acetylation of H3 and H4 is reduced following curcumin and garcinol treatment, although this effect was dose-dependent (Fig. 5.1A). At doses above 10 μM a marked induction of H4K16ac was observed (Fig. 5.1B, C and Fig. 5.2). This result indicates that a cancer associated PTM i.e. hypoacetylation of H4K16, can be modulated by small molecule treatment. The increase in H4K16ac was accompanied by increased expression of the DNA damage regulator TIP60 (Fig. 5.4), which was previously reported to acetylate H4K16 *in vivo* (Doyon et al., 2006). However, hMOF, which has been claimed to be responsible for most of the cellular acetylation of H4K16, did not show any increased expression. siRNA knockdown of TIP60 in cell treated with garcinol will be performed by other members of the group to confirm whether TIP60 is responsible for increased H4K16 acetylation in response to garcinol.

Consistent with these data, marked increases in H3K56 acetylation and $\gamma\text{H2A.X}$, and other DNA damage markers including p53, phospho BRCA1 and phospho ATM were observed following garcinol treatment (Fig 5.5 and 5.7). This

provides a strong indication that these effects are associated with a cell stress such as DNA damage invoked by the treatment with garcinol compounds. In contrast garcinol compounds induced a marked reduction of H3K18ac (Fig. 5.1B). This PTM is deposited by CBP/p300 and is required for S phase progression in fibroblasts (Horwitz et al., 2008, Ferrari et al., 2008). This shows that garcinol action *in vivo* is plieotropic. Although it may inhibit CBP/p300 activity and thus block H3K18 acetylation, it also affects expression of other HATs and histone modulators, leading to other effects on histone PTMs. Conversely, garcinol treatment did not block H3K18 acetylation in the non-transformed MRC-5 cells (Fig. 5.2). These results are consistent with the observed effects on cell cycle arrest and reduction of the numbers of cells in S phase. Interestingly, H3K56 has been reported to be acetylated by CBP/p300 (Das et al., 2009). Thus, our result suggests that other HATs may target this residue after DNA damage, or distinct mechanisms are involved in H3K18 or H3K56 acetylation.

In addition to effects on histone acetylation, HATi compounds also induced expression of p53 protein and altered p53 acetylation profiles (Fig. 5.7 and Fig. 5.8). Remarkably, while curcumin inhibited acetylation of the C-terminal activation domain of p53, it strongly enhanced TIP60-dependent acetylation of K120 within the DNA binding domain. Garcinol markedly increased the three p53 acetylation marks. This was accompanied by a switch in the subcellular localisation of p53K120ac from the nucleus to the cytoplasm. This highlights the profound effects that drug-like molecules such as garcinol can have on the growth of tumour cells in culture by reprogramming key PTMs in histones and p53.

In addition to effects on acetylation garcinol induced a very strong increase in cellular levels of H4K20me3 in MCF7 cells and MRC5 (Fig. 5.2 and Fig. 5.3); however, this was not observed for another methylation, i.e. H3K9me3 (Fig. 5.2 and 5.3). As for H4K16ac, H4K20me3 is considered a hallmark of cancer, thus this provides another example of the reversal of loss of a histone PTM associated with cancer. Our data showed that garcinol induced an increase in SUV20H2 suggesting that this might be responsible for the observed increase in H4K20 trimethylation. This was confirmed by siRNA experiments showing that the increase in H4K20me3 induced by garcinol is blocked by knockdown of SUV420H2 (Fig. 5.3).

Curcumin had distinct effects on the cell cycle causing an arrest in G2/M (Fig. 5.12). This was also reflected by differential effects on histone and p53 PTMs which were less robust and we did not observe an induction of DNA damage markers to the same extent as garcinol compounds. We did note that curcumin induced expression of SUV39H1, which we have shown to be a good prognostic indicator in breast tumours.

Moreover, curcumin and garcinol were found to have opposing effects on expression of p21, the p53 dependent protein (Eldeiry et al., 1993) and the transcription factor C-MYC (Fig. 5.10). These effects on p21/C-MYC expression may be related to the differential effects of curcumin and garcinol on p53 acetylation at K373 which can alter p53 activity (Knights et al., 2006b). Moreover, the altered cell cycle profile following HATi treatment in MCF-7 (Fig. 5.11 and Fig. 5.12) and in MRC-5 cells (Fig. 5.13) may be a consequence of

HATi-induced histone and p53 PTMs. Finally we found that curcumin and LTK14 treatment sensitize the MCF-7, the breast cancer tumour cell line to etoposide treatment (Fig.5.14), which may propose a potential chemotherapeutic application of such small molecules in medical practice. Future studies in the lab will include mouse xenograft models of breast tumours, to explore the breast tumour response to HATi treatment.

CONCLUDING REMARKS

Conventional histopathological diagnostic reports for breast cancer cases constitute histopathological typing, tumour grade, size, stage and nodal metastasis and lymphovascular invasion status. Additionally, immunoreactivity for ER, PR and HER2 is also included. In spite of the involvement of those variables with patient prognosis and tumour outcome (Elston and Ellis, 1991, Costa et al., 2002, Pritchard et al., 2006), these conventional variables remain unable to predict tumour behaviour, especially in response to treatment (Alizadeh et al., 2001). Histopathological diagnosis is basically a descriptive and rather subjective methodology, although digital imaging analysis may be available in the future .It is increasingly recognised that new approaches that characterize the complex genetic alterations that are involved in different tumour s need to be developed (Stange et al., 2006).

Cytogenetic and molecular genetic analysis of breast cancer samples demonstrates that various genetic alterations including amplification of oncogenes and mutation or loss of tumour suppressor genes are involved in tumour development and seem to be pathognomonic for the development or progression of a specific histological subtype (Beckmann et al., 1997). High throughout genomic studies have managed to classify breast cancer into biologically and clinically distinct groups based on gene expression profiles (Perou et al., 2000, Sorlie et al., 2001, Sorlie et al., 2003, Sotiriou et al., 2003). Those classifications are basically based on ‘genetic model’ as a cause of cancer (Feinberg, 2004) without taking in to consideration the epigenetic model of cancer (Li et al., 2005b). Genome wide epigenetic profiling and transcriptional profiling may soon provide a better understanding of the biology of breast tumours and identify

cohorts of biomarkers that predict outcome. However, the cost is currently prohibitive for a practical application. Thus PCR or antibody detection of panels of biomarkers is the best current approach.

In an earlier study based on the same breast cancer tissue cohort, Abdel El-Reheim *et al* (2005) characterized breast cancer tumours according the immunodetection of groups of proteins related to epithelial cell differentiation, hormonal receptors, growth factors receptors and gene products that known to be altered in some forms of breast cancer. The study revealed an association between those variables and tumour outcome and patient survival. Clustering of breast cancer cases into biological classes that characterized by distinctive expression of a group of variable (see previously in Introduction) revealed a significant association between those cluster classes with clinical and pathological variables. However that study did not profile the epigenetic aspect of breast tumours.

Our recent study in the same breast cohort profiled the global modification of histone PTMs and revealed an association with tumour types, conventional histopathological and biological variables. In addition cluster analysis of Histone PTMs revealed a distinctive hyper-modified class (which characterized by high levels of histone PTMs) as a class correlated with longer patient survival and better tumour outcome. However further study will be required to explore in depth the relationship between high levels of those marks and cellular function, or understand how those histone PTMs are regulated in breast cancer tumours.

In Chapter 3 I tried to explore the profile of histone H4K16ac and its regulatory axis in breast cancer. I determined the levels of several members of the H4K16ac regulatory axis among breast cancer tumour various types, subtypes; correlated their levels to conventional prognostic factors and assessed the impact of their level in breast cancer tissue on tumour outcome and patient survival. According to my knowledge, although H4K16ac and hMOF levels were previously studied in breast tumours (Elsheikh et al., 2009, Pfister et al., 2008), this study was the first to explore H4K16ac regulatory axis in breast cancer or other tumours. High levels of H4K16ac, hMOF, and SUV39H1 were correlated with better tumour outcome and patient survival. Previous study on smaller number of cases (298) reported down regulation of hMOF and low acetylation levels of H4K16 in breast tumours in compare to normal tissue (Pfister et al., 2008). Our study-according to my knowledge- is the first to study the protein level of SUV39H1 in breast cancer or any other tumour tissue. However, analysis of SUV39H1 mRNA levels in fresh frozen tissue from 219 colorectal cancers patients revealed elevated SUV39H1 levels in 25% of 219 colorectal cancers. In addition, global analysis of H4K16ac regulatory axis levels revealed their potential classification into distinctive clusters. High (H4K16ac, hMOF, SUV39H1) cluster was correlated with favourable tumour grade and longer patient survival. Other classes were correlated with poor prognosis and poorly differentiated tumours. Those cluster classes were characterized by either low levels of H4K16ac or distorted relationship between the members of H4K16ac regulatory axis. Interestingly, the distorted SIRT1/DBC1 relationship was also reported previously in breast cancer tumours (Sung et al., 2010).

Exploring histone H2A variant expression levels in breast tumours revealed a significant correlation with steroid hormone receptors levels. Consistently with H2A.Z involvement in ER signalling in breast cancer cells (Svotelis et al., 2009b). High levels of H2A.Z in breast tumours were correlated with favourable tumour grade and patient survival; which in contrast to previous study reported high levels of H2A.Z as a poor prognostic marker in breast cancer (Hua et al., 2008).

In chapter four, I also explored in breast cancer tissue the level of a number of p53 acetylation sites and their regulators. The results revealed positive correlation between high levels of p53 acetylation and better tumour outcome, especially the p53K373ac and p53k386ac. Acetylation of p53 was found correlated with favourable tumour histopathological and biological variables. I noticed differences between nuclear and cytoplasmic p53K120ac levels among tumour cores assessed which may denote a differences in the function of acetylated p53 at K120 depending on its localization whether nuclear or cytoplasmic.

Global analysis of the different p53 PTMs and their modulators revealed that breast cancer can be classified into prognostically and biological distinct groups depending on their H-score pattern. The cluster analysis suggests acetylation of p53 as favourable mark in breast cancer. High levels of both SUV39H1 and p53K373ac were found significantly correlated with favourable tumour outcome and patient survival. In addition, p53 acetylation at K386 was also found correlated with favourable tumour outcome and patient survival in

breast tumours, especially if combined with high levels of hMOF. This is consistent with the critical role for hMOF in acetylating p53 in inducing apoptosis (Rea et al., 2007), suggesting an integrated apoptotic pathway in breast cancer groups characterized by high levels of both hMOF and p53 acetylation.

This study has shown that small molecule inhibitors can be used to alter histone and p53 modifications in breast cancer cells. In the case of garcinol compounds, these actions are pleiotropic and may be due to indirect effects (such as induction of DNA damage responses, as well as through direct HAT inhibitor function. My results identified reduced bulk acetylation of H3 and H4 following curcumin and garcinol treatment using pan-acetyl antibodies. However, when we used antibodies to detect specific histone PTMs, a marked induction of H4K16ac and H4K20me3 was observed, both of which are suppressed in breast cancer and other tumours (Elsheikh et al., 2009, Van Den Broeck et al., 2008).

Curcumin induced expression of SUV39H1, a good outcome marker in breast cancer however we could not identify any change in H3K9me3, the SUV39H1 target. Garcinol compounds markedly induced a range of DNA damage markers including H3K56ac levels (Das et al., 2009), γ H2A.X, and phospho BRCA1/ATM levels (Fig. 5.1, 5.2 and 5.5). As shown in Figure 6.1 this was due in part to increased expression of chromatin regulators such as TIP60 and CBP levels which is likely to account for the observed increase in H4K16 and H3K56 acetylation. In addition to having important effects on histone PTMs, garcinol was also found to increase a profound change in the acetylation status of p53. Garcinol induced p53 acetylation at K373/382 and K386 which mediated by CBP/p300;

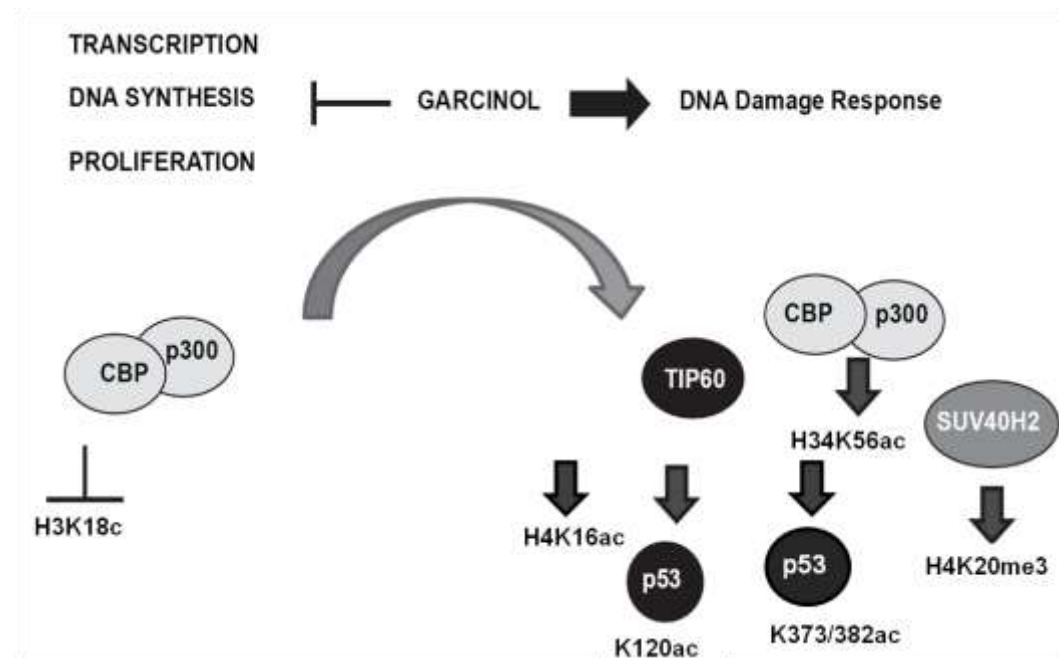
p53K120ac which catalysed by TIP60 in response to DNA damage. Moreover, the subcellular localisation of p53 was altered from the nucleus to the cytoplasm. While the mechanism responsible for this translocation is unclear, we note that acetylation regulates nuclear/ cytoplasmic trafficking through importin/exportin pathways (Bannister et al., 2000, Ryan et al., 2010).

We identified curcumin/garcinol- induced cell cycle changes in MCF-7 cells, in the form of failure of S phase progression, which consistent with the marked reduction of H3K18ac which catalysed by CBP/p300 (Horwitz et al., 2008); and a marked built up of SubG1 population following isogarcinol treatment. Curcumin treatment was previously reported to cause antiproliferative effect through G2/M arrest in many cell lines including colon and Rhabdomyosarcoma cell lines (Goel et al., 2001, Hanif et al., 1997, Beevers, 2006). Small molecules HDACi like SAHA caused growth arrest, differentiation, and/or apoptosis of many tumour types *in vitro* and *in vivo* (Butler et al., 2002). SAHA also caused an inhibition of proliferation in MCF-7 cells; accumulation of cells in a in G (1) then G (2)-M phase of the cell cycle in a dose-dependent manner (Munster et al., 2001).

HATi treatment induced an induction of p53 and p53 PTMs, which are likely to impact on p53 transcriptional activity, as observed through the distinct effects on p21 and c-MYC expression. This may also be linked to the observed effects of HATi treatment on cell cycle progression. We found that curcumin and LTK14 treatment altered long term MCF-7 cellular proliferation and sensitized the cells to etoposide treatment which reflected on the ability of MCF-7 cell to

form visible cell colonies. Trichostatin A and Valproic acid which are HDACi have also been shown to sensitize drug resistant MCF-7 tumour cells to etoposide, the topoisomerase II inhibitor, with concomitant increase in H4K16ac (Hajji et al., 2009). My results show that HATi treatment (curcumin and garcinol) is able to induce H4K16ac in more than one cell line, and sensitizes the MCF-7 cells to etoposide. Collectively, our results propose a potential chemotherapeutic application of such small molecules in medical practice.

6.1: The Possible Pathways Through Which Garcinol Treatment Alters Cell Proliferation.



This cartoon demonstrates the effects of garcinol treatment on histone and p53 acetylation. Garcinol induces a DNA damage response manifested by TIP60 and SUV420H2 over expression that enhances H4K16 acetylation (H4K16ac) and H4K20 trimethylation (H4K20me3). DNA synthesis is blocked as demonstrated by reduced H3K18ac. H3K56 acetylation is enhanced suggesting targeting by CBP/p300 or other HATs upon garcinol treatment. Garcinol induces p53 expression although p53 transcription activity is reduced. DNA damage induces p53 acetylation at K120, K373/382 which may trigger its function in cell cycle regulation/apoptosis

Future Work

In future work I could extend the panel of study to include PTMs other than acetylation and methylation of histone and p53 PTMs as phosphorylation, ubiquitination, sumoylation, and ADP-ribosylation (Khorasanizadeh, 2004, Dai and Gu, 2010). Those modifications are also important in mitosis and chromosomal condensation, cell cycle progression, DNA damage response, tumour proliferation and others (Bannister and Kouzarides, 2011). Another set of enzymes ‘Clippases’ that can remove histone N-terminal tails (Best and Carey, 2010, Bannister and Kouzarides, 2011) have been identified in yeast. Evaluation of those enzymes could be a part of my future study in relationship to breast cancer tumour outcome.

REFERENCES

- AAGAARD, L., LAIBLE, G., SELENKO, P., SCHMID, M., DORN, R., SCHOTTA, G., KUHFITTIG, S., WOLF, A., LEBERSORGER, A., SINGH, P. B., REUTER, G. & JENUWEIN, T. (1999) Functional mammalian homologues of the *Drosophila* PEV-modifier Su(var)3-9 encode centromere-associated proteins which complex with the heterochromatin component M31. *EMBO Journal*, 18, 1923-38.
- AAGAARD, L., SCHMID, M., WARBURTON, P. & JENUWEIN, T. (2000) Mitotic phosphorylation of SUV39H1, a novel component of active centromeres, coincides with transient accumulation at mammalian centromeres. *Journal of Cell Science*, 113, 817-29.
- ABBOTT, D. W., LASZCZAK, M., LEWIS, J. D., SU, H., MOORE, S. C., HILLS, M., DIMITROV, S. & AUSIO, J. (2004) Structural characterization of macroH2A containing chromatin. *Biochemistry*, 43, 1352-1359.
- ABD EL-REHIM, D. M., BALL, G., PINDER, S. E., RAKHA, E. A., PAISH, C., ROBERTSON, J. F. R., MACMILLAN, D., BLAMEY, R. W. & ELLIS, I. O. (2005) High throughput protein expression analysis using tissue microarray technology of a large well characterised series identifies biologically distinct classes of breast cancer confirming recent cDNA expression analyses. *Int J Cancer*, 116, 340 - 350.
- ABD EL-REHIM, D. M., PINDER, S. E., PAISH, C. E., BELL, J., BLAMEY, R. W., ROBERTSON, J. F., NICHOLSON, R. I. & ELLIS, I. O. (2004a) Expression of luminal and basal cytokeratins in human breast carcinoma. *J Pathol*, 203, 661-71.
- ABD EL-REHIM, D. M., PINDER, S. E., PAISH, C. E., BELL, J. A., RAMPAUL, R. S., BLAMEY, R. W., ROBERTSON, J. F., NICHOLSON, R. I. & ELLIS, I. O. (2004b) Expression and co-expression of the members of the epidermal growth factor receptor (EGFR) family in invasive breast carcinoma. *Br J Cancer*, 91, 1532-42.
- AFONSO, N. & BOUWMAN, D. (2008) Lobular carcinoma in situ. *Eur J Cancer Prev*, 17, 312-6.
- AGGARWAL, B. B. & HARIKUMAR, K. B. (2009) Potential therapeutic effects of curcumin, the anti-inflammatory agent, against neurodegenerative, cardiovascular, pulmonary, metabolic, autoimmune and neoplastic diseases. *International Journal of Biochemistry & Cell Biology*, 41, 40-59.
- AHMED, S., DUL, B., QIU, X. & WALWORTH, N. C. (2007) Msc1 acts through histone H2A.Z to promote chromosome stability in *Schizosaccharomyces pombe*. *Genetics*, 177, 1487-97.
- AKHTAR, A. & BECKER, P. B. (2000) Activation of transcription through histone H4 acetylation by MOF, an acetyltransferase essential for dosage compensation in *Drosophila*. *Mol Cell*, 5, 367-75.
- ALARCON-VARGAS, D. & RONAI, Z. (2002) p53-Mdm2--the affair that never ends. *Carcinogenesis*, 23, 541-7.
- ALESKANDARANY, M. A., RAKHA, E. A., AHMED, M. A., POWE, D. G., ELLIS, I. O. & GREEN, A. R. (2010) Clinicopathologic and molecular significance of phospho-Akt expression in early invasive breast cancer. *Breast Cancer Research and Treatment*, 127, 407-416.
- ALIZADEH, A. A., ROSS, D. T., PEROU, C. M. & VAN DE RIJN, M. (2001) Towards a novel classification of human malignancies based on gene expression patterns. *Journal of Pathology*, 195, 41-52.

- ALLRED, D. C., WU, Y., MAO, S., NAGTEGAAL, I. D., LEE, S., PEROU, C. M., MOHSIN, S. K., O'CONNELL, P., TSIMELZON, A. & MEDINA, D. (2008) Ductal Carcinoma In situ and the Emergence of Diversity during Breast Cancer Evolution. *Clin Cancer Res*, 14, 370-378.
- ALTAF, M., AUGER, A., COVIC, M. & COTE, J. (2009) Connection between histone H2A variants and chromatin remodeling complexes. *Biochemistry & Cell Biology*, 87, 35-50.
- ALTAF, M., UTLEY, R. T., LACOSTE, N., TAN, S., BRIGGS, S. D. & COTE, J. (2007) Interplay of chromatin modifiers on a short basic patch of histone H4 tail defines the boundary of telomeric heterochromatin. *Molecular Cell*, 28, 1002-1014.
- AMMON, H. P. & WAHL, M. A. (1991) Pharmacology of Curcuma longa. *Planta Med*, 57, 1-7.
- ANANTHARAMAN, V. & ARAVIND, L. (2008) Analysis of DBC1 and its homologs suggests a potential mechanism for regulation of sirtuin domain deacetylases by NAD metabolites. *Cell Cycle*, 7, 1467-72.
- ANGELOV, D., MOLLA, A., PERCHE, P. Y., HANS, F., COTE, J., KHOCHBIN, S., BOUVET, P. & DIMITROV, S. (2003) The histone variant macroH2A interferes with transcription factor binding and SWI/SNF nucleosome remodeling. *Molecular Cell*, 11, 1033-1041.
- ARAYA, I., NARDOCCI, G., MORALES, J. P., VERA, M. I., MOLINA, A. & ALVAREZ, M. (2010) MacroH2A subtypes contribute antagonistically to the transcriptional regulation of the ribosomal cistron during seasonal acclimatization of the carp fish. *Epigenetics & Chromatin*, 3.
- ARENAS-MENA, C., WONG, K. S. & ARANDI-FOROSHANI, N. R. (2007) Histone H2A.Z expression in two indirectly developing marine invertebrates correlates with undifferentiated and multipotent cells. *Evolution & Development*, 9, 231-43.
- ARIF, M., KUMAR, G. V. P., NARAYANA, C. & KUNDU, T. K. (2007) Autoacetylation induced specific structural changes in histone acetyltransferase domain of p300: Probed by surface enhanced Raman spectroscopy. *Journal of Physical Chemistry B*, 111, 11877-11879.
- ARIF, M., PRADHAN, S. K., THANUJA, G. R., VEDAMURTHY, B. M., AGRAWAL, S., DASGUPTA, D. & KUNDU, T. K. (2009) Mechanism of p300 specific histone acetyltransferase inhibition by small molecules. *J Med Chem*, 52, 267-77.
- ARIMBASSERI, A. G. & BHARGAVA, P. (2008) Chromatin structure and expression of a gene transcribed by RNA polymerase III are independent of H2A.Z deposition. *Molecular & Cellular Biology*, 28, 2598-607.
- ASHBURNER, B. P., WESTERHEIDE, S. D. & BALDWIN, A. S. (2001) The p65 (RelA) subunit of NF-kappa B interacts with the histone deacetylase (HDAC) corepressors HDAC1 and HDAC2 to negatively regulate gene expression. *Molecular and Cellular Biology*, 21, 7065-7077.
- AUSTOKER, J. (2003) Breast self examination. *BMJ*, 326, 1-2.
- BABIARZ, J. E., HALLEY, J. E. & RINE, J. (2006) Telomeric heterochromatin boundaries require NuA4-dependent acetylation of histone variant H2A.Z in *Saccharomyces cerevisiae*. *Genes & Development*, 20, 700-10.
- BACHMAN, K. E., PARK, B. H., RHEE, I., RAJAGOPALAN, H., HERMAN, J. G., BAYLIN, S. B., KINZLER, K. W. & VOGELSTEIN, B. (2003)

- Histone modifications and silencing prior to DNA methylation of a tumor suppressor gene. *Cancer Cell*, 3, 89-95.
- BACHMEIER, B. E., NERLICH, A. G., IANCU, C. M., CILLI, M., SCHLEICHER, E., VENE, R., DELL'EVA, R., JOCHUM, M., ALBINI, A. & PFEFFER, U. (2007) The chemopreventive polyphenol Curcumin prevents hematogenous breast cancer metastases in immunodeficient mice. *Cellular Physiology and Biochemistry*, 19, 137-152.
- BADAL, V., CHUANG, L. S., TAN, E. H., BADAL, S., VILLA, L. L., WHEELER, C. M., LI, B. F. & BERNARD, H. U. (2003) CpG methylation of human papillomavirus type 16 DNA in cervical cancer cell lines and in clinical specimens: genomic hypomethylation correlates with carcinogenic progression. *J Virol*, 77, 6227-34.
- BALASUBRAMANYAM, K., ALTAF, M., VARIER, R. A., SWAMINATHAN, V., RAVINDRAN, A., SADHALE, P. P. & KUNDU, T. K. (2004a) Polyisoprenylated Benzophenone, Garcinol, a Natural Histone Acetyltransferase Inhibitor, Represses Chromatin Transcription and Alters Global Gene Expression. *J. Biol. Chem.*, 279, 33716-33726.
- BALASUBRAMANYAM, K., SWAMINATHAN, V., RANGANATHAN, A. & KUNDU, T. K. (2003) Small molecule modulators of histone acetyltransferase p300. *J Biol Chem*, 278, 19134-40.
- BALASUBRAMANYAM, K., VARIER, R. A., ALTAF, M., SWAMINATHAN, V., SIDDAPPA, N. B., RANGA, U. & KUNDU, T. K. (2004b) Curcumin, a Novel p300/CREB-binding Protein-specific Inhibitor of Acetyltransferase, Represses the Acetylation of Histone/Nonhistone Proteins and Histone Acetyltransferase-dependent Chromatin Transcription. *J. Biol. Chem.*, 279, 51163-51171.
- BANDYOPADHYAY, D., CURRY, J. L., LIN, Q. S., RICHARDS, H. W., CHEN, D. H., HORNSBY, P. J., TIMCHENKO, N. A. & MEDRANO, E. E. (2007) Dynamic assembly of chromatin complexes during cellular senescence: implications for the growth arrest of human melanocytic nevi. *Aging Cell*, 6, 577-591.
- BANDYOPADHYAY, D., MISHRA, A. & MEDRANO, E. E. (2004) Overexpression of histone deacetylase 1 confers resistance to sodium butyrate-mediated apoptosis in melanoma cells through a p53-mediated pathway. *Cancer Research*, 64, 7706-7710.
- BANNISTER, A. J. & KOUZARIDES, T. (2011) Regulation of chromatin by histone modifications. *Cell Research*, 21, 381-395.
- BANNISTER, A. J., MISKA, E. A., GORLICH, D. & KOUZARIDES, T. (2000) Acetylation of importin-alpha nuclear import factors by CBP/p300. *Current Biology*, 10, 467-470.
- BANNISTER, A. J., ZEGERMAN, P., PARTRIDGE, J. F., MISKA, E. A., THOMAS, J. O., ALLSHIRE, R. C. & KOUZARIDES, T. (2001) Selective recognition of methylated lysine 9 on histone H3 by the HP1 chromo domain. *Nature*, 410, 120-4.
- BARRETT, S. V. (2010) Breast cancer. *J R Coll Physicians Edinb*, 40, 335-9.
- BARRY, J., FRITZ, M., BRENDER, J. R., SMITH, P. E. S., LEE, D. K. & RAMAMOORTHY, A. (2009) Determining the Effects of Lipophilic Drugs on Membrane Structure by Solid-State NMR Spectroscopy: The Case of the Antioxidant Curcumin. *Journal of the American Chemical Society*, 131, 4490-4498.

- BARSKI, A., CUDDAPAH, S., CUI, K., ROH, T. Y., SCHONES, D. E., WANG, Z., WEI, G., CHEPELEV, I. & ZHAO, K. (2007) High-resolution profiling of histone methylations in the human genome.[see comment]. *Cell*, 129, 823-37.
- BECKMANN, M. W., NIEDERACHER, D., SCHNURCH, H. G., GUSTERSON, B. A. & BENDER, H. G. (1997) Multistep carcinogenesis of breast cancer and tumour heterogeneity. *Journal of Molecular Medicine-Jmm*, 75, 429-439.
- BEEVERS, F. L. L. L. S. H. (2006) Curcumin inhibits the mammalian target of rapamycin-mediated signaling pathways in cancer cells. *International Journal of Cancer*, 119, 757-764.
- BELLODI, C., KINDLE, K., BERNASSOLA, F., COSSARIZZA, A., DINSDALE, D., MELINO, G., HEERY, D. & SALOMONI, P. (2006) A cytoplasmic PML mutant inhibits p53 function. *Cell Cycle*, 5, 2688-92.
- BENETTI, R., GONZALO, S., JACO, I., SCHOTTA, G., KLATT, P., JENUWEIN, T. & BLASCO, M. A. (2007) Suv4-20h deficiency results in telomere elongation and derepression of telomere recombination. *Journal of Cell Biology*, 178, 925-936.
- BERGER, S. L. (2002) Histone modifications in transcriptional regulation. *Curr Opin Genet Dev*, 12, 142-8.
- BERNSTEIN, E., DUNCAN, E. M., MASUI, O., GIL, J., HEARD, E. & ALLIS, C. D. (2006) Mouse polycomb proteins bind differentially to methylated histone H3 and RNA and are enriched in facultative heterochromatin. *Molecular and Cellular Biology*, 26, 2560-2569.
- BEST, J. D. & CAREY, N. (2010) Epigenetic opportunities and challenges in cancer. *Drug Discovery Today*, 15, 65-70.
- BESTOR, T. H. (2003) Unanswered questions about the role of promoter methylation in carcinogenesis. *Ann NY Acad Sci*, 983, 22-7.
- BHAUMIK, S. R., SMITH, E. & SHILATIFARD, A. (2007) Covalent modifications of histones during development and disease pathogenesis. *Nat Struct Mol Biol*, 14, 1008-1016.
- BICAKU, E., MARCHION, D. C., SCHMITT, M. L. & MUNSTER, P. N. (2008) Selective inhibition of histone deacetylase 2 silences progesterone receptor-mediated signaling. *Cancer Research*, 68, 1513-1519.
- BINDA, O., NASSIF, C. & BRANTON, P. E. (2008) SIRT1 negatively regulates HDAC1-dependent transcriptional repression by the RBP1 family of proteins. *Oncogene*.
- BLAMEY, R. W., WILSON, A. R. & PATNICK, J. (2000) ABC of breast diseases: screening for breast cancer. *BMJ*, 321, 689-93.
- BORROW, J., STANTON, V. P., JR., ANDRESEN, J. M., BECHER, R., BEHM, F. G., CHAGANTI, R. S., CIVIN, C. I., DISTECHE, C., DUBE, I., FRISCHAUF, A. M., HORSMAN, D., MITELMAN, F., VOLINIA, S., WATMORE, A. E. & HOUSMAN, D. E. (1996) The translocation t(8;16)(p11;p13) of acute myeloid leukaemia fuses a putative acetyltransferase to the CREB-binding protein. *Nat Genet*, 14, 33-41.
- BRADY, M. E., OZANNE, D. M., GAUGHAN, L., WAITE, I., COOK, S., NEAL, D. E. & ROBSON, C. N. (1999) Tip60 is a nuclear hormone receptor coactivator. *Journal of Biological Chemistry*, 274, 17599-604.

- BREATHNACH, R. & CHAMBON, P. (1981) ORGANIZATION AND EXPRESSION OF EUKARYOTIC SPLIT GENES-CODING FOR PROTEINS. *Annual Review of Biochemistry*, 50, 349-383.
- BREUER, A., KANDEL, M., FISSELER-ECKHOFF, A., SUTTER, C., SCHWAAB, E., LUCK, H. J. & DU BOIS, A. (2007) BRCA1 germline mutation in a woman with metaplastic squamous cell breast cancer. *Onkologie*, 30, 316-8.
- BRICKNER, D. G., CAJIGAS, I., FONDUFÉ-MITTENDORF, Y., AHMED, S., LEE, P. C., WIDOM, J. & BRICKNER, J. H. (2007) H2A.Z-mediated localization of genes at the nuclear periphery confers epigenetic memory of previous transcriptional state. *Plos Biology*, 5, e81.
- BRICKNER, J. H. (2009) Transcriptional memory at the nuclear periphery. *Current Opinion in Cell Biology*, 21, 127-33.
- BRUCE, K., MYERS, F. A., MANTOUVALOU, E., LEFEVRE, P., GREAVES, I., BONIFER, C., TREMETHICK, D. J., THORNE, A. W. & CRANE-ROBINSON, C. (2005) The replacement histone H2A.Z in a hyperacetylated form is a feature of active genes in the chicken. *Nucleic Acids Research*, 33, 5633-9.
- BUCHEN, L. (2011) MISSING THE MARK. *Nature*, 471, 428-432.
- BUDILLON, A., DI GENNARO, E., BRUZZESE, F., DELRIO, P., CARAGLIA, M. & AVALLONE, A. (2005) Suberoylanilide hydroxamic acid (SAHA) potentiates the anti-tumour effects of 5-fluorouracil and raltitrexed in colon cancer cells through the inhibition of thymidilate synthase expression. *Annals of Oncology*, 16, 33-34.
- BUERGER, H., SIMON, R., SCHAFER, K. L., DIALLO, R., LITTMANN, R., POREMBA, C., VAN DIEST, P. J., DOCKHORN-DWORNICZAK, B. & BOCKER, W. (2000) Genetic relation of lobular carcinoma in situ, ductal carcinoma in situ, and associated invasive carcinoma of the breast. *Mol Pathol*, 53, 118-21.
- BULYNKO, Y. A., HSING, L. C., MASON, R. W., TREMETHICK, D. J. & GRIGORYEV, S. A. (2006) Cathepsin L stabilizes the histone modification landscape on the Y chromosome and pericentromeric heterochromatin. *Molecular & Cellular Biology*, 26, 4172-84.
- BUTLER, L. M., ZHOU, X., XU, W. S., SCHER, H. I., RIFKIND, R. A., MARKS, P. A. & RICHON, V. M. (2002) The histone deacetylase inhibitor SAHA arrests cancer cell growth, up-regulates thioredoxin-binding protein-2, and down-regulates thioredoxin. *Proc Natl Acad Sci U S A*, 99, 11700-5.
- CAI, R. L., YAN-NEALE, Y., CUETO, M. A., XU, H. & COHEN, D. (2000) HDAC1, a histone deacetylase, forms a complex with Hus1 and Rad9, two G(2)/M checkpoint Rad proteins. *Journal of Biological Chemistry*, 275, 27909-27916.
- CAI, Y., JIN, J., GOTTSCHALK, A. J., YAO, T., CONAWAY, J. W. & CONAWAY, R. C. (2006) Purification and assay of the human INO80 and SRCAP chromatin remodeling complexes. *Methods (Duluth)*, 40, 312-7.
- CALISKAN, M., GATTI, G., SOSNOVSKIKH, I., ROTMENSZ, N., BOTTERI, E., MUSMECI, S., ROSALI DOS SANTOS, G., VIALE, G. & LUINI, A. (2008) Paget's disease of the breast: the experience of the European

- institute of oncology and review of the literature. *Breast Cancer Res Treat.*
- CAMP, R. L., CHARETTE, L. A. & RIMM, D. L. (2000) Validation of tissue microarray technology in breast carcinoma. *Laboratory Investigation*, 80, 1943-1949.
- CAO, X. & SUDHOFF, T. C. (2001) A transcriptionally [correction of transcriptively] active complex of APP with Fe65 and histone acetyltransferase Tip60.[see comment][comment][erratum appears in Science 2001 Aug 24;293(5534):1436]. *Science*, 293, 115-20.
- CARNEIRO, M. L. B., PORFIRIO, E. P., OTAKE, A. H., CHAMMAS, R., BAO, S. N. & GUILLO, L. A. (2010) Morphological Alterations and G0/G1 Cell Cycle Arrest Induced by Curcumin in Human SK-MEL-37 Melanoma Cells. *Brazilian Archives of Biology and Technology*, 53, 343-352.
- CHA, E. J., NOH, S. J., KWON, K. S., KIM, C. Y., PARK, B. H., PARK, H. S., LEE, H., CHUNG, M. J., KANG, M. J., LEE, D. G., MOON, W. S. & JANG, K. Y. (2009) Expression of DBC1 and SIRT1 Is Associated with Poor Prognosis of Gastric Carcinoma. *Clinical Cancer Research*, 15, 4453-4459.
- CHANG, H. H., CHIANG, C. P., HUNG, H. C., LIN, C. Y., DENG, Y. T. & KUO, M. Y. P. (2009) Histone deacetylase 2 expression predicts poorer prognosis in oral cancer patients. *Oral Oncology*, 45, 610-614.
- CHAUHAN, D. P. (2002) Chemotheapeutic potential of curcumin for colorectal cancer. *Current Pharmaceutical Design*, 8, 1695-1706.
- CHEKHUN, V. F., LUKYANOVA, N. Y., KOVALCHUK, O., TRYNDYAK, V. P. & POGRIBNY, I. P. (2007) Epigenetic profiling of multidrug-resistant human MCF-7 breast adenocarcinoma cells reveals novel hyper- and hypomethylated targets. *Mol Cancer Ther*, 6, 1089-1098.
- CHEN, C. Y., J, D. O., Q, Z., A, J. F., JR., B, V. & M, B. K. (1994) Interactions between p53 and MDM2 in a mammalian cell cycle checkpoint pathway. *Proceedings of the National Academy of Sciences of the United States of America*, 91, 2684-2688.
- CHEN, I. Y., LYPOWY, J., PAIN, J., SAYED, D., GRINBERG, S., ALCENDOR, R. R., SADOSHIMA, J. & ABDELLATIF, M. (2006) Histone H2A.z is essential for cardiac myocyte hypertrophy but opposed by silent information regulator 2alpha. *Journal of Biological Chemistry*, 281, 19369-77.
- CHEN, L., FAN, Y., LANG, R. G., GUO, X. J., SUN, Y. L., CUI, L. F., LIU, F., WEI, J., ZHANG, X. M. & FU, L. (2008a) Breast carcinoma with micropapillary features: clinicopathologic study and long-term follow-up of 100 cases. *Int J Surg Pathol*, 16, 155-63.
- CHEN, L. H., LI, Z. Y., ZWOLINSKA, A. K., SMITH, M. A., CROSS, B., KOOMEN, J., YUAN, Z. M., JENUWEIN, T., MARINE, J. C., WRIGHT, K. L. & CHEN, J. D. (2010) MDM2 recruitment of lysine methyltransferases regulates p53 transcriptional output. *EMBO Journal*, 29, 2538-2552.
- CHEN, Z.-Q., JIE, X. & MO, Z.-N. (2008b) [Curcumin inhibits growth, induces G1 arrest and apoptosis on human prostatic stromal cells by regulating Bcl-2/Bax]. *Zhongguo Zhong Yao Za Zhi*, 33, 2022-5.

- CHENG, A. S. L., JIN, V. X., FAN, M. Y., SMITH, L. T., LIYANARACHCHI, S., YAN, P. S., LEU, Y. W., CHAN, M. W. Y., PLASS, C., NEPHEW, K. P., DAVULURI, R. V. & HUANG, T. H. M. (2006) Combinatorial analysis of transcription factor partners reveals recruitment of c-MYC to estrogen receptor-alpha responsive promoters. *Molecular Cell*, 21, 393-404.
- CHENG, H. L., MOSTOSLAVSKY, R., SAITO, S., MANIS, J. P., GU, Y., PATEL, P., BRONSON, R., APPELLA, E., ALT, F. W. & CHUA, K. F. (2003) Developmental defects and p53 hyperacetylation in Sir2 homolog (SIRT1)-deficient mice. *Proc Natl Acad Sci U S A*, 100, 10794-9.
- CHERRIER, T., SUZANNE, S., REDEL, L., CALAO, M., MARBAN, C., SAMAH, B., MUKERJEE, R., SCHWARTZ, C., GRAS, G., SAWAYA, B. E., ZEICHNER, S. L., AUNIS, D., VAN LINT, C. & ROHR, O. (2009) p21(WAF1) gene promoter is epigenetically silenced by CTIP2 and SUV39H1. *Oncogene*, 28, 3380-9.
- CHO, M., UEMURA, H., KIM, S. C., KAWADA, Y., YOSHIDA, K., HIRAO, Y., KONISHI, N., SAGA, S. & YOSHIKAWA, K. (2001) Hypomethylation of the MN/CA9 promoter and upregulated MN/CA9 expression in human renal cell carcinoma. *Br J Cancer*, 85, 563-7.
- CHOUDHURI, T., PAL, S., DAS, T. & SA, G. (2005) Curcumin selectively induces apoptosis in deregulated cyclin D1 expressed cells at G2 phase of cell cycle in a p53-dependent manner. *J. Biol. Chem.*, M410670200.
- CHUIKOV, S., KURASH, J. K., WILSON, J. R., XIAO, B., JUSTIN, N., IVANOV, G. S., MCKINNEY, K., TEMPST, P., PRIVES, C., GAMBLIN, S. J., BARLEV, N. A. & REINBERG, D. (2004) Regulation of p53 activity through lysine methylation. *Nature*, 432, 353-360.
- CLOOS, P. A. C., CHRISTENSEN, J., AGGER, K., MAIOLICA, A., RAPPSILBER, J., ANTAL, T., HANSEN, K. H. & HELIN, K. (2006) The putative oncogene GASC1 demethylates tri- and dimethylated lysine 9 on histone H3. *Nature*, 442, 307-311.
- COL, E., CARON, C., CHABLE-BESSIA, C., LEGUBE, G., GAZZERI, S., KOMATSU, Y., YOSHIDA, M., BENKIRANE, M., TROUCHE, D. & KHOCHBIN, S. (2005) HIV-1 Tat targets Tip60 to impair the apoptotic cell response to genotoxic stresses. *EMBO Journal*, 24, 2634-45.
- COLEMAN, M. P. (2000) Trends in breast cancer incidence, survival, and mortality. *Lancet*, 356, 590-1; author reply 593.
- COLLINS, H. M., KINDLE, K. B., MATSUDA, S., RYAN, C., TROKE, P. J., KALKHOVEN, E. & HEERY, D. M. (2006) MOZ-TIF2 alters cofactor recruitment and histone modification at the RAR β 2 promoter: differential effects of MOZ fusion proteins on CBP- and MOZ-dependent activators. *J Biol Chem*, 281, 17124-33.
- COMMANDEUR, J. N. & VERMEULEN, N. P. (1996) Cytotoxicity and cytoprotective activities of natural compounds. The case of curcumin. *Xenobiotica*, 26, 667-80.
- COSTA, S. D., LANGE, S., KLINGA, K., MERKLE, E. & KAUFMANN, M. (2002) Factors influencing the prognostic role of oestrogen and progesterone receptor levels in breast cancer - results of the analysis of 670 patients with 11 years of follow-up. *European Journal of Cancer*, 38, 1329-1334.

- COSTANZI, C. & PEHRSON, J. R. (1998) Histone macroH2A1 is concentrated in the inactive X chromosome of female mammals. *Nature*, 393, 599-601.
- COX, D. R. (1972) REGRESSION MODELS AND LIFE-TABLES. *Journal of the Royal Statistical Society Series B-Statistical Methodology*, 34, 187-&.
- CREYGHTON, M. P., MARKOULAKI, S., LEVINE, S. S., HANNA, J., LODATO, M. A., SHA, K., YOUNG, R. A., JAENISCH, R. & BOYER, L. A. (2008) H2AZ is enriched at polycomb complex target genes in ES cells and is necessary for lineage commitment. *Cell*, 135, 649-61.
- CUI, K., ZANG, C., ROH, T. Y., SCHONES, D. E., CHILDS, R. W., PENG, W. & ZHAO, K. (2009) Chromatin signatures in multipotent human hematopoietic stem cells indicate the fate of bivalent genes during differentiation.[see comment]. *Cell Stem Cell*, 4, 80-93.
- CZERMIN, B., SCHOTTA, G., HULSMANN, B. B., BREHM, A., BECKER, P. B., REUTER, G. & IMHOF, A. (2001) Physical and functional association of SU(VAR)3-9 and HDAC1 in Drosophila. *EMBO Reports*, 2, 915-919.
- CZVITKOVICH, S., SAUER, S., PETERS, A. H., DEINER, E., WOLF, A., LAIBLE, G., OPRAVIL, S., BEUG, H. & JENUWEIN, T. (2001) Over-expression of the SUV39H1 histone methyltransferase induces altered proliferation and differentiation in transgenic mice. *Mechanisms of Development*, 107, 141-53.
- DAI, C. & GU, W. (2010) p53 post-translational modification: deregulated in tumorigenesis. *Trends in Molecular Medicine*, 16, 528-536.
- DAS, C., LUCIA, M. S., HANSEN, K. C. & TYLER, J. K. (2009) CBP/p300-mediated acetylation of histone H3 on lysine 56. *Nature*, 459, 113-7.
- DAS, P. M. & SINGAL, R. (2004) DNA Methylation and Cancer. *J Clin Oncol*, 22, 4632-4642.
- DAUJAT, S., BAUER, U. M., SHAH, V., TURNER, B., BERGER, S. & KOUZARIDES, T. (2002) Crosstalk between CARM1 methylation and CBP acetylation on histone H3. *Curr Biol*, 12, 2090-7.
- DE GASPERI, M. J., CAVAZOS, D. & DEGRAFFENRIED, L. A. (2009) Curcumin Modulates Tamoxifen Response in Resistant Breast Cancer Cells. *Cancer Research*, 69, 679S-679S.
- DE RUIJTER, A. J. M., VAN GENNIP, A. H., CARON, H. N., KEMP, S. & VAN KUILENBURG, A. B. P. (2003) Histone deacetylases (HDACs): characterization of the classical HDAC family. *Biochemical Journal*, 370, 737-749.
- DE SMET, C., DE BACKER, O., FARAONI, I., LURQUIN, C., BRASSEUR, F. & BOON, T. (1996) The activation of human gene MAGE-1 in tumor cells is correlated with genome-wide demethylation. *Proc Natl Acad Sci U S A*, 93, 7149-53.
- DENU, J. M. (2005) The Sir2 family of protein deacetylases. *Current Opinion in Chemical Biology*, 9, 431-440.
- DERKS, S., BOSCH, L. J., NIJESSEN, H. E., MOERKERK, P. T., VAN DEN BOSCH, S. M., CARVALHO, B., MONGERA, S., VONCKEN, J. W., MEIJER, G. A., DE BRUIJNE, A. P., HERMAN, J. G. & VAN ENGELAND, M. (2009) Promoter CpG island hypermethylation- and H3K9me3 and H3K27me3-mediated epigenetic silencing targets the deleted in colon cancer (DCC) gene in colorectal carcinogenesis without

- affecting neighboring genes on chromosomal region 18q21. *Carcinogenesis*, 30, 1041-8.
- DHILLON, N., OKI, M., SZYJKA, S. J., APARICIO, O. M. & KAMAKAKA, R. T. (2006) H2A.Z functions to regulate progression through the cell cycle. *Molecular & Cellular Biology*, 26, 489-501.
- DINTZIS, H. M. (1961) ASSEMBLY OF PEPTIDE CHAINS OF HEMOGLOBIN. *Proceedings of the National Academy of Sciences of the United States of America*, 47, 247-&.
- DOMLOGE, N., BAUZA, E., ROUX, E., PERRIN, A., GONDTRAN, C., BOTTO, J. M. & DAL FARRA, C. (2005) SIRT1, the human homologue of Sir2, a gene involved in regulating life span, is expressed in human skin and in cultured skin cells. *Journal of Investigative Dermatology*, 125, 043.
- DORMANN, H. L., TSENG, B. S., ALLIS, C. D., FUNABIKI, H. & FISCHLE, W. (2006) Dynamic regulation of effector protein binding to histone modifications - The biology of HP1 switching. *Cell Cycle*, 5, 2842-2851.
- DOYEN, C. M., AN, W., ANGELOV, D., BONDARENKO, V., MIETTON, F., STUDITSKY, V. M., HAMICHE, A., ROEDER, R. G., BOUVET, P. & DIMITROV, S. (2006) Mechanism of polymerase II transcription repression by the histone variant macroH2A. *Mol Cell Biol*, 26, 1156-64.
- DOYON, Y., CAYROU, C., ULLAH, M., LANDRY, A. J., COTE, V., SELLECK, W., LANE, W. S., TAN, S., YANG, X. J. & COTE, J. (2006) ING tumor suppressor proteins are critical regulators of chromatin acetylation required for genome expression and perpetuation. *Molecular Cell*, 21, 51-64.
- DOYON, Y., SELLECK, W., LANE, W. S., TAN, S. & COTE, J. (2004) Structural and functional conservation of the NuA4 histone acetyltransferase complex from yeast to humans. *Mol Cell Biol*, 24, 1884-96.
- DRAKER, R. & CHEUNG, P. (2009) Transcriptional and epigenetic functions of histone variant H2A.Z. *Biochemistry & Cell Biology*, 87, 19-25.
- DRYHURST, D., THAMBIRAJAH, A. A. & AUSIO, J. (2004) New twists on H2A.Z: a histone variant with a controversial structural and functional past. *Biochem Cell Biol*, 82, 490-7.
- DUDZIEC, E., GOEPEL, J. R. & CATTO, J. W. F. (2011) Global epigenetic profiling in bladder cancer. *Epigenomics*, 3, 35-45.
- DUGAS-BREIT, S., LI, W., MARSHALL, C., GELFAND, J. & SEYKORA, J. T. (2005) Curcumin modulates growth regulatory signaling pathways and promotes G2/M growth arrest in human keratinocytes. *Journal of Investigative Dermatology*, 124, 562.
- EGELHOFER, T. A., MINODA, A., KLUGMAN, S., LEE, K., KOLASINSKA-ZWIERZ, P., ALEKSEYENKO, A. A., CHEUNG, M.-S., DAY, D. S., GADEL, S., GORCHAKOV, A. A., GU, T., KHARCHENKO, P. V., KUAN, S., LATORRE, I., LINDER-BASSO, D., LUU, Y., NGO, Q., PERRY, M., RECHTSTEINER, A., RIDDLE, N. C., SCHWARTZ, Y. B., SHANOWER, G. A., VIELLE, A., AHRINGER, J., ELGIN, S. C. R., KURODA, M. I., PIRROTTA, V., REN, B., STROME, S., PARK, P. J., KARPEN, G. H., HAWKINS, R. D. & LIEB, J. D. (2011) An assessment of histone-modification antibody quality. *Nature Structural & Molecular Biology*, 18, 91-+.

- EGGER, G., LIANG, G., APARICIO, A. & JONES, P. A. (2004) Epigenetics in human disease and prospects for epigenetic therapy. *Nature*, 429, 457-63.
- EICHENBAUM, K. D., RODRIGUEZ, Y., MEZEI, M. & OSMAN, R. (2009) The energetics of the acetylation switch in p53-mediated transcriptional activation. *Proteins-Structure Function and Bioinformatics*, 78, 447-456.
- ELDEIRY, W. S., TOKINO, T., VELCULESCU, V. E., LEVY, D. B., PARSONS, R., TRENT, J. M., LIN, D., MERCER, W. E., KINZLER, K. W. & VOGELSTEIN, B. (1993) WAF1, A POTENTIAL MEDIATOR OF P53 TUMOR SUPPRESSION. *Cell*, 75, 817-825.
- ELISEEVA, E. D., VALKOV, V., JUNG, M. & JUNG, M. O. (2007) Characterization of novel inhibitors of histone acetyltransferases. *Mol Cancer Ther*, 6, 2391-8.
- ELLINGER, J., KAHL, P., VON DER GATHEN, J., ROGENHOFER, S., HEUKAMP, L. C., GUTGEMANN, I., WALTER, B., HOFSTADTER, F., BUTTNER, R., MULLER, S. C., BASTIAN, P. J. & VON RUECKER, A. (2010) Global Levels of Histone Modifications Predict Prostate Cancer Recurrence. *Prostate*, 70, 61-69.
- ELSHEIKH, S. E., GREEN, A. R., RAKHA, E. A., POWE, D. G., AHMED, R. A., COLLINS, H. M., SORIA, D., GARIBALDI, J. M., PAISH, C. E., AMMAR, A. A., GRAINGE, M. J., BALL, G. R., ABDELGHANY, M. K., MARTINEZ-POMARES, L., HEERY, D. M. & ELLIS, I. O. (2009) Global histone modifications in breast cancer correlate with tumor phenotypes, prognostic factors, and patient outcome. *Cancer Res*, 69, 3802-9.
- ELSTON, C. W. (1984) THE ASSESSMENT OF HISTOLOGICAL DIFFERENTIATION IN BREAST-CANCER. *Australian and New Zealand Journal of Surgery*, 54, 11-15.
- ELSTON, C. W. & ELLIS, I. O. (1991) Pathological prognostic factors in breast cancer. I. The value of histological grade in breast cancer: experience from a large study with long-term follow-up. *Histopathology*, 19, 403 - 410.
- EPAND, R. F., MARTINUO, J. C., FORNALLAZ-MULHAUSER, M., HUGHES, D. W. & EPAND, R. M. (2002) The apoptotic protein tBid promotes leakage by altering membrane curvature. *J Biol Chem*, 277, 32632-9.
- ESSMANN, F., ENGELS, I. H., TOTZKE, G., SCHULZE-OSTHOFF, K. & JANICKE, R. U. (2004) Apoptosis resistance of MCF-7 breast carcinoma cells to ionizing radiation is independent of p53 and cell cycle control but caused by the lack of caspase-3 and a caffeine-inhibitable event. *Cancer Research*, 64, 7065-7072.
- ESTELLER, M. (2007a) Cancer epigenomics: DNA methylomes and histone-modification maps. *Nat Rev Genet*, 8, 286-298.
- ESTELLER, M. (2007b) Cancer epigenomics: DNA methylomes and histone-modification maps. *Nat Rev Genet*, 8, 286-98.
- FAIOLA, F., LIU, X., LO, S., PAN, S., ZHANG, K., LYMAR, E., FARINA, A. & MARTINEZ, E. (2005) Dual regulation of c-Myc by p300 via acetylation-dependent control of Myc protein turnover and coactivation of Myc-induced transcription. *Molecular & Cellular Biology*, 25, 10220-34.
- FAN, J. Y., ZHOU, J. & TREMETHICK, D. J. (2007) Quantitative analysis of HP1alpha binding to nucleosomal arrays. *Methods (Duluth)*, 41, 286-90.

- FANG, J., FENG, Q., KETEL, C. S., WANG, H. B., CAO, R., XIA, L., ERDJUMENT-BROMAGE, H., TEMPST, P., SIMON, J. A. & ZHANG, Y. (2002) Purification and functional characterization of SET8, a nucleosomal histone H4-lysine 20-specific methyltransferase. *Current Biology*, 12, 1086-1099.
- FAUSTINO, N. A. & COOPER, T. A. (2003) Pre-mRNA splicing and human disease. *Genes & Development*, 17, 419-437.
- FEINBERG, A. P. (2004) The epigenetics of cancer etiology. *Semin Cancer Biol*, 14, 427-32.
- FENG, L., LIN, T., URANISHI, H., GU, W. & XU, Y. (2005) Functional Analysis of the Roles of Posttranslational Modifications at the p53 C Terminus in Regulating p53 Stability and Activity. *Mol. Cell. Biol.*, 25, 5389-5395.
- FERRARI, R., PELLEGRINI, M., HORWITZ, G. A., XIE, W., BERK, A. J. & KURDISTANI, S. K. (2008) Epigenetic reprogramming by adenovirus e1a. *Science*, 321, 1086-8.
- FIDLEROVA, H., KALINOVA, J., BLECHOVA, M., VELEK, J. & RASKA, I. (2009) A new epigenetic marker: The replication-coupled, cell cycle-dependent, dual modification of the histone H4 tail. *Journal of Structural Biology*, 167, 76-82.
- FINGERMAN, I. M., DU, H.-N. & BRIGGS, S. D. (2008) In Vitro Histone Methyltransferase Assay. *Cold Spring Harbor Protocols*, 2008, pdb.prot4939-.
- FISCHLE, W. (2009) Tip60-ing the balance in DSB repair. *Nature Cell Biology*, 11, 1279-1281.
- FORD, J., JIANG, M. & MILNER, J. (2005a) Cancer-specific functions of SIRT1 enable human epithelial cancer cell growth and survival. *Cancer Research*, 65, 10457-10463.
- FORD, J., JIANG, M. & MILNER, J. (2005b) Cancer-Specific Functions of SIRT1 Enable Human Epithelial Cancer Cell Growth and Survival. *Cancer Res*, 65, 10457-10463.
- FORTSON, W. S., KAYARTHODI, S., FUJIMURA, Y., XU, H. L., MATTHEWS, R., GRIZZLE, W. E., RAO, V. N., BHAT, G. K. & REDDY, E. S. P. (2011) Histone deacetylase inhibitors, valproic acid and trichostatin-A induce apoptosis and affect acetylation status of p53 in ERG-positive prostate cancer cells. *International Journal of Oncology*, 39, 111-119.
- FRAGA, M. F., BALLESTAR, E., VILLAR-GAREA, A., BOIX-CHORNET, M., ESPADA, J., SCHOTTA, G., BONALDI, T., HAYDON, C., ROPERO, S., PETRIE, K., IYER, N. G., PEREZ-ROSADO, A., CALVO, E., LOPEZ, J. A., CANO, A., CALASANZ, M. J., COLOMER, D., PIRIS, M. A., AHN, N., IMHOF, A., CALDAS, C., JENUWEIN, T. & ESTELLER, M. (2005) Loss of acetylation at Lys16 and trimethylation at Lys20 of histone H4 is a common hallmark of human cancer. *Nat Genet*, 37, 391-400.
- FU, M., WANG, C., ZHANG, X. & PESTELL, R. G. (2004) Acetylation of nuclear receptors in cellular growth and apoptosis. *Biochemical Pharmacology*, 68, 1199-1208.

- FU, Y., SINHA, M., PETERSON, C. L. & WENG, Z. (2008) The insulator binding protein CTCF positions 20 nucleosomes around its binding sites across the human genome. *PLoS Genetics*, 4, e1000138.
- GALEA, M. H., BLAMEY, R. W., ELSTON, C. E. & ELLIS, I. O. (1992) The Nottingham Prognostic Index in primary breast cancer. *Breast Cancer Res Treat*, 22, 207 - 219.
- GALLUZZI, L., MORSELLI, E., KEPP, O., TAJEDDINE, N. & KROEMER, G. (2008) Targeting p53 to mitochondria for cancer therapy. *Cell Cycle*, 7, 1949-1955.
- GARCIA-MANERO, G., YANG, H., BUESO-RAMOS, C., FERRAJOLI, A., CORTES, J., WIERDA, W. G., FADERL, S., KOLLER, C., MORRIS, G., ROSNER, G., LOBODA, A., FANTIN, V. R., RANDOLPH, S. S., HARDWICK, J. S., REILLY, J. F., CHEN, C., RICKER, J. L., SECRIST, J. P., RICHON, V. M., FRANKEL, S. R. & KANTARJIAN, H. M. (2008) Phase 1 study of the histone deacetylase inhibitor vorinostat (suberoylanilide hydroxamic acid [SAHA]) in patients with advanced leukemias and myelodysplastic syndromes. *Blood*, 111, 1060-6.
- GATEI, M., SCOTT, S. P., FILIPPOVITCH, I., SORONIKA, N., LAVIN, M. F., WEBER, B. & KHANNA, K. K. (2000) Role for ATM in DNA damage-induced phosphorylation of BRCA1. *Cancer Research*, 60, 3299-+.
- GAYTHER, S. A., BATLEY, S. J., LINGER, L., BANNISTER, A., THORPE, K., CHIN, S. F., DAIGO, Y., RUSSELL, P., WILSON, A., SOWTER, H. M., DELHANTY, J. D., PONDER, B. A., KOUZARIDES, T. & CALDAS, C. (2000) Mutations truncating the EP300 acetylase in human cancers. *Nat Genet*, 24, 300-3.
- GERVAIS, A. L. & GAUDREAU, L. (2009) Discriminating nucleosomes containing histone H2A.Z or H2A based on genetic and epigenetic information. *BMC Molecular Biology*, 10, 18.
- GEVRY, N., CHAN, H. M., LAFLAMME, L., LIVINGSTON, D. M. & GAUDREAU, L. (2007) p21 transcription is regulated by differential localization of histone H2A.Z. *Genes & Development*, 21, 1869-81.
- GIANGASPERO, F., WELLEK, S., MASOKA, J., GESSI, M., KLEIHUES, P. & OHGAKI, H. (2006) Stratification of medulloblastoma on the basis of histopathological grading. *Brain Pathology*, 16, 228.
- GILES, R. H., PETERS, D. J. & BREUNING, M. H. (1998) Conjunction dysfunction: CBP/p300 in human disease. *Trends Genet*, 14, 178-83.
- GLOZAK, M. A. & SETO, E. (2007) Histone deacetylases and cancer. *Oncogene*, 26, 5420-5432.
- GOEL, A., BOLAND, C. R. & CHAUHAN, D. P. (2001) Specific inhibition of cyclooxygenase-2 (COX-2) expression by dietary curcumin in HT-29 human colon cancer cells. *Cancer Lett*, 172, 111-8.
- GOH, A. M., COFFILL, C. R. & LANE, D. P. The role of mutant p53 in human cancer. *Journal of Pathology*, 223, 116-126.
- GOUSSIA, A. C., STEFANOU, D. G., KARAIOSIFIDI, E. C. & AGNANTIS, N. J. (2006) DCIS histopathology from a historical perspective. *Eur J Gynaecol Oncol*, 27, 282-5.
- GRAFF, J. R., HERMAN, J. G., LAPIDUS, R. G., CHOPRA, H., XU, R., JARRARD, D. F., ISAACS, W. B., PITHA, P. M., DAVIDSON, N. E. & BAYLIN, S. B. (1995) E-cadherin expression is silenced by DNA

- hypermethylation in human breast and prostate carcinomas. *Cancer Res*, 55, 5195-9.
- GREAVES, I. K., RANGASAMY, D., RIDGWAY, P. & TREMETHICK, D. J. (2007) H2A.Z contributes to the unique 3D structure of the centromere. *Proceedings of the National Academy of Sciences of the United States of America*, 104, 525-30.
- GREEN, D. R. & KROEMER, G. (2009) Cytoplasmic functions of the tumour suppressor p53. *Nature*, 458, 1127-1130.
- GREESON, N. T., SENGUPTA, R., ARIDA, A. R., JENUWEIN, T. & SANDERS, S. L. (2008) Di-methyl H4 Lysine 20 Targets the Checkpoint Protein Crb2 to Sites of DNA Damage. *Journal of Biological Chemistry*, 283, 33168-33174.
- GRIER, J. D., XIONG, S. B., ELIZONDO-FRAIRE, A. C., PARANT, J. M. & LOZANO, G. (2006) Tissue-specific differences of p53 inhibition by Mdm2 and Mdm4. *Molecular and Cellular Biology*, 26, 192-198.
- GRONER, A. C., MEYLAN, S., CIUFFI, A., ZANGGER, N., AMBROSINI, G., DENERVERAUD, N., BUCHER, P. & TRONO, D. (2010) KRAB-Zinc Finger Proteins and KAP1 Can Mediate Long-Range Transcriptional Repression through Heterochromatin Spreading. *PLoS Genetics*, 6.
- GUILLEMETTE, B., BATAILLE, A. R., GEVRY, N., ADAM, M., BLANCHETTE, M., ROBERT, F. & GAUDREAU, L. (2005) Variant histone H2A.Z is globally localized to the promoters of inactive yeast genes and regulates nucleosome positioning. *Plos Biology*, 3, e384.
- GUILLEMETTE, B. & GAUDREAU, L. (2006) H2A.Z: un variant d'histone qui orne les promoteurs des gènes. *M S-Medecine Sciences*, 22, 941-6.
- GUPTA, A., GUERIN-PEYROU, T. G., SHARMA, G. G., PARK, C., AGARWAL, M., GANJU, R. K., PANDITA, S., CHOI, K., SUKUMAR, S., PANDITA, R. K., LUDWIG, T. & PANDITA, T. K. (2008) The mammalian ortholog of Drosophila MOF that acetylates histone H4 lysine 16 is essential for embryogenesis and oncogenesis. *Molecular & Cellular Biology*, 28, 397-409.
- GURTNER, A., FUSCHI, P., MAGI, F., COLUSSI, C., GAETANO, C., DOBBELSTEIN, M., SACCHI, A. & PIAGGIO, G. (2008) NF-Y dependent epigenetic modifications discriminate between proliferating and postmitotic tissue. *PLoS ONE [Electronic Resource]*, 3, e2047.
- HABASHY, H., POWE, D., RAKHA, E., BALL, G., PAISH, C., GEE, J., NICHOLSON, R. & ELLIS, I. (2008a) Forkhead-box A1 (FOXA1) expression in breast cancer and its prognostic significance. *European Journal of Cancer*, 44, 1541 - 1551.
- HABASHY, H. O., POWE, D. G., RAKHA, E. A., BALL, G., MACMILLAN, R. D., GREEN, A. R. & ELLIS, I. O. (2009) The prognostic significance of PELP1 expression in invasive breast cancer with emphasis on the ER-positive luminal-like subtype. *Breast Cancer Res Treat*, 120, 603-12.
- HABASHY, H. O., POWE, D. G., RAKHA, E. A., BALL, G., PAISH, C., GEE, J., NICHOLSON, R. I. & ELLIS, I. O. (2008b) Forkhead-box A1 (FOXA1) expression in breast cancer and its prognostic significance. *European Journal of Cancer*, 44, 1541-1551.
- HABUCHI, T., LUSCOMBE, M., ELDER, P. A. & KNOWLES, M. A. (1998) Structure and methylation-based silencing of a gene (DBCCR1) within a

- candidate bladder cancer tumor suppressor region at 9q32-q33. *Genomics*, 48, 277-88.
- HAJJI, N., WALLENBORG, K., VLACHOS, P., FULLGRABE, J., HERMANSON, O. & JOSEPH, B. (2009) Opposing effects of hMOF and SIRT1 on H4K16 acetylation and the sensitivity to the topoisomerase II inhibitor etoposide. *Oncogene*, 29, 2192-204.
- HAJJI, N., WALLENBORG, K., VLACHOS, P., NYMAN, U., HERMANSON, O. & JOSEPH, B. (2008) Combinatorial action of the HDAC inhibitor trichostatin A and etoposide induces caspase-mediated AIF-dependent apoptotic cell death in non-small cell lung carcinoma cells. *Oncogene*, 27, 3134-44.
- HALKIDOU, K., GNANAPRAGASAM, V. J., MEHTA, P. B., LOGAN, I. R., BRADY, M. E., COOK, S., LEUNG, H. Y., NEAL, D. E. & ROBSON, C. N. (2003) Expression of Tip60, an androgen receptor coactivator, and its role in prostate cancer development. *Oncogene*, 22, 2466-77.
- HAMAGUCHI, M., METH, J. L., VON KLITZING, C., WEI, W., ESPOSITO, D., RODGERS, L., WALSH, T., WELCSH, P., KING, M. C. & WIGLER, M. H. (2002) DBC2, a candidate for a tumor suppressor gene involved in breast cancer. *Proceedings of the National Academy of Sciences of the United States of America*, 99, 13647-13652.
- HAN, M. K., SONG, E. K., GUO, Y., OU, X., MANTEL, C. & BROXMEYER, H. E. (2008) SIRT1 regulates apoptosis and Nanog expression in mouse embryonic stem cells by controlling p53 subcellular localization. *Cell Stem Cell*, 2, 241-51.
- HANIF, R., QIAO, L., SHIFF, S. J. & RIGAS, B. (1997) Curcumin, a natural plant phenolic food additive, inhibits cell proliferation and induces cell cycle changes in colon adenocarcinoma cell lines by a prostaglandin-independent pathway. *Journal of Laboratory and Clinical Medicine*, 130, 576-584.
- HARMS, K. L. & CHEN, X. B. (2007) Histone deacetylase 2 modulates p53 transcriptional activities through regulation of p53-DNA binding activity. *Cancer Research*, 67, 3145-3152.
- HASEGAWA, K. & YOSHIKAWA, K. (2008) Necdin regulates p53 acetylation via Sirtuin1 to modulate DNA damage response in cortical neurons. *Journal of Neuroscience*, 28, 8772-84.
- HASSIG, C. A., TONG, J. K., FLEISCHER, T. C., OWA, T., GRABLE, P. G., AYER, D. E. & SCHREIBER, S. L. (1998) A role for histone deacetylase activity in HDAC1-mediated transcriptional repression. *Proceedings of the National Academy of Sciences of the United States of America*, 95, 3519-3524.
- HATTORI, T., COUSTRY, F., STEPHENS, S., EBERSPAECHER, H., TAKIGAWA, M., YASUDA, H. & DE CROMBRUGGHE, B. (2008) Transcriptional regulation of chondrogenesis by coactivator Tip60 via chromatin association with Sox9 and Sox5. *Nucleic Acids Research*, 36, 3011-24.
- HAUGSTEN, E. M., WIEDLOCHA, A., OLSNES, S. & WESCHE, J. (2010) Roles of Fibroblast Growth Factor Receptors in Carcinogenesis. *Molecular Cancer Research*, 8, 1439-1452.

- HEERY, D. M. & FISCHER, P. M. (2007) Pharmacological targeting of lysine acetyltransferases in human disease: a progress report. *Drug Discov Today*, 12, 88-99.
- HILFIKER, A., HILFIKER-KLEINER, D., PANNUTI, A. & LUCCHESI, J. C. (1997a) mof, a putative acetyl transferase gene related to the Tip60 and MOZ human genes and to the SAS genes of yeast, is required for dosage compensation in Drosophila. *EMBO J*, 16, 2054-60.
- HILFIKER, A., HILFIKER-KLEINER, D., PANNUTI, A. & LUCCHESI, J. C. (1997b) mof, a putative acetyl transferase gene related to the Tip60 and MOZ human genes and to the SAS genes of yeast, is required for dosage compensation in Drosophila. *Embo Journal*, 16, 2054-2060.
- HORWITZ, G. A., ZHANG, K., MCBRIAN, M. A., GRUNSTEIN, M., KURDISTANI, S. K. & BERK, A. J. (2008) Adenovirus small e1a alters global patterns of histone modification. *Science*, 321, 1084-5.
- HSIAO, K.-Y. & MIZZEN, C. (2010) Functional interactions between lysine 20 methylation and lysine 16 acetylation on histone H4 in DNA damage responses. *Proceedings of the American Association for Cancer Research Annual Meeting*, 51, 1185.
- HU, J. & COLBURN, N. H. (2005) Histone deacetylase inhibition down-regulates cyclin D1 transcription by inhibiting nuclear factor-kappaB/p65 DNA binding. *Mol Cancer Res*, 3, 100-9.
- HU, Z., FAN, C., OH, D. S., MARRON, J. S., HE, X., QAQISH, B. F., LIVASY, C., CAREY, L. A., REYNOLDS, E., DRESSLER, L., NOBEL, A., PARKER, J., EWEND, M. G., SAWYER, L. R., WU, J., LIU, Y., NANDA, R., TRETIKOVA, M., RUIZ ORRICO, A., DREHER, D., PALAZZO, J. P., PERREARD, L., NELSON, E., MONE, M., HANSEN, H., MULLINS, M., QUACKENBUSH, J. F., ELLIS, M. J., OLOPADE, O. I., BERNARD, P. S. & PEROU, C. M. (2006) The molecular portraits of breast tumors are conserved across microarray platforms. *BMC Genomics*, 7, 96.
- HUA, S., KALLEN, C. B., DHAR, R., BAQUERO, M. T., MASON, C. E., RUSSELL, B. A., SHAH, P. K., LIU, J., KHRAMTSOV, A., TRETIKOVA, M. S., KRAUSZ, T. N., OLOPADE, O. I., RIMM, D. L. & WHITE, K. P. (2008) Genomic analysis of estrogen cascade reveals histone variant H2A.Z associated with breast cancer progression. *Molecular Systems Biology*, 4, 188.
- HUANG, J., PEREZ-BURGOS, L., PLACEK, B. J., SENGUPTA, R., RICHTER, M., DORSEY, J. A., KUBICEK, S., OPRAVIL, S., JENUWEIN, T. & BERGER, S. L. (2006) Repression of p53 activity by Smyd2-mediated methylation. *Nature*, 444, 629-632.
- HUANG, J., SENGUPTA, R., ESPEJO, A. B., LEE, M. G., DORSEY, J. A., RICHTER, M., OPRAVIL, S., SHIEKHATTAR, R., BEDFORD, M. T., JENUWEIN, T. & BERGER, S. L. (2007) p53 is regulated by the lysine demethylase LSD1. *Nature*, 449, 105-108.
- IKURA, T., OGRYZKO, V. V., GRIGORIEV, M., GROISMAN, R., WANG, J., HORIKOSHI, M., SCULLY, R., QIN, J. & NAKATANI, Y. (2000) Involvement of the TIP60 Histone Acetylase Complex in DNA Repair and Apoptosis. *Cell*, 102, 463-473.
- IMBRIANO, C., GURTNER, A., COCCHIARELLA, F., DI AGOSTINO, S., BASILE, V., GOSTISSA, M., DOBBELSTEIN, M., DEL SAL, G.,

- PIAGGIO, G. & MANTOVANI, R. (2005) Direct p53 transcriptional repression: In vivo analysis of CCAAT-containing G(2)/M promoters. *Molecular and Cellular Biology*, 25, 3737-3751.
- ISSA, J. P., GARCIA-MANERO, G., GILES, F. J., MANNARI, R., THOMAS, D., FADERL, S., BAYAR, E., LYONS, J., ROSENFELD, C. S., CORTES, J. & KANTARJIAN, H. M. (2004) Phase 1 study of low-dose prolonged exposure schedules of the hypomethylating agent 5-aza-2'-deoxycytidine (decitabine) in hematopoietic malignancies. *Blood*, 103, 1635-40.
- ITO, A., KAWAGUCHI, Y., LAI, C. H., KOVACS, J. J., HIGASHIMOTO, Y., APPELLA, E. & YAO, T. P. (2002) MDM2-HDAC1-mediated deacetylation of p53 is required for its degradation. *EMBO Journal*, 21, 6236-6245.
- ITOH, Y., SUZUKI, T. & MIYATA, N. (2008) Isoform-selective histone deacetylase inhibitors. *Current Pharmaceutical Design*, 14, 529-544.
- IYER, N. G., OZDAG, H. & CALDAS, C. (2004) p300/CBP and cancer. *Oncogene*, 23, 4225-4231.
- JACKSON, J. G., POST, S. M. & LOZANO, G. (2010) Regulation of tissue- and stimulus-specific cell fate decisions by p53 in vivo. *Journal of Pathology*, 223, 127-136.
- JAGODZINSKI, M. W. Ł. A. P. P. (2006) The role of DNA methylation in cancer development. *FOLIA HISTOCHEMICA ET CYTOBIOLOGICA*, 44, 11.
- JANG, K. Y., HWANG, S. H., KWON, K. S., KIM, K. R., CHOI, H. N., LEE, N. R., KWAK, J. Y., PARK, B. H., PARK, H. S., CHUNG, M. J., KANG, M. J., LEE, D. G., KIM, H. S., SHIM, H. & MOON, W. S. (2008) SIRT1 expression is associated with poor prognosis of diffuse large B-cell lymphoma. *American Journal of Surgical Pathology*, 32, 1523-31.
- JANG, K. Y., KIM, K. S., HWANG, S. H., KWON, K. S., KIM, K. R., PARK, H. S., PARK, B. H., CHUNG, M. J., KANG, M. J., LEE, D. G. & MOON, W. S. (2009) Expression and prognostic significance of SIRT1 in ovarian epithelial tumours. *Pathology*, 41, 366-71.
- JANICKE, R. U., ENGELS, I. H., DUNKERN, T., KAINA, B., SCHULZE-OSTHOFF, K. & PORTER, A. G. (2001) Ionizing radiation but not anticancer drugs causes cell cycle arrest and failure to activate the mitochondrial death pathway in MCF-7 breast carcinoma cells. *Oncogene*, 20, 5043-5053.
- JANSSON, M., DURANT, S. T., CHO, E.-C., SHEAHAN, S., EDELMANN, M., KESSLER, B. & LA THANGUE, N. B. (2008) Arginine methylation regulates the p53 response. *Nat Cell Biol*, 10, 1431-1439.
- JENUWEIN, T. & ALLIS, C. D. (2001) Translating the histone code. *Science*, 293, 1074-80.
- JEPPESEN, P. & TURNER, B. M. (1993) The inactive X chromosome in female mammals is distinguished by a lack of histone H4 acetylation, a cytogenetic marker for gene expression. *Cell*, 74, 281-9.
- JHA, S., SHIBATA, E. & DUTTA, A. (2008) Human Rvb1/Tip49 is required for the histone acetyltransferase activity of Tip60/NuA4 and for the downregulation of phosphorylation on H2AX after DNA damage. *Molecular & Cellular Biology*, 28, 2690-700.

- JIN, C. & FELSENFELD, G. (2007) Nucleosome stability mediated by histone variants H3.3 and H2A.Z. *Genes & Development*, 21, 1519-29.
- JONES, P. A., ARCHER, T. K., BAYLIN, S. B., BECK, S., BERGER, S., BERNSTEIN, B. E., CARPTEN, J. D., CLARK, S. J., COSTELLO, J. F., DOERGE, R. W., ESTELLER, M., FEINBERG, A. P., GINGERAS, T. R., GREALLY, J. M., HENIKOFF, S., HERMAN, J. G., JACKSON-GRUSBY, L., JENUWEIN, T., JIRTLE, R. L., KIM, Y. J., LAIRD, P. W., LIM, B., MARTIENSSEN, R., POLYAK, K., STUNNENBERG, H., TLSTY, T. D., TYCKO, B., USHIJIMA, T., ZHU, J. D., PIRROTTA, V., ALLIS, C. D., ELGIN, S. C., RINE, J., WU, C., AMER ASSOC CANC RES HUMAN, E. & EUROPEAN UNION NETWORK, E. (2008) Moving AHEAD with an international human epigenome project. *Nature*, 454, 711-715.
- JUNG-HYNES, B., NIHAL, M., ZHONG, W. & AHMAD, N. (2009) Role of sirtuin histone deacetylase SIRT1 in prostate cancer. A target for prostate cancer management via its inhibition? *Journal of Biological Chemistry*, 284, 3823-32.
- KAKAR, S., PUANGSUVAN, N., STEVENS, J. M., SERENAS, R., MANGAN, G., SAHAI, S. & MIHALOV, M. L. (2000) HER-2/neu assessment in breast cancer by immunohistochemistry and fluorescence in situ hybridization: comparison of results and correlation with survival. *Mol Diagn*, 5, 199-207.
- KALOCSAY, M., HILLER, N. J. & JENTSCH, S. (2009) Chromosome-wide Rad51 spreading and SUMO-H2A.Z-dependent chromosome fixation in response to a persistent DNA double-strand break. *Molecular Cell*, 33, 335-43.
- KAMINE, J., ELANGOVAN, B., SUBRAMANIAN, T., COLEMAN, D. & CHINNADURAI, G. (1996) Identification of a cellular protein that specifically interacts with the essential cysteine region of the HIV-1 Tat transactivator. *Virology*, 216, 357-66.
- KAPOOR-VAZIRANI, P., KAGEY, J. D., POWELL, D. R. & VERTINO, P. M. (2008) Role of hMOF-Dependent Histone H4 Lysine 16 Acetylation in the Maintenance of TMS1/ASC Gene Activity. *Cancer Res*, 68, 6810-6821.
- KAPOOR, A., GOLDBERG, M. S., CUMBERLAND, L. K., RATNAKUMAR, K., SEGURA, M. F., EMANUEL, P. O., MENENDEZ, S., VARDABASSO, C., LEROY, G., VIDAL, C. I., POLSKY, D., OSMAN, I., GARCIA, B. A., HERNANDO, E. & BERNSTEIN, E. (2010) The histone variant macroH2A suppresses melanoma progression through regulation of CDK8. *Nature*, 468, 1105-U509.
- KASPER, L. H., BOUSSOUAR, F., NEY, P. A., JACKSON, C. W., REHG, J., VAN DEURSEN, J. M. & BRINDLE, P. K. (2002) A transcription-factor-binding surface of coactivator p300 is required for haematopoiesis. *Nature*, 419, 738-743.
- KAWAI, H., LI, H. C., AVRAHAM, S., JIANG, S. X. & AVRAHAM, H. K. (2003) Overexpression of histone deacetylase HDAC1 modulates breast cancer progression by negative regulation of estrogen receptor alpha. *International Journal of Cancer*, 107, 353-358.
- KAWASHIMA, S., OGAWARA, H., TADA, S., HARATA, M., WINTERSBERGER, U., ENOMOTO, T. & SEKI, M. (2007) The INO80

- complex is required for damage-induced recombination. *Biochemical & Biophysical Research Communications*, 355, 835-41.
- KHORASANIZADEH, S. (2004) The nucleosome: from genomic organization to genomic regulation. *Cell*, 116, 259-72.
- KIM, E. J., KHO, J. H., KANG, M. R. & UM, S. J. (2007) Active regulator of SIRT1 cooperates with SIRT1 and facilitates suppression of p53 activity. *Mol Cell*, 28, 277-90.
- KIM, E. J. & UM, S. J. (2008) SIRT1: roles in aging and cancer. *BMB reports*, 41, 751-6.
- KIM, J. E., CHEN, J. & LOU, Z. (2008) DBC1 is a negative regulator of SIRT1. *Nature*, 451, 583-6.
- KIMURA, A. & HORIKOSHI, M. (1998) Tip60 acetylates six lysines of a specific class in core histones in vitro. *Genes to Cells*, 3, 789-800.
- KINDLE, K. B., TROKE, P. J., COLLINS, H. M., MATSUDA, S., BOSSI, D., BELLODI, C., KALKHOVEN, E., SALOMONI, P., PELICCI, P. G., MINUCCI, S. & HEERY, D. M. (2005) MOZ-TIF2 inhibits transcription by nuclear receptors and p53 by impairment of CBP function. *Mol Cell Biol*, 25, 988-1002.
- KITABAYASHI, I., AIKAWA, Y., NGUYEN, L. A., YOKOYAMA, A. & OHKI, M. (2001) Activation of AML1-mediated transcription by MOZ and inhibition by the MOZ-CBP fusion protein. *Embo Journal*, 20, 7184-7196.
- KNIGHTS, C. D., CATANIA, J., DI GIOVANNI, S., MURATOGLU, S., PEREZ, R., SWARTZBECK, A., QUONG, A. A., ZHANG, X., BEERMAN, T., PESTELL, R. G. & AVANTAGGIATI, M. L. (2006a) Distinct p53 acetylation cassettes differentially influence gene-expression patterns and cell fate. *J Cell Biol*, 173, 533-44.
- KNIGHTS, C. D., CATANIA, J., DI GIOVANNI, S., MURATOGLU, S., PEREZ, R., SWARTZBECK, A., QUONG, A. A., ZHANG, X. J., BEERMAN, T., PESTELL, R. G. & AVANTAGGIATI, M. L. (2006b) Distinct p53 acetylation cassettes differentially influence gene-expression patterns and cell fate. *Journal of Cell Biology*, 173, 533-544.
- KOJIMA, K., OHHASHI, R., FUJITA, Y., HAMADA, N., AKAO, Y., NOZAWA, Y., DEGUCHI, T. & ITO, M. (2008) A role for SIRT1 in cell growth and chemoresistance in prostate cancer PC3 and DU145 cells. *Biochemical & Biophysical Research Communications*, 373, 423-8.
- KOMAKI, K., SAKAMOTO, G., SUGANO, H., MORIMOTO, T. & MONDEN, Y. (1988) Mucinous carcinoma of the breast in Japan. A prognostic analysis based on morphologic features. *Cancer*, 61, 989-96.
- KONDO, Y., SHEN, L. & ISSA, J. P. (2003) Critical role of histone methylation in tumor suppressor gene silencing in colorectal cancer. *Mol Cell Biol*, 23, 206-15.
- KONONEN, J., BUBENDORF, L., KALLIONIEMI, A., BARLUND, M., SCHRAML, P., LEIGHTON, S., TORHORST, J., MIHATSCH, M. J., SAUTER, G. & KALLIONIEMI, O. P. (1998) Tissue microarrays for high-throughput molecular profiling of tumor specimens. *Nature Medicine*, 4, 844-847.
- KRAMER, O. H. (2009) HDAC2: a critical factor in health and disease. *Trends in Pharmacological Sciences*, 30, 647-655.

- KRISHNAN, V., CHOW, M. Z. Y., WANG, Z. M., ZHANG, L., LIU, B. H., LIU, X. G. & ZHOU, Z. J. (2011) Histone H4 lysine 16 hypoacetylation is associated with defective DNA repair and premature senescence in Zmpste24-deficient mice. *Proceedings of the National Academy of Sciences of the United States of America*, 108, 12325-12330.
- KRUCHEN, A., JOHANN, P. D., HANDGRETINGER, R. & MULLER, I. (2010) Effect of the HDAC inhibitor SAHA on the immunmodulatory properties of MSC and tumour stroma cells. *Bone Marrow Transplantation*, 45, S178-S178.
- KRUSCHE, C., WÜLFING, P., KERSTING, C., VLOET, A., BÖCKER, W., KIESEL, L., BEIER, H. & ALFER, J. (2005) Histone deacetylase-1 and -3 protein expression in human breast cancer: a tissue microarray analysis. *Breast Cancer Research and Treatment*, 90, 15-23.
- KRUSE, J. P. & GU, W. (2009) Modes of p53 Regulation. *Cell*, 137, 609-622.
- KURASH, J. K., LEI, H., SHEN, Q., MARSTON, W. L., GRANDA, B. W., FAN, H., WALL, D., LI, E. & GAUDET, F. (2008) Methylation of p53 by Set7/9 mediates p53 acetylation and activity in vivo. *Mol Cell*, 29, 392-400.
- KUSCH, T., FLORENS, L., MACDONALD, W. H., SWANSON, S. K., GLASER, R. L., YATES, J. R., 3RD, ABMAYR, S. M., WASHBURN, M. P. & WORKMAN, J. L. (2004) Acetylation by Tip60 is required for selective histone variant exchange at DNA lesions. *Science*, 306, 2084-7.
- KUTALA, V. K., KARUPPAIYAH, S., WEIR, N. M., TONG, L. Y., VISWANATH, S. & KUPPUSAMY, P. (2006) Curcumin induced G2/M arrest and apoptosis by enhancing superoxide generation and inhibiting Akt activity in chemoresistant human ovarian cancer cells. *Free Radical Biology and Medicine*, 41, S111-S111.
- KWON, H.-S. & OTT, M. (2008) The ups and downs of SIRT1. *Trends in Biochemical Sciences*, 33, 517-525.
- LAGGER, G., O'CARRROLL, D., REMBOLD, M., KHIER, H., TISCHLER, J., WEITZER, G., SCHUETTENGRUBER, B., HAUSER, C., BRUNMEIR, R., JENUWEIN, T. & SEISER, C. (2002) Essential function of histone deacetylase 1 in proliferation control and CDK inhibitor repression. *EMBO Journal*, 21, 2672-2681.
- LALL, S. (2008) Sinister symphony in e1a. *Nat Struct Mol Biol*, 15, 1005-1005.
- LANE, D. P. (1992) CANCER - P53, GUARDIAN OF THE GENOME. *Nature*, 358, 15-16.
- LANGLEY, E., PEARSON, M., FARETTA, M., BAUER, U. M., FRYE, R. A., MINUCCI, S., PELICCI, P. G. & KOUZARIDES, T. (2002) Human SIR2 deacetylates p53 and antagonizes PML/p53-induced cellular senescence. *EMBO J*, 21, 2383-96.
- LAVERY, D. N. & BEVAN, C. L. (2011) Androgen Receptor Signalling in Prostate Cancer: The Functional Consequences of Acetylation. *Journal of Biomedicine and Biotechnology*.
- LEE, E. H., PARK, S. K., PARK, B., KIM, S. W., LEE, M. H., AHN, S. H., SON, B. H., YOO, K. Y. & KANG, D. (2010) Effect of BRCA1/2 mutation on short-term and long-term breast cancer survival: a systematic review and meta-analysis. *Breast Cancer Research and Treatment*, 122, 11-25.

- LEE, H., KIM, K. R., NOH, S. J., PARK, H. S., KWON, K. S., PARK, B. H., JUNG, S. H., YOUN, H. J., LEE, B. K., CHUNG, M. J., KOH, D. H., MOON, W. S. & JANG, K. Y. (2011) Expression of DBC1 and SIRT1 is associated with poor prognosis for breast carcinoma. *Human Pathology*, 42, 204-213.
- LEE, J. H., KIM, E. K., CHOI, S., NAM, K. J., KIM, D. C. & CHO, S. H. (2008) Metaplastic breast carcinoma with extensive osseous differentiation: A case report. *Breast*, 17, 314-6.
- LEE, J. T. & GU, W. (2009) The multiple levels of regulation by p53 ubiquitination. *Cell Death Differ*, 17, 86-92.
- LEMIEUX, K., LAROCHELLE, M. & GAUDREAU, L. (2008) Variant histone H2A.Z, but not the HMG proteins Nhp6a/b, is essential for the recruitment of Swi/Snf, Mediator, and SAGA to the yeast GAL1 UAS(G). *Biochemical & Biophysical Research Communications*, 369, 1103-7.
- LI, C. I., MOE, R. E. & DALING, J. R. (2003) Risk of mortality by histologic type of breast cancer among women aged 50 to 79 years. *Arch Intern Med*, 163, 2149-53.
- LI, C. I., URIBE, D. J. & DALING, J. R. (2005a) Clinical characteristics of different histologic types of breast cancer. *British Journal of Cancer*, 93, 1046-52.
- LI, J., LIN, Q., YOON, H. G., HUANG, Z. Q., STRAHL, B. D., ALLIS, C. D. & WONG, J. (2002) Involvement of histone methylation and phosphorylation in regulation of transcription by thyroid hormone receptor. *Molecular & Cellular Biology*, 22, 5688-97.
- LI, L.-C., CARROLL, P. R. & DAHIYA, R. (2005b) Epigenetic Changes in Prostate Cancer: Implication for Diagnosis and Treatment. *J. Natl. Cancer Inst.*, 97, 103-115.
- LI, Q., KE, Q. D. & COSTA, M. (2009a) Alterations of histone modifications by cobalt compounds. *Carcinogenesis*, 30, 1243-1251.
- LI, Q., LIN, S., WANG, X., LIAN, G., LU, Z., GUO, H., RUAN, K., WANG, Y., YE, Z., HAN, J. & LIN, S. C. (2009b) Axin determines cell fate by controlling the p53 activation threshold after DNA damage. *Nature Cell Biology*, 11, 1128-34.
- LI, X. Z., CORSA, C. A. S., PAN, P. W., WU, L. P., FERGUSON, D., YU, X. C., MIN, J. R. & DOU, Y. L. (2011) MOF and H4 K16 Acetylation Play Important Roles in DNA Damage Repair by Modulating Recruitment of DNA Damage Repair Protein Mdc1. *Molecular and Cellular Biology*, 30, 5335-5347.
- LI, X. Z., WU, L. P., CORSA, C. A. S., KUNKEL, S. & DOU, Y. L. (2009c) Two Mammalian MOF Complexes Regulate Transcription Activation by Distinct Mechanisms. *Molecular Cell*, 36, 290-301.
- LI, Z., CHEN, L., KABRA, N., WANG, C., FANG, J. & CHEN, J. (2009d) Inhibition of SUV39H1 Methyltransferase Activity by DBC1. *J. Biol. Chem.*, 284, 10361-10366.
- LI, Z. Y., CHEN, L. H., KABRA, N. H., WANG, C. G., FANG, J. & CHEN, J. D. (2009e) Inhibition of SUV39H1 Methyltransferase Activity by DBC1. *Journal of Biological Chemistry*, 284, 10361-10366.
- LIN, J. K., PAN, M. H. & LIN-SHIAU, S. Y. (2000) Recent studies on the biofunctions and biotransformations of curcumin. *Biofactors*, 13, 153-8.

- LINDEMAN, L. C., WINATA, C. L., AANES, H., MATHAVAN, S., ALESTROM, P. & COLLAS, P. (2010) Chromatin states of developmentally-regulated genes revealed by DNA and histone methylation patterns in zebrafish embryos. *International Journal of Developmental Biology*, 54, 803-813.
- LIU, B. L., CHENG, J. X., ZHANG, X. A., WANG, R., ZHANG, W., LIN, H., XIAO, X. A., CAI, S., CHEN, X. Y. & CHENG, H. (2010) Global Histone Modification Patterns as Prognostic Markers to Classify Glioma Patients. *Cancer Epidemiology Biomarkers & Prevention*, 19, 2888-2896.
- LIU, E. Y., WU, J., CAO, W. D., ZHANG, J. N., LIU, W. P., JIANG, X. F. & ZHANG, X. A. (2007) Curcumin induces G2/M cell cycle arrest in a p53-dependent manner and upregulates ING4 expression in human glioma. *Journal of Neuro-Oncology*, 85, 263-270.
- LIU, X., WANG, L., ZHAO, K. H., THOMPSON, P. R., HWANG, Y., MARMORSTEIN, R. & COLE, P. A. (2008) The structural basis of protein acetylation by the p300/CBP transcriptional coactivator. *Nature*, 451, 846-850.
- LOBJOIS, V., FRONGIA, C., JOZAN, S., TRUCHET, I. & VALETTE, A. (2009) Cell cycle and apoptotic effects of SAHA are regulated by the cellular microenvironment in HCT116 multicellular tumour spheroids. *European Journal of Cancer*, 45, 2402-2411.
- LOUHELAINEN, J. P., HURST, C. D., PITTS, E., NISHIYAMA, H., PICKETT, H. A. & KNOWLES, M. A. (2006) DBC1 re-expression alters the expression of multiple components of the plasminogen pathway. *Oncogene*, 25, 2409-19.
- LUGER, K. (2003) Structure and dynamic behavior of nucleosomes. *Curr Opin Genet Dev*, 13, 127-35.
- LUND, A. H. & VAN LOHUIZEN, M. (2004a) Epigenetics and cancer. *Genes Dev*, 18, 2315-2335.
- LUND, A. H. & VAN LOHUIZEN, M. (2004b) Epigenetics and cancer. *Genes Dev*, 18, 2315-35.
- MACALUSO, M., CINTI, C., RUSSO, G., RUSSO, A. & GIORDANO, A. (2003) pRb2/p130-E2F4/5-HDAC1-SUV39H1-p300 and pRb2/p130-E2F4/5-HDAC1-SUV39H1-DNMT1 multimolecular complexes mediate the transcription of estrogen receptor-alpha in breast cancer. *Oncogene*, 22, 3511-7.
- MACALUSO, M., MONTANARI, M., MARSHALL, C. M., GAMBONE, A. J., TOSI, G. M., GIORDANO, A. & MASSARO-GIORDANO, M. (2006) Cytoplasmic and nuclear interaction between Rb family proteins and PAI-2: a physiological crosstalk in human corneal and conjunctival epithelial cells. *Cell Death & Differentiation*, 13, 1515-22.
- MALYUCHIK, S. S. & KIYAMOVA, R. G. (2008) Medullary breast carcinoma. *Exp Oncol*, 30, 96-101.
- MANTELINGU, K., KISHORE, A. H., BALASUBRAMANYAM, K., KUMAR, G. V., ALTAF, M., SWAMY, S. N., SELVI, R., DAS, C., NARAYANA, C., RANGAPPA, K. S. & KUNDU, T. K. (2007a) Activation of p300 histone acetyltransferase by small molecules altering enzyme structure: probed by surface-enhanced Raman spectroscopy. *J Phys Chem B*, 111, 4527-34.

- MANTELINGU, K., REDDY, B. A., SWAMINATHAN, V., KISHORE, A. H., SIDDAPPA, N. B., KUMAR, G. V., NAGASHANKAR, G., NATESH, N., ROY, S., SADHALE, P. P., RANGA, U., NARAYANA, C. & KUNDU, T. K. (2007b) Specific inhibition of p300-HAT alters global gene expression and represses HIV replication. *Chem Biol*, 14, 645-57.
- MANUYAKORN, A., PAULUS, R., FARRELL, J., DAWSON, N. A., TZE, S., CHEUNG-LAU, G., HINES, O. J., REBER, H., SELIGSON, D. B., HORVATH, S., KURDISTANI, S. K., GUHA, C. & DAWSON, D. W. (2010) Cellular Histone Modification Patterns Predict Prognosis and Treatment Response in Resectable Pancreatic Adenocarcinoma: Results From RTOG 9704. *Journal of Clinical Oncology*, 28, 1358-1365.
- MARINE, J. C. & LOZANO, G. (2010) Mdm2-mediated ubiquitylation: p53 and beyond. *Cell Death Differ*, 17, 93-102.
- MARQUARD, L., GJERDRUM, L. M., CHRISTENSEN, I. J., JENSEN, P. B., SEHESTED, M. & RALFKIAER, E. (2008) Prognostic significance of the therapeutic targets histone deacetylase 1, 2, 6 and acetylated histone H4 in cutaneous T-cell lymphoma. *Histopathology*, 53, 267-277.
- MARQUES, M., LAFLAMME, L., GERVAIS, A. L. & GAUDREAU, L. (2010) Reconciling the positive and negative roles of histone H2A.Z in gene transcription. *Epigenetics*, 5, 267-272.
- MARTIN, C. & ZHANG, Y. (2005) The diverse functions of histone lysine methylation. *Nat Rev Mol Cell Biol*, 6, 838-849.
- MARTINEZ, R., SETIEN, F., VOELTER, C., CASADO, S., QUESADA, M. P., SCHACKERT, G. & ESTELLER, M. (2007) CpG island promoter hypermethylation of the pro-apoptotic gene caspase-8 is a common hallmark of relapsed glioblastoma multiforme. *Carcinogenesis*, 28, 1264-8.
- MASUMOTO, H., HAWKE, D., KOBAYASHI, R. & VERREAUULT, A. (2005) A role for cell-cycle-regulated histone H3 lysine 56 acetylation in the DNA damage response. *Nature*, 436, 294-8.
- MATSUMOTO, M., FURIHATA, M. & OHTSUKI, Y. (2006) Posttranslational phosphorylation of mutant p53 protein in tumor development. *Med Mol Morphol*, 39, 79-87.
- MATTERA, L., ESCAFFIT, F., PILLAIRE, M. J., SELVES, J., TYTECA, S., HOFFMANN, J. S., GOURRAUD, P. A., CHEVILLARD-BRIET, M., CAZAUX, C. & TROUCHE, D. (2009) The p400/Tip60 ratio is critical for colorectal cancer cell proliferation through DNA damage response pathways. *Oncogene*, 28, 1506-17.
- MAZOUNI, C., BONNIER, P., GOUBAR, A., ROMAIN, S. & MARTIN, P. M. (2010)
 -) Is quantitative oestrogen receptor expression useful in the evaluation of the clinical prognosis? Analysis of a homogeneous series of 797 patients with prospective determination of the ER status using simultaneous EIA and IHC. *Eur J Cancer*.
- MCCARTY, K. S., JR., MILLER, L. S., COX, E. B., KONRATH, J. & MCCARTY, K. S., SR. (1985) Estrogen receptor analyses. Correlation of biochemical and immunohistochemical methods using monoclonal antireceptor antibodies. *Arch Pathol Lab Med*, 109, 716-21.
- MCGOVERN, P. E., CHRISTOFIDOU-SOLOMIDOU, M., WANG, W., DUKE, F., DAVIDSON, T. & EL-DEIRY, W. S. (2010) Anticancer

- activity of botanical compounds in ancient fermented beverages (Review). *International Journal of Oncology*, 37, 5-14.
- MCPHERSON, K., STEEL, C. M. & DIXON, I. M. (2000) ABC of breast diseases. Breast cancer-epidemiology, risk factors, and genetics *British Medical Journal*, 321, 624-628.
- MEEK, D. W. & ANDERSON, C. W. (2009) Posttranslational modification of p53: cooperative integrators of function. *Cold Spring Harb Perspect Biol*, 1, a000950.
- MELCHER, M., SCHMID, M., AAGAARD, L., SELENKO, P., LAIBLE, G. & JENUWEIN, T. (2000) Structure-function analysis of SUV39H1 reveals a dominant role in heterochromatin organization, chromosome segregation, and mitotic progression. *Molecular and Cellular Biology*, 20, 3728-3741.
- MILLAR, C. B., XU, F., ZHANG, K. & GRUNSTEIN, M. (2006) Acetylation of H2AZ Lys 14 is associated with genome-wide gene activity in yeast. *Genes Dev*, 20, 711-22.
- MILLER, B., WEEDON-FEKJAER, H., HAKULINEN, T., TRYGGVADOTTIR, L., STORM, H. H., TALBACK, M. & HALDORSEN, T. (2005) The influence of mammographic screening on national trends in breast cancer incidence. *Eur.J.Cancer Prev*, 14, 117-128.
- MILNE, J. C., LAMBERT, P. D., SCHENK, S., CARNEY, D. P., SMITH, J. J., GAGNE, D. J., JIN, L., BOSS, O., PERNI, R. B., VU, C. B., BEMIS, J. E., XIE, R., DISCH, J. S., NG, P. Y., NUNES, J. J., LYNCH, A. V., YANG, H. Y., GALONEK, H., ISRAELIAN, K., CHOY, W., IFFLAND, A., LAVU, S., MEDVEDIK, O., SINCLAIR, D. A., OLEFSKY, J. M., JIROUSEK, M. R., ELLIOTT, P. J. & WESTPHAL, C. H. (2007) Small molecule activators of SIRT1 as therapeutics for the treatment of type 2 diabetes. *Nature*, 450, 712-716.
- MITTRA, I., BAUM, M., THORNTON, H., HOUGHTON, J. & (2000) Is clinical breast examination an acceptable alternative to mammographic screening? *British Medical Journal*, 321, 1071-1073
- MIYAKE, K., YOSHIZUMI, T., IMURA, S., SUGIMOTO, K., BATMUNKH, E., KANEMURA, H., MORINE, Y. & SHIMADA, M. (2008) Expression of hypoxia-inducible factor-1alpha, histone deacetylase 1, and metastasis-associated protein 1 in pancreatic carcinoma: correlation with poor prognosis with possible regulation. *Pancreas*, 36, e1-9.
- MIYAMOTO, N., IZUMI, H., NOGUCHI, T., NAKAJIMA, Y., OHMIYA, Y., SHIOTA, M., KIDANI, A., TAWARA, A. & KOHNO, K. (2008) Tip60 is regulated by circadian transcription factor clock and is involved in cisplatin resistance. *Journal of Biological Chemistry*, 283, 18218-26.
- MONTGOMERY, R. L., DAVIS, C. A., POTTHOFF, M. J., HABERLAND, M., FIELITZ, J., QI, X. X., HILL, J. A., RICHARDSON, J. A. & OLSON, E. N. (2007) Histone deacetylases 1 and 2 redundantly regulate cardiac morphogenesis, growth, and contractility. *Genes & Development*, 21, 1790-1802.
- MONTI, S., TAMAYO, P., MESIROV, J. & GOLUB, T. (2003) Consensus clustering: A resampling-based method for class discovery and visualization of gene expression microarray data. *Machine Learning*, 52, 91-118.

- MOSASHVILLI, D., KAHL, P., MERTENS, C., HOLZAPFEL, S., ROGENHOFER, S., HAUSER, S., BUTTNER, R., VON RUECKER, A., MULLER, S. C. & ELLINGER, J. (2010) Global histone acetylation levels: Prognostic relevance in patients with renal cell carcinoma. *Cancer Science*, 101, 2664-2669.
- MULLER-TIDOW, C., KLEIN, H. U., HASCHER, A., ISKEN, F., TICKENBROCK, L., THOENNISSEN, N., AGRAWAL-SINGH, S., TSCHANER, P., DISSELHOFF, C., WANG, Y. P., BECKER, A., THIEDE, C., EHNINGER, G., ZUR STADT, U., KOSCHMIEDER, S., SEIDL, M., MULLER, F. U., SCHMITZ, W., SCHLENKE, P., MCCLELLAND, M., BERDEL, W. E., DUGAS, M. & SERVE, H. (2010) Profiling of histone H3 lysine 9 trimethylation levels predicts transcription factor activity and survival in acute myeloid leukemia. *Blood*, 116, 3564-3571.
- MUNSTER, P. N., TROSO-SANDOVAL, T., ROSEN, N., RIFKIND, R., MARKS, P. A. & RICHON, V. M. (2001) The Histone Deacetylase Inhibitor Suberoylanilide Hydroxamic Acid Induces Differentiation of Human Breast Cancer Cells. *Cancer Res*, 61, 8492-8497.
- MURR, R., LOIZOU, J. I., YANG, Y. G., CUENIN, C., LI, H., WANG, Z. Q. & HERCEG, Z. (2006) Histone acetylation by Trrap-Tip60 modulates loading of repair proteins and repair of DNA double-strand breaks.[see comment]. *Nature Cell Biology*, 8, 91-9.
- NATIONAL INSTITUTE FOR CLINICAL EXCELLENCE, N. (2002) Guidance on Cancer Services - Improving outcomes in breast cancer - Manual Update, London.
- NEMOTO, S., FERGUSSON, M. M. & FINKEL, T. (2004) Nutrient availability regulates SIRT1 through a forkhead-dependent pathway. *Science*, 306, 2105-2108.
- NEVE, R. M., CHIN, K., FRIDLYAND, J., YEH, J., BAEHNER, F. L., FEVR, T., CLARK, L., BAYANI, N., COPPE, J. P., TONG, F., SPEED, T., SPELLMAN, P. T., DEVRIES, S., LAPUK, A., WANG, N. J., KUO, W. L., STILWELL, J. L., PINKEL, D., ALBERTSON, D. G., WALDMAN, F. M., MCCORMICK, F., DICKSON, R. B., JOHNSON, M. D., LIPPMAN, M., ETHIER, S., GAZDAR, A. & GRAY, J. W. (2006) A collection of breast cancer cell lines for the study of functionally distinct cancer subtypes. *Cancer Cell*, 10, 515-27.
- NIELSEN, S. J., SCHNEIDER, R., BAUER, U. M., BANNISTER, A. J., MORRISON, A., O'CARROLL, D., FIRESTEIN, R., CLEARY, M., JENUWEIN, T., HERRERA, R. E. & KOUZARIDES, T. (2001) Rb targets histone H3 methylation and HP1 to promoters.[see comment]. *Nature*, 412, 561-5.
- NIELSEN, T. O., HSU, F. D., JENSEN, K., CHEANG, M., KARACA, G., HU, Z., HERNANDEZ-BOUSSARD, T., LIVASY, C., COWAN, D. & DRESSLER, L. (2004) Immunohistochemical and clinical characterization of the basal-like subtype of invasive breast carcinoma. *Clin Cancer Res*, 10, 5367 - 5374.
- NISHIOKA, K., CHUIKOV, S., SARMA, K., ERDJUMENT-BROMAGE, H., ALLIS, C. D., TEMPST, P. & REINBERG, D. (2002a) Set9, a novel histone H3 methyltransferase that facilitates transcription by precluding

- histone tail modifications required for heterochromatin formation. *Genes & Development*, 16, 479-89.
- NISHIOKA, K., RICE, J. C., SARMA, K., ERDJUMENT-BROMAGE, H., WERNER, J., WANG, Y. M., CHUIKOV, S., VALENZUELA, P., TEMPST, P., STEWARD, R., LIS, J. T., ALLIS, C. D. & REINBERG, D. (2002b) PR-Set7 is a nucleosome-specific methyltransferase that modifies lysine 20 of histone H4 and is associated with silent chromatin. *Molecular Cell*, 9, 1201-1213.
- NISHIYAMA, H., HORNIGOLD, N., DAVIES, A. M. & KNOWLES, M. A. (1999a) A sequence-ready 840-kb PAC contig spanning the candidate tumor suppressor locus DBC1 on human chromosome 9q32-q33. *Genomics*, 59, 335-8.
- NISHIYAMA, H., TAKAHASHI, T., KAKEHI, Y., HABUCHI, T. & KNOWLES, M. A. (1999b) Homozygous deletion at the 9q32-33 candidate tumor suppressor locus in primary human bladder cancer. *Genes, Chromosomes & Cancer*, 26, 171-5.
- NOSHO, K., SHIMA, K., IRAHARA, N., KURE, S., FIRESTEIN, R., BABA, Y., TOYODA, S., CHEN, L., HAZRA, A., GIOVANNUCCI, E. L., FUCHS, C. S. & OGINO, S. (2009) SIRT1 histone deacetylase expression is associated with microsatellite instability and CpG island methylator phenotype in colorectal cancer. *Modern Pathology*, 22, 922-32.
- O'CARRROLL, D., SCHERTHAN, H., PETERS, A. H., OPRAVIL, S., HAYNES, A. R., LAIBLE, G., REA, S., SCHMID, M., LEBERSORGER, A., JERRATSCH, M., SATTLER, L., MATTEI, M. G., DENNY, P., BROWN, S. D., SCHWEIZER, D. & JENUWEIN, T. (2000) Isolation and characterization of Suv39h2, a second histone H3 methyltransferase gene that displays testis-specific expression. *Molecular & Cellular Biology*, 20, 9423-33.
- O'SULLIVAN-COYNE, G., MCKENNA, S. & O'SULLIVAN, G. C. (2007) Curcumin induced G2/M checkpoint arrest in oesophageal cancer cells is a better predictor of cytotoxicity than apoptosis. *Proceedings of the American Association for Cancer Research Annual Meeting*, 48, 803.
- O'SULLIVAN-COYNE, G., O'SULLIVAN, G. C., O'DONOVAN, T. R., PIWOCKA, K. & MCKENNA, S. L. (2009) Curcumin induces apoptosis-independent death in oesophageal cancer cells. *British Journal of Cancer*, 101, 1585-1595.
- OKAZAKI, T., OGATA, E. & FUJITA, T. (2000) Histone deacetylase (HDAC) 2, but not HDAC1, is required for negative gene regulation by vitamin D: A novel mechanism of negative gene regulation By the liganded nuclear hormone receptors (NRs). *Journal of Bone and Mineral Research*, 15, 1169.
- OPPIKOFER, M., KUENG, S., MARTINO, F., SOEROES, S., HANCOCK, S. M., CHIN, J. W., FISCHLE, W. & GASSER, S. M. (2011) A dual role of H4K16 acetylation in the establishment of yeast silent chromatin. *Embo Journal*, 30, 2610-2621.
- OREN, M. (1999) Regulation of the p53 tumor suppressor protein. *J Biol Chem*, 274, 36031-4.
- OSHIMO, Y., NAKAYAMA, H., ITO, R., KITADAI, Y., YOSHIDA, K., CHAYAMA, K. & YASUI, W. (2003) Promoter methylation of cyclin D2 gene in gastric carcinoma. *Int J Oncol*, 23, 1663-70.

- OTT, J. J., ULLRICH, A., MASCARENHAS, M. & STEVENS, G. A. (2010) Global cancer incidence and mortality caused by behavior and infection. *J Public Health (Oxf)*.
- OUARARHNI, K., HADJ-SLIMANE, R., AIT-SI-ALI, S., ROBIN, P., MIETTON, F., HAREL-BELLAN, A., DIMITROV, S. & HAMICHE, A. (2006) The histone variant mH2A1.1 interferes with transcription by down-regulating PARP-1 enzymatic activity. *Genes & Development*, 20, 3324-3336.
- OZDAG, H., TESCHENDORFF, A. E., AHMED, A. A., HYLAND, S. J., BLENKIRON, C., BOBROW, L., VEERAKUMARASIVAM, A., BURTT, G., SUBKHANKULOVA, T., ARENDS, M. J., COLLINS, V. P., BOWTELL, D., KOUZARIDES, T., BRENTON, J. D. & CALDAS, C. (2006) Differential expression of selected histone modifier genes in human solid cancers. *Bmc Genomics*, 7.
- PANNETIER, M., JULIEN, E., SCHOTTA, G., TARDAT, M., SARDET, C., JENUWEIN, T. & FEIL, R. (2008) PR-SET7 and SUV4-20H regulate H4 lysine-20 methylation at imprinting control regions in the mouse. *Embo Reports*, 9, 998-1005.
- PANTEL, K. & BRAKENHOFF, R. H. (2004) Dissecting the metastatic cascade. *Nat Rev Cancer*, 4, 448-56.
- PARK, C., KIM, G. Y., KIM, G. D., CHOI, B. T., PARK, Y. M. & CHOI, Y. H. (2006) Induction of G2/M arrest and inhibition of cyclooxygenase-2 activity by curcumin in human bladder cancer T24 cells. *Oncology Reports*, 15, 1225-1231.
- PARKIN, D. M., BRAY, F., FERLAY, J. & PISANI, P. (2001) Estimating the world cancer burden: Globocan 2000. *Int J Cancer*, 94, 153-6.
- PEDERSEN, L., ZEDELER, K., HOLCK, S., SCHIODT, T. & MOURIDSEN, H. T. (1995) Medullary carcinoma of the breast. Prevalence and prognostic importance of classical risk factors in breast cancer. *Eur J Cancer*, 31A, 2289-95.
- PEHRSON, J. R., COSTANZI, C. & DHARIA, C. (1997) Developmental and tissue expression patterns of histone MacroH2A1 subtypes. *Journal of Cellular Biochemistry*, 65, 107-113.
- PEHRSON, J. R. & FRIED, V. A. (1992) MACROH2A, A CORE HISTONE CONTAINING A LARGE NONHISTONE REGION. *Science*, 257, 1398-1400.
- PEI, H., ZHANG, L., LUO, K., QIN, Y., CHESI, M., FEI, F., BERGSAGEL, P. L., WANG, L., YOU, Z. & LOU, Z. (2011) MMSET regulates histone H4K20 methylation and 53BP1 accumulation at DNA damage sites. *Nature*, 470, 124-U144.
- PEROU, C. M., SORLIE, T., EISEN, M. B., VAN DE RIJN, M., JEFFREY, S. S., REES, C. A., POLLACK, J. R., ROSS, D. T., JOHNSEN, H., AKSLEN, L. A., FLUGE, O., PERGAMENSCHIKOV, A., WILLIAMS, C., ZHU, S. X., LONNING, P. E., BORRESEN-DALE, A. L., BROWN, P. O. & BOTSTEIN, D. (2000) Molecular portraits of human breast tumours. *Nature*, 406, 747-52.
- PETERSEN, O. W., GUDJONSSON, T., VILLADSEN, R., BISSELL, M. J. & RONNOV-JESSEN, L. (2003) Epithelial progenitor cell lines as models of normal breast morphogenesis and neoplasia. *Cell Prolif*, 36 Suppl 1, 33-44.

- PFISTER, S., REA, S., TAIPALE, M., MENDRZYK, F., STRaub, B., ITTRICH, C., THUERIGEN, O., SINN, H. P., AKHTAR, A. & LICHTER, P. (2008) The histone acetyltransferase hMOF is frequently downregulated in primary breast carcinoma and medulloblastoma and constitutes a biomarker for clinical outcome in medulloblastoma. *International Journal of Cancer*, 122, 1207-1213.
- PIJNAPPEL, R. S. A. R. (2008) Breast Calcifications - Differential diagnosis and BIRADS.
- PILLUS, L. (2008) MYSTs mark chromatin for chromosomal functions. *Current Opinion in Cell Biology*, 20, 326-33.
- PLACEK, B. J., HARRISON, L. N., VILLERS, B. M. & GLOSS, L. M. (2005) The H2A.Z/H2B dimer is unstable compared to the dimer containing the major H2A isoform. *Protein Science*, 14, 514-22.
- POGRIBNY, I. P., ROSS, S. A., TRYNDYAK, V. P., POGRIBNA, M., POIRIER, L. A. & KARPINETS, T. V. (2006) Histone H3 lysine 9 and H4 lysine 20 trimethylation and the expression of Suv4-2Oh2 and Suv-39h1 histone methyltransferases in hepatocarcinogenesis induced by methyl deficiency in rats. *Carcinogenesis*, 27, 1180-1186.
- POGRIBNY, I. P., TRYNDYAK, V. P., MUSKHELISHVILI, L., RUSYN, I. & ROSS, S. A. (2007) Methyl deficiency, alterations in global histone modifications, and carcinogenesis. *Journal of Nutrition*, 137, 216S-222S.
- POLJAKOVA, J., HREBACKOVA, J., HRABETA, J., ECKSCHLAGER, T., FREI, E. & STIBOROVA, M. (2009) Ellipticine combined with histone deacetylase inhibitors, valproic acid and trichostatin A, is an effective DNA damage strategy in neuroblastoma cells. *Febs Journal*, 276, 336-336.
- POLYAK, K. (2008) Is Breast Tumor Progression Really Linear? *Clin Cancer Res*, 14, 339-341.
- PRITCHARD, K. I., SHEPHERD, L. E., O'MALLEY, F. P., ANDRULIS, I. L., TU, D. S., BRAMWELL, V. H., LEVINE, M. N. & NATL CANC INST CANADA CLIN, T. (2006) HER2 and responsiveness of breast cancer to adjuvant chemotherapy. *New England Journal of Medicine*, 354, 2103-2111.
- PRUITT, K., ZINN, R. L., OHM, J. E., MCGARVEY, K. M., KANG, S. H., WATKINS, D. N., HERMAN, J. G. & BAYLIN, S. B. (2006) Inhibition of SIRT1 reactivates silenced cancer genes without loss of promoter DNA hypermethylation. *PLoS Genet*, 2, e40.
- QUINN, M. & ALLEN, E. (1995) Changes in incidence of and mortality from breast cancer in England and Wales since introduction of screening. United Kingdom Association of Cancer Registries. *BMJ*, 311, 1391-5.
- RAHMAN, S. & ISLAM, R. (2011) Mammalian Sirt1: insights on its biological functions. *Cell Communication and Signaling*, 9.
- RAISNER, R. M., HARTLEY, P. D., MENEGHINI, M. D., BAO, M. Z., LIU, C. L., SCHREIBER, S. L., RANDO, O. J. & MADHANI, H. D. (2005) Histone variant H2A.Z marks the 5' ends of both active and inactive genes in euchromatin.[erratum appears in Cell. 2008 Jul 11;134(1):188]. *Cell*, 123, 233-48.
- RAISNER, R. M. & MADHANI, H. D. (2008) Genomewide screen for negative regulators of sirtuin activity in *Saccharomyces cerevisiae* reveals 40 loci and links to metabolism. *Genetics*, 179, 1933-44.

- RAKHA, E. A., EL-SAYED, M. E., LEE, A. H., ELSTON, C. W., GRAINGE, M. J., HODI, Z., BLAMEY, R. W. & ELLIS, I. O. (2008) Prognostic significance of Nottingham histologic grade in invasive breast carcinoma. *J Clin Oncol*, 26, 3153-8.
- RAKHA, E. A., PUTTI, T. C., ABD EL-REHIM, D. M., PAISH, C., GREEN, A. R., POWE, D. G., LEE, A. H., ROBERTSON, J. F. & ELLIS, I. O. (2006) Morphological and immunophenotypic analysis of breast carcinomas with basal and myoepithelial differentiation. *J Pathol*, 208, 495-506.
- RANGASAMY, D., BERVEN, L., RIDGWAY, P. & TREMETHICK, D. J. (2003) Pericentric heterochromatin becomes enriched with H2A.Z during early mammalian development. *EMBO Journal*, 22, 1599-607.
- RAVINDRAN, J., PRASAD, S. & AGGARWAL, B. B. (2009) Curcumin and cancer cells: how many ways can curry kill tumor cells selectively? *AAPS J*, 11, 495-510.
- REA, S., EISENHABER, F., O'CARRROLL, N., STRAHL, B. D., SUN, Z. W., SCHMID, M., OPRAVIL, S., MECHTLER, K., PONTING, C. P., ALLIS, C. D. & JENUWEIN, T. (2000) Regulation of chromatin structure by site-specific histone H3 methyltransferases. *Nature*, 406, 593-599.
- REA, S., XOURI, G. & AKHTAR, A. (2007) Males absent on the first (MOF): from flies to humans. *Oncogene*, 26, 5385-94.
- REDON, C., PILCH, D., ROGAKOU, E., SEDELNIKOVA, O., NEWROCK, K. & BONNER, W. (2002) Histone H2A variants H2AX and H2AZ. *Current Opinion in Genetics & Development*, 12, 162-169.
- RENTHAL, W., CARLE, T. L., MAZE, I., COVINGTON, H. E., 3RD, TRUONG, H. T., ALIBHAI, I., KUMAR, A., MONTGOMERY, R. L., OLSON, E. N. & NESTLER, E. J. (2008) Delta FosB mediates epigenetic desensitization of the c-fos gene after chronic amphetamine exposure. *Journal of Neuroscience*, 28, 7344-9.
- RENZ, D. M., BALTZER, P. A., BOTTCHER, J., THAHER, F., GAJDA, M., CAMARA, O., RUNNEBAUM, I. B. & KAISER, W. A. (2008) Magnetic resonance imaging of inflammatory breast carcinoma and acute mastitis. A comparative study. *Eur Radiol*.
- REYNOIRD, N., ROUSSEAU, S. & KHOCHBIN, S. (2010) Epigenetic perturbations and cancer: innovative therapeutic strategies against cancer. *Bulletin Du Cancer*, 97, 1265-1274.
- RICHARDS, M. A., SMITH, P., RAMIREZ, A. J., FENTIMAN, I. S. & RUBENS, R. D. (1999) The influence on survival of delay in the presentation and treatment of symptomatic breast cancer. *British Journal of Cancer*, 79, 858-64.
- RIMM, D. L. (2001) Impact of microarray technologies on cytopathology - Overview of technologies and commentary on current and future implications for pathologists and cytopathologists. *Acta Cytologica*, 45, 111-114.
- RODRIGUEZ, A., DIEZ, C., CAAMANO, J. N., DE FRUTOS, C., ROYO, L. J., MUÑOZ, M., IKEDA, S., FACAL, N., ALVAREZ-VIEJO, M. & GOMEZ, E. (2007) Retinoid receptor-specific agonists regulate bovine in vitro early embryonic development, differentiation and expression of genes related to cell cycle arrest and apoptosis. *Theriogenology*, 68, 1118-27.

- RODRIGUEZ, M. S., DESTERRO, J. M. P., LAIN, S., LANE, D. P. & HAY, R. T. (2000) Multiple C-terminal lysine residues target p53 for ubiquitin-proteasome-mediated degradation. *Molecular and Cellular Biology*, 20, 8458-8467.
- ROELFSEMA, J. H. & PETERS, D. J. (2007) Rubinstein-Taybi syndrome: clinical and molecular overview. *Expert Rev Mol Med*, 9, 1-16.
- ROGEL, A., POPLIKER, M., WEBB, C. G. & OREN, M. (1985) p53 cellular tumor antigen: analysis of mRNA levels in normal adult tissues, embryos, and tumors. *Mol. Cell. Biol.*, 5, 2851-2855.
- RONG, Y. S. (2008) Loss of the histone variant H2A.Z restores capping to checkpoint-defective telomeres in Drosophila. *Genetics*, 180, 1869-75.
- ROSAI, J. (2004) Rosai and Ackerman's Surgical Pathology. 2.
- ROSSETTO, D., TRUMAN, A. W., KRON, S. J. & COTE, J. (2010) Epigenetic Modifications in Double-Strand Break DNA Damage Signaling and Repair. *Clinical Cancer Research*, 16, 4543-4552.
- ROTH, S. Y., DENU, J. M. & ALLIS, C. D. (2001) Histone acetyltransferases. *Annual Review of Biochemistry*, 70, 81-120.
- RUDEK, M. A., ZHAO, M., HE, P., HARTKE, C., GILBERT, J., GORE, S. D., CARDUCCI, M. A. & BAKER, S. D. (2005) Pharmacokinetics of 5-azacitidine administered with phenylbutyrate in patients with refractory solid tumors or hematologic malignancies. *J Clin Oncol*, 23, 3906-11.
- RUHL, D. D., JIN, J., CAI, Y., SWANSON, S., FLORENS, L., WASHBURN, M. P., CONAWAY, R. C., CONAWAY, J. W. & CHRIVIA, J. C. (2006) Purification of a human SRCAP complex that remodels chromatin by incorporating the histone variant H2A.Z into nucleosomes. *Biochemistry*, 45, 5671-7.
- RUTHENBURG, A. J., ALLIS, C. D. & WYSOCKA, J. (2007) Methylation of lysine 4 on histone H3: Intricacy of writing and reading a single epigenetic mark. *Molecular Cell*, 25, 15-30.
- RYAN, C. M., KINDLE, K. B., COLLINS, H. M. & HEERY, D. M. (2010) SUMOylation regulates the nuclear mobility of CREB binding protein and its association with nuclear bodies in live cells. *Biochemical and Biophysical Research Communications*, 391, 1136-1141.
- SAFER, B. (1989) NOMENCLATURE OF INITIATION, ELONGATION AND TERMINATION FACTORS FOR TRANSLATION IN EUKARYOTES - RECOMMENDATIONS 1988. *European Journal of Biochemistry*, 186, 1-3.
- SAHU, R. P., BATRA, S. & SRIVASTAVA, S. K. (2009) Activation of ATM/Chk1 by curcumin causes cell cycle arrest and apoptosis in human pancreatic cancer cells. *British Journal of Cancer*, 100, 1425-1433.
- SAINSBURY, J. R., ANDERSON, T. J. & MORGAN, D. A. (2000) ABC of breast diseases: breast cancer
British Medical Journal, 321
745-750.
- SAKAGUCHI, A. & STEWARD, R. (2007) Aberrant monomethylation of histone H4 lysine 20 activates the DNA damage checkpoint in Drosophila melanogaster. *Journal of Cell Biology*, 176, 155-162.
- SANDERS, S. L., PORTOSO, M., MATA, J., BAHLER, J., ALLSHIRE, R. C. & KOUZARIDES, T. (2004) Methylation of histone H4 lysine 20 controls recruitment of Crb2 to sites of DNA damage. *Cell*, 119, 603-614.

- SASAKI, K., YAMAGATA, T. & MITANI, K. (2008) Histone deacetylase inhibitors trichostatin A and valproic acid circumvent apoptosis in human leukemic cells expressing the RUNX1 chimera. *Cancer Science*, 99, 414-422.
- SCHOTTA, G., EBERT, A., KRAUSS, V., FISCHER, A., HOFFMANN, J., REA, S., JENUWEIN, T., DORN, R. & REUTER, G. (2002) Central role of Drosophila SU(VAR)3-9 in histone H3-K9 methylation and heterochromatic gene silencing. *EMBO Journal*, 21, 1121-31.
- SCHOTTA, G., LACHNER, M., SARMA, K., EBERT, A., SENGUPTA, R., REUTER, G., REINBERG, D. & JENUWEIN, T. (2004) A silencing pathway to induce H3-K9 and H4-K20 trimethylation at constitutive heterochromatin. *Genes Dev*, 18, 1251-62.
- SCHOTTA, G., SENGUPTA, R., KUBICEK, S., MALIN, S., KAUER, M., CALLEN, E., CELESTE, A., PAGANI, M., OPRAVIL, S., DE LA ROSA-VELAZQUEZ, I. A., ESPEJO, A., BEDFORD, M. T., NUSSENZWEIG, A., BUSSLINGER, M. & JENUWEIN, T. (2008) A chromatin-wide transition to H4K20 monomethylation impairs genome integrity and programmed DNA rearrangements in the mouse. *Genes & Development*, 22, 2048-61.
- SCHWARZ, D. S., HUTVAGNER, G., HALEY, B. & ZAMORE, P. D. (2002) Evidence that siRNAs function as guides, not primers, in the Drosophila and human RNAi pathways. *Mol Cell*, 10, 537-48.
- SELIGSON, D. B., HORVATH, S., MCBRIAN, M. A., MAH, V., YU, H., TZE, S., WANG, Q., CHIA, D., GOODGLICK, L. & KURDISTANI, S. K. (2009) Global Levels of Histone Modifications Predict Prognosis in Different Cancers. *Am J Pathol*, 174, 1619-1628.
- SELIGSON, D. B., HORVATH, S., SHI, T., YU, H., TZE, S., GRUNSTEIN, M. & KURDISTANI, S. K. (2005) Global histone modification patterns predict risk of prostate cancer recurrence. *Nature*, 435, 1262-6.
- SELVI, B. R., MOHANKRISHNA, D. V., OSTWAL, Y. B. & KUNDU, T. K. (2010) Small molecule modulators of histone acetylation and methylation: A disease perspective. *Biochimica Et Biophysica Acta-Gene Regulatory Mechanisms*, 1799, 810-828.
- SHAO, Z. M., SHEN, Z. Z., LIU, C. H., SARTIPPOUR, M. R., GO, V. L., HEBER, D. & NGUYEN, M. (2002) Curcumin exerts multiple suppressive effects on human breast carcinoma cells. *International Journal of Cancer*, 98, 234-240.
- SHEPPARD, D. G., WHITMAN, G. J., FORNAGE, B. D., STELLING, C. B., HUYNH, P. T. & SAHIN, A. A. (2000) Tubular Carcinoma of the Breast: Mammographic and Sonographic Features. *Am. J. Roentgenol.*, 174, 253-257.
- SHI, D., POP, M. S., KULIKOV, R., LOVE, I. M., KUNG, A. L. & GROSSMAN, S. R. (2009) CBP and p300 are cytoplasmic E4 polyubiquitin ligases for p53. *Proc Natl Acad Sci U S A*, 106, 16275-80.
- SHI, X., KACHIRSKAIA, I., YAMAGUCHI, H., WEST, L. E., WEN, H., WANG, E. W., DUTTA, S., APPELLA, E. & GOZANI, O. (2007) Modulation of p53 Function by SET8-Mediated Methylation at Lysine 382. *Molecular Cell*, 27, 636-646.

- SHIA, W. J., LI, B. & WORKMAN, J. L. (2006) SAS-mediated acetylation of histone H4 Lys 16 is required for H2A.Z incorporation at subtelomeric regions in *Saccharomyces cerevisiae*. *Genes & Development*, 20, 2507-12.
- SHISHODIA, S., AMIN, H. M., LAI, R. & AGGARWAL, B. B. (2005) Curcumin (diferuloylmethane) inhibits constitutive NF-kappa B activation, induces G1/S arrest, suppresses proliferation, and induces apoptosis in mantle cell lymphoma. *Biochemical Pharmacology*, 70, 700-713.
- SHOGREN-KNAAK, M., ISHII, H., SUN, J. M., PAZIN, M. J., DAVIE, J. R. & PETERSON, C. L. (2006) Histone H4-K16 acetylation controls chromatin structure and protein interactions. *Science*, 311, 844-7.
- SIMS, R. J. & REINBERG, D. (2008) Is there a code embedded in proteins that is based on post-translational modifications? *Nat Rev Mol Cell Biol*, 9, 815-820.
- SINGLETARY, S. E., ALLRED, C., ASHLEY, P., BASSETT, L. W., BERRY, D., BLAND, K. I., BORGEN, P. I., CLARK, G., EDGE, S. B., HAYES, D. F., HUGHES, L. L., HUTTER, R. V., MORROW, M., PAGE, D. L., RECHT, A., THERIAULT, R. L., THOR, A., WEAVER, D. L., WIEAND, H. S. & GREENE, F. L. (2002) Revision of the American Joint Committee on Cancer staging system for breast cancer. *Journal of Clinical Oncology*, 20, 3628-36.
- SNOWDEN, A. W., GREGORY, P. D., CASE, C. C. & PABO, C. O. (2002) Gene-specific targeting of H3K9 methylation is sufficient for initiating repression in vivo. *Curr Biol*, 12, 2159-66.
- SOMASUNDARAM, S., EDMUND, N. A., MOORE, D. T., SMALL, G. W., SHI, Y. Y. & ORLOWSKI, R. Z. (2002) Dietary Curcumin Inhibits Chemotherapy-induced Apoptosis in Models of Human Breast Cancer. *Cancer Res*, 62, 3868-3875.
- SORIA, D., GARIBALDI, J. M., AMBROGI, F., GREEN, A. R., POWE, D., RAKHA, E., MACMILLAN, R. D., BLAMEY, R. W., BALL, G., LISBOA, P. J., ETCHELLS, T. A., BORACCHI, P., BIGANZOLI, E. & ELLIS, I. O. (2010) A methodology to identify consensus classes from clustering algorithms applied to immunohistochemical data from breast cancer patients. *Comput Biol Med*, 40, 318-30.
- SORLIE, T., PEROU, C. M., TIBSHIRANI, R., AAS, T., GEISLER, S., JOHNSEN, H., HASTIE, T., EISEN, M. B., VAN DE RIJN, M., JEFFREY, S. S., THORSEN, T., QUIST, H., MATESE, J. C., BROWN, P. O., BOTSTEIN, D., EYSTEIN LONNING, P. & BORRESEN-DALE, A. L. (2001) Gene expression patterns of breast carcinomas distinguish tumor subclasses with clinical implications. *Proc Natl Acad Sci U S A*, 98, 10869-74.
- SORLIE, T., TIBSHIRANI, R., PARKER, J., HASTIE, T., MARRON, J. S., NOBEL, A., DENG, S., JOHNSEN, H., PESICH, R., GEISLER, S., DEMETER, J., PEROU, C. M., LONNING, P. E., BROWN, P. O., BORRESEN-DALE, A. L. & BOTSTEIN, D. (2003) Repeated observation of breast tumor subtypes in independent gene expression data sets. *Proc Natl Acad Sci U S A*, 100, 8418-23.
- SOTIRIOU, C., NEO, S. Y., MCSHANE, L. M., KORN, E. L., LONG, P. M., JAZAERI, A., MARTIAT, P., FOX, S. B., HARRIS, A. L. & LIU, E. T. (2003) Breast cancer classification and prognosis based on gene

- expression profiles from a population-based study. *Proceedings of the National Academy of Sciences of the United States of America*, 100, 10393-8.
- SOUZA, P. P., VOLKEL, P., TRINEL, D., VANDAMME, J., ROSNOBLET, C., HELIOT, L. & ANGRAND, P. O. (2009) The histone methyltransferase SUV420H2 and Heterochromatin Proteins HP1 interact but show different dynamic behaviours. *BMC Cell Biology*, 10, 41.
- SQUATRITO, M., GORRINI, C. & AMATI, B. (2006) Tip60 in DNA damage response and growth control: many tricks in one HAT. *Trends in Cell Biology*, 16, 433-42.
- STANGE, D. E., RADLWIMMER, B., SCHUBERT, F., TRAUB, F., PICH, A., TOEDT, G., MENDRZYK, F., LEHMANN, U., EILS, R., KREIPE, H. & LICHTER, P. (2006) High-resolution genomic profiling reveals association of chromosomal aberrations on 1q and 16p with histologic and genetic subgroups of invasive breast cancer. *Clinical Cancer Research*, 12, 345-352.
- STANTE, M., MINOPOLI, G., PASSARO, F., RAIA, M., VECCHIO, L. D. & RUSSO, T. (2009) Fe65 is required for Tip60-directed histone H4 acetylation at DNA strand breaks. *Proceedings of the National Academy of Sciences of the United States of America*, 106, 5093-8.
- STERNER, D. E. & BERGER, S. L. (2000) Acetylation of histones and transcription-related factors. *Microbiol Mol Biol Rev*, 64, 435-59.
- STROUHAL, E. & NEMECKOVA, A. (2009) Palaeopathological diagnosis after 2500 years. The case of Imakhetkherresnet, sister of priest Iufaa. *Prague Med Rep*, 110, 102-13.
- SUN, Y., JIANG, X., CHEN, S., FERNANDES, N. & PRICE, B. D. (2005) A role for the Tip60 histone acetyltransferase in the acetylation and activation of ATM. *Proceedings of the National Academy of Sciences of the United States of America*, 102, 13182-7.
- SUN, Y., JIANG, X. & PRICE, B. D. (2011) Tip60: connecting chromatin to DNA damage signaling. *Cell Cycle*, 9, 930-6.
- SUN, Y. L., JIANG, X. F., XU, Y., AYRAPETOV, M. K., MOREAU, L. A., WHETSTINE, J. R. & PRICE, B. D. (2009) Histone H3 methylation links DNA damage detection to activation of the tumour suppressor Tip60. *Nature Cell Biology*, 11, 1376-U273.
- SUNG, J. Y., KIM, R., KIM, J. E. & LEE, J. (2010) Balance between SIRT1 and DBC1 expression is lost in breast cancer. *Cancer Science*, 101, 1738-1744.
- SUTCLIFFE, E. L., PARISH, I. A., HE, Y. Q., JUELICH, T., TIERNEY, M. L., RANGASAMY, D., MILBURN, P. J., PARISH, C. R., TREMETHICK, D. J. & RAO, S. (2009) Dynamic histone variant exchange accompanies gene induction in T cells. *Molecular & Cellular Biology*, 29, 1972-86.
- SVOTELIS, A., GEVRY, N. & GAUDREAU, L. (2009a) Regulation of gene expression and cellular proliferation by histone H2A.Z. *Biochemistry & Cell Biology*, 87, 179-88.
- SVOTELIS, A., GEVRY, N., GRONDIN, G. & GAUDREAU, L. (2009b) H2A.Z overexpression promotes cellular proliferation of breast cancer cells. *Cell Cycle*, 9, 364-70.

- SVOTELIS, A., GEVRY, N., GRONDIN, G. & GAUDREAU, L. (2010) H2A.Z overexpression promotes cellular proliferation of breast cancer cells. *Cell Cycle*, 9, 364-370.
- SYEED, N., HUSAIN, S. A., SAMEER, A. S., CHOWDHRI, N. A. & SIDDIQI, M. A. (2010) Mutational and promoter hypermethylation status of FHIT gene in breast cancer patients of Kashmir. *Mutat Res.*
- SYKES, S. M., MELLERT, H. S., HOLBERT, M. A., LI, K., MARMORSTEIN, R., LANE, W. S. & MCMAHON, S. B. (2006) Acetylation of the p53 DNA-binding domain regulates apoptosis induction. *Molecular Cell*, 24, 841-851.
- TACHIBANA, M., UEDA, J., FUKUDA, M., TAKEDA, N., OHTA, T., IWANARI, H., SAKIHAMA, T., KODAMA, T., HAMAKUBO, T. & SHINKAI, Y. (2005) Histone methyltransferases G9a and GLP form heteromeric complexes and are both crucial for methylation of euchromatin at H3-K9. *Genes Dev.*, 19, 815-826.
- TAIPALE, M., REA, S., RICHTER, K., VILAR, A., LICHTER, P., IMHOFF, A. & AKHTAR, A. (2005) hMOF Histone Acetyltransferase Is Required for Histone H4 Lysine 16 Acetylation in Mammalian Cells. *Mol. Cell. Biol.*, 25, 6798-6810.
- TAIRA, N., NIHIRA, K., YAMAGUCHI, T., MIKI, Y. & YOSHIDA, K. (2007) DYRK2 is targeted to the nucleus and controls p53 via Ser46 phosphorylation in the apoptotic response to DNA damage. *Mol Cell*, 25, 725-38.
- TANG, Y., LUO, J., ZHANG, W. & GU, W. (2006a) Tip60-dependent acetylation of p53 modulates the decision between cell-cycle arrest and apoptosis.[see comment]. *Molecular Cell*, 24, 827-39.
- TANG, Y., LUO, J. Y., ZHANG, W. Z. & GU, W. (2006b) Tip60-dependent acetylation of p53 modulates the decision between cell-cycle arrest and apoptosis. *Molecular Cell*, 24, 827-839.
- TANG, Y., ZHAO, W. H., CHEN, Y., ZHAO, Y. M. & GU, W. (2008) Acetylation is indispensable for p53 activation (vol 133, pg 612, 2008). *Cell*, 133, 1290-1290.
- TANYI, J., TORY, K., BÁNKFALVI, A., SHRÖDER, W., RATH, W. & FÜZESI, L. (1999) Analysis of p53 Mutation and Cyclin D1 Expression in Breast Tumors. *Pathology and Oncology Research*, 5, 90-94.
- THAMBIRAJAH, A. A., LI, A., ISHIBASHI, T. & AUSIO, J. (2009) New developments in post-translational modifications and functions of histone H2A variants. *Biochemistry & Cell Biology*, 87, 7-17.
- THOMAS, T., DIXON, M. P., KUEH, A. J. & VOSS, A. K. (2008) Mof (MYST1 or KAT8) is essential for progression of embryonic development past the blastocyst stage and required for normal chromatin architecture. *Molecular & Cellular Biology*, 28, 5093-105.
- THOMAS, T. & VOSS, A. K. (2007) The diverse biological roles of MYST histone acetyltransferase family proteins. *Cell Cycle*, 6, 696-704.
- TJEERTES, J. V., MILLER, K. M. & JACKSON, S. P. (2009) Screen for DNA-damage-responsive histone modifications identifies H3K9Ac and H3K56Ac in human cells. *EMBO J*, 28, 1878-89.
- TOLEDO, F. & WAHL, G. M. (2007) MDM2 and MDM4: p53 regulators as targets in anticancer therapy. *Int J Biochem Cell Biol*, 39, 1476-82.

- TOT, T. (2010) The origins of early breast carcinoma. *Semin Diagn Pathol*, 27, 62-8.
- TRAUERNICHT, A. M., KIM, S. J., KIM, N. H. & BOYER, T. G. (2007) Modulation of estrogen receptor alpha protein level and survival function by DBC-1. *Molecular Endocrinology*, 21, 1526-1536.
- TROKE, P. J. F., KINDLE, K. B., COLLINS, H. M. & HEERY, D. M. (2006) MOZ fusion proteins in acute myeloid leukaemia. IN ROBERTS, S. G. E. W. R. O. J. W. R. J. (Ed.) *Transcription*.
- TRYNDYAK, V. P., KOVALCHUK, O. & POGRIBNY, I. P. (2006) Loss of DNA methylation and histone H4 lysine 20 trimethylation in human breast cancer cells is associated with aberrant expression of DNA methyltransferase 1, Suv4-20h2 histone methyltransferase and methyl-binding proteins. *Cancer Biol Ther*, 5, 65-70.
- TSAPROUNI, L. G., ITO, K., POWELL, J. J., ADCOCK, I. M. & PUNCHARD, N. (2011) Differential patterns of histone acetylation in inflammatory bowel diseases. *Journal of Inflammation-London*, 8.
- TSENG, R. C., LEE, C. C., HSU, H. S., TZAO, C. & WANG, Y. C. (2009) Distinct HIC1-SIRT1-p53 Loop Dereulation in Lung Squamous Carcinoma and Adenocarcinoma Patients. *Neoplasia*, 11, 763-U65.
- TSEREL, L., KOLDE, R., REBANE, A., KISAND, K., ORG, T., PETERSON, H., VILO, J. & PETERSON, P. (2010) Genome-wide promoter analysis of histone modifications in human monocyte-derived antigen presenting cells. *BMC Genomics*, 11, 642.
- TUSCHL, T. & BORKHARDT, A. (2002) Small interfering RNAs: a revolutionary tool for the analysis of gene function and gene therapy. *Molecular Interventions*, 2, 158-67.
- TYTECA, S., VANDROMME, M., LEGUBE, G., CHEVILLARD-BRIET, M. & TROUCHE, D. (2006) Tip60 and p400 are both required for UV-induced apoptosis but play antagonistic roles in cell cycle progression. *EMBO Journal*, 25, 1680-9.
- TZAO, C., TUNG, H.-J., JIN, J.-S., SUN, G.-H., HSU, H.-S., CHEN, B.-H., YU, C.-P. & LEE, S.-C. (2008) Prognostic significance of global histone modifications in resected squamous cell carcinoma of the esophagus. *Mod Pathol*, 22, 252-260.
- VAN 'T VEER, L. J., DAI, H., VAN DE VIJVER, M. J., HE, Y. D., HART, A. A., MAO, M., PETERSE, H. L., VAN DER KOY, K., MARTON, M. J., WITTEVEEN, A. T., SCHREIBER, G. J., KERKHOVEN, R. M., ROBERTS, C., LINSLEY, P. S., BERNARDS, R. & FRIEND, S. H. (2002) Gene expression profiling predicts clinical outcome of breast cancer. *Nature*, 415, 530-6.
- VAN ATTIKUM, H. & GASSEN, S. M. (2009) Crosstalk between histone modifications during the DNA damage response. *Trends in Cell Biology*, 19, 207-17.
- VAN DEN BROECK, A., BRAMBILLA, E., MORO-SIBILOT, D., LANTUEJOUL, S., BRAMBILLA, C., EYMIN, B., KHOCHBIN, S. & GAZZERI, S. (2008) Loss of Histone H4K20 Trimethylation Occurs in Preneoplasia and Influences Prognosis of Non-Small Cell Lung Cancer. *Clinical Cancer Research*, 14, 7237-7245.
- VAQUERO, A., SCHER, M., ERDJUMENT-BROMAGE, H., TEMPST, P., SERRANO, L. & REINBERG, D. (2007) SIRT1 regulates the histone

- methyl-transferase SUV39H1 during heterochromatin formation. *Nature*, 450, 440-444.
- VAQUERO, A., SCHER, M., LEE, D., ERDJUMENT-BROMAGE, H., TEMPST, P. & REINBERG, D. (2004) Human SirT1 interacts with histone H1 and promotes formation of facultative heterochromatin. *Mol Cell*, 16, 93-105.
- VAQUERO, A., SCHER, M. B., LEE, D. H., SUTTON, A., CHENG, H. L., ALT, F. W., SERRANO, L., STERNGLANZ, R. & REINBERG, D. (2006) SirT2 is a histone deacetylase with preference for histone H4 Lys 16 during mitosis. *Genes Dev*, 20, 1256-61.
- VEMPATI, R. K., JAYANI, R. S., NOTANI, D., SENGUPTA, A., GALANDE, S. & HALDAR, D. (2010) p300-mediated Acetylation of Histone H3 Lysine 56 Functions in DNA Damage Response in Mammals. *Journal of Biological Chemistry*, 285, 28553-28564.
- VENKATASUBRAHMANYAM, S., HWANG, W. W., MENEGHINI, M. D., TONG, A. H. & MADHANI, H. D. (2007) Genome-wide, as opposed to local, antisilencing is mediated redundantly by the euchromatic factors Set1 and H2A.Z. *Proceedings of the National Academy of Sciences of the United States of America*, 104, 16609-14.
- VERGER, P., CHAMBOLLE, M., BABAYOU, P., LE BRETON, S. & VOLATIER, J. L. (1998) Estimation of the distribution of the maximum theoretical intake for ten additives in France. *Food Addit Contam*, 15, 759-66.
- VOSS, A. K., COLLIN, C., DIXON, M. P. & THOMAS, T. (2009) Moz and Retinoic Acid Coordinately Regulate H3K9 Acetylation, Hox Gene Expression, and Segment Identity. *Developmental Cell*, 17, 674-686.
- VOUSDEN, K. H. & LANE, D. P. (2007) p53 in health and disease. *Nat Rev Mol Cell Biol*, 8, 275-283.
- WAKO, T. & FUKUI, K. (2007) Beyond genome sequences: Epigenetics and the chromatin state. *Proceedings of the National Academy of Sciences India Section B-Biological Sciences*, 77, 73-84.
- WANG, H., CAO, R., XIA, L., ERDJUMENT-BROMAGE, H., BORCHERS, C., TEMPST, P. & ZHANG, Y. (2001) Purification and functional characterization of a histone H3-lysine 4-specific methyltransferase. *Molecular Cell*, 8, 1207-17.
- WANG, Y., LIANG, Y. & VANHOUTTE, P. M. (2011) SIRT1 and AMPK in regulating mammalian senescence: A critical review and a working model. *Febs Letters*, 585, 986-994.
- WANG, Y. L., ZHANG, H., LI, N., WANG, X. H., HAO, J. F. & ZHAO, W. P. (2009a) Potential mechanisms involved in resistant phenotype of MCF-7 breast carcinoma cells to ionizing radiation induced apoptosis. *Nuclear Instruments & Methods in Physics Research Section B-Beam Interactions with Materials and Atoms*, 267, 1001-1006.
- WANG, Z. B., ZANG, C. Z., CUI, K. R., SCHONES, D. E., BARSKI, A., PENG, W. Q. & ZHAO, K. J. (2009b) Genome-wide Mapping of HATs and HDACs Reveals Distinct Functions in Active and Inactive Genes. *Cell*, 138, 1019-1031.
- WATSON, J. D. & CRICK, F. H. C. (1953a) GENETICAL IMPLICATIONS OF THE STRUCTURE OF DEOXYRIBONUCLEIC ACID. *Nature*, 171, 964-967.

- WATSON, J. D. & CRICK, F. H. C. (1953b) MOLECULAR STRUCTURE OF NUCLEIC ACIDS - A STRUCTURE FOR DEOXYRIBOSE NUCLEIC ACID. *Nature*, 171, 737-738.
- WEICHERT, W. (2009) HDAC expression and clinical prognosis in human malignancies. *Cancer Letters*, 280, 168-176.
- WEICHERT, W., RÄSKE, A., GEKELER, V., BECKERS, T., EBERT, M. P., PROSS, M., DIETEL, M., DENKERT, C. & RÄCKEN, C. (2008a) Association of patterns of class I histone deacetylase expression with patient prognosis in gastric cancer: a retrospective analysis. *The Lancet Oncology*, 9, 139-148.
- WEICHERT, W., RÄSKE, A., NIESPOREK, S., NOSKE, A., BUCKENDAHL, A.-C., DIETEL, M., GEKELER, V., BOEHM, M., BECKERS, T. & DENKERT, C. (2008b) Class I Histone Deacetylase Expression Has Independent Prognostic Impact in Human Colorectal Cancer: Specific Role of Class I Histone Deacetylases In vitro and In vivo. *Clinical Cancer Research*, 14, 1669-1677.
- WEICHERT, W., ROSKE, A., GEKELER, V., BECKERS, T., STEPHAN, C., JUNG, K., FRITZSCHE, F. R., NIESPOREK, S., DENKERT, C., DIETEL, M. & KRISTIANSEN, G. (2008c) Histone deacetylases 1, 2 and 3 are highly expressed in prostate cancer and HDAC2 expression is associated with shorter PSA relapse time after radical prostatectomy. *Br J Cancer*, 98, 604-610.
- WEIGELT, B., PETERSE, J. L. & VAN 'T VEER, L. J. (2005) Breast cancer metastasis: markers and models. *Nat Rev Cancer*, 5, 591-602.
- WEIR, N. M., SELVENDIRAN, K., KUTALA, V. K., TONG, L. Y., VISHWANATH, S., RAJARAM, M., TRIDANDAPANI, S., ANANT, S. & KUPPUSAMY, P. (2007) Curcumin induces G2/M arrest and apoptosis in cisplatin-resistant human ovarian cancer cells by modulating Akt and p38 MAPK. *Cancer Biology & Therapy*, 6, 178-184.
- WESTLAKE S, C. N. (2008) Cancer incidence and mortality: trends in the United Kingdom and constituent countries, 1993 to 2004. In: Health Statistics Quarterly No 38.
- WIENCKE, J. K., ZHENG, S., MORRISON, Z. & YEH, R. F. (2008) Differentially expressed genes are marked by histone 3 lysine 9 trimethylation in human cancer cells. *Oncogene*, 27, 2412-21.
- WILEY (1990) Finding groups in data: an introduction to cluster analysis. . Wiley series in probability and mathematical statistics. *Applied probability and statistics*.
- WILLIS-MARTINEZ, D., RICHARDS, H. W., TIMCHENKO, N. A. & MEDRANO, E. E. (2009) Role of HDAC1 in senescence, aging, and cancer. *Experimental Gerontology*, 45, 279-285.
- WOLF, D., RODOVA, M., MISKA, E. A., CALVET, J. P. & KOUZARIDES, T. (2002) Acetylation of beta-catenin by CREB-binding protein (CBP). *J Biol Chem*, 277, 25562-7.
- WOODWARD, W. A., STROM, E. A., TUCKER, S. L., MCNEESE, M. D., PERKINS, G. H., SCHECHTER, N. R., SINGLETARY, S. E., THERIAULT, R. L., HORTOBAGYI, G. N., HUNT, K. K. & BUCHHOLZ, T. A. (2003) Changes in the 2003 American Joint Committee on Cancer staging for breast cancer dramatically affect stage-specific survival. *Journal of Clinical Oncology*, 21, 3244-8.

- XU, L., CHEN, Y., SONG, Q., XU, D., WANG, Y. & MA, D. (2009a) PDCD5 interacts with Tip60 and functions as a cooperator in acetyltransferase activity and DNA damage-induced apoptosis. *Neoplasia (New York)*, 11, 345-54.
- XU, L. J., CHEN, Y. Y., SONG, Q. S., XU, D., WANG, Y. & MA, D. L. (2009b) PDCD5 Interacts with Tip60 and Functions as a Cooperator in Acetyltransferase Activity and DNA Damage-Induced Apoptosis. *Neoplasia*, 11, 345-U46.
- XU, Y. & PRICE, B. D. (2011) Chromatin dynamics and the repair of DNA double strand breaks. *Cell Cycle*, 10, 261-267.
- YANG, X.-J. & SETO, E. (2008) The Rpd3/Hda1 family of lysine deacetylases: from bacteria and yeast to mice and men. *Nat Rev Mol Cell Biol*, 9, 206-218.
- YANG, X., YAN, L. & DAVIDSON, N. E. (2001) DNA methylation in breast cancer. *Endocr Relat Cancer*, 8, 115-127.
- YANG, X. J. & ULLAH, M. (2007a) MOZ and MORF, two large MYSTic HATs in normal and cancer stem cells. *Oncogene*, 26, 5408-5419.
- YANG, X. J. & ULLAH, M. (2007b) MOZ and MORF, two large MYSTic HATs in normal and cancer stem cells. *Oncogene*, 26, 5408-19.
- YOSHIDA, K., YOSHIDA, S. H., SHIMODA, C. & MORITA, T. (2003) Expression and radiation-induced phosphorylation of histone R2AX in mammalian cells. *Journal of Radiation Research*, 44, 47-51.
- YUAN, J., PU, M., ZHANG, Z. & LOU, Z. (2009) Histone H3-K56 acetylation is important for genomic stability in mammals.[see comment]. *Cell Cycle*, 8, 1747-53.
- YUE, W. W., HASSLER, M., ROE, S. M., THOMPSON-VALE, V. & PEARL, L. H. (2007) Insights into histone code syntax from structural and biochemical studies of CARM1 methyltransferase. *EMBO J*, 26, 4402-12.
- ZHANG, H., RAKHA, E. A., BALL, G. R., SPITERI, I., ALESKANDARANY, M., PAISH, E. C., POWE, D. G., MACMILLAN, R. D., CALDAS, C., ELLIS, I. O. & GREEN, A. R. (2009) The proteins FABP7 and OATP2 are associated with the basal phenotype and patient outcome in human breast cancer. *Breast Cancer Research and Treatment*, 121, 41-51.
- ZHANG, K., FAIOLA, F. & MARTINEZ, E. (2005) Six lysine residues on c-Myc are direct substrates for acetylation by p300. *Biochemical & Biophysical Research Communications*, 336, 274-80.
- ZHAO, W. H., KRUSE, J. P., TANG, Y., JUNG, S. Y., QIN, J. & GU, W. (2008) Negative regulation of the deacetylase SIRT1 by DBC1. *Nature*, 451, 587-U11.
- ZHAO, Y., LU, S. L., WU, L. P., CHAI, G. L., WANG, H. Y., CHEN, Y. Q., SUN, J., YU, Y., ZHOU, W., ZHENG, Q. H., WU, M., OTTERSON, G. A. & ZHU, W. G. (2006) Acetylation of p53 at lysine 373/382 by the histone deacetylase inhibitor depsipeptide induces expression of p21(Waf1/Cip1). *Molecular and Cellular Biology*, 26, 2782-2790.
- ZHENG, M. Z., EKMEKCIOLLU, S., WALCH, E. T., TANG, C. H. & GRIMM, E. A. (2004) Inhibition of nuclear factor-kappa B and nitric oxide by curcumin induces G(2)/M cell cycle arrest and apoptosis in human melanoma cells. *Melanoma Research*, 14, 165-171.
- ZHOU, H., BEEVERS, C. S. & HUANG, S. (2011) The targets of curcumin. *Curr Drug Targets*, 12, 332-47.

- ZHOU, Q.-M., ZHANG, H., LU, Y.-Y., WANG, X.-F. & SU, S.-B. (2009) Curcumin reduced the side effects of mitomycin C by inhibiting GRP58-mediated DNA cross-linking in MCF-7 breast cancer xenografts. *Cancer Science*, 100, 2040-2045.
- ZHOU, Y. & GRUMMT, I. (2005) The PHD finger/bromodomain of NoRC interacts with acetylated histone H4K16 and is sufficient for rDNA silencing. *Current Biology*, 15, 1434-8.
- ZHU, F., XIA, X., LIU, B., SHEN, J., HU, Y. & PERSON, M. (2007) IKKalpha shields 14-3-3sigma, a G(2)/M cell cycle checkpoint gene, from hypermethylation, preventing its silencing. *Molecular Cell*, 27, 214-27.
- ZIMMERMANN, S., KIEFER, F., PRUDENZIATI, M., SPILLER, C., HANSEN, J., FLOSS, T., WURST, W., MINUCCI, S. & GOTTLICHER, M. (2007) Reduced body size and decreased intestinal tumor rates in HDAC2-mutant mice. *Cancer Research*, 67, 9047-9054.
- ZINK, A., ROHRBACH, H., SZEIMIES, U., HAGEDORN, H. G., HAAS, C. J., WEYSS, C., BACHMEIER, B. & NERLICH, A. G. (1999) Malignant tumors in an ancient Egyptian population. *Anticancer Research*, 19, 4273-4277.
- ZIPPO, A., SERAFINI, R., ROCCHIGIANI, M., PENNACCHINI, S., KREPELOVA, A. & OLIVIERO, S. (2009) Histone crosstalk between H3S10ph and H4K16ac generates a histone code that mediates transcription elongation. *Cell*, 138, 1122-36.
- ZUPKOVITZ, G., TISCHLER, J., POSCH, M., SADZAK, I., RAMSAUER, K., EGGER, G., GRAUSENBURGER, R., SCHWEIFER, N., CHIOCCHA, S., DECKER, T. & SEISER, C. (2006) Negative and positive regulation of gene expression by mouse histone deacetylase 1. *Molecular and Cellular Biology*, 26, 7913-7928.

APPENDIX

Appendix 1: List for Antibodies Used in the study and Working Concentration used in Each Technique.

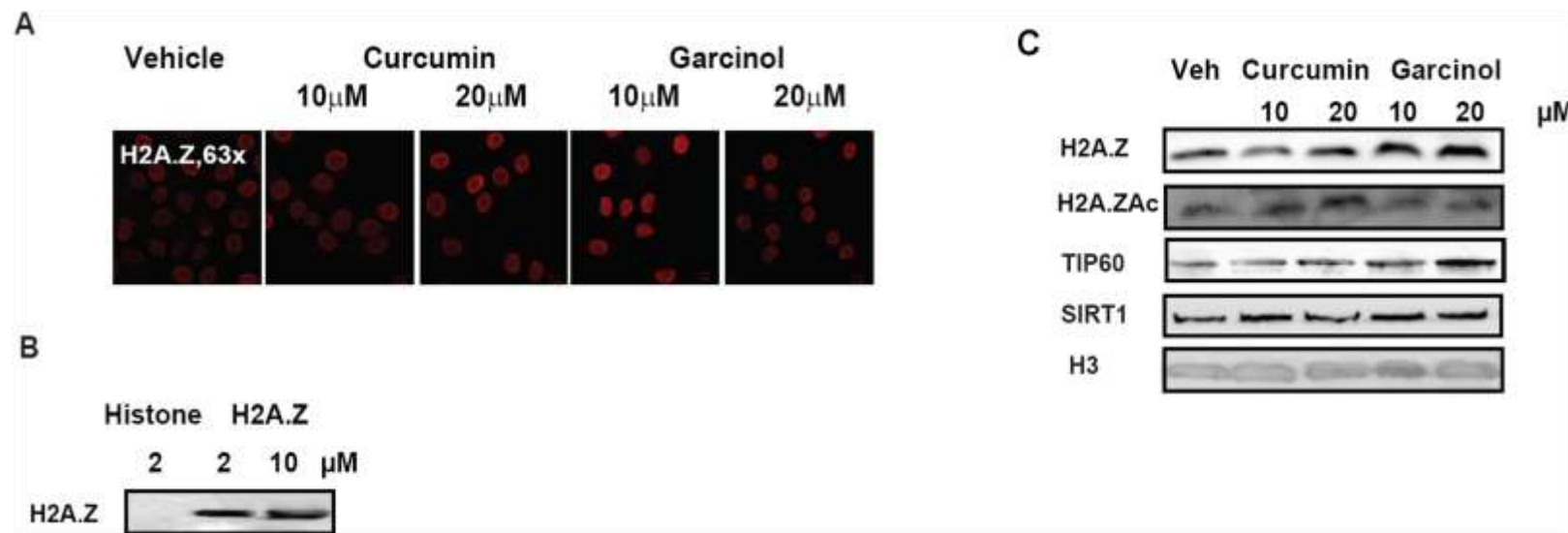
Antibody Name	Description	Catalogue No.	Lot No.	Application/ dilution					Provider	
				IF	WB	FACS	IHC			
							Con.	Antigen Retrieval		
Anti-Actin (C-2)	Ms Mono	Sc-8432			1/5000				Santa Cruz	
Anti-H2A	Rb						1/500	Citrate	Dr. Dimitrove	
Anti-H2A.Z(688)	Rb			1/50	1/500		1/25	Citrate	Dr. Dimitrove	
Anti-H2A.Z(2595)	Rb						1/50	Citrate	Dr. Dimitrove	
Anti-H2A.Z (acetyl K4+K7+K11)	Sh Poly	ab18262	618318		1/500		1/5	Citrate	Abcam	
Anti-Histone H3 (N-20)	Gt Poly	sc-8653			1/2000				Santa Cruz	
Anti-acetyl-Histone H3	Rb Poly	06-599	21514	1/100	1/2000				Upstate, Millipore	
Anti-H3K18ac	Rb Poly	ab1991		1/200	1/500				Abcam	
Anti-acetyl-Histone H4	Rb Poly			1/00						
Anti-H4K16ac	Rb	06762	31884	1/100	1/200	1/100	1/20	EDTA	Upstate, Millipore	
Anti-H3K9me3	Rb	ab8898		1/300	1/250	1/100	1/300	Citrate	Abcam	
Anti-H4K20me3	Rb Poly	ab9053		1/200	1/500	1/100			Abcam	
Anti-PCAF (C-16)	Gt Poly	sc-6300			1/500				Santa Cruz	
Anti-CBP (A-22)	Rb Poly	sc-369	E2406	1/50	1/500		1/50	Citrate	Santa Cruz	
Anti-p300 (N-15)	Rb Poly	sc-584			1/250				Santa Cruz	
MOZ (N-19)	Rb Poly	sc-5713		1/10					Santa Cruz	
Anti-MORF	Rb Poly	ab58823		1/10			1/75	Citrate	Abcam	
Anti-hMOF	Ms Mono	ab54276		1/100			1/8	Proteinase k	Abcam	
Anti-Tip60	Ms Mono	ab54277	405324	1/200			1/5,000	Citrate	Abcam	
Anti-HDAC1(H-51)	Rb Poly	sc-7872		1/15			1/15	EDTA	Santa Cruz	
Anti-HDAC2 (H-54)	Rb Poly	sc-7899		1/50			1/50	Citrate	Santa Cruz	
Anti-SIRT1	Rb Mono	ab32441		1/00	1/100		1/25	Citrate	Abcam	
Anti-SUV39H1	Rb Poly	ab33056		1/10	1/125		1/25	Proteinase k	Abcam	

Anti-SUV420h1/2	Rb Poly	Ab18186	864861		1/100	1/100			
Anti-DBC1	Ms Mono	Ab57608	528169	1/25			1/25	Citrate	Abcam
Anti-p53									
Anti-p53(DO-1)	Ms Mono	sc-126			1/500				Santa Cruz
Anti-Ac-p53 (K386)	Rb Poly	ab52172		1/200	1/00	1/200	1/200	Citrate	Abcam
Anti-Acp53 (K120)	Ms Mono	Ab78316		1.100	1/500	1/500	1/50	Citrate	Abcam
Anti-Acp53 (K373)	Rb Mono	Ab62376		1/100	1/500	1/400	1/100 0	Citrate	Abcam
Anti-Acp53 (K373& K382)	Rb poly	06-758	22561		1/500				Abcam
Anti-p21 (C-19)	Rb Poly	sc-397			1/250				Santa Cruz
Anti-C-Myc (9E10)	Ms	sc-40			1/250				Santa Cruz
Anti-IRF-1	Rb Poly	ab26109					1/100		Abcam
Anti-H3K56ac	Rb Poly				1/500		1/200	Citrate	A Collaborator
FITC Anti-BrdU	Ms Mono	556028	17253			1/50			BD Pharmingen
DNA Damage Antibody Kit									
Anti-Phospho-ATM (Ser1981)	Ms	4526			1/500				Cell Signaling
Anti-Phospho-ATR (Ser 428)	Rb	2853			1/500				Cell Signaling
Anti-Phospho-BRCA1 (1524)	Rb	9009			1/500				Cell Signaling
Anti- Phospho-H2A.X (Ser139)	Rb	2577			1/250				Cell Signaling
Anti-Hb1(D-15)	Gt Poly	Sc-10217					1/500		Santa Cruz
Anti-Abobec3	Rb Poly	ARP46114_P0 50					1/75		AVIVA SYSTEMS BIOLOGY

Where RB, Rabbit; Ms, Mouse; Sh, Sheep; Gt, Goat; Poly, Polyclonal; Mono, Monoclonal; IHC, immunohistochemistry; IF,

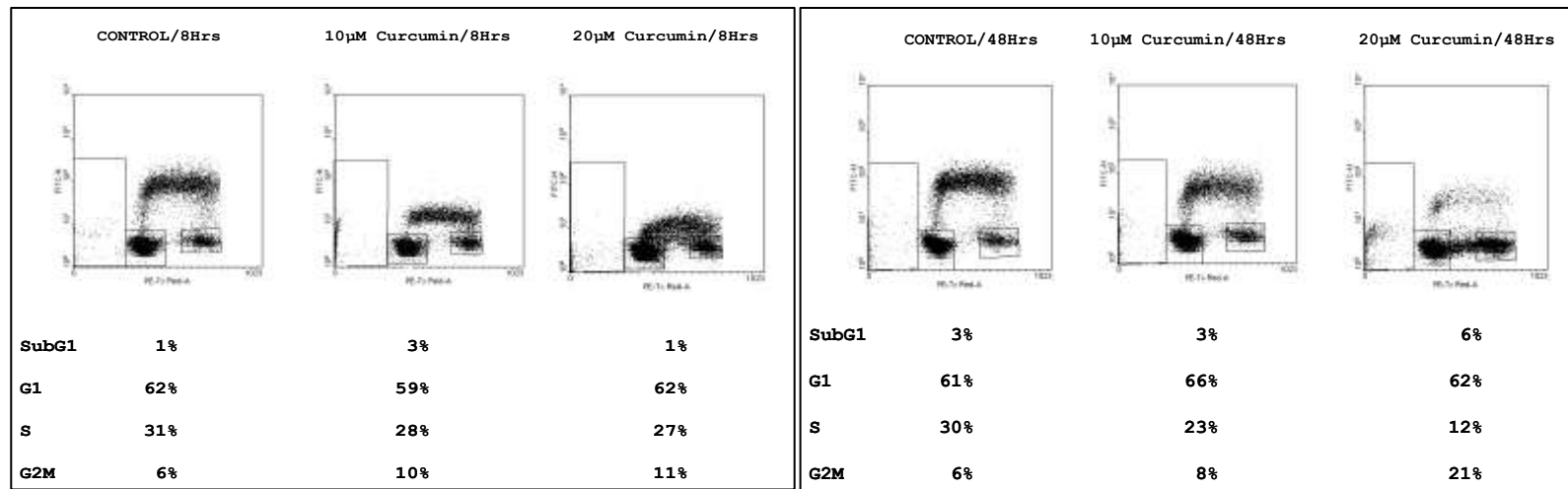
immunofluorescence; WB, Western Blotting.

Appendix 2: HATi Alters H2A.Z and its Acetylated Form Level in MCF-7 Cells.



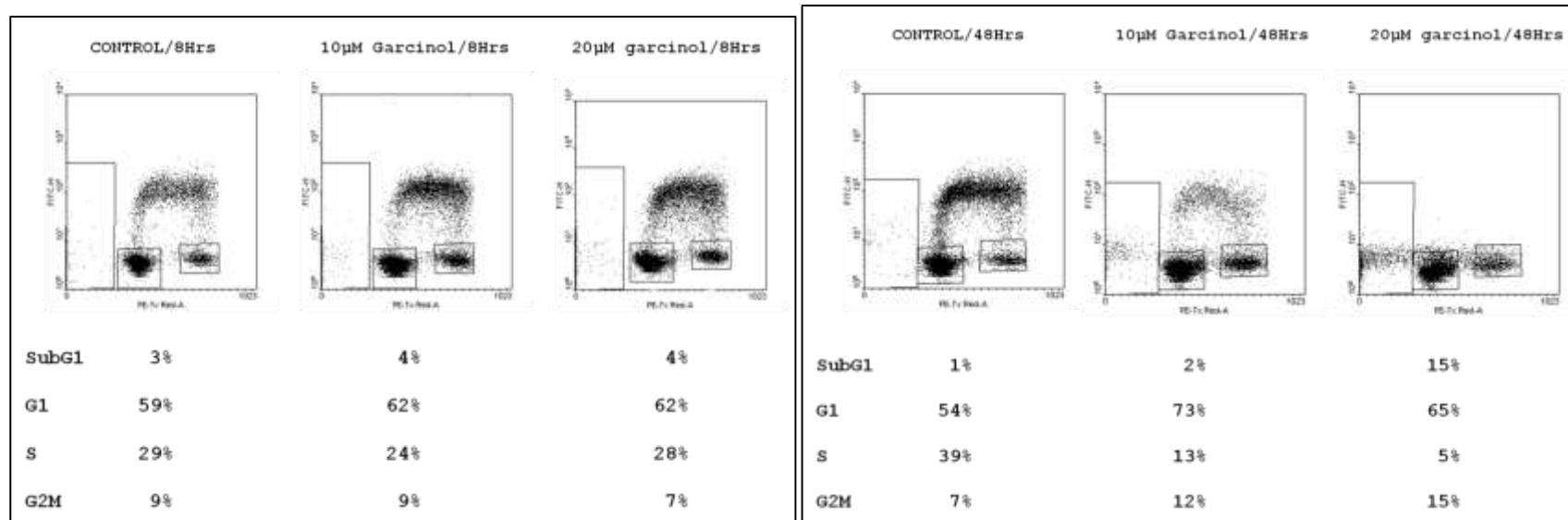
A, Immunofluorescence staining of MCF-7 cells for H2A.Z following 24hrs of HATi treatment; garcinol treatment induces increases H2A.Z levels; **B**, H2A.Z antibody is specific for H2A.Z, no immunoreactivity to core histone was seen; **C**, Western blotting for MCF-7 cells treated with curcumin or garcinol for 24 hours, garcinol induces H2A.Z levels, curcumin increases acetylation of H2A.Z. TIP60 is markedly increased following garcinol treatment. No considerable changes in SIRT1 level were detected. H3 was used as a loading control.

Appendix 3: Curcumin Treatment for 8 and 48 Hours Alters Cell Cycle progression in MCF-7 Cells



Cell cycle analysis of MCF-7 cells treated with curcumin for 8 (Left panel) or (Right panel) 48 hrs. No significant changes have been noted after 8 hrs of treatment; however, marked reduction in S phase cells were observed after 48 hrs.

Appendix 4: Garcinol Treatment for 8 and 48 Hours Alters Cell Cycle progression in MCF-7 Cells



Cell cycle analysis of MCF-7 cells treated with garcinol for 8 (Left panel) or 48 (Right panel) hrs. No significant changes have been noted after 8 hrs of treatment; however, 48 hrs of treatment caused a marked loss in S phase cells and an increased (Sub G1) cells.

ELSEVIER LICENSE
TERMS AND CONDITIONS

Oct 11, 2011

This is a License Agreement between magdy Abdelghany ("You") and Elsevier ("Elsevier") provided by Copyright Clearance Center ("CCC"). The license consists of your order details, the terms and conditions provided by Elsevier, and the payment terms and conditions.

All payments must be made in full to CCC. For payment instructions, please see information listed at the bottom of this form.

Supplier	Elsevier Limited The Boulevard, Langford Lane Kidlington, Oxford, OX5 1GB, UK
Registered Company Number	1982084
Customer name	magdy Abdelghany
Customer address	168 woodside road, beeston, nottingham, Nottingham, other NG9 2TT
License number	2765831315375
License date	Oct 11, 2011
Licensed content publisher	Elsevier
Licensed content publication	Trends in Molecular Medicine
Licensed content title	p53 post-translational modification: deregulated in tumorigenesis
Licensed content author	Chao Dai, Wei Gu
Licensed content date	November 2010
Licensed content volume number	16
Licensed content issue number	11
Number of pages	9
Start Page	528
End Page	536
Type of Use	reuse in a book/textbook
Requestor type	author of new work
Intended publisher of new work	American Chemical Society
Portion	figures/tables/illustrations
Number of figures/tables/illustrations	1
Format	both print and electronic
Are you the author of this Elsevier article?	No
Will you be translating?	No
Order reference number	

Title of the book	Profiling post Translational Modifications of Histone and p53 in Human Breast Carcinoma
Publisher of the book	American Chemical Society
Author of the book	Magdy Korashy Abdelghany
Expected publication date	Oct 2011
Estimated size of the book (number of pages)	350
Elsevier VAT number	GB 494 6272 12
Permissions price	0.00 USD
VAT/Local Sales Tax	0.0 USD / 0.0 GBP
Total	0.00 USD
Terms and Conditions	

INTRODUCTION

1. The publisher for this copyrighted material is Elsevier. By clicking "accept" in connection with completing this licensing transaction, you agree that the following terms and conditions apply to this transaction (along with the Billing and Payment terms and conditions established by Copyright Clearance Center, Inc. ("CCC"), at the time that you opened your Rightslink account and that are available at any time at <http://myaccount.copyright.com>).

GENERAL TERMS

2. Elsevier hereby grants you permission to reproduce the aforementioned material subject to the terms and conditions indicated.

3. Acknowledgement: If any part of the material to be used (for example, figures) has appeared in our publication with credit or acknowledgement to another source, permission must also be sought from that source. If such permission is not obtained then that material may not be included in your publication/copies. Suitable acknowledgement to the source must be made, either as a footnote or in a reference list at the end of your publication, as follows:

"Reprinted from Publication title, Vol./edition number, Author(s), Title of article / title of chapter, Pages No., Copyright (Year), with permission from Elsevier [OR APPLICABLE SOCIETY COPYRIGHT OWNER]." Also Lancet special credit - "Reprinted from The Lancet, Vol. number, Author(s), Title of article, Pages No., Copyright (Year), with permission from Elsevier."

4. Reproduction of this material is confined to the purpose and/or media for which permission is hereby given.

5. Altering/Modifying Material: Not Permitted. However figures and illustrations may be altered/adapted minimally to serve your work. Any other abbreviations, additions, deletions and/or any other alterations shall be made only with prior written authorization of Elsevier Ltd. (Please contact Elsevier at permissions@elsevier.com)

6. If the permission fee for the requested use of our material is waived in this instance, please be advised that your future requests for Elsevier materials may attract a fee.

7. Reservation of Rights: Publisher reserves all rights not specifically granted in the combination of (i) the license details provided by you and accepted in the course of this licensing transaction, (ii)